



**Brunel**  
University  
London

**Conceptual Design and Development of a Research Tool: - The  
Vagina-on-chip (VOC)**

**A thesis submitted for the degree of  
Doctor of Philosophy**

**By**

**Angel Kayalvilli Naveenathayalan**

**College of Engineering, Design and Physical Sciences  
Department of Mechanical and Aerospace Engineering**

**Brunel University**

**October 2020**

## Abstract

Bacterial Vaginosis is one of the most common vaginal infection that affect 50% of women globally between the ages of 14-49, yet its aetiology remains unknown. Antibiotics or vaginal creams are usually prescribed to women to treat the infection however, reoccurrence is common after a year of treatment. Therefore, this condition desperately needs a new approach to developing an effective treatment. The aim of this thesis was to develop a microfluidic platform that can realistically mimic the *in vivo* vaginal epithelium tissue as an *in vitro* system which can then be used by clinicians and researchers to gain a better understanding of bacterial vaginosis (BV). The Vagina-on-chip (VOC) was developed using multiple techniques that combined micro-engineering, 3D printing, electrospinning, and cell culture to mimic the mechanical, biochemical and physical aspects of vaginal tissue.

VOC platform comprised of three layers, top and bottom microfluidic channels to provide nutrients to the central layer, the membrane held in suspension to support the growth of vaginal tissue. The membrane was fabricated using natural and synthetic polymers via electrospinning technique. Composite membrane made with gelatine (GE) and polycaprolactone (PCL), a mixture of natural and synthetic polymers was found to be the optimal membrane for cell culture. This membrane was chosen due to its fibre size ( $257.25 \pm 72.92\text{nm}$ ) and wettability CA ( $29.66^\circ$ ) which provided a large surface area and hydrophilic exterior to support growth and cell adhesion of vaginal cells. Mechanical testing revealed that composite membrane exhibited similar mechanical properties to vaginal epithelium from non-prolapsed women. The composite membrane had a stress failure at 1.6MPa with strain failure at 12%. Cell viability assays were also conducted on the membranes to test for biocompatibility, which confirmed the composite membrane to be the most appropriate membrane for the VOC platform. Scanning electron microscopy was performed to visualise cell attachment on all membranes which showed the vaginal cells merging to the fibres of PCL/GE, PCL/COL and composite membrane indicating that these as-spun scaffolds promoted cellular attachments and spreading. Together with these results, the first VOC platform prototype was constructed. Due to its early stages in development, further experimentation and optimisation is required to evaluate its performance, to support the growth of vaginal tissue and potentially becoming a realistic research tool to study BV.

## **Acknowledgments**

First and foremost, I would like to express my gratitude and appreciation to both my principal supervisor Dr Ruth Mackay and second supervisor Dr Elisabete Silva for their endless, advice, support and guidance, time and patience throughout my PhD, especially during the last stages of writing my thesis. They both have encouraged me to keep going and never stop, to quote them 'Keep on trucking'. It has been a long and hard journey to the finish line, but they have supported me all the way, thank you so much. I would also like to acknowledge my research development advisor Professor Wamadeva Balachandran for his advice and support during my PhD degree especially during my reviews, to tackle this multidisciplinary project with a little more confidence.

I would like to extend my appreciation and say a massive thank you to all my friends at Brunel University Shima Abdullateef, Aya Aly, Femke Cappon, Dr Pascal Craw, Dr Luq Ereku, Alessandro Giudici, Nauman Hafeez, Racheal Kerslake, Dr Rebecca Leese, Irene Ruiz Rodriguez, Samira Safari, Dr Tom Stead, and Dr Shavini Wijesuriya for all your continuous support, advice, encouragement, humour and most of all your friendship over the years and throughout my PhD studies. You have all made every day being in the office, labs and catchups fun and entertaining especially when I needed it the most during the hard and difficult times. I also would like to take this opportunity to say a special thank you Emily De-Bodene, Deborah De Jong, Kudakwashe Chiwanga, Palwinder Kaur, Dr Phoebe Maund, Luana Osório and Punyaporn Saengnuan for their outstanding support and advice in the labs. Working with you all has been a great pleasure.

I would like to sincerely thank EPSRC for funding my PhD studies for 3.5 years and a special thank you to Dr Raina Ficharova from Brigham Womens Hospital, Harvard, USA for providing the cell line for my research.

Finally, I would like to say thank you to my family for their continuous support and inspiration, their endless love and encouragement during my PhD has been amazing. Without them I would not have been able to reach my goal and for that I am very grateful.

## Dedication

To my ever-supporting family and friends

## Table of Contents

Abstract .....	i
Acknowledgments .....	ii
Dedication.....	iii
Table of Contents .....	iv
List of Figures .....	viii
List of Tables .....	xii
List of Abbreviations.....	xiii
List of Symbols .....	xv
1.1 Aim.....	1
1.2 Objectives.....	1
1.3 Description of Chapters.....	2
1.4 Background .....	3
1.5 Contributing Risks Factors.....	4
1.6 Physiology of the vagina .....	5
1.6.1 Anatomy of the vagina .....	5
1.6.2 Vaginal Microbiota and Acidic Environment .....	7
1.7 Diagnostic Measurements.....	8
1.7.1 Treatment of BV.....	9
1.8 Limitations of current models .....	9
1.8.1 Organ - on -chip .....	10
Chapter 2- Literature Review .....	11
2.1 2D modelling of Vaginal Tissue.....	11
2.1.1. 2D vs 3D cell culture .....	16
2.2 3D modelling of Vaginal tissue .....	18
2.2.1 Organ-on-a-chip.....	22
2.2.2 Female reproductive OOC systems .....	27
2.3 Scaffold Fabrication .....	29
2.3.1 Photolithography .....	29
2.3.2 Soft lithography .....	31
2.3.3 Electrospinning .....	32
2.3.4 Bio-plotting.....	35
2.4 Microfluidics.....	37

2.4.1	Stereolithography .....	37
2.4.2	Fused Deposition Modelling .....	40
2.4.3	Material Jetting.....	42
2.4.4	Lego Microfluidics .....	43
2.5	Summary .....	44
<b>Chapter 3 – Microfluidic Design of the VOC platform and fabrication processes .....</b>		<b>46</b>
3.1	Engineering Design Process .....	47
3.2	Design Concept .....	49
3.3	Product Design Requirements .....	49
3.4	Materials .....	51
3.5	Methodology .....	51
3.5.1	PDMS for fabricating VOC layers .....	51
3.5.2	Soft Lithography Process for Creating VOC Moulds .....	52
3.5.3	Design and Fabrication of VOC Moulds .....	53
3.5.4	Assembling VOC Moulds into Steel Casing .....	53
3.5.5	Preparing PDMS mixture .....	54
3.5.6	Removing VOC PDMS layer of moulds .....	55
3.5.7	Bonding of the VOC PDMS layers.....	55
3.6	Design iterations and evaluation .....	56
3.6.1	Initial Design .....	56
3.6.2	Design 7 – The Final Model.....	58
3.7	Assembling of VOC platform .....	59
3.7.1	Channel Dimension .....	60
3.7.2	Top and Base VOC Moulds .....	60
3.7.3	Central top and base membrane layers .....	61
3.8	Testing of VOC platform.....	61
3.9	Summary .....	62
<b>Chapter 4 – Electrospun Membrane Fabrication and Evaluation .....</b>		<b>64</b>
4.1	Requirement for a suitable membrane.....	65
4.2	Biopolymers .....	66
4.2.1	Gelatin.....	66
4.2.2	Collagen.....	66
4.3	Synthetic polymer.....	67

4.2.3	Poly ( $\epsilon$ -caprolactone) .....	67
4.4	Materials and Methods.....	67
4.4.1	Materials .....	67
4.5	Preparation of spinning solutions.....	68
4.5.1	Single solutions.....	68
4.5.2	Composite solution .....	68
4.5.3	Co-axial solution .....	68
4.5.4	Crosslinking .....	69
4.6	Electrospinning setup and single method .....	69
4.6.1	Co-axial spinning.....	70
4.6.2	Evaluation of Fibre Diameter and Morphology .....	71
4.6.3	Fibre Diameter Measurement .....	72
4.6.4	Contact angle measurements .....	72
4.6.5	Uniaxial Tensile Measurements.....	73
4.7	Results.....	74
4.7.1	Morphology of Membranes.....	74
4.7.2	Stress-strain Curves.....	77
4.7.3	Contact Angle .....	79
4.8	Electrostatics Forces .....	81
4.9	Summary .....	83
<b>Chapter 5 – Assessment of VOC membrane biocompatibility using VK2/E6E7 (vaginal epithelial cells) .....</b>		<b>85</b>
5.1	Materials .....	85
5.1.1	Cell line.....	85
5.1.2	Growth Media for VK2/E6E7 .....	85
5.1.3	Growth Media for Resuspending .....	87
5.1.4	Trypsin – EDTA (0.05%), phenol red .....	87
5.2	Methodology.....	87
5.2.1	Thawing and culturing of VK2/E6E7 cells .....	87
5.2.2	Maintaining cells.....	88
5.2.3	Health of a cell line .....	88
5.2.4	Subculture cells.....	89
5.2.5	Cell counting.....	90
5.2.6	Cryopreservation of cells.....	91

5.2.7	Observing cells .....	92
5.3	Cell viability test (MTT) – Electrospun membranes (24 well plate) .....	93
5.3.1	Set up of experiment.....	94
5.4	Statistical Analysis .....	96
5.5	Results and discussion .....	96
5.5.1	MTT results conducted on Electrospun membranes .....	96
5.5.2	Cell morphology observations on membranes .....	101
5.5.3	Fluorescent staining o VK2/E6E7 cells on membranes.....	101
5.5.4	SEM imaging of VK2/E6E7 cells on membranes.....	103
5.6	Summary .....	106
Chapter 6	– Discussion and VOC Platform Integration .....	108
6.1	VOC Integration .....	112
Chapter 7	– Conclusion .....	115
7.1	Contribution to knowledge .....	116
8.1	Set up of ELVEFLOW Experiment .....	118
References	.....	121
Appendix A	.....	147
9.1	Top VOC Mould Dimensions.....	147
9.1.1	Top VOC Mould Annotations.....	148
9.2	Central Top VOC Mould Dimensions.....	149
9.2.1	Central Top VOC Mould Annotations.....	150
9.3	Central Base VOC Mould Dimensions .....	151
9.3.1	Central Base VOC Mould Annotations .....	152
9.4	Base VOC Mould Dimensions .....	153
9.4.1	Base VOC Mould Annotations .....	154
9.5	Top Plate Casing for VOC Mould Dimensions.....	155
9.5.1	Top Plate Casing for VOC Mould Trimetric View.....	156
9.6	Bottom Plate Casing for VOC Mould Dimensions .....	157
9.7	VOC Mould in Casing Assembly .....	158
9.7.1	Assembly of the VOC Platform .....	159



## List of Figures

Figure 1 The anatomy of the vagina, created with BioRender.com .....	6
Figure 1.2 Histology image presenting the layers of the vagina (Sugiritama, 2009).....	7
Figure 1.3 Vaginal epithelial cells: (A) Normal vaginal epithelial cells surrounded by the microflora Lactobacillus, rod like shaped bacteria; (B) Vaginal epithelial cells surrounded by bacteria Gardnerella vaginalis forming clue cells is normally found in vaginal samples obtained from women with BV (Todar, 2008).....	8
Figure 2.1. Causes of recurrent of BV and potential strategies to reduce its prevalence (Bradshaw and Brotman, 2015a) .....	14
Figure 2.2. Comparison between 2D cell culture and 3D cell culture highlighting the key difference when growing cells in 2D environment in comparison to cells growing in a 3D matrix (Ustyugov et al., 2018). .....	17
Figure 2.3. SEM presenting the 3D organotypic vagina epithelial cell model, (A) presents single layer of vaginal cells after 19-21 days during early development a low magnification;(B) Low magnification SEM of multiple flatten vaginal cell layers after 39-42 days during late development (C); high magnification of boxed area in (A) and (D) high magnification of boxed area in (B) (Hjelm et al., 2010).....	19
Figure 2.4. Presents the physiological structures of vaginal cells from the 3D model A) SEM of secretory vesicles (B) TEM of microfolds (rugae) indicated by the arrows and C) TEM of long microvilli on adjacent walls. Scale bar (A) 20 $\mu\text{m}$ (B & C) 2 $\mu\text{m}$ (Hjelm et al., 2010). .....	20
Figure 2.5. Presents SEM of structural characteristics of endometrial epithelial cell aggregates on the EEC model after 21 days at magnification of x250, x1200 and x4000 respectively. (A) Microbeads covered in single layer of endometrial epithelial cells; (B) The white arrows indicates cells proliferation at different stages and the microvilli present on the cell surface; (C) The while arrows highlighting the microvilli and secretory/mucus material visible on the surface of the cells (Laniewski et al., 2017). .....	21
Figure 2.6. SEM of vaginal bacterial species and N. gonorrhoeae effectively colonising in the 3D endometrial epithelial cell model. The EEC model was infected for 24 hours with (A) L. crispatus VPI-3199; (B) G. vaginalis JCP8066 and (C) N. gonorrhoeae MS11 which showed the characteristic morphologies of each bacterium attaching to the surface of the EEC aggregates. Photoshop CS51, Adobe was used to colour the bacteria (A) L. crispatus in purple; (B) G. vaginalis in green and (C) N. gonorrhoeae in blue (Laniewski et al., 2017). ....	22
Figure 2.7. Schematic drawing of Human-on-a-chip and how each chip is interconnected. Each chip has been designed to mimic the organ level functions ( Ingber, 2017). .....	23
Figure 2.8. (A) multi-layered lung-on-a-chip microfluidic device (B) two cell cultured layers separated by a porous PDMS membrane. Vacuum chamber on either side allows the membrane to be stretched (Huh <i>et al.</i> , 2013).....	25
Figure 2.9. A multi-layered Gut-on-chip microfluidic device constructed with two cell cultured layers separated by a porous PDMS membrane lined with human villus intestinal	

epithelium and human vascular endothelium under fluid flow and peristalsis like strain forces on either side of the membrane. (Bein <i>et al.</i> , 2018). .....	26
Figure 2.10. Draper microfluidic platform FemKUBE. The bottom layer consists of air channels which controls the flow of media through the middle layer. The media is transported to the top layer where chamber house cell culture or with fresh media and used media for experimental analysis (Woodruff, 2013b). .....	28
Figure 2.11. EVATAR, a microfluidic representation of the female reproductive tract that contains compartments with different 3D cells culture from the ovaries, uterus, and the vagina. The liver is also included for the purpose of evaluating hormonal levels in response to drugs (Xiao <i>et al.</i> , 2017). .....	29
Figure 2.12 Presents the step by step process conducted in Photolithography to create precise and small masks known as SU-8 wafers for microfabrication applications (Verma <i>et al.</i> , 2013). .....	30
Figure 2.13. Presents the step by step process conducted in Soft lithography to create embossed elastomeric stamps made with PDMS (Microfluidics Background, 2020). .....	32
Figure 2.14 Present the set-up of the electrospinning apparatus (Garg and Bowlin, 2011)..	33
Figure 2.15. Presents images of 3D bio plotted constructs with heterogeneous and complex structures (A) a mandible of bone; (B) an ear cartilage with ear lobe; (C) a kidney with renal pelvis ;(D) a liver ;(E) a heart cross-section and (F) an arterial tree (Yi <i>et al.</i> ,2017)..	36
Figure 2.16 Present the set up for SLA printing which uses photopolymer and UV laser beam to build an object layer by layer (Fasnacht, 2017)..	38
Figure 2.17 Demonstrates the Top-down SLA printer (Varotsis, 2020a). .....	39
Figure 2.18. Presents SLA 3D printer Formlabs (Ward, 2015). .....	39
Figure 2.19 Demonstrates the bottom-up SLA printer (Varotsis, 2020a). .....	40
Figure 2.20 Ultimaker 2+ is an example of FDM printer, which uses filaments to build an object through material extrusion process (Professional 3D printing made accessible   Ultimaker, 2011). .....	40
Figure 2.21 Presents the printing process of FDM (Varotsis, 2020a) .....	41
Figure 2.22 The Objet Polyjet printer uses material jetting to cure photocurable resin (Fasnacht, 2017)..	42
Figure 2.23. Presents the printing process MJ printing (Bournias Varotsis, 2019). .....	43
Figure 2.24 Fluid flow through microfluidic Lego® (Vittayarukkul and Lee, 2017)..	44
Figure 3.1 The engineering design process followed to design and develop the VOC platform. ....	46
Figure 3.2 Concept design of the VOC platform. ....	49
Figure 3.3 Schematic illustration of the three major steps involved in the soft lithography..	52
Figure 3.4 Full casting assembly of VOC mould housed in a steel casing to fabricate the PDMS layers of the VOC platform.....	53

Figure 3.5 Tubing attached to the in/outlets of the top layer for a secure connection. ....	54
Figure 3.6 Surface modification of PDMS after oxygen plasma treatment (Pasirayi <i>et al.</i> , 2012). ....	55
Figure 3.8 Presents the SolidWorks and 3D printed moulds for the VOC platform (A) Top VOC mould; (B) Base VOC mould; (C) Central top mould and (D) Central base mould. ....	58
Figure 3.9 Final VOC platform in exploded view showing the separate layers in order (A) Top VOC layer; (B) Central top layer; (C) Electrospun membrane; (D) Central base layer and (E) Base VOC layer. ....	59
Figure 3.10 Final assembly of the VOC platform from a top view and isometric view with the membrane at the centre held in suspension between the channels. ....	59
Figure 3.11 (A) Top VOC mould with extra in/outlet circled in red and (B) Base VOC mould with no extra in/outlets. ....	60
Figure 3.12 Three independent VOC chips (A) an empty VOC platform; (B) VOC platform with membrane between the two fluidic channels and (C) flow experiment conducted on VOC platform with colour dyes. ....	62
Figure 4.1 Electrospinning setup manufactured by AC solutions Ltd, UK. ....	70
Figure 4.2 (A) Co-axial electrospinning set up; (B) Schematic of co-axial fibres with core (PCL) and shell (GEL or COL). ....	71
Figure 4.3 (A) Sputter coater device (OM-SC7640, UK); (B) 1 cm x 2 cm electrospun samples placed onto stub holders using carbon tape to sputter coat samples in gold for 2 mins. ....	72
Figure 4.4 FTA 32A goniometer instrument use to measure contact angle of membranes ...	73
Figure 4.5 TSTS350, (Linkam Scientific Instruments, UK) measuring the tensile strength of an electrospun membrane under 20N load cell and pulled in the y-axis direction with a speed of 250µm/sec until sample failure. (A) sample at the stationary position; (B) Sample at failure. ....	74
Figure 4.6. SEM of electrospun membranes (A) PCL membrane (2000x); (C) PCL/GE membrane (2000x); (E) PCL/COL membrane (2700x); (G) Composite membrane (4000x) with their respective fibre diameter distributions (B) PCL membrane; (D) PCL/GE membrane; (F) PCL/COL membrane and (H) Composite membrane. ....	76
Figure 4.7. Stress -Strain curves on all electrospun membranes (n = 4) ....	77
Figure 4.8 Stress -Strain curves of PCL/GE and Composite electrospun membranes (n=2). ..	78
Figure 4.9 Contact angle measurement table presenting the angles for spreading to no wetting which informs whether a surface is hydrophobic of hydrophilic (Solving the Problems of Plastics Adhesion   Adhesion Bonding, 2012). ....	79
Figure 4.10 Water contact angle of PCL, PCL/GEL, PCL/COL and Composite membranes at 0 seconds and 5 seconds (n=4). ....	80
Figure 5.1 Growth curve presenting the four phases' cells go through during cell culture. Lag phase, cells grow slowly adapting to their environment. The log phase is where cells	

experience exponential growth by consuming the nutrients from the growth media. At the stationary phase cell growth begins to reduced significantly leading to the death phase where cells die, caused by lack of nutrients and inhabitable conditions (Straube and Müller, 2016). .....89

Figure 5.2 Cells observed on days 3,6 and 8 on the Lecia microscope x40 magnification.....92

Figure 5.3 The yellow dye (MMT) is reduced by the mitochondrial reductase enzyme which forms insoluble formazan crystals (Riss. T.L, et al 2004). .....94

Figure 5.4 24 well plate with membranes held down in the well with nitrile O-rings to prevent samples from floating during experiments. ....95

Figure 5.5. Represents all membranes cell viability in relation to the control (P <0.05) after 24hrs (n=4). .....97

Figure 5.6. Represents all membranes cell viability in relation to the control (P <0.05) after 72hrs (n=4). .....97

Figure 5.7. Represents all membranes cell viability in relation to the control (P <0.05) after 168 hrs (n=4) .....98

Figure 5.8 Fluorescent microscopy images of DAPI staining of VK2/E6E7 cells on (A) PCL/GE; (B) PCL/COL and (C) composite (PCL/GE) membrane at x10 magnification.....102

Figure 5.9 Scanning Electron Microscopy image of VK2/E6E7 cells on (A and B) PCL/GE coaxial membrane x2000 magnification.....103

Figure 5.10 Scanning Electron Microscopy image of VK2/E6E7 cells on (A, B and C) PCL/COL coaxial membrane x2000 magnification.....104

Figure 5.11 Scanning Electron Microscopy image of VK2/E6E7 cells on PCL/COL coaxial membrane x2000 magnification.....105

Figure 5.12 Interaction of bone-marrow stromal cells with gelatin/PCL composite fibrous scaffolds after 7 days of cell culture: cell interaction with scaffold, at 1000 x magnification (Zhang et al., 2005) .....106

Figure 6.1 presents the potential layers of the VOC platform (created in BioRender.com) .112

Figure 6.2(A) 3D printed VOC platform in VeroClear; (B) Design concept for TPU VOC platform. ....113

Figure 8.1 Integrated VOC platform under flow experiment through with the Elveflow system. ....118

## List of Tables

Table 1.1 Four diagnostic makers for the Amsel Criteria assessment of BV prevalence .....	8
Table 3.1 Design requirements for the VOC platform.....	50
Table 3.2 Summary table of the VOC designs presenting the features, evaluation and benefits of each design. ....	57
Table 4.1 Parameter settings used for electrospinning nanofiber membranes.....	70
Table 4.2 Evaluation of passive In vitro cell adhesion intervention and stages .....	82
Table 5.1. Ingredients for VK2/E6E7 Keratinocyte serum free medium. ....	86
Table 5.2. Components required freezing media .....	91

## List of Abbreviations

2D	Two Dimensional
3D	Three Dimensional
AA	Glacial Acetic Acid
ABS	Acrylonitrile Butadiene Styrene
AV	Atopobium Vaginae
BV	Bacterial Vaginosis
CaCl <sub>2</sub>	Calcium Chloride
CFD	Computer Fluidic Dynamics
CFU	Colony Forming Units
CO <sub>2</sub>	Carbon Dioxide
COL	Collagen
CS	Cellulose Sulphate
CT	Chlamydia Trachomastis
DI	Deionised water
DMEM/F12	Dulbecco's Modified Eagle Medium/Nutrient Mixture F-12
DMSO	Dimethyl Sulfoxide
DNA	Deoxyribonucleic Acid
ECM	Extracellular Matrix
Ect1/E6E7	Ectocervical
EEC	Endometrial Epithelial Cell
EGF	Epidermal Growth Factor
Endo1/E6E7	Endocervical
EVATAR	Female Reproductive Tract and Liver
FDM	Fused Deposition Modelling
FFF	Fused Filament Fabrication
GEL	Gelatin
GTA	Glutaraldehyde
GV	Gardnerella Vaginalis
HBSS	Hank's Balanced Salt Solution
HEC	Hydroxyethyl Cellulose
HIV	Human Immunodeficiency Virus
HRT	Hormone Replace Therapy
HSV-2	Herpes Simplex Virus Type 2
HUVEC	Human Umbilical Vein Endothelial Cells
ID	Inner Diameter
ISO	International Organisation for Standardisation
IPA	Isopropyl Alcohol
LB	Lactobacillus
LOC	Lab – on– chip
MJ	Material Jetting
MTT	(3-(4,5-dimethylthiazol-2-yl)-2,5-diphenyltetrazolium bromide

NGU	Non-Gonococcal Urethritis
OD	Outer Diameter
P/S	Penicillin -Streptomycin
PA	Polyamide Nylon
PBS	Phosphate Buffer Solution
PCL	Poly ( $\epsilon$ -caprolactone)
PCR	Polymerase Chain Reaction
PDMS	Polydimethylsiloxane
PETG	Polyethylene Terephthalate Glycol
PID	Pelvic Inflammatory Disease
PLA	Poly Lactic Acid
PTFE	Polytetrafluoroethylene
RGD	Arginylglycylaspartic
SLA	Stereolithography
STI	Sexually Transmitted Infection
STL	Stereolithography
SU-8	Silicon Wafer
TEM	Transmission Electron Microscopy
TFE	2, 2, 2-Trifluoroethanol
TLR	Toll-like Receptors
TPU	Polyurethane
UTI	Urinary tract infections
UV	Ultraviolet
VK2/E6E7	Vaginal Epithelium
VOC	Vagina -on-chip

## List of Symbols

°	Degree
°c	Degrees Centigrade
μL	Microliters
μm	Microns
Cm	Centimetre
mL	Millilitres
mm	Millimetres
∅	Diameter
pL	Picolitres



# Chapter 1 - Introduction

Bacterial vaginosis (BV) is the most common vaginal syndrome that affects women of reproductive age between 14-49. Approximately 50% of women from the developing world and 33% from the developed world are affected by this condition on a global basis. It remains a formidable problem in women's genital health as clinicians and microbiologist are yet to fully understand its aetiology. At present, there no effective long-term treatment for BV and the need for a new approach to model and manage BV is necessary, to gain a better understanding of the condition. A new platform, with the ability to mimic the function of the vaginal tissues and sustain the human microbiome will provide researchers and clinicians a working platform to develop new and alternative treatments for BV and to improve female healthcare.

## 1.1 Aim

The aim of this project is to develop a microfluidic device that can mimic the *in-vivo* vaginal tissue, within an *in-vitro* system.

A combination of techniques including 3D printing, electrospinning, and micro engineering will be used to make the Vagina-on-a-Chip (VOC). The purpose of the VOC is to have a realistic platform that represents the human physiology of the vagina, which can be used to study factors that disrupt the vaginal microbiome, understand the interaction between vaginal epithelial cells and bacterial strains. The VOC also has the potential to replace animal testing and provide as a realistic platform that can be used by researchers and clinicians to find better or improved treatment for BV and other pathogens that may affect the homeostasis of the vagina.

## 1.2 Objectives

To fulfil the aim of the project the following objectives were considered throughout the research:

- 1) To develop a 3D microfluidic VOC device.
- 2) To develop a biocompatible membrane to support the growth of squamous epithelial cells.
- 3) To optimise the growth of vaginal epithelial cells

- 4) To evaluate the membranes through mechanical and biological studies
- 5) To integrate the membrane into the microfluidic VOC system.

### **1.3 Description of Chapters**

This section provides a brief description of what each chapter will be discussing throughout the thesis.

- **Chapter 2 Literature review**

This chapter will consist of a thorough literature review on previous systems that have studied vaginal tissue in 2D and 3D systems. An overview of current research done on OOC system and studies related to female health. Methods of fabrication for the microfluidic devices and cellular scaffolds are reviewed.

- **Chapter 3 Design and Microfabrication**

This chapter will cover the steps taken to design and create the VOC platform.

- **Chapter 4 Electrospinning and membrane fabrication**

Chapter 4 describes and explains the process of fabricating the electrospun membrane.

- **Chapter 5 Cell work**

Chapter 5 explains the process taken to culture vaginal epithelium cells and validated using assays and fluorescence microscopy work.

- **Chapter 6 Discussion**

Chapter 6 describes the results from experiments conducted in previous chapters.

- **Chapter 7 Conclusion**

The final chapter will conclude the thesis and identify the contribution to knowledge

- **Chapter 8 Future Work**

This chapter will define the potential future work that can be conducted for further research development of the project.

## 1.4 Background

BV occurs when the natural balance of healthy vaginal microflora with an acidic pH of 3.8-4.5 is disrupted. This occurs due to an overgrowth of anaerobic bacteria including *Gardnerella vaginalis* (GV), *Atopobium vaginae* (AV); and many other anaerobic species and genital mycoplasmas which causes the ecosystem of the vagina to alter, resulting in a more neutral pH of > 4.5 (Boskey, 2005; Bradshaw and Sobel, 2016). BV is known to be a polymicrobial infection that is poorly understood as approximately 400 bacterial species are associated with the infection therefore making it difficult for clinicians and researchers to identify the specific bacterium that cause BV to occur (Easmon *et al.*, 1992).

The healthy vaginal microbiota primarily contains *Lactobacillus* spp. (LB) including *L. crispatus*, *L. jensenii* and *L. iners* (Forsum *et al.*, 2005); these bacteria play a vital role in the hosts defence against pathogens by producing antimicrobial molecules, lactic acid and bacteriocins which help maintain vaginal pH (Truter and Graz, 2013). Vaginal lactobacilli are regulated by hormones circulating through the body which cause the vaginal epithelia cells to produce glycogen. Glycogen has a specific role in inhibiting BV occurrence. Glycogen is metabolised by the LB producing lactic acid which is responsible for normal vaginal acidic conditions (Turovskiy *et al.*, 2012). Hydrogen peroxide produced by LB inhibits bacterial overgrowth and further inhibits bacteria from attaching to the walls of the vagina.

About 50% of women who experience BV are asymptomatic (Hoffmann *et al.*, 2014). Those who are symptomatic experience abnormal watery, thin or greyish colour discharge. There is a noticeable change in the pH of the vagina when BV is present. The vaginal pH increases to pH > 4.5 and in severe cases develop a fishy smelling odour which mainly occurs during menstruation or after having sexual intercourse (Watson, 2019).

Whilst BV is not a sexually transmitted infection (STI), 1 in 3 women will be affected by this condition at some point in their lives as it is associated with sexual behaviour (Truter and Graz, 2013). Women with BV are susceptible to STIs including *Chlamydia trachomatis*, *Neisseria gonorrhoea* and human immunodeficiency virus (HIV) (Gillet *et al.*, 2011). This is due to the depletion of the protective *Lactobacillus* spp. in the vagina. GV was identified as the first pathogenic species to create a polymicrobial biofilm that strongly attaches to vaginal epithelium; this becomes a scaffold for other microorganisms to adhere to (Truter and Graz,

2013). This GV biofilm acts as a barrier that prevents the immune system and antibiotics penetrating and eliminating underlying bacteria. The biofilm is composed of polysaccharides, proteins and nucleic acids, which due to their distinct gene expression and physical structure increases in bacterial resistance to many negative stimuli such as vaginal cream and gels, immune defence and antibiotics (Patterson *et al.*, 2007). This causes the survival rate of GV to increase, even with the presence of LB producing hydrogen peroxide and lactic acid; this results in a high risk of BV reoccurrence and other biofilm related infections.

### **1.5 Contributing Risks Factors**

The cause of changes to bacteria levels in the vagina are unknown but contributing risks factors such as having multiple or changing partners, douching and using scented soaps increase the risk of infection. BV is associated with significant health risks that if left untreated can lead to reproductive and obstetric issues increasing the consequences of pelvic inflammatory disease (PID) which can lead to infertility, premature birth and miscarriages (Gillet *et al.*, 2011; Bitew *et al.*, 2017). A recent study by (Nye *et al.*, 2020) examined whether women with symptomatic BV were at risk of having recurrence with *Mycoplasma genitalium* (MG). MG is an emerging STI known to effect women's health especially in acute or chronic conditions such as PID and premature birth, however it is an infection that is usually underdiagnosed as the pathogen is difficult to culture and is often asymptomatic. As it is associated with non-gonococcal urethritis (NGU) it is possible to detected MG through polymerase chain reaction (PCR) to ensure diagnosis. The study showed prevalence of MG infection was higher in women with vaginitis caused by BV, however, this was indicated independently by Nugent score for MG only and not associated with clinician manifestation of BV. If left untreated, BV would present a significant risk of developing symptomatic MG. It was recommended that, better management of BV would be beneficial to decrease the likelihood of women transmitting and developing pathogenic infections like MG (Nye *et al.*, 2020) which can be difficult to treat and is beginning to show high levels of antimicrobial resistance. Patients with MG are usually given common antibiotics like moxifloxacin to treat the infection by damaging the cell wall of bacteria, however MG does not have a cell wall and therefore such treatment is not always effective (Johnson, 2020).

## **1.6 Physiology of the vagina**

The vagina is an organ that is part of the female reproductive system and is involved in a multitude of functions due to the response of hormonal changes. These changes are experienced throughout a woman's life span, especially during puberty, menstruation, pregnancy and menopause (Gold and Shrimanker, 2019). The vagina plays a vital role during childbirth, intercourse, and female sexual arousal. During childbirth and pregnancy, the vagina is also known as the birth canal which provides a pathway for the mother to safely deliver the baby naturally from the uterus to the outside world.

During childbirth, the vagina is able to expand and stretch to more than three times its normal diameter (Brusie, 2019). During sexual intercourse and sexual arousal, the vagina can increase in length and width of up to 10cm in response to pressure. As the walls of the vagina are made up of an elastic mucous membrane that is able to stretch and contract with the aid of the pelvic muscles to the size of the penis and other objects resulting in sexual pleasure and fertilisation. During menstruation, the vagina acts as a passage for menstrual flow and tissue to leave the uterus.

Another function of the vagina is its immune defence to protect the female reproductive system against harmful pathogens by maintaining a natural balance of commensal bacteria in the vaginal microflora, chemical signalling and maintaining the internal acidic pH environment (Gold and Shrimanker, 2019; Taylor, 2020). As described previously, the normal vaginal flora contains *Lactobacillus* spp., which produce a protective barrier by producing lactic acid and hydrogen peroxide preventing bacteria from attaching to the inner walls of the vagina. Lactic acid helps maintain a low pH in the vagina whereas hydrogen peroxide kills the bacteria; both are important in managing the healthy ecosystem in the vagina (NHS England, 2018)

### **1.6.1 Anatomy of the vagina**

The vagina is a fibromuscular canal about 8cm in length and 3cm in diameter. The upper region of the vagina connects to the cervix (womb) of the uterus leading towards the lower region, vulva the opening of the vagina. The vaginal canal is situated between the urethra and the bladder seen in Figure 1.

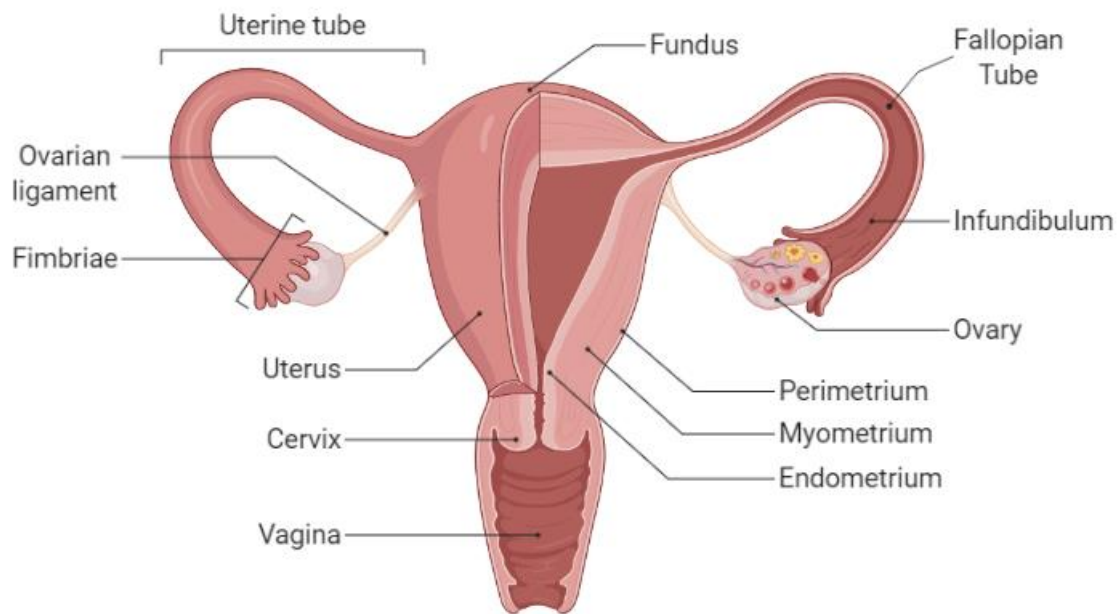


Figure 1 The anatomy of the vagina, created with BioRender.com

The vaginal wall consists of three layers, the mucosa, muscularis, adventitia. The mucosa is composed of a thin layer of nonkeratinizing stratified squamous epithelium that is situated on loose connective tissue known as lamina propria which contains no glands making it flexible (J.Paavone, 1983; Siddique, 2003). However, the mucus that lubricates the vaginal walls is due to the Bartholin's glands located in the labia, outside the vagina ensuring that the area is always moist (NHS England, 2018a).

The vaginal epithelial cells are found in the mucosa layer in the form of folds called rugae which are supported by oestrogen and provides an increased surface area for extension. The second layer, the vaginal muscular, contains smooth muscle made from collagen and elastin that are present as inner circular and outer longitudinal fibres which offers the capacity of the vagina to expand and contract providing support during sexual intercourse and childbirth (Siddique, 2003). Lastly, the outer layer called the adventitia is made up of dense fibroelastic connective tissue which provides the vagina support from its surrounding structures. The outer layer of the adventitia also contains blood and lymphatic vessels, nerves and nerve sensory endings (Figure 1.2).

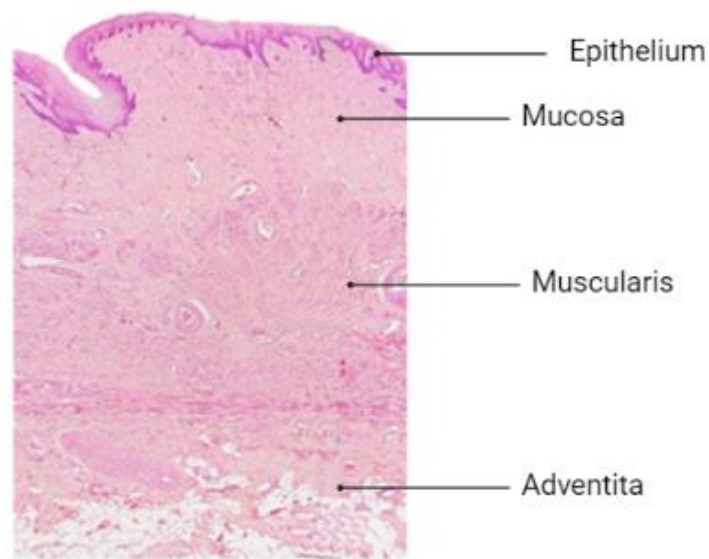


Figure 1.2 Histology image presenting the layers of the vagina (Sugiritama, 2009).

### 1.6.2 Vaginal Microbiota and Acidic Environment

The vagina is a very complex ecosystem which contains approximately 7-9 CFU/ml of *Lactobacillus* spp. in the vaginal fluid (Aleshkin, Voropaeva and Shenderov, 2006). With *Lactobacillus* being the predominant bacteria species found in vaginal microflora is known to be the most aciduric bacteria amongst acidophilic lactic acid bacteria making it thrive in an environment with a low pH of 4 (Vaneechoutte, 2017). The production of *Lactobacillus* spp. changes over a woman's life, at the beginning, a young premenarchal girl's vaginal microbiota is more neutral/alkaline, but as oestrogen levels increase with ovary function the microbiota changes causing the pH to decrease (Devillard *et al.*, 2004). As the vaginal epithelium thickens the level of glycogen builds within the tissue. The *Lactobacillus* spp. metabolise the glycogen and as this breaks down it increases the production of lactic acid resulting in a low pH environment of between 3.8-4.5 (Devillard *et al.*, 2004). The low pH ecosystem helps maintain the natural microflora, protect and prevent disease causing microorganisms to enter the vagina, kill sperm and produce immunological protection against bacterial growth (Gold and Shrimanker, 2019). With the combination of lactic acid and hydrogen peroxide the vagina is also known to be a self-cleansing organ, however contributing risk factors such as douching or washing out the vagina with scented soaps can disrupt the natural balance of microflora causing irritation and an increased risk of infection and syndromes including bacterial vaginosis to occur. (Gordon Betts *et al.*, 2013).

## 1.7 Diagnostic Measurements

In women, the normal healthy vaginal environment consists of having a white discharge, high in viscosity, with a pH of 3.5-4 and presence no odour but these conditions change when the vaginal ecosystem is disrupted by anaerobic bacteria causing syndromes like BV to occur. To diagnose BV, clinicians use two standard methods known as the Amsel's diagnostic criteria and the Nugent scoring system. Amsel's criteria consists of 4 markers (Eriksson, 2011) seen in Table 1.1. If 3 out of 4 markers are consistent with the presence of BV, then this indicates a positive diagnosis.

Table 1.1 Four diagnostic makers for the Amsel Criteria assessment of BV prevalence (Eriksson, 2011).

Diagnostic Markers	Amsel Criteria for the Diagnosis of BV
1	Presence of vaginal discharge – if thin, white/grey discharge coats the vaginal walls.
2	pH of vaginal secretion – if pH of vaginal discharge is >4.5.
3	Whiff test – if by adding 10% of potassium hydroxide solution (KOH) to vaginal discharge produces a fishy smell is which is the usual outcome from vaginal specimen from women with BV.
4	Microscopic examination of vaginal epithelia cells – if >20% of vaginal epithelia cells are surrounded by anaerobic bacteria called clue cells.

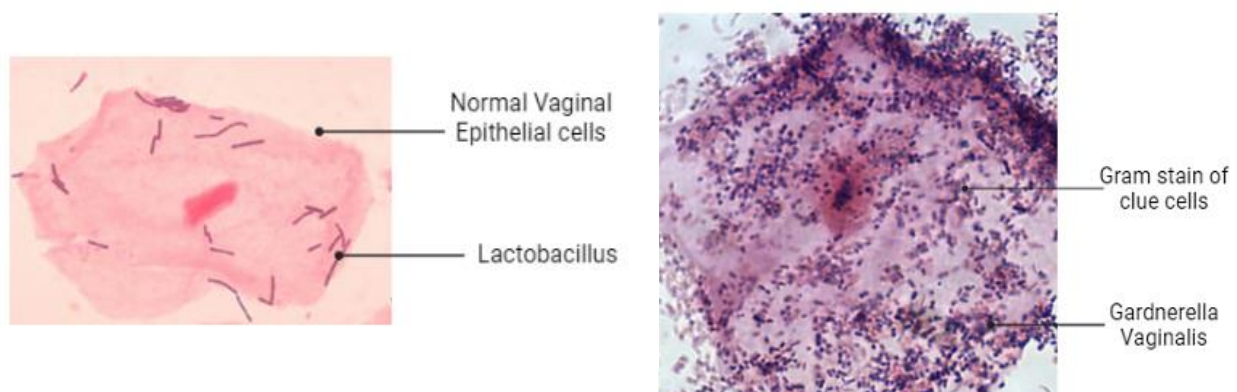


Figure 1.3 Vaginal epithelial cells: (A) Normal vaginal epithelial cells surrounded by the microflora Lactobacillus, rod like shaped bacteria; (B) Vaginal epithelial cells surrounded by bacteria Gardnerella vaginalis forming clue cells is normally found in vaginal samples obtained from women with BV (Todar, 2008).



The Nugent score is a Gram stain scoring system that is used to assess the alteration in the vaginal flora (Sha *et al.*, 2005). Vaginal swabs are used to collect samples to create vaginal smears which are then fixated on microscopic slides and stained for analyses. The Nugent score is calculated by evaluating the presence of bacteria morphotypes which are classified into 3 categories: gram-positive rods, gram-negative coccobacilli form and curved gram-negative rods. Scores of 0-3 is considered normal (*Lactobacillus Spp.*), scores of 4-6 represent a mixture of bacteria and scores of 7-10 indicates the presences of BV (reduction of *Lactobacillus Spp.*) with an increase in other pathogenic bacteria (Martin and Marrazzo, 2016).

### **1.7.1 Treatment of BV**

Women are usually prescribed first line medication which include the choice of antibiotics metronidazole taken orally for 5-7 days or to apply clindamycin vaginal cream/ gel with a cure rate of 60-70% (Thulkar *et al.*, 2010). 50% of women experience reoccurrence within 6-12 months of treatment (Bradshaw and Brotman, 2015b). Studies have been conducted using alternative therapies using probiotics and prebiotics combined with antibiotics were recommended to women with BV to revitalise the native microflora. Although these treatments are promising and have been shown to improve the cure rate of BV in patients, further analysis is required. This is due to the limited evidence showing probiotics provide any real benefit or impact for women with BV (Senok *et al.*, 2009; Huang, *et al.*, 2014; Wang, *et al.*, 2019; van de Wijgert *et al.*, 2020). Senok *et al.*, 2009 and Bradshaw and Brotman, 2015 both expressed the need for a standardised protocol to analyse and evaluate alternative therapies; the effect that probiotics have on patients with BV must be conducted in well-designed randomised clinical trials with a larger patient population for prolonged treatment of 6-12 months.

### **1.8 Limitations of current models**

Several studies have attempted to use nonhuman primates animal models which include the pig tailed macaque, chimpanzees and murine to research and advance our understanding of BV pathogenesis factors that affect the vaginal microbiota, the role of the biofilm, transmission mechanisms and enhancement of other infection (Herbst-Kralovetz *et al.*, 2016). However, these models impede the opportunity to gain a better understanding of the

condition as they do not truly mimic the human vaginal environment. The vaginal environment of these animal models usually have a pH > 5 and differ in the content of vaginal microbiota in comparison to the microflora found in the human vagina (Bradshaw and Brotman, 2015; Herbst-Kralovetz *et al.*, 2016; Martin and Marrazzo, 2016). A study conducted by Johnson *et al.*, 1984 initiated *G. vaginalis* vaginal colonization in pig tailed macaques and chimpanzee models, but these models failed to express clue cells or detect any changes in pH (Johnson *et al.*, 1984). Noticeably it can be difficult to establish the human microbiome in an animal model due to their native microbiome being highly resilient. This will be discussed in greater depth in Chapter 2.

### **1.8.1 Organ - on -chip**

With animal models being expensive and failing to predict human response to new medication as they are unable to mimic human pathophysiology, there is a need to find alternative ways to model human diseases *in vitro* to develop new treatment and personalised medication ( Ingber, 2017). New studies are now being focused on the latest technology, Organ-on-Chip (OOC), where organs of interest are being created using multidisciplinary research and techniques including 3D printing, microengineering and tissue engineering to use small scale tissues to mimic organ like functions. The OOC is designed to provide researchers a potential platform that could replace animal testing and provide a realistic model to capture and monitor the initiation, progression and treatment of a specific disease or syndrome of interest.

## Chapter 2- Literature Review

In this section, a thorough literature review has been conducted on three distinctive areas that are required in order to create an organ on a chip device: cellular/tissue culture, scaffold fabrication and microfluidics. By identifying the knowledge currently available in the literature, the information will then be combined to design and create the VOC.

### 2.1 2D modelling of Vaginal Tissue

The vagina is a complicated ecosystem, however not much is known about the vagina, especially the regulation of microbiological flora. A study done by (Fichorova *et al.*, 2011) observed the novel vaginal microflora colonisation model which provided a new insight into microbicide mechanism of action. To understand how the vaginal microflora regulated the epithelial and bacterial components in order to maintain homeostasis. Human immortalised endocervical (End1/E6E7), ectocervical (Ect1 /E6E7) and vaginal (Vk2/E6E7) cell lines were cultured to compare the physical properties of the monolayers of vaginal tissue to 3D cell culture of VEC-100 tissues, derived from primary human ectocervical epithelial cells. These cells used a permeable membrane to support the 3D culture which resembled the bactericidal and immune properties of normal tissue origin. Both cultures were used to study the effects of bacteria found in women with BV including (*L. acidophilus* and *L. crispatus*).

The aim of this study was to improve the preclinical and phase I safety of women acquiring human immunodeficiency virus (HIV) during phase II and III clinical trials of microbicides. The cultures were exposed to cellulose sulphate (CS) and hydroxyethylcellulose (HEC) to understand how both the vaginal epithelium and microbiome interact with these drugs and why pre-clinical models failed. Overall, the results showed interaction between the drug, epithelium and microflora. The work showed evidence that the microbiome of the vagina regulates the immunity of the epithelial layer (Fichorova *et al.*, 2011).

Another study by Devillard *et al.* examined a novel approach to understanding the vaginal microflora but this time in postmenopausal women under hormone replacement therapy. Devillard *et al.* investigated the use of new molecular technologies to identify vaginal bacterial species. 19 postmenopausal women were provided with oestrogen therapy, and vaginal flora was observed over a period of three months and analysed using polymerase chain reaction

(PCR), DNA sequencing and gel electrophoresis. Oestrogen plays a vital role in menopausal women as it stimulates proliferation of vaginal epithelial cells and produces high levels of glycogen. As discussed in Chapter 1, increased glycogen is broken down by *Lactobacillus* Spp. in the vagina to help maintain pH (Boskey ER *et al.*, 1999). Following menopause, women are more likely to sustain infections that affect the lower genital tract due to a reduction of oestrogen secretion; this further causes the depletion of *Lactobacillus* Spp. which and therefore microorganisms associated with BV and urinary tract infections (UTIs) can colonise (Ginkel *et al.*, 1993).

Medications such as vaginal estriol cream has shown a great impact on restoring the *Lactobacillus* Spp. bacteria and reduce the rate of (UTIs) (Ginkel *et al.*, 1993). Due to the complex anaerobic conditions and nutrients required to grow vaginal microorganisms many microbiological techniques have been used to recover the bacteria, but this has been difficult. However, using PCR and gel electrophoresis has made it possible to identify bacterial composition of the vagina in pre- and post-menopausal women (Burton and Reid, 2002; Burton, Cadieux and Reid, 2003).

Devillard *et al.* 2004 conducted a study to investigate the vaginal microflora in postmenopausal women under hormone replacement therapy to determine the effect of oral intake of hormone replace therapy (HRT) and premarin-conjugated equine oestrogen on the vaginal flora (Devillard *et al.*, 2004). The 19 women who took part in the study did not have a sign of UTI or any other vaginal infections. The women given HRT were observed and swab samples were obtained every 30 days over a period of 3 months. DNA was extracted from the bacteria present on the vaginal swabs and bacterial species were identified following PCR, gel electrophoresis and DNA sequencing analysis. The vaginal flora of all subjects contained *Lactobacillus* Spp., 44% of the samples contained other species such as *Gardnerella vaginalis* and *Escherichia coli* at a low percentage rate. The two main *Lactobacillus* Spp. bacteria found in the samples were *L. iners* and *L. crispatus*. This study indicates that the HRT has shown to maintain a stable environment of vaginal microflora by restoring *Lactobacillus* Spp. to ensure a healthy vagina for menopausal women, as well as reducing the risk of urogenital infection (Devillard *et al.*, 2004).

Bradshaw and Brotmans' review on 'Making inroads into improving treatment of bacterial vaginosis – striving for long term cure' expresses the fact that BV is a common vaginal infection that affect women on a global basis and is understood to be an enigma in women's health due to its unknown aetiology. BV is known to affect women during pregnancy i.e., low birth weight and miscarriages. Though BV is not classed as a sexually transmitted infection (STI), it is associated with STIs due to its high prevalence rate. This review also discusses the function of *Lactobacillus* Spp. microbiota and other bacterial species found in the vagina and how clinicians are determined to find a long-term cure for this condition to improve women's health. The aetiology and pathology of BV is not yet fully understood however, the depletion of *Lactobacillus* Spp. microbiota increase the prevalence of BV to occur. "*Most vaginal Lactobacillus* Spp. provide broad-spectrum protection against pathogens through production of potent antimicrobial molecules, bacteriocins and lactic acid" (Aroutcheva *et al.*, 2001; Boskey *et al.*, 2001; Donia *et al.*, 2014).

It is still unknown what causes the recurrence of BV whether, due to the current antibiotics or other external factors like douching or being reinfected through STI (Ness *et al.*, 2002). Figure 2.1 presents the potential strategies that can be used to reduce the likelihood of BV recurring. It also depicts what causes BV to reoccur, for example, women who are affected by BV are prone to being infected with an STI, especially those who have multiple sexual partners over a lifetime (Fethers *et al.*, 2008). Overall, the article concludes that there have been no advances for new treatments to improve the cure rate for BV. Recent studies have only just started to understand the environment of the vagina and the importance of vaginal microbiome and how the changes within its composition can affect women's health (Bradshaw and Brotman, 2015a).

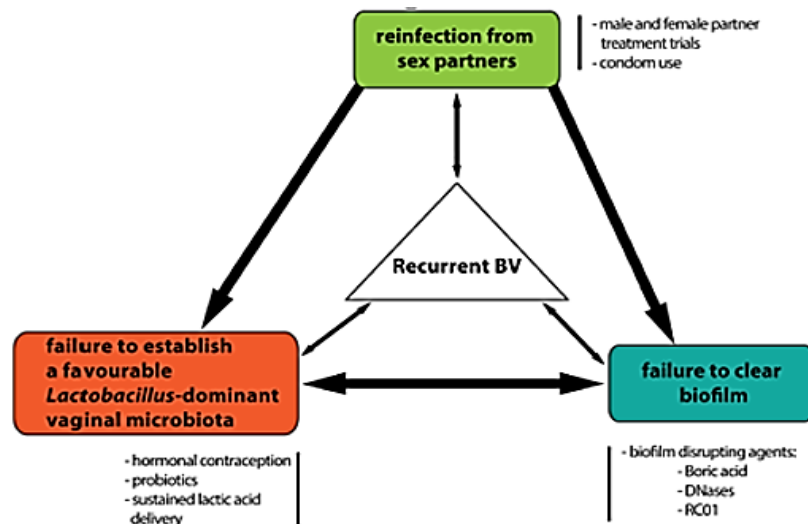


Figure 2.1. Causes of recurrent of BV and potential strategies to reduce its prevalence (Bradshaw and Brotman, 2015a).

Bradshaw and Brotman clearly state that clinicians and researchers are making the need for a new system that would be able to manage BV, find better treatment and develop effective prevention strategies to reduce the recurrence of any BV associated conditions as a priority (Bradshaw and Brotman, 2015a).

A study by Gilbert et al. (2013) observed the clinical features of BV in a murine model of vaginal infection with GV. BV, a dysbiosis of vaginal flora is characterised by the shift in balance of dominating *Lactobacillus* Spp. replaced by a polymicrobial mixture of anaerobic bacteria and Gram-negative bacilli (Gilbert *et al.*, 2013). Women with BV are prone to STIs and can experience adverse effects during pregnancy such as premature birth. Furthermore, several bacterial species are associated with BV the causes of the condition through biochemical, cellular and clinical features remain elusive. GV, the most frequent bacterial species isolated from BV patients is also known to be the first bacterium implicated in the pathogenesis of BV which causes cytolytic toxin production and the formation of biofilm (Gilbert *et al.*, 2013). The most important diagnostic feature of BV through culutre is the presence of clue cells, this is when bacteria associated with BV such as GV coat or interact with the vaginal epithelial cells.

Vaginal samples from women with BV have indicated bacteria adhering to the surface of the cells. In order to understand whether *G. vaginalis* plays a vital role in initiating clue cells, a murine model, displaying BV characteristics was used to examine the GV vaginal infection.

The murine vaginal infection model demonstrated that GV was adequate in causing BV phenotypes suggesting that this particular bacterial species contributes to the aetiology of BV. The study compared clinical specimens from women with BV against the murine model which revealed vaginal epithelial cell exfoliation and bacterial adherence to the vaginal epithelial cells in comparison to specimens with normal flora. It was also noted that the murine model expressed similar phenotypic features parallel to human BV making the system an ideal experiment tool that has the potential to gain a better understanding of the role GV plays in the vagina ( Gilbert *et al.*, 2013).

In the study done by (Rosa R. Yu, *et al.*, 2009) the vaginal *Lactobacillus* Spp. colonisation and live microbial environment was investigated using a Chinese rhesus macaque (*Macaca mulatta*) model. The study was conducted to establish a model that would closely relate to human physiology and sensitive to mucosal HIV infection. Due to the depletion of vaginal lactobacilli, the vagina is prone to bacterial infections and increases the risk of acquiring other conditions such as HIV and herpes simplex virus type 2 (HSV-2). Amongst the animal models used which include rats, mice, dogs, hamsters and guinea pigs it has been reported that these models contain a low number of vaginal lactobacilli compared to the vaginal flora found in women at the reproductive age, and therefore are not suitable for such studies regarding the microbial environment of the vagina.

Though these animal models have been used in previous studies, they unfortunately do not accurately mimic the human female lower reproductive tract as they have an oestrous cycle, as well as reproductive physiology and anatomy differ from that of humans (Pot *et al.*, 1993; Patton *et al.*, 1996; Noguchi K, Tsukumi K, 2003; Poonia *et al.*, 2006). The aim of the study was to select an animal model that expresses similar characteristics to human physiology, the Chinese rhesus macaque was selected as its reproductive system shares many similarities to the human reproductive system. The model was developed to test colonisation, efficacy and the safety of a new biological approach, that would use a 'live' recombinant human vaginal *Lactobacillus* Spp. to test topical microbicides against mucosal transmission of pathogen in the vagina (Rosa R. Yu *et al.*, 2009).

To develop the macaque model for examining *Lactobacillus* Spp. based microbicides, microflora samples were obtained from both the vagina and rectum of 13 female Chinese rhesus macaques and analysed with cultivated bacteria recognised by 16S rRNA gene

sequencing. It was reported that 12 out of 13 macaque models maintained a large number of lactobacilli colonies with *Lactobacillus johnsonii* being the predominant species. *Lactobacillus Spp.* derived from the vagina and rectum of the same model presented different genetic and biochemical profiles indicating that microflora from the rectum may not be a reservoir for harbouring endogenous vaginal *Lactobacillus Spp.* Vaginal flora found in healthy women of child bearing age is normally dominated by *Lactobacillus acidophilus* complex which contains six distinct species: *L. acidophilus*, *L. crispatus*, *L. gasseri*, *L. gallinarum*, *L. amylovorus*, and *L. johnsonii*. (Johnson *et al.*, 1980; Lauer, Helming and Kandler, 1980; Fujisawa *et al.*, 1992; Zhou *et al.*, 2004).

Through molecular techniques, *L. gasseri*, *L. jensenii*, *L. crispatus*, and *L. iners* have been indicated to be the dominating *Lactobacillus Spp.* found in the human vagina of reproductive women. The interesting discovery of finding *L. acidophilus* complex in the vagina of macaque models suggested that the microenvironment is similar to that of the human vagina and therefore having the ability to maintain the growth of vaginal lactobacilli. Due to the similarities between the rhesus macaque and human vaginal microflora this animal model has shown good potential in offering support for pre-clinical evaluation of safety and efficacy of the *Lactobacillus Spp.* based microbicides. Animal testing is however costly, has ethical problems, and can never fully replicate the human vagina and associated microbiome.

### **2.1.1. 2D vs 3D cell culture**

Two dimensional (2D) cell culture is the most common *in vitro* technique used to biological experiments and often used to improve our understanding of cell interactions, tissue morphology, mechanism of diseases and response to drug treatment (Kapałczyńska *et al.*, 2018). In 2D adherent cell culture, cells are normally grown in plastic culture flasks or petri dishes where cells cultivate as monolayers and adhere to the surface Figure. 2.2. Researchers generally use this technique due to its simplicity, cost effectiveness and ease of observation for results analysis. Many studies have been done on 2D cell culture making it easier to compare results from previous literature (Khoruzhenko, 2011). However, there are limitations to 2D cell culture as this method does not truly represent how cells grow and function in the human body. Cells in the human body experience mechanical forces of stress, strain, shear,



gravity, tension and compression on a daily basis which, cells grown in 2D are not exposed too.

2D cell culture is normally used to test new drugs in the pharmaceutical industry, but due to lack of predictivity can lead to an increase failure during clinical trials and cost for the development of new drugs (Khoruzhenko, 2011). Though 2D cell culture is a simple and easy process where cells are grown within a controlled environment, cells must be well maintained to avoid contamination. Cells are fed growth media which contain vital nutrients for cells to grow, but as the media is consumed by the cells, cells also release waste products making the environment toxic causing cell death and reduction of nutrients

3D cell culture is a method that is not as commonly used as 2D cell culture but is a technique that better represents human tissue *in vitro*. Growing cells in 3D has the ability to exhibit how cells behave in response to diseases and treatment. These biomimetic tissue models provide an accurate representation of *in vivo* scenario in this case physiology, structural complexity, cell to cell interactions and establishing a homeostatic environment for a specific length of time . 3D models are sometimes linked with microfluidics which increases the complexity of this system. The integration of flow is crucial for all functioning tissue which enables cells to communicate through differentiation and metabolic adaptation. Microfluidics allows for the continuous supply of nutrients distributed to cells, supporting growth to emulate *in vivo* tissues.

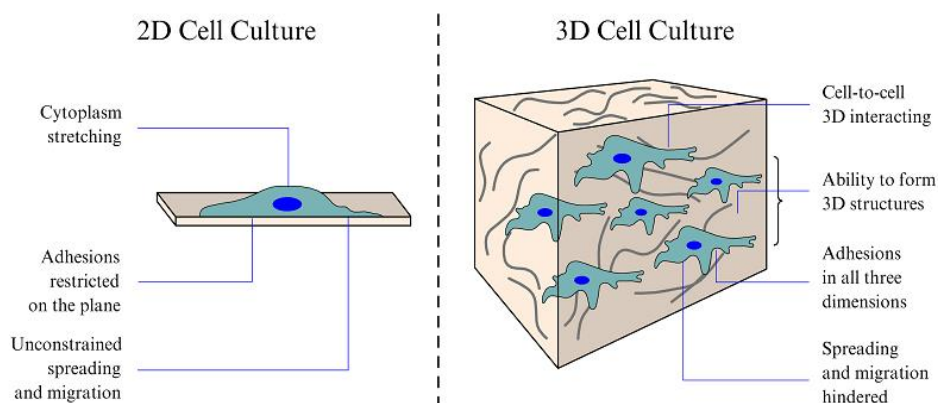


Figure 2.2. Comparison between 2D cell culture and 3D cell culture highlighting the key difference when growing cells in 2D environment in comparison to cells growing in a 3D matrix (Ustyugov et al., 2018).

With such models being available, they have the potential to replace animal testing and provide a realistic solution to understanding diseases and responses to new drugs and treatment in an efficient way. However, 3D cell culture models can be expensive, time consuming and complex in nature making it difficult to analyse results. For example, microscopic analysis can become difficult due to their large scale. Needless to say, this method has potential in biomedical research to offer a greater understanding of cell culture in a profound and realistic way.

## **2.2 3D modelling of Vaginal tissue**

The vaginal epithelium is characterised by sheets of stratified squamous epithelial that express tissue-specific proteins, produce mucus glycoproteins and support enzymatic and pathological defence. The cells also exhibit morphological structures which include, cell to cell adhesion features, microfolds and micro-ridges (Fichorova, Rheinwald and Anderson, 1997; Hjelm *et al.*, 2010). The cells play a vital role in the immunological response to pathogens through toll-like receptors (TLR) which produces cytokines, chemokines and signalling pathways (Fichorova and Anderson, 1999; Quayle, 2002; Herbst-Kralovetz *et al.*, 2008). It is these physiological attributes of the vaginal epithelial cells that are required to develop a 3D model which can be used to study syndromes and infections that affect the vagina along with further treatment.

A study done by Hjelm, *et al.*, (2010) developed an *in vitro* 3D organotypic human vaginal epithelial cell model using the rotating wall vessel (RWV) bioreactor technology which managed to capture the *in vivo* environment, structural and functional properties of vaginal epithelial cells which exhibited stratified squamous epithelia with microvilli, microfolds and tight junctions. The 3D model was used as a platform to carry out toxicity tests of microbicides targeting STI infections, replacing existing system such as surgical explants and animal models (Hjelm *et al.*, 2010).

To develop the organotypic human vaginal epithelial cell model the human vaginal cells were grown on porous collagen coated microbeads cultivated in the RWV bioreactor rotating under a low fluid shear conditions which created 3D vaginal epithelial cell aggregates. The experiment was carried out in 2 stages, early and late development. After 1-21 days in the rotating culture scanning electron microscopy (SEM) presented monolayer of vaginal cells on

the microbeads during early development as shown in Figure 2.3. Cells at this time point varied in size and presented convex apical cell shape with light microvilli structures.

After 39-42 days cells SEM and transmission electron microscopy (TEM) were used to confirm surface morphology presenting differentiation and polarisation of 3D vaginal epithelial cell aggregates during late development. The aggregates were densely packed with microvilli at different lengths, vaginal microfolds known as rugae and micro-ridges as well as secretory vesicles of mucus/deposits between adjacent cells on the apical cell surface which can be seen in Figure 2.4 (Hjelm *et al.*, 2010). With this model being able to produce 3D cell culture expressing *in vivo* like structures it was considered that it would be used as a potential platform to screen microbicide compounds and improve safety as an effective early clinical study.

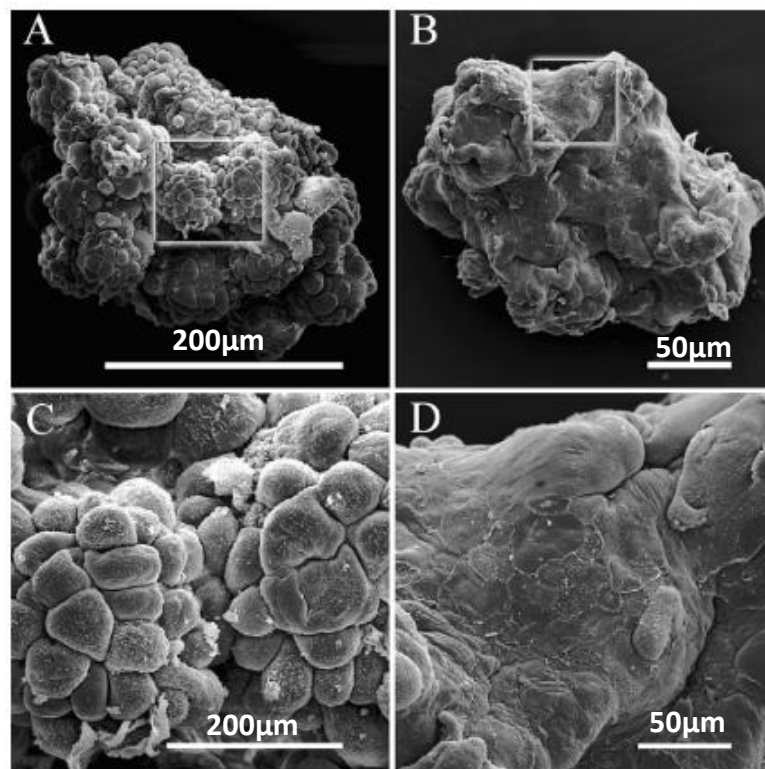


Figure 2.3. SEM presenting the 3D organotypic vagina epithelial cell model, (A) presents single layer of vaginal cells after 19-21 days during early development a low magnification;(B) Low magnification SEM of multiple layers of flattened vaginal cell layers after 39-42 days during late development (C); high magnification of boxed area in (A) and (D) high magnification of boxed area in (B) (Hjelm *et al.*, 2010).

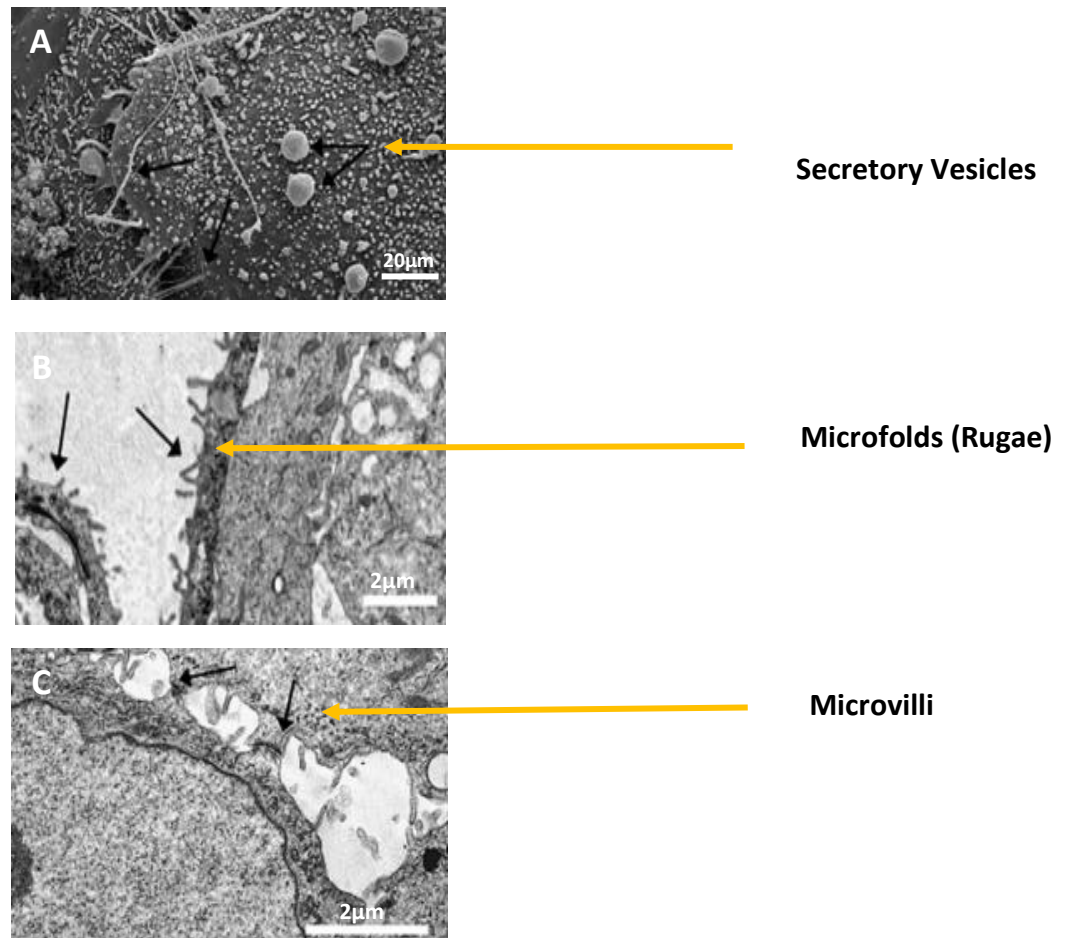


Figure 2.4. Presents the physiological structures of vaginal cells from the 3D model A) SEM of secretory vesicles (B) TEM of microfolds (rugae) indicated by the arrows and C) TEM of long microvilli on adjacent walls. Scale bar (A) 20 μm (B & C) 2 μm (Hjelm et al., 2010).

Another study by Łaniewski et al. (2017) developed a human 3D endometrial epithelial cell model to study host interactions with vaginal bacteria and *Neisseria gonorrhoeae* (Laniewski et al., 2017). This model was created again using the RWV bioreactor technology (Radtke and Herbst-Kralovetz, 2012) with the previously established endometrial epithelial cell line HEC-1A. This cell line was isolated from a patient in 1968 with stage 1A endometrial cancer (Kuramoto, Tamura and Notake, 1972). Cells were first cultured as monolayers in flasks before being transferred to the RWV bioreactor which contained porous collagen coated microcarrier beads. Cells were rotated under a low fluid shear microgravity environment which maintains the cells in free fall. This allows the cells to attach to the microbeads which act as a scaffold for them to form 3D aggregates (Figure 2.5).

The endometrial epithelial cell (EEC) model demonstrated complex structures and functions including cell differentiation and microvilli as well as membrane associated mucins and TLRs.

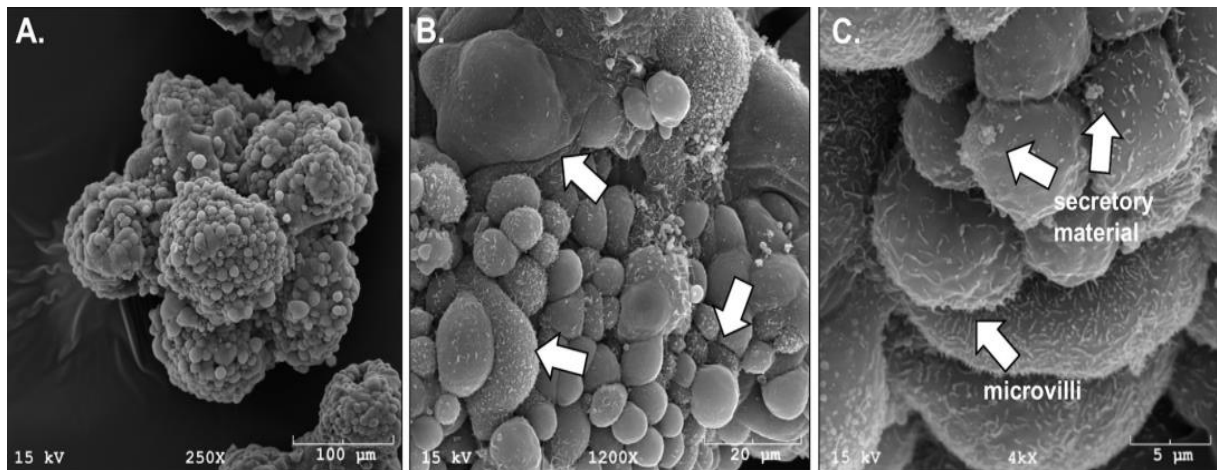


Figure 2.5. Presents SEM of structural characteristics of endometrial epithelial cell aggregates on the EEC model after 21 days at magnification of x250, x1200 and x4000 respectively. (A) Microbeads covered in single layer of endometrial epithelial cells; (B) The white arrows indicates cells proliferation at different stages and the microvilli present on the cell surface; (C) The while arrows highlighting the microvilli and secretory/mucus material visible on the surface of the cells (Laniewski et al., 2017).

The EEC model was exposed to native and pathogenic bacteria to conduct infection studies. Three bacterial species were derived from the vagina, cervix and the uterus; *L. crispatus* the common bacterial species found in the microflora of the vagina, Figure 2.6. GV a predominant bacterium associated with BV and *Neisseria gonorrhoeae* a bacterial species responsible for sexually transmitted gonorrhoea (Laniewski et al., 2017). The EEC model is known to be one of the first reported bioreactor models using this particular cell line to study host interactions with human EEC. From the infection studies the results demonstrated all that vaginal bacterial species and *N. gonorrhoeae* had formed colonies on the EEC aggregates. Gonococci was reported to produce dramatic changes in morphology to the cortex of the epithelial cells.

The EEC model is one of the first 3D bioreactor models to use this particular cell line to study host interactions with human EEC and to present bacterial colonies interacting with 3D cells at their crevice and folds; which can not be captured using traditional 2D cell culture. Overall, from the experiments conducted in this study it was concluded that the EEC is a robust working 3D model that has the potential to be used as a research tool to challenge the system with microbials to achieve a better understanding of the host immune response (Laniewski et al., 2017).

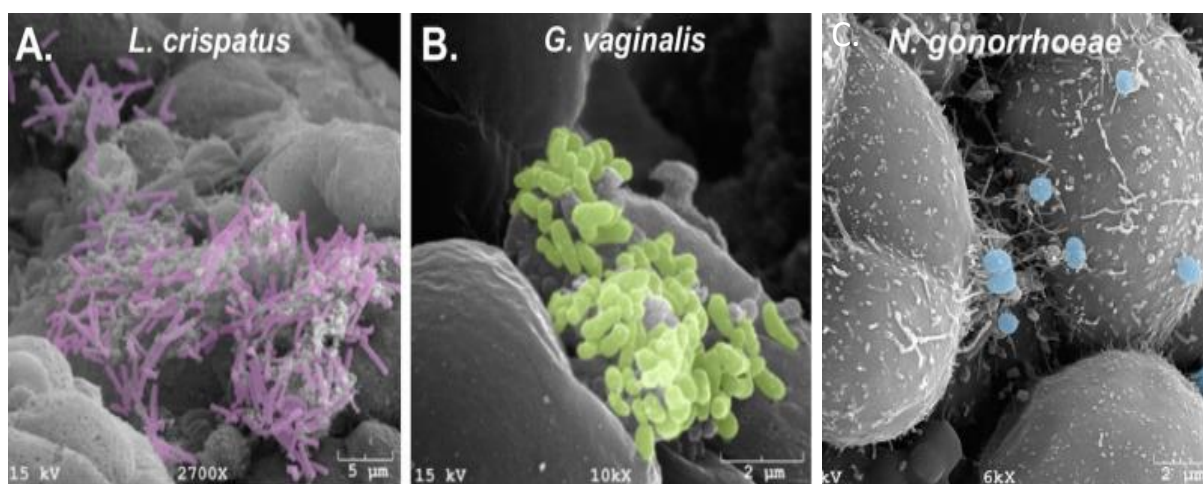


Figure 2.6. SEM of vaginal bacterial species and *N. gonorrhoeae* effectively colonising in the 3D endometrial epithelial cell model. The EEC model was infected for 24 hours with (A) *L. crispatus* VPI-3199; (B) *G. vaginalis* JCP8066 and (C) *N. gonorrhoeae* MS11 which showed the characteristic morphologies of each bacterium attaching to the surface of the EEC aggregates. Photoshop CS51, Adobe was used to colour the bacteria (A) *L. crispatus* in purple; (B) *G. vaginalis* in green and (C) *N. gonorrhoeae* in blue (Laniewski et al., 2017).

RWV bioreactor technology is a useful method that captures the *in vivo* structural and functional properties of cells of interest by maintaining cell suspension through slow rotation. The model provides cell aggregates in 3D, closely resembling native tissue but experience minimal mechanical forces. Therefore, it does not truly represent or replicate how cells normally grow in the human body and the mechanical forces they experience on a daily basis. In order to improve this method, mechanical forces must be considered to mimic the *in vivo* conditions. An alternative method organ-on-chip has taken this into consideration, it has the ability to mimic the function of an organ of interest with the mechanical forces being applied to replicate the corresponding environment.

### 2.2.1 Organ-on-a-chip

Organ-on-a-chip (OOC) is a new microfluidic method that is evolving in the biomedical engineering field. It is an alternative method to understanding human disease *in vitro*, helping to reduce the use of animal testing. OOCs are bioinspired microdevices that can mimic the whole human organ function and potentially replace animal testing. These devices can be used by researchers to model diseases and develop new drugs to improve healthcare at a low cost. An OOC is multichannel 3D microfluidic cell culture chip that has been designed to recreate the functional unit of an organ or organs to mimic the biochemical, mechanical and physiological aspects that cells experience in *in vivo*.

Donald Ingber's group at the Wyss Institute research, Harvard university have created various OOCs that include the lungs, kidneys, skin and bone marrow as seen in Figure 2.7. The group has developed an automated instrument that links to multiple OOCs via common microfluidic channels. The device has been designed to mimic the human body, control fluidic flow and cell feasibility allowing for real time observation of cell culture and interconnected biochemical, biomechanical and physiological properties. This new system is called the body-on-a-chip which has the ability to respond to new drug development providing a platform for testing as well as ensuring the efficacy and safety of the drugs (Human Organs-on-Chips, 2017).

To create the human-on-a-chip, each device was fabricated using a clear flexible polymer that contained hollow microfluidic channels lined with living human cells depending on the organ on interest; this was interfaced with human endothelial cells to create an artificial vascular system. In order to mimic similar physical microenvironment that cells experience under normal circumstances, mechanical forces were applied to the system establish breathing motion for the lungs and peristalsis like deformation for the intestine.

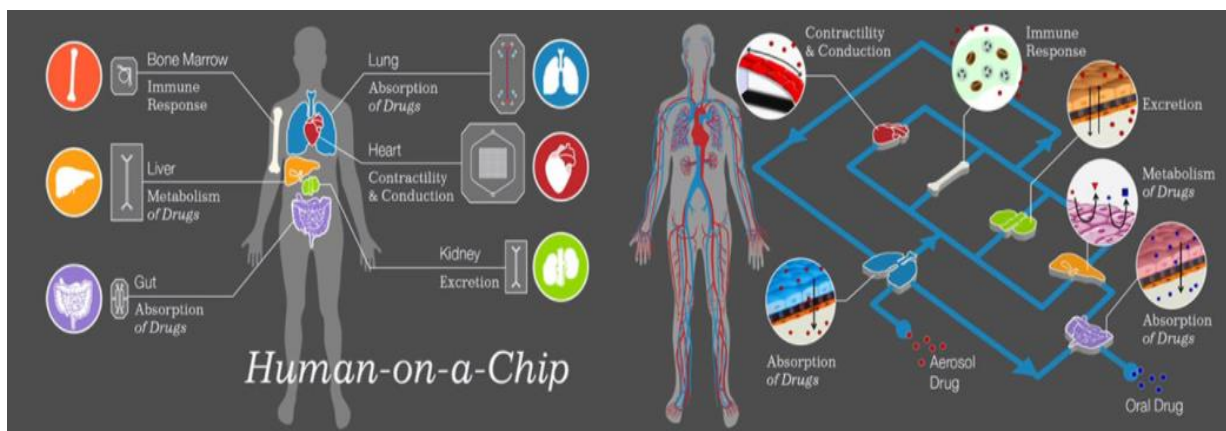


Figure 2.7. Schematic drawing of Human-on-a-chip and how each chip is interconnected. Each chip has been designed to mimic the organ level functions ( Ingber, 2017).

A study by Huh et al. in 2013 observed the evolution of OOCs. This describes OOCs as micro engineered biomimetic systems that provide a platform for the mimicry of a living organs combined with microfluidic channels to replicate a functional unit. These microdevices can be used to test new drugs and create realistic *in vitro* models to study various diseases. Huh created the lung-on-a-chip device where microfabrication techniques were used to develop the first model.

The design was inspired to capture the mechanism of breathing in the human lungs by producing alveolar air sacs, which induces filling of the lungs with air and stretching of the alveolar epithelium and then compared to the vascular endothelium in the surrounding capillaries (Huh *et al.*, 2013a). Two parallel elastomeric microchannel layers were fabricated with dimensions of 400  $\mu\text{m}$  wide x 100  $\mu\text{m}$  high and separated by a thin (10 $\mu\text{m}$ ) flexible porous membrane made from Polydimethylsiloxane (PDMS) (Huh *et al.*, 2010). Huh *et al.* chose these specific dimensions for the channels to resemble the average diameter of an alveolus in the human lungs. The membrane was then coated with extracellular matrix (ECM) collagen or fibronectin to support the growth of human alveolar epithelial cells on the upper channel and pulmonary microvascular endothelial cells on the lower channel for 5 days to form monolayers on either side of the membrane.

During the cell culturing process, the channels provided nutrient flow to the cells and metabolic waste was removed. Once cells had reached confluence, media was removed from the upper channel to form an air-liquid interface on the surface of the alveolar epithelium which stimulates cell differentiation and express tissue specific functions. During this stage media continued to flow in the lower channel mimicking the dynamic flow in the pulmonary capillary blood vessels which provided oxygen and nutrients to the epithelial layer via the endothelium.

To create the breathing functionality on the chip to mimic the mechanically active alveolar-capillary interface of the human lungs, hollow vacuum chambers surrounded either side of the of the membrane and vacuum pumps were used to stretched and relax the PDMS membrane containing both the epithelial and endothelial monolayers (Figure 2.8). This produced a cyclic suction which replicated the rhythmic breathing momentum similarly observed in the air sacs of living human lungs (Huh *et al.*, 2013a).

Fabricating the microdevice took around 3.5 days. The device was able to reproduce complex organ level including the responses to bacteria and inflammatory cytokines in the alveolar spaces which cannot be monitored in conventional *in vitro* cultures. With this approach Huh *et al.* 2013 further developed a nanotoxicology model to evaluate the effects of breathing nanoparticle toxicities and extra pulmonary absorption which was not possible using static cultures. Furthermore, OOC microdevices have shown their capability in providing an alternative solution to conventional cell culture models, replacing animal models and



reducing the cost of clinical trials for screening of newly developed drugs and toxicology applications (Huh *et al.*, 2010).

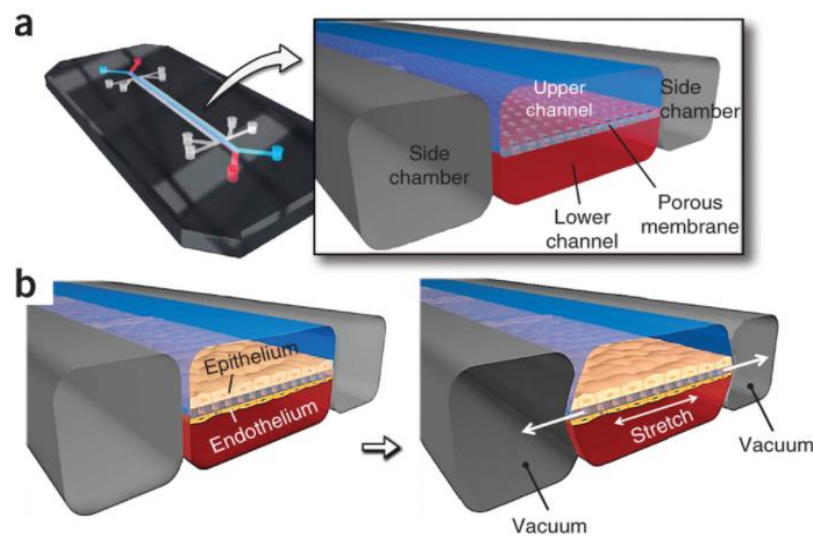


Figure 2.8. (A) multi-layered lung-on-a-chip microfluidic device (B) two cell cultured layers separated by a porous PDMS membrane. Vacuum chamber on either side allows the membrane to be stretched (Huh *et al.*, 2013)

The Gut-on-a-Chip was developed using the same approach by Bein *et al.* 2018 to investigate the human intestinal physiology and pathophysiology. The human intestines are responsible for many functions in the gut which includes digestion, secretion, absorption and motility. The intestine provides a protective epithelial layer between the digestive environment and the rest of the body. The intestine is known to regulate systematic physiology by metabolising drugs and communicate with other organs like the liver and pancreas through a portal flow.

The intestinal microflora plays an important role in maintaining the homeostasis of intestinal health and immune modulation. Analysis of gut microbiome interacting with human intestinal cells have been limited due to the difficulty in co-culturing microbes found in gut with intestine epithelial cells for more than 1 day through conventional cultural models or organoid models.

The gut-on-chip was fabricated in a similar way to the lung-on-chip. The microdevice contained 2 hollow microfluidic channels with dimensions of less than 1mm wide in order to support laminar flow of nutrients to cells during culturing process. The channels were again separated by a porous membrane made from PDMS at thickness of <math>20\mu\text{m}</math> (Figure 2.9). The membrane was coated with ECM to support the growth of the intestinal epithelium on the upper channel and capillary endothelium on the lower channel to re-create the intestinal tissue-tissue interface. The membrane is surrounded by 2 hollow channels on either side to

which vacuum cyclic suction is applied in order to stretch and relax the membrane with adherent intestinal epithelial cells. This was done to replicate the mechanical forces cells experience during peristalsis (Bein *et al.*, 2018).

Under these conditions the human Caco-2 intestinal epithelial cells were able to form villus and produce mucus inside the dynamic platform. With the continuous flow of nutrients provided to the cells and the formation of villi and mucus, the platform provided the opportunity for co-culturing cells with commensal microbes for example *Lactobacillus rhamnosus* which was applied into direct contact with the epithelial cells through the upper channel for 5 days (Bein *et al.*, 2018).

The interaction of *Lactobacillus rhamnosus* did not compromise the integrity of the barrier of the intestinal cells. From this the gut-on-chip showed that it was possible to co-culture cells with natural microflora expressing similarities to normal human ileum.

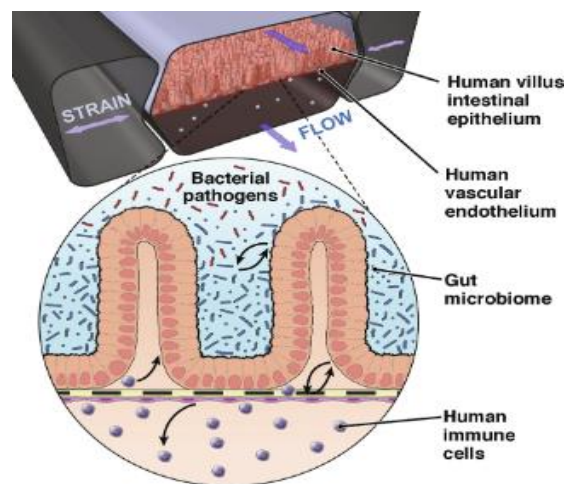


Figure 2.9. A multi-layered Gut-on-chip microfluidic device constructed with two cell cultured layers separated by a porous PDMS membrane lined with human villus intestinal epithelium and human vascular endothelium under fluid flow and peristalsis like strain forces on either side of the membrane. (Bein *et al.*, 2018).

The chip was used to understand the complex immune microbiome inflammatory interactions and chronic inflammatory diseases e.g., inflammatory bowel disease (IBD). With the ability to express organ like functions, the gut-on-chip provides researchers with a new insight to understanding the biological, chemical and mechanical properties within the intestinal microenvironment its structure, function and physiology of living human intestines. The model also offers a new approach into developing personalised medication (Bein *et al.*, 2018).

### 2.2.2 Female reproductive OOC systems

Many OOC devices have been developed as discussed previously, there is some research into the female reproductive system. Recent studies done by Woodruff's group focus on understanding women's health with more knowledge by studying the female reproductive system in further detail including blood clots and production of hormones that affect the body to sexual health (Woodruff, 2013b).

Limited knowledge can be derived from examining conventional cell culture and animal models. This encourages the need for a new model that can be used to analyse how the reproductive system works and eventually be used as a testing platform for the development of new drugs for better treatment to improve female healthcare.

A 3D model of female reproductive system is under development by Woodruff's group. The systems goal is to amalgamate the reproductive organs into a network system to form a chip called FemKUBE, Figure 2.10. The device contains the main reproductive tissue that make up the female reproductive system, "*ovarian follicles, fallopian tube, uterus, endocervix, and ectocervix*" (Woodruff, 2013b)

The group has established 3D cell culture using the steroid hormones oestrogen and progesterone, this allowed the device to mimic menstrual cycle which no *in vitro* assessment has ever accomplished. A new microfluidic device has also been created for ovarian follicles which *in vitro* creates the menstrual cycle over 28 days. Both these platforms will lead to establishing a full system that can mimic the whole female reproductive system (Woodruff, 2013b)

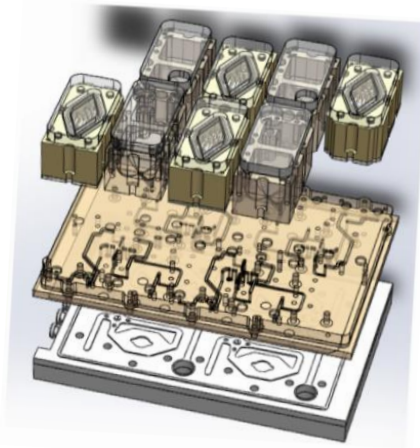


Figure 2.10. Draper microfluidic platform FemKUBE. The bottom layer consists of air channels which controls the flow of media through the middle layer. The media is transported to the top layer where chamber house cell culture or with fresh media and used media for experimental analysis (Woodruff, 2013b).

Woodruff has also recently developed the EVATAR which is a small device that depicts the female reproductive tract and the liver on an interconnected microfluidic chip. The platform contains 3D models which sustain five different tissues working together which include the ovaries, fallopian tube, uterus, cervix, vagina and the liver. A specifically formulated fluid which acts as blood is pumped through the system to the organs allowing each tissue to communicate with one another via secreted substances such as hormones. With this functionality the platform is able to resemble how different organ tissue would normally work together in the human body (Woodruff, 2013a).

The EVATAR was designed to study endometriosis, fibroids and cancers that affect the female reproductive system as well as be used to evaluate and test the development of new drugs. Woodruff states that previous studies were inhibited as each organ required its own specific media, therefore a universal media was developed; the media has similar properties to blood.

Applying this blood like media to the platform allowed tissues to communicate through the media. To conclude with the development of such a platform that closely represents the female reproductive system the EVATAR provides researchers the opportunity to study and gain a better understanding of the basic hormonal and cellular function in the reproductive tract. Furthermore, the platform will be used to understand various types of cancers, STIs and benign tumours that affected the female reproductive system.

The addition of a liver-on-a-chip within the platform allows the device to monitor how drugs affect women in response to hormonal levels. The main goal for the EVATAR is to eventually

be combined with the human on a chip platform to make one integrated system that can then be used to evaluate the effects of drugs on the modelled human body before performing clinical trials with human participants (Figure 2.11)(NIH, 2017).

As seen in Figure 2.11 the EVATAR platform is an open compartmentalised device designed for different tissues of the reproductive system to communicate with each other in order to understand hormonal changes and cellular functions. Building on their research, the VOC platform will be designed to mimic the function of the vagina in an enclosed microfluidic chip. Microflora of the vagina will be introduced to the VOC platform to establish the vaginal microbiome environment. The purpose of the VOC is to achieve a realistic model of the human vaginal ecosystem to study interactions between cells and bacterial strains. This approach has the prospective to gain a better understanding of BV and other pathogens that may affect the vagina as well as have a research tool to develop new and effective treatment for BV to improve female healthcare.

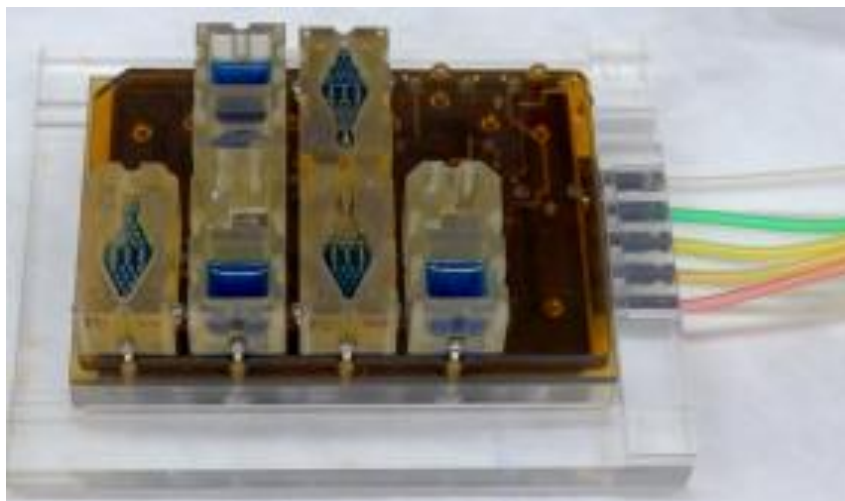


Figure 2.11. EVATAR, a microfluidic representation of the female reproductive tract that contains compartments with different 3D cells culture from the ovaries, uterus, and the vagina. The liver is also included for the purpose of evaluating hormonal levels in response to drugs (Xiao *et al.*, 2017).

## 2.3 Scaffold Fabrication

There are many techniques have been used to fabricate scaffolds for OOC devices which include photolithography, soft lithography, electrospinning, bio-plotting and 3D printing.

### 2.3.1 Photolithography

Photolithography sometimes known as optical lithography or UV lithography is a common process used in microfabrication to pattern designs onto a thin film called a silicon wafer or

other suitable substrates. Light is used to transfer specific geometric patterns via a photomask or an optical mask onto a photosensitive chemical photoresist spun on top of the wafer or substrate. The photoresist is exposed to UV light to create the specific pattern for example a microfluidic channel. The photoresist then undergoes a series of chemical treatments which etches the patterns on to the material or deposits new material onto the pattern of interest depending on the material placed under the photoresist. SU-8 is a common material used to fabricate microfluidic channels; un-crosslinked SU-8 is dissolved in a developer. Once the SU-8 mould is fabricated on a silicon wafer, it can be used repeatedly to fabricate several replicates of the design depending on the purpose of application. Though the process is well known it is a technique that requires specialised and expensive equipment, is time consuming and involves working with highly toxic chemicals. Even with these limitations it is still a technique that is commonly used especially in OOC application due to its ability to capture small intricate detail (Figure 2.12) (Pleil, 2009).

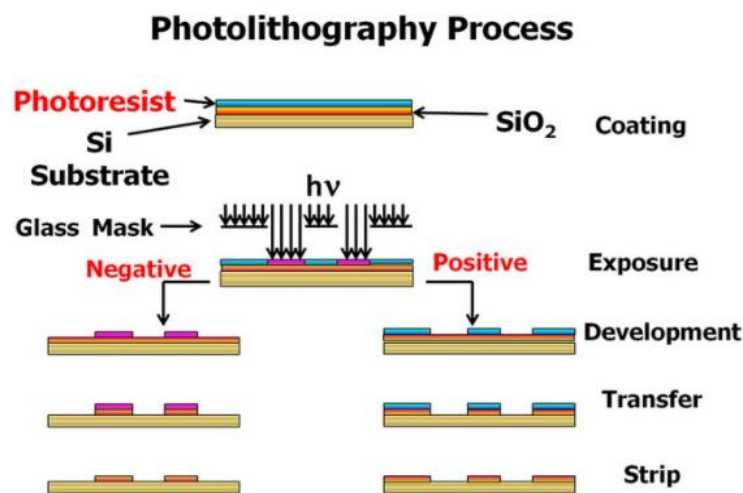


Figure 2.12 Presents the step by step process conducted in Photolithography to create precise and small masks known as SU-8 wafers for microfabrication applications (Verma *et al.*, 2013).

Photolithography is the most common method used to create moulds for OOC fabrication to form porous membranes made from PDMS. Huh *et al.*, created flexible PDMS membranes for the lung-on-chip and gut-on-chip in which PDMS was poured onto the silicon master (SU-8 wafer) that contained an array of microfabricated circular pillars with dimension of 10 µm in diameter and 30 µm in height. PDMS was carefully poured onto the wafer and spread evenly avoiding any air bubbles (Huh *et al.*, 2013). The SU-8 master was also used to create the microfluidic channels as both the Lung-on-a-chip and Gut-on-a-chip channels were designed

to replicates the average diameter of an alveolus in human lungs and intestinal villus of the human gut.

Though this method provides an ideal approach for creating membranes with small pore sizes for supporting the growth of 3D cell culture, the pores have shown to vary in size and thickness resulting in an uneven surface. This may be due to the handling of fabricating flexible porous membranes using PDMS. Though the PDMS membrane has shown promising results in both the lung-on-chip and gut-on-chip it has been reported that there are some varying results in terms of chip fabrication and testing. Small feature like the pores on the membrane varied in height. PDMS is also known to absorb hydrophobic molecules which could potentially compromise accuracy of drug efficacy and toxicity testing. This is due to its poor chemical resistance to certain solvents (Ingber *et al.*, 2013). Furthermore, it has been recommend that an alternative material can be used to create ultrathin porous membrane to mimic the extra cellular matrix (ECM) material that could be implemented in future OOC models (Ingber *et al.*, 2013).

### **2.3.2 Soft lithography**

Soft lithography is a fabrication technique that uses a combination of 3D printing, moulding, and embossing using an elastomeric stamp. The technique provides a low costing and convenient method to replicating a 3D design which is commonly used in microfluidics, cell biology, lab-on-a-chip applications (Qin, Xia and Whitesides, 2010). This method can also be used to create scaffolds to support tissue engineering applications in relation to OOC research.

In soft lithography, the photolithography process is still being used to create pattern SU-8 wafer to act as master (Figure 2.13). However, 3D printing is an alternative and easier method to create moulds with the desired design of interest which, can then be used repeatedly for creating elastomeric stamps. PDMS is cast over the moulds and left to set for 2-4 hours in an oven at 45°C or left to cure at ambient temperature for 24 hrs. PDMS is then removed from the 3D printed or SU-8 mould to reveal the embossed design and is then sealed against a suitable substrate i.e., glass or PDMS. Soft lithography process uses a wide range of elastomeric material like PDMS, to capture the embossed structure from the master. This method is seen as a cost-effective alternative approach to rapid prototyping.

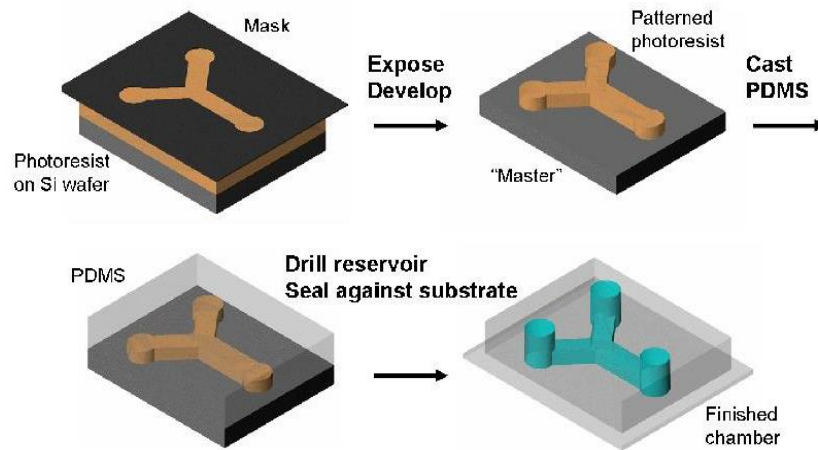


Figure 2.13. Presents the step by step process conducted in Soft lithography to create embossed elastomeric stamps made with PDMS (Microfluidics Background, 2020).

### 2.3.3 Electrospinning

Electrospinning is a process that uses electrostatic forces to draw polymer solution creating nanoscale fibrous structures. The fibrous structure can be used for various applications (Z.-M. Huang *et al.*, 2003), including wound dressing (Khil *et al.*, 2003; Min *et al.*, 2004) tissue engineering scaffolds (Fertala, Han and Ko, 2001; Jin *et al.*, 2002; Zong *et al.*, 2003) and drug delivery platforms (Verreck *et al.*, 2003; Ashammakhi *et al.*, 2012).

Electrospinning is a method that uses a high electrostatic field to draw a polymer solution, under a low pressure, from a needle tip to a metallic surface to create fibres. A polymer solution is placed in a syringe, this is driven towards a needle tip through tubing by a syringe pump. As the electrostatic field strengthen the Coulombic repulsion forces causes the droplet to change shape, this is called the Taylor cone.

An increase in electrostatic strength causes a charged jet stream of polymer solution to eject from the apex of the Taylor cone (Reneker *et al.*, 2000). The charged solutions travel in a vertical trajectory for a short distance, this is when the polymer solution goes through a liquid to a solid phase. The solution undergoes bending instability which results to further thinning of the solution before reaching the ground collector (Figure 2.14) (Reneker *et al.*, 2000).



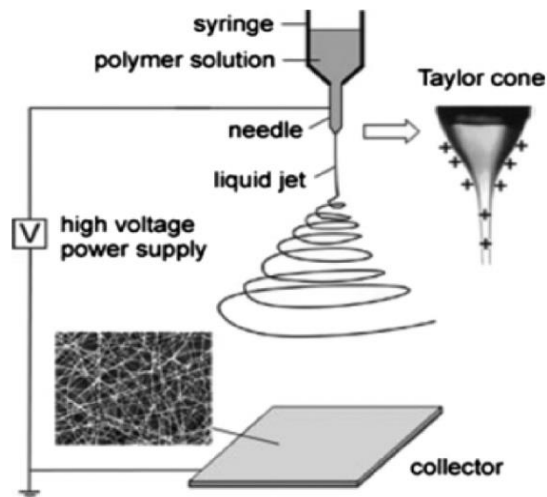


Figure 2.14 Present the set-up of the electrospinning apparatus (Garg and Bowlin, 2011)

Electrospun fibres contain unique characteristics which are ideal for tissue engineering and other biomedical application. This is due to the high surface area to volume or mass ratio and high surface area of pores varying in size (Choktaweessap *et al.*, 2007). For tissue engineering, fibrous scaffolds are produced using biodegradable and biocompatible polymers. These membranes can be spun with a diameter ranging from microns to nanometres. Such small fibres can imitate the structural dimension of an extracellular matrix of tissue and organs (Huang *et al.*, 2004). Human cells can attach and organise themselves around these structural membranes if the diameter of the fibres is smaller than the cells (Laurencin *et al.*, 1999).

There are several parameters that are considered for an electrospinning experiment such as concentration (wt. %), humidity (%), temperature ( $^{\circ}\text{C}$ ), voltage (kV), height (cm) and flow rate (mL/hr) (Laurencin *et al.*, 1999). However, to be able to spin a biopolymer/polymer solution, there are five solution properties that must be considered which are conductivity, surface tension, solvent volatility, solution phase transitions and viscosity (Li and Wang, 2013; Teo, 2015)

**Conductivity** – Solvents selected for dissolving the polymer must have some conductivity. By increasing the conductivity of the solution, it has shown to improve the quality of fibres. By adding an organic or inorganic salt to spike the solution it can also lower the voltage required for electrospinning and reduces the formation of beads (Teo, 2015).

**Surface tension** – The charged solution must overcome the surface tension of the solution. Surface tension reduces per unit mass of a liquid. Water has a high surface tension which

makes it difficult to electrospin causing the charged jet to form droplets or causes bead formation. By adding solvents such as acetic acid to water this reduced the surface tension and reduces the formation of beads producing smooth fibres (Teo, 2015).

**Solvent volatility** – When the charged jet travels towards the ground collector, fibres are formed and solidified due to solvent evaporation. Using a low volatility solvent can cause wet fibres to be formed whereas using a high volatility solvent this can cause the solution to solidify at the tip of the spinneret (Teo, 2015).

**Solution phase transition** – Is the interaction between polymer and solvent in terms of solubility at various temperatures (Teo, 2015).

**Viscosity** – This is one of the main properties to consider for electrospinning as a high viscosity solution may not spin. This may be due to insufficient electrical charge to stretch the solution to form fibres. The solution concentration must be lowered to avoid gel like solution and have sufficient viscosity to be stretched into fibres (Teo, 2015).

Gelatin, a natural biopolymer is derived from collagen, both have similar compositions and biological properties but dissolving gelatin in water is unsuitable for electrospinning. This is due to gelatin being a polyelectrolyte polymer and therefore needs treatment (cross-linking) with a high polarity organic solvent such as 2, 2, 2-trifluoroethanol (TFE) which allows gelatin to be directly spun into ultrafine fibres. It is known that collagen cannot be electrospun alone as molecular chains of collagen denature under strong solvents causing collagen to lose its native triple helical structure resulting in gelatin and therefore inhibiting collagen from electrospinning. Therefore, blending with another biodegradable synthetic polymer such as poly ( $\epsilon$ -caprolactone) PCL for the solution to be suitable for electrospinning is required (Laurencin *et al.*, 1999).

Zhang et al. produced gelatin nanofibers, however in order to improve the water resistance ability and thermomechanical performance for potential biomedical application, gelatin was crosslinked with glutaraldehyde (GTA) vapour for 3 days which preserved the fibrous morphology. The gelatin fibrous scaffold was placed into water at 37°C to check its stability and did not dissolve. The scaffold was used to study cell proliferation by culturing human dermal fibroblast for 1,3,5 and 7 days. Cells expanded over the duration of the cell culture experiments however, further cell expansion may have inhibited due to the cytotoxicity

residual of GTA left on the cells. This paper has shown that cell culture was successful on biopolymer membranes made from gelatin, but crosslinking is required to enhance the fibres thermomechanical and thermal stability performance (Yi, L *et al.*, 2017).

Huang *et al* investigated electrospinning gelatin dissolved in water, the solution was unable to produce fibres. TFE was used to dissolved gelatin which successfully produced nanofibers of 100nm – 340nm. Various solutions were made to spin from 5% - 12% w/v. Overall 7.5% w/v mass concentration gave the best results of electrospun fibres with an average size of 140nm and no bead formation comparing to the other mass concentrations (Huang *et al.*, 2004).

A newly optimised method has been observed in Horuz and Belibağlı paper where the L<sub>9</sub> orthogonal array and S/N ratio Taguchi's method (effects four conditions flow rate, voltage applied, distance between tip and collector and concentration levels of acetic acid) was employed to find the optimal conditions for electrospinning gelatin with acetic acid. The experiments gave better (bead-free, smaller diameter and smooth) nanofibers (Horuz and Belibağlı, 2017).

#### **2.3.4 Bio-plotting**

3D printing is a process that is becoming popular in the diverse areas such as medicine, aerospace engineering and tissue engineering. 3D printing is the process of building complex structures layer by layer, but it also can adopt various materials. It has been applied in tissue engineering research for building patient specific shapes with complicated porous designs such bone and ear cartilage, Figure 2.15. 3D printing involving cell is called 3D bioprinting which involves the construction of anatomy and physiology of desired tissues. This requires precise patterning and layering of various cellular compositions and biomaterials (Yi, *et al.*, 2017).

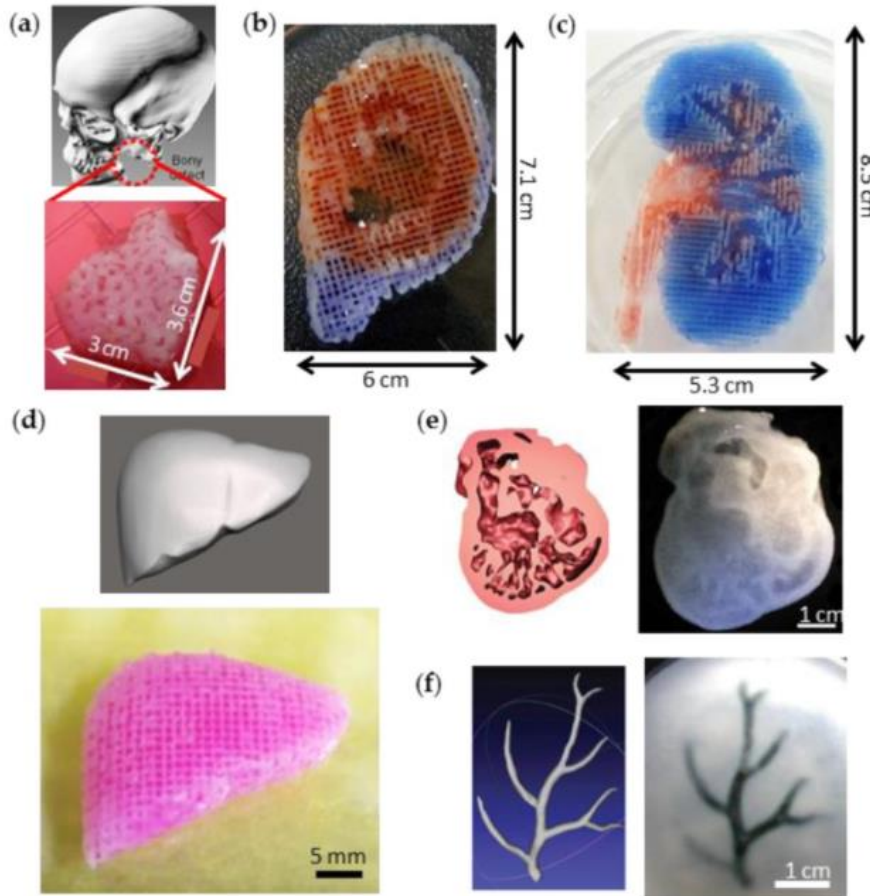


Figure 2.15. Presents images of 3D bio plotted constructs with heterogeneous and complex structures (A) a mandible of bone; (B) an ear cartilage with ear lobe; (C) a kidney with renal pelvis ;(D) a liver ;(E) a heart cross-section and (F) an arterial tree (Yi *et al.*,2017).

For 3D printing of OOC, biocompatible materials are available as printing ink, depending on the function and of the chip. The printing ink can be divided into two categories natural and synthetic. Natural materials such as collagen, gelatin, alginate and fibrin are formed by hydrogels also known as bioinks and are normally used to encapsulate cells in 3D cell printing. The bioinks are high in water content and viscoelastic which protects the cells during printing. Synthetic materials can adopt to any purpose for printing. Biocompatible synthetic polymers are normally low in cytotoxicity and bioinert, they are also stiff and rigid which makes them suitable for cell support framework for 3D cell -printing.

Biocompatible polymers with non-degradable properties can ideally be used to 3D print housing components for an OOC. Materials such as PCL and PDMS can be used to print various parts of a device. Though PCL has biodegradable properties it can be used to print implantable devices that will last just over a year. Whereas PDMS, a silicon polymer is known for its flexibility and toughness that makes it useful to generate microfluidic devices which can be

used for cell culturing. PDMS is transparent which allows visualisation of cell culture or transporting of fluids. However, making PDMS chips can be an intensive process, but due to its reversible and irreversible bonding to glass and plastic and other materials it can be printed as an outer wall compartment as storage for cell media and hydrogels (Yi, *et al.*, 2017). 3D printing of OOCs has shown the ability that this technique can be used to print such device, but this technology is at the preliminary stages and many aspects will need to be considered in the future for this process to fully develop into a working progress.

## **2.4 Microfluidics**

Microfluidics refers to the behaviour of manipulating and precisely controlling fluids at a small scale ranging from microliters  $10^{-6}$  to picolitres  $10^{-9}$ . It is a technique that is used through multidisciplinary fields from engineering, biology, nanotechnology to chemistry and biotechnology. The use of microfluidics evolved during the development of lab-on-a-chip (LOC) devices which brought the likes of biology and chemistry research onto one single platform. With the support of technology such as 3D printing microfluidic devices can easily be fabricated, reducing the time it takes from a concept into a chip. 3D printing is seen as the alternative method to conventional methods such as using SU-8 modelling (Fertala, Han and Ko, 2001). Stereolithography (SLA), Fused Deposition Modelling (FDM) and Material Jetting (MJ) are some of the most common 3D printing methods used to fabricate microfluidic chips.

### **2.4.1 Stereolithography**

Stereolithography (SLA) is a form of additive manufacturing process that belongs to the photopolymerization family. The method of printing involves creating an object through curing a polymer resin layer by layer via ultraviolet (UV) laser beam. For SLA printing, materials used are photosensitive thermoset polymers and usually come in resin form (Varotsis, 2020b).

### 2.4.1.1 Method

As seen in Figure 2.16, the build platform is positioned in the tank containing the liquid resin which is set just above the surface of the resin. The SLA printer uses UV lasers to form the next layer by selectively curing and solidifying the photopolymer resin. Mirrors are placed at the corners of the build plate which determines the laser beam pathways.

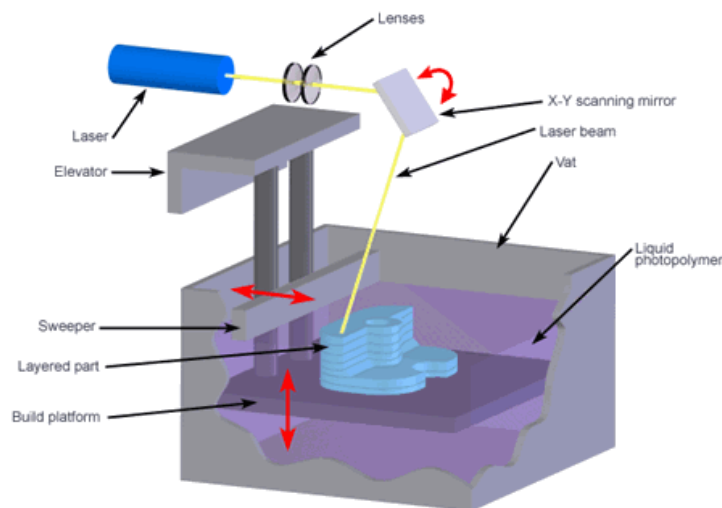


Figure 2.16 Present the set up for SLA printing which uses photopolymer and UV laser beam to build an object layer by layer (Fasnacht, 2017).

The cross-section area where the model is being printed is scanned to ensure the part being printed is completely solid before moving onto the next layer. As each layer finishes the build plate gradually moves at a safe distance for the sweeper blade to recoat the surface. The sequence of steps is repeated until the print is finished. After printing, the prints are left to cure under UV light before being removed. Prints are solidified through the process of photopolymerization, as resin contains monomer carbon chains, these chains become active under the UV laser causing the material to solidify as it creates unbreakable bonds between each monomer chain (Varotsis, 2020b).

SLA printers typical print height ranges between 25-100 microns, 100 microns being the optimum height for most applications. The build size is important depending on the SLA printer. There are 2 types of SLA setups: 1) top-down orientation and 2) bottom-up orientation. The top-down method places lasers above the tank where the build plate starts from the top and gradually moves down the resin vat as each layer is formed. The parts are built facing upwards, Figure 2.17. Whereas the bottom-up method the lasers are placed under the resin tank. The tank contains a transparent bottom coated in silicone which allows

the lasers to pass through and prevents the cured resin sticking to the bottom surface. As the build plate gradually moves up each layer is cured and detached from the bottom surface of the tank, this process is called the peeling step (Varotsis, 2020b).

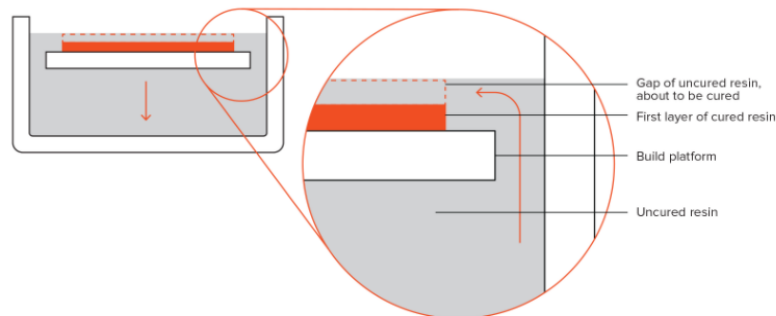


Figure 2.17 Demonstrates the Top-down SLA printer (Varotsis, 2020a).

The bottom-up method is mainly used for desktop SLA printers like the Formlabs (Figure 2.18), which is easier to use and manufacture but the build size is limited due to forces being applied during the peeling step process which can lead to print failures, Figure 2.19. However, the top-down method is mainly used for larger scale prints which provides a greater accuracy in printing and faster built time but at a higher cost (Varotsis, 2020b). The main advantage of using an SLA printer is that it has the ability to fabricate parts with very high dimensional accuracy, in detail and provides a smooth finish.

However SLA prints are not ideal for using as prototypes as parts can become brittle and when exposed to sunlight or extreme heat can cause the prints to warp and change in mechanical properties and visual appearance (Varotsis, 2020b).



Figure 2.18. Presents SLA 3D printer Formlabs (Ward, 2015).

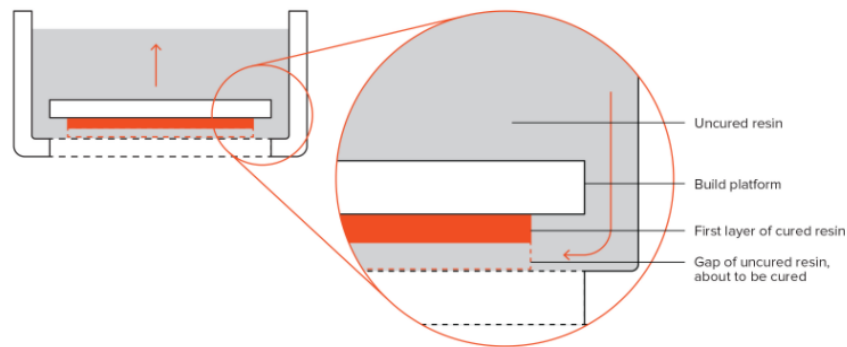


Figure 2.19 Demonstrates the bottom-up SLA printer (Varotsis, 2020a).

## 2.4.2 Fused Deposition Modelling

Fused Deposition Modelling (FDM) or Fused Filament Fabrication (FFF) is another additive manufacturing method that uses material extrusion as its main process. This printing method is often used to create basic prototypes for testing. The FDM printer like the Ultimaker 2+, builds an object layer by layer as it deposits melted material on a defined pathway (Figure 2.0) (Varotsis, 2020a).



Figure 2.20 Ultimaker 2+ is an example of FDM printer, which uses filaments to build an object through material extrusion process (Professional 3D printing made accessible | Ultimaker, 2011).



### 2.4.2.1 Method

The FDM uses thermoplastic polymers in filament form. The filament is loaded onto the printer and nozzle is set to the desired temperature depending on the filament being used. The filament is fed through to the extrusion head to the nozzle where the filament begins to melt. The extrusion head is connected to a 3-axis system which allows the nozzles to be moved in the x, y and z directions. The melted filament is extruded onto the build plate as thin strands and deposits layer by layer onto a predefined location where the layers cool and solidifies.

Depending on the design, areas are usually filled by the extrusion head passing over multiple times. Once the layer is completed, the extrusion head moves up and deposits the next layer. This process is repeated which can be seen in Figure 2.21 until the designed part is completed. Support can also be added to the design to support the part during the building process. Once the print has finished the build plate is then left to cool down before removing the printed sample (Varotsis, 2020a) .

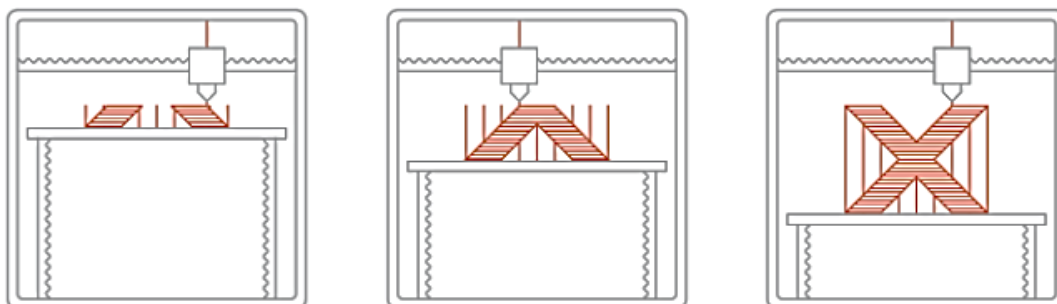


Figure 2.21 Presents the printing process of FDM (Varotsis, 2020a) .

Usually, desktop FDM printers have a build size of 200 X 200 X 200mm whilst the printers used in industry have a build size of 1000 x1000 x 1000mm. FDM printer can print layers with a height ranging from 50-400 microns. Nozzles can be changed to refine the strands of filaments to increase the proximity of each layer creating a finer mesh. Layers printed at the optimum height of 200 microns provides a smooth finish with the ability to capture curved geometry. However, warping is known to be one of the major defects in FDM printing. This happens when extruded material cools during solidification which causes the dimensions of the layers to decrease. As areas of the print cool and solidify at different rates the dimensions

also change, resulting in layers to be pull upwards. To prevent warping monitoring the temperature of the build plate and increasing adhesion to the build plate is recommended (Varotsis, 2020b).

The advantage of using FDM is that there is a wide range of material that can be utilised from commodity thermoplastic such as poly lactic acid (PLA) and acrylonitrile butadiene styrene (ABS) to engineering materials like polyamide nylon (PA), polyurethane (TPU) and polyethylene terephthalate glycol (PETG). For high performance, materials such as polyether ether ketone (PEEK) known for its excellent mechanical and chemical resistance properties that can also be used at higher temperatures are suitable for engineering applications that requires such properties. In comparison to other printing techniques FDM is the most cost effective method used to fabricate prototypes but is not suitable for creating moulds or designs with such intricate detail due to the high surface roughness after printing (Varotsis, 2020a).

### 2.4.3 Material Jetting

Material jetting (MJ) is a forms of additive manufacturing process that runs in a similar way to a 2D printer. A print head similar to those used in inkjet printing distributes droplets of photosensitive material layer by layer, solidifying under UV light (Figure 2.22). MJ printers mainly uses thermoset photopolymer which include acrylics, ABS and transparent material which come in resin form. This form of 3D printing provides accuracy in dimensions and a smooth surface finish (Bournias Varotsis, 2019).

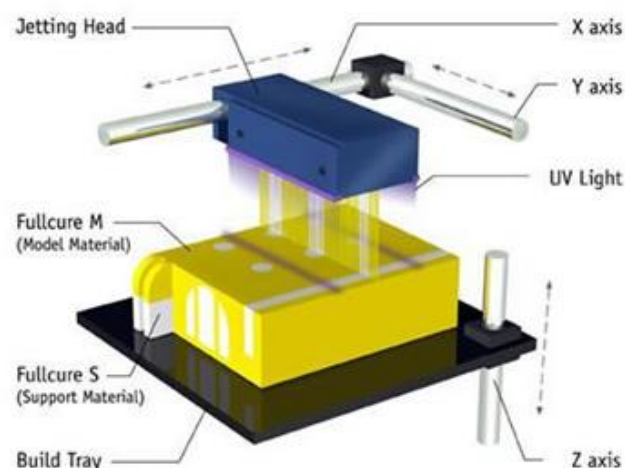


Figure 2.22 The Objet Polyjet printer uses material jetting to cure photocurable resin (Fasnacht, 2017).

### 2.4.3.1 Method

To operate MJ printing, first the resin is heated to temperature of 30-60 °C for the resin to reach optimum viscosity. The printer head then travels over the build plate where it deposits several tiny droplets on a designated location. A UV light source is attached to the printer head which solidifies the material creating the first layer of the print. Once a layer is completed the build plate moves down as each layer builds. This process repeats until print is complete (Figure 2.23). With MJ printing, the support structures are always included in the print. The support material is easily removed or can be dissolved leaving a smooth finished print. Both MJ and SLA methods use photosensitive polymers that undergo photopolymerization to solidify the material, however MJ printers do not need further post-curing to achieve optimised prints due to the small height of 16-32microns being used to print the layers (Bournias Varotsis, 2019).

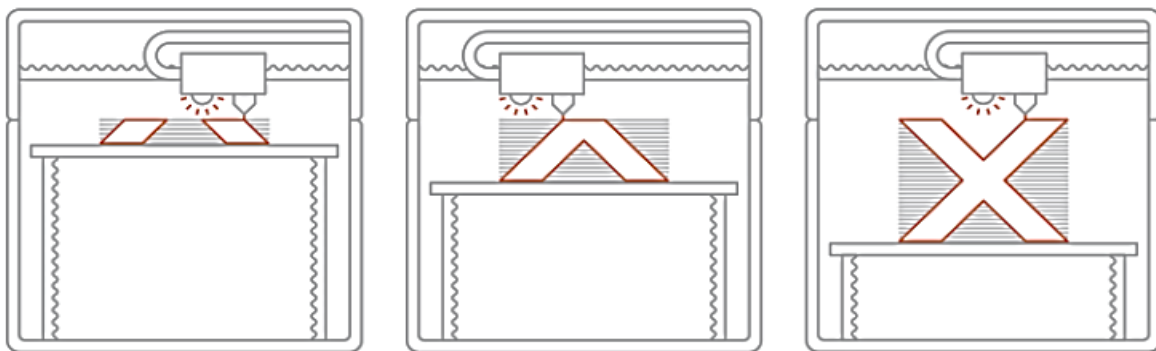


Figure 2.23. Presents the printing process MJ printing (Bournias Varotsis, 2019).

MJ method is one of the most accurate additive manufacturing methods amongst other 3D printing methods. The printer has a dimensional accuracy of  $\pm 0.1\%$  with a typical lower limit of  $\pm 0.1$  mm. Sometimes parts printed using this method can experience warping, but it is not as common as SLA and FDM because MJ usually prints at room temperature making it easier to build larger parts with greater accuracy. However, MJ prints are suitable for non-heavy use due to poor mechanical properties and degradation of material over a period of time.

### 2.4.4 Lego Microfluidics

In most OOC devices the alignment of the layers has never been expressed in detail though this is seen as an integral part to the OOC design. Alignment aids the combing of individual

layers into one working device as channels, inlets and outlets must be aligned correctly to avoid faulty chip. If any of the layers are misaligned during the assembling process, this can cause the chip to not function properly causing issues, like leakage, the attachment of tubing, inserting of membrane and bonding between layers.

It is vital that alignment is checked during the design process before chips are fabricated for prototyping. Fail to identify the misalignment can be costly, time consuming and waste in materials and resources. Vittayaraukskul and Lee's (2017) paper discussed Lego® like modular microfluidic platform by using Lego® like designs to mass produce simple 3D microfluidic devices (Figure 2.24). The idea was to promote the reversible pressure sealing as well as automatic alignment(Vittayaraukskul and Lee, 2017) .

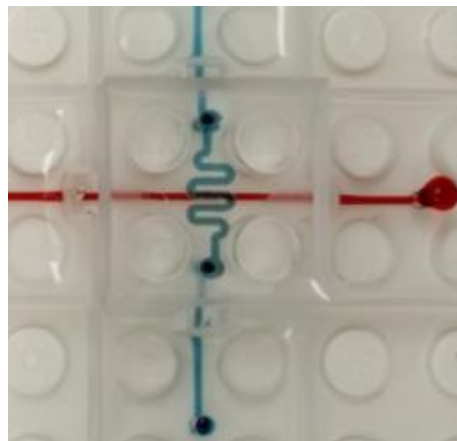


Figure 2.24 Fluid flow through microfluidic Lego® (Vittayaraukskul and Lee, 2017).

Inspired by this concept of the automatic alignment feature, alignment posts will be implemented on the design of the VOC platform. With this feature the layers will be easy to assemble and detached for further experimental use. The alignment posts will provide an interlocking system similar to Lego®. This will benefit the chip by providing better layer attachment and sealing between layers.

## 2.5 Summary

After conducting a thorough literature review on the previous and current studies done regarding female health care for the treatment of BV and there is no model that only models the vagina or a system that can host the innate response to understanding what causes BV and how it can be managed to reduce the chances of recurrence. Therefore, a gap has been

identified in the knowledge. To create a device that can be used to understand BV and to find better treatment to improve female health.

The following objectives will be considered in this thesis: -

**1. Microfluidics: To develop a new organ-on-a-chip device for the study of BV:**

By using microfluidic techniques and 3D printing (material jetting) to design and create 3 layered VOC platform that will house a biocompatible membrane held in suspension to support the growth of squamous epithelial cells. The VOC will consist of microfluidic channels designed to provide nutrients to the cells. The platform will be attached to an automated system that will control and monitor flow and pressure for testing and to stimulate the environment of the human vagina.

**2. Electrospinning: To create a porous biocompatible and biodegradable membrane onto which different cell types can be seeded and proliferate.**

To create functional, physiological vaginal micro tissues within the device - creating biocompatible, stretchable porous membranes using electrospinning technique which will act as a scaffold to support the growth of 3D vaginal epithelium tissue. The membrane will be made with synthetic and natural biodegradable polymers such as gelatin, collagen and polycaprolactone. Immortalised epithelial cells line VK2/E6E7 will be seeded on to the membrane and cultured for short- and long-term experiments on membranes alone and within the chip to establish vaginal tissue. The microfluidic channels on top and bottom will distribute growth media to cells continuously. Live/dead cell assays and fluorescence microscopy will be used to validate cells.

**3. Cell culture: To create 3D vaginal tissues in vitro.**

To seed bacteria associated with the normal microflora and bacterial vaginosis. *Lactobacillus* Spp. species will be added to the vaginal epithelial cells to identify the optimal percentage required for cells to grow which will then be added to the VOC to mimic the human vaginal microbiome. This can then be compared as a healthy model vs unhealthy model that is seeded with BV bacterial strains.

## Chapter 3 – Microfluidic Design of the VOC platform and fabrication processes

OOC platforms are seen as one of the latest emerging technologies to capture the attention of biomedical research worldwide. They are addressed as biomimetic systems developed on microfluidic chips that combine multidisciplinary research in engineering, cell biology, microenvironments, and biomaterials to stimulate the tissue - tissue interactions and mechanical stimulation of the organ of interest. The platform provides an insight to the 3D structural and functional characterisation of human physiology and its environment (Sun *et al.*, 2020; Wu *et al.*, 2020). These OOC platforms are the development of a novel approach for *in vitro* disease modelling, to study complex human diseases and conditions which can then be used to produce new drugs and treatment, testing of toxicity (drugs and chemicals) and potentially an alternative method to animal testing (Huh *et al.*, 2013). The main purpose for the development of the VOC platform was to create a realistic model that truly represents the function and physiology of the human vagina and its environment to gain a better understanding of bacterial vaginosis. To create and manufacture an OOC platform design requirements and engineering principles must be considered before fabricating such a complex device which can be a challenging process (Yang, *et al.*, 2017). Figure 3.1. shows the engineering principles that were considered whilst designing and creating the VOC platform.

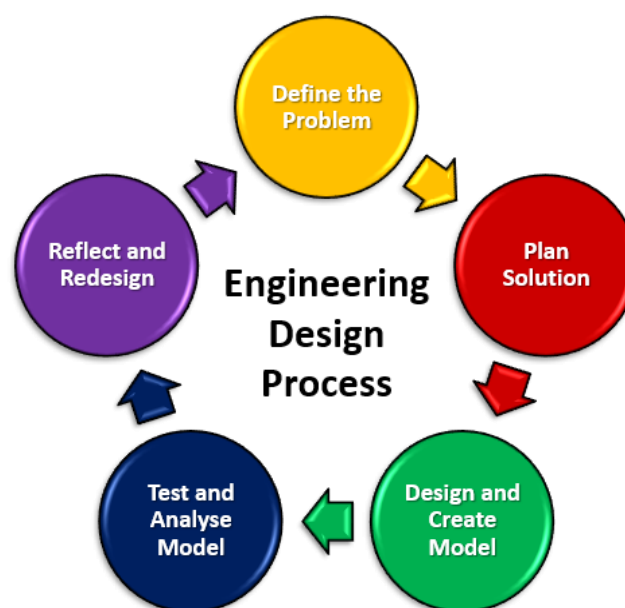


Figure 3.1 The engineering design process followed to design and develop the VOC platform.

In the previous chapter a thorough literature review was conducted to identify the previous and current models used to study vaginal epithelial tissue as well as OOC models that have been developed to study organs of interests including the lungs, liver and gut. However, the literature indicated the lack of OOC devices that have successfully cultured 3D cells with their natural microbiome. The gut-on-chip is currently the only model that has shown promising results in studying the interactions between the host cells and its natural microbiome. With reference to this model the VOC platform has been designed to support the development of 3D vaginal tissue and to include the vaginal microbiome, to create a realistic *in vitro* environment. Once established, the VOC platform has the potential to investigate the initiation, progression, and treatment of bacterial vaginosis.

### 3.1 Engineering Design Process

To create the VOC platform an engineering design process was followed seen in Figure 3.1 to identify the design requirements for the VOC platform.

**Define the Problem:** - As discussed, BV is a common vaginal infection that affects women of childbearing age and if left untreated can lead to complication such as premature births, miscarriages, and pelvic inflammatory disease. The vagina contains a natural balance of healthy bacteria *Lactobacillus spp.*, which promote the production of lactic acid; these bacteria are responsible for maintaining a low the pH of the vagina. However, when this environment becomes disrupted infections like BV can occur due to an overgrowth of anaerobic bacteria. Therefore, a novel approach must be considered to understand the complexity of BV and how it could help develop new and improved treatment of the infection.

To construct the VOC platform, different type of materials and methodology must be considered. 3D printing and soft lithography will be used to make the layers of the VOC platform using PDMS. The device must also contain a membrane made from biodegradable material that is porous, biocompatible and exhibits good mechanical properties to support the growth of vaginal tissue. Electrospinning technique will be used to fabricate such membranes using biopolymer and synthetic polymers to form ultrafine fibres mats with multiple arrangements and morphological structures. These fibres usually have a diameter ranging from micrometres to nanometres. The fibrous mats provide features like porosity and large surface area ideal for application like wound dressing, drug delivery applications and

tissue engineering. In this research the electrospun mats will be used as scaffolds to support the growth of vaginal tissue at the centre of the VOC platform.

The VOC platform embodies the function of vaginal tissue; therefore, the type of cells that will be utilised in this platform must be considered for modelling an *in vitro* system to mimic the *in vivo* behaviour. To fully mimic the vaginal environment the microbiome of the vagina must also be included in the design of the platform. This is so to establish a healthy system that truly represents the human vaginal environment where bacteria induce the biofilm formation on the epithelium membrane.

**Plan Solution:** - To design and develop a novel 3D microfluidic tool, VOC, which can be used as a research tool to investigate the initiation, progression, and treatment of BV, by combining multidisciplinary techniques that will mimic the mechanical, biochemical and physical aspects of the vaginal tissue. The main aim is to create a viable VOC platform to study the factors that cause an interruption in the vaginal microbiome and the interaction between the vaginal epithelial cells and bacteria strains, to improve female healthcare.

**Design and Create Model:** - The designs behind the VOC platform were derived from the lung-on-a-chip, Liver-on-a-chip and gut-on-a-chip with a similar concept of channels crossing over each other whilst being separated by a semi permeable porous membrane. The use of multiple techniques such as 3D printing, soft lithography, microfluidics, and electrospinning were used to fabricate the VOC platforms which is described further in methods section 3.5.

**Test and Analyse:** - VOC designs were tested using a Fusion 200 two channel syringe pump – (KR Analytical, UK) with green and blue food colouring dyes to check and analyse the performance of the chip design, the alignment of the layers, the bonding between the layers and positioning of the membrane. A steady flow rate of 15  $\mu\text{L/hr}$  was used replicate the dynamic flow that is experienced by the cells and tissues in the vagina.

**Reflect and Redesign:** - From the analysis conducted through the experimental stages of the VOC experiments, results were then analysed to identify any challenges. Once identified, the process of re-designing and further iterations were conducted, re-tested and analysed, until the final design had been optimised and met the desired design requirements of a fully functioning device.



### 3.2 Design Concept

The aim of the VOC is to create a realistic platform that truly represents the human vagina and its microbiome environment. The VOC design consists of three layers (Figure 3.2). The top and bottom layers feature the fluidic channels, designed and positioned to flow over and under the central layer, to provide continuous supply of nutrients to the vaginal cells grown at the centre of the chip. The central layer consists of a biocompatible membrane, fabricated using the electrospinning technique, seen in chapter 4. The VOC has been designed to support and hold the membrane in suspension like a gasket which forms the middle layer of the VOC platform. The purpose of the electrospun membrane is to mimic the natural ECM for vaginal epithelial cells to grow and form 3D vaginal tissue. The platform contains two microfluidic channels, to support the future prospects of using more than one cell type. For the first VOC prototype VK2/E6E7 vaginal epithelial cells will be used. All components of the VOC are fabricated individually and then amalgamated into one single platform as seen in Figure 3.2.

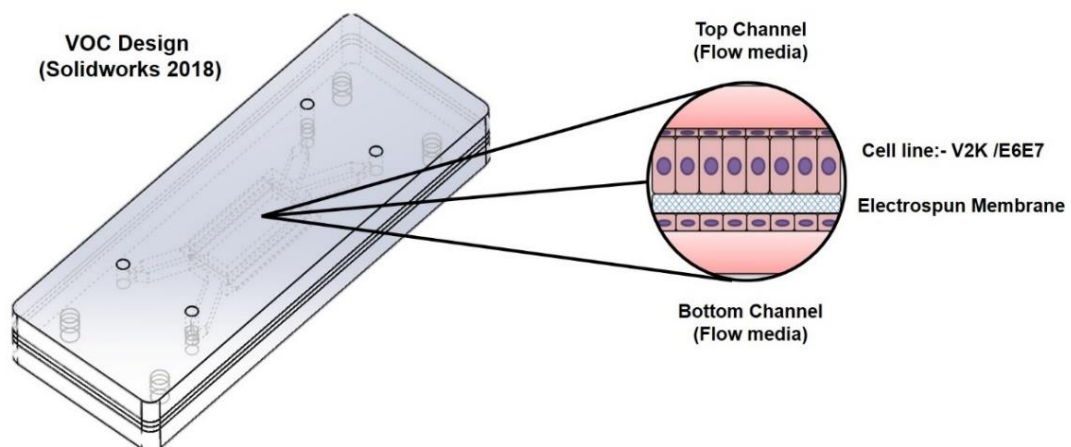


Figure 3.2 Concept design of the VOC platform.

### 3.3 Product Design Requirements

Currently, OOC devices that have been established in the market have not been created under any official International Organisation for Standardisation (ISO). Therefore, there are no specific requirements to designing the ideal OOC platform. However, from literature common principles such as the design, materials and size have been taken into consideration to develop the VOC. Table 3.1 presents the design requirements for the VOC and how these measures will be used to develop and manufacture and working design.

Table 3.1 Design requirements for the VOC platform.

Design Requirements		
Design	Dimensions	Reason
<b>Size of chip</b>	Length 75 mm Width 25 mm	The size of a glass slide, for ease of handling the chip during testing. Ideal for microscopy evaluation.
<b>Size of channels</b>	Length ~ 10 mm Width 2.75 mm	Large channels to provide nutrients to the cells at the centre of the chip. First design to work at macroscale once optimised can be scaled down to microscale.
<b>Size membrane</b>	Length ~ 20 mm Width 8 mm	To provide the cells a large surface area to grow. Also, to obtain a sufficient sample for further testing. Small electrospun membrane can be difficult to handle therefore, a realistic sample size can be easier to manufacture and handle during assembling of the VOC platform.
<b>Size of in/outlets</b>	1 mm diameter	To ensure tubing can be attached to the 3D printed mould securing a tight seal between the tubing and the layer of the chip. When PDMS cures, the tubing will then be attached to the layer of the chip. This method will prevent the tubing from detaching, blocking, and leaking.
<b>Lego alignment posts</b>	1.50 mm diameter	For the alignment of the different layers. This will help with the alignment of the channels over the membrane. The post will help with the sealing of the chip as well as provide the flexibility in detaching the layers to obtain samples for further testing. The post will provide a plug and play system have Lego® bricks use.

### **3.4 Materials**

The following equipment and materials were used to fabricate the VOC chips. Poly(dimethylsiloxane) (PDMS) (Qsil 216, ACC Silicones Ltd, UK), 3D printed moulds made from VeroWhite resin (Stratasys, US), Steel casing (Brunel, UK), Polytetrafluoroethylene (PTFE) tubing 1.58mm OD x 0.5mm ID (Sigma Aldrich, UK), Silicone tubing 0.5mm OD X 1.00mm ID (Atlec, UK), Isopropyl Alcohol (IPA), nitrogen gas, Corona Plasma Treater (BlackHole Lab, FRA), Fusion 200 Two channel syringe pump (KR Analytical Ltd, UK) , Syringe (BD Plastics, UK), Blunt needles End 22G (RS, UK) and electrospun membranes (see chapter 4).

### **3.5 Methodology**

To design and develop the VOC platform, SolidWorks 2017 was used to draw and design the VOC moulds. These drawings were then converted, and 3D printed into moulds. The soft lithography method was then used to create the individual layers of the VOC. This method was selected as it is cost effective, captured micron-scale features, easy to fabricate and manufacture chips for prototyping, further details can be seen in section 3.5.1-3.5.3.

#### **3.5.1 PDMS for fabricating VOC layers**

PDMS is a flexible elastomer silicon based organic polymer that is often used in prototyping and testing microfluidic applications including lab-on-chip (LOC) and OOC devices. PDMS is normally selected as the ideal material for such applications due to its versatile properties of being biocompatible, cost effective, permeable for gas exchange and optically transparent (Charati and Stern, 1998; Marois and Be, 2001; Leclerc, Sakai and Fujii, 2003).

PDMS is also easy to use and is excellent for moulding, but one key feature is that it has the ability to bond irreversibly to glass or onto itself. This is done by activating the surface with plasma treatment to form a permanent bond (Haubert, Drier and Beebe, 2006). However, to ensure good bonding between any surfaces i.e., glass or PDMS all surfaces must be clean. Any dust or contaminant on the surface can hinder the bonding effect which can lead to many issues, for example leaking between layers and incomplete bonding during experiments.

### 3.5.2 Soft Lithography Process for Creating VOC Moulds

The process of soft lithography which consists of using a 3D printed mould or an SU-8 wafer discussed previously in chapter 2 which can be used multiple times to manufacture microfluidic chips. PDMS was selected as the main material for creating the VOC layers due to the many benefits it provides as mentioned above (3.5.1.) To make the VOC layers the soft lithography process is followed as depicted in Figure 3.3. The moulds are used as stamps. PDMS is then poured on top of the moulds and allowed to set for a required time. Depending on the size of the mould and the volume of PDMS used, curing time for PDMS can vary between 2-4hrs in the oven at 45°. Once the PDMS has cured, the PDMS layer is then slowly removed to reveal the negative print of the positive mould (step 3 of Figure 3.3). This is a favourable technique often used in microfluidic fabrication, due to being a cost-effective process. This method was used successfully to make the individual layers of the VOC platform which is explained further in section 3.5.3.

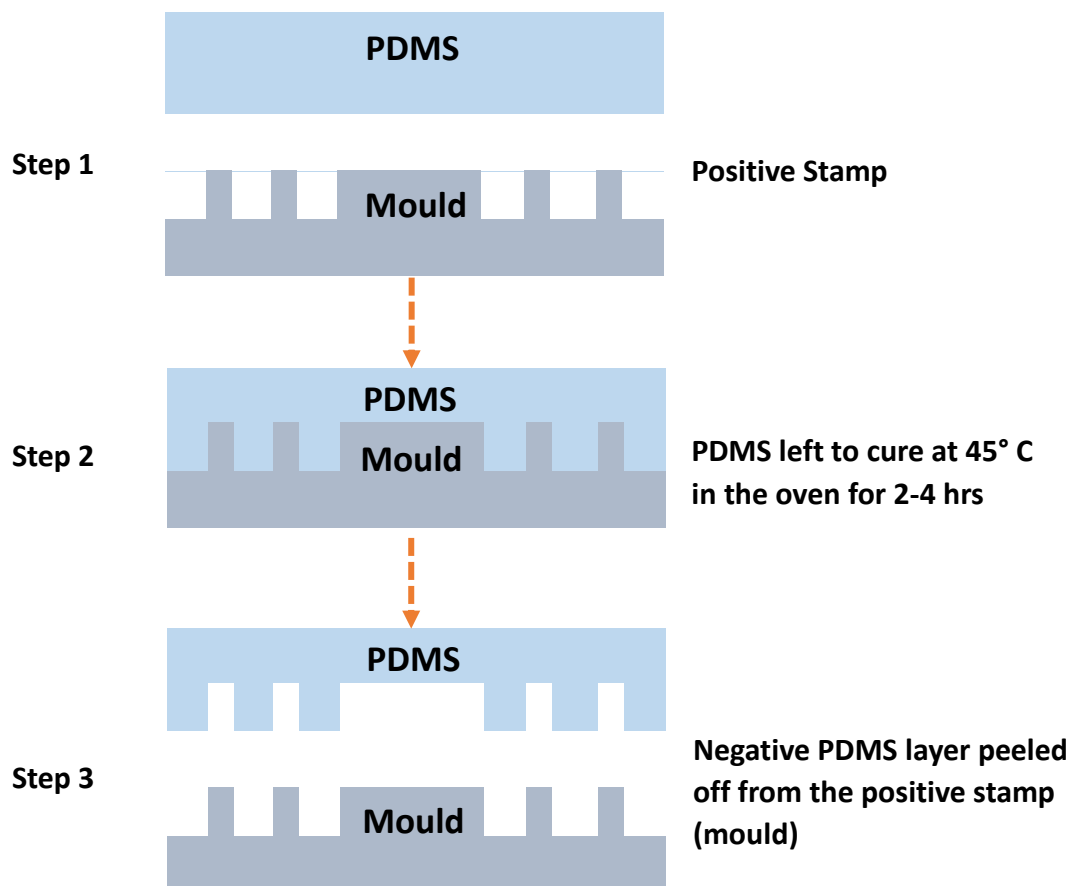


Figure 3.3 Schematic illustration of the three major steps involved in the soft lithography.

### 3.5.3 Design and Fabrication of VOC Moulds

To create the VOC platform, moulds were first designed using computer aid design software (CAD) SolidWorks 2017 and saved as stereolithography (STL) files. The designs were then 3D printed using the Objet 30 to create the VOC moulds. Polyjet, also known as material jetting, is a form of 3D printing that uses a photosensitive polymer resin i.e., VeroWhite. Designs were printed layer by layer and then solidified using ultraviolet light (UV) resulting in a rigid and highly detailed print. The method was chosen to create the moulds as it provides prints with a smooth surface finish and captures the micron- scale features in the design. With a smooth surface finish, PDMS layers are easily removable from the mould. The resulting smooth surface of the PDMS layers also provides an improvement in the bonding between layers.

### 3.5.4 Assembling VOC Moulds into Steel Casing

To make the VOC PDMS layers, 3D printed moulds were enclosed into a steel casing seen in Figure 3.4 and sealed with M8 screws. The casing was designed and made to fit the VOC moulds with a dimension of 30 x 80 mm whilst providing a final chip dimension of 25 x 75 mm. Moulds were cleaned with Isopropyl Alcohol (IPA) followed by rinsing with deionised water (DI) and left to dry. To ensure moulds were contaminant free the moulds were left under the UV for 20mins before use.

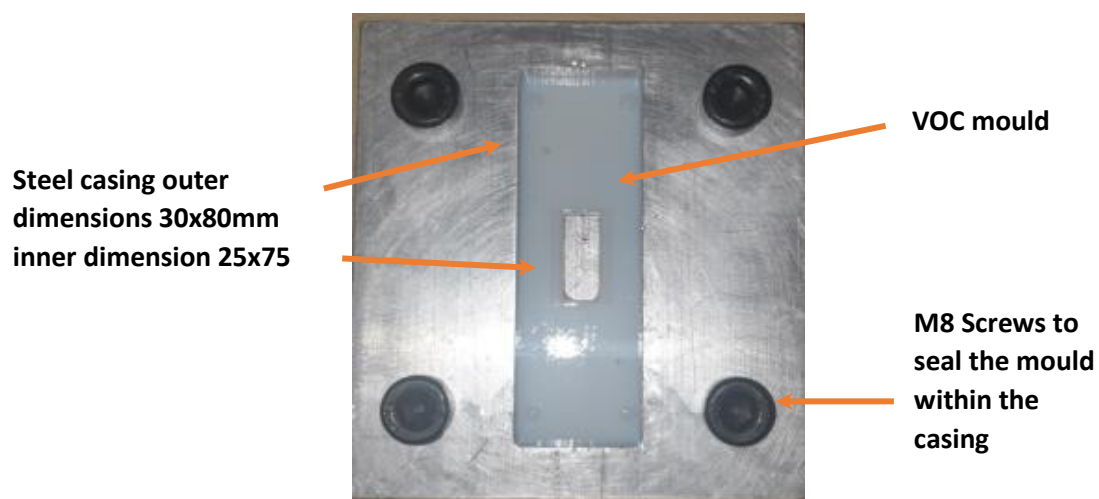
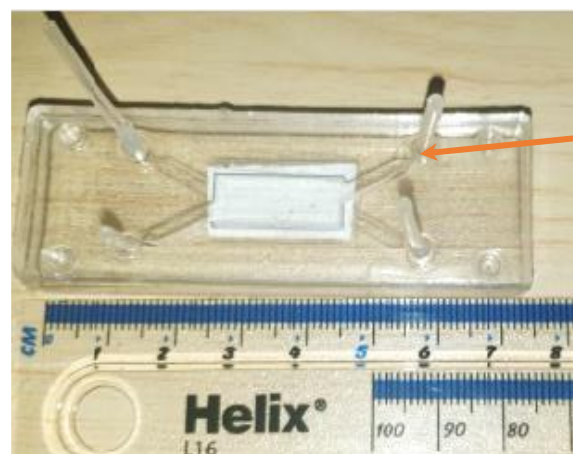


Figure 3.4 Full casting assembly of VOC mould housed in a steel casing to fabricate the PDMS layers of the VOC platform.

The custom-made steel casing undergoes the same cleansing treatment to avoid contamination. The mould is then placed into the steel casing and is tightly sealed to ensure no leakage of PDMS. Nitrogen gas is then used to remove any dust particles on the surface of the mould, this is to ensure a clean surface before adding PDMS to the moulds. The top steel plate has a depth of 2mm to create 2mm thick PDMS layers for the top and base of the VOC platform. Another steel casing was used to make 1mm thick PDMS layers to make the central layers that would support the membrane held in suspension. See appendix for full engineering drawings of steel casing for the VOC moulds.

### 3.5.5 Preparing PDMS mixture

To prepare the PDMS for the VOC moulds, a 1:10 (mL) ratio of Part QsilA: QsilB (ACC Silicones, UK) were measured to a final volume of 20mL and manually stirred for 3mins. The PDMS mixture is then placed into a vacuum desiccator and degassed for approximately 20mins until all air bubbles have been removed, leaving a clear viscous solution (Branavan *et al.*, 2016). For the top VOC mould tubing of 0.5mm OD X 1.00mm ID (Atlec, BEL) was added to the inlets and outlets, this is so the tubing would attach to the PDMS whilst curing, creating a tight seal to avoid leakage at the inlets and outlets during testing; a problem commonly encountered in microfluidics (Figure 3.5). The desired mould is usually cleaned and sterilised before securely enclosing the mould into the steel casing. The PDMS is then carefully poured on top of the mould at close proximity to avoid creating additional air bubbles. The moulds are placed into an oven at 45°C for 2-4 hours for the PDMS to cure. Due To the moulds being fabricated in Verowhite material, the moulds can only withstand a maximum temperature of 50°C, if exceeded the moulds' physical form alters significantly due to the low glass transition temperature of the material (Verowhite - Sculpteo, FRA).



Tubing attached to the in/outlets of the two PDMS layer of the VOC.

Figure 3.5 Tubing attached to the in/outlets of the top layer for a secure connection.

### 3.5.6 Removing VOC PDMS layer of moulds

After 2-4 hrs of curing time, the PDMS layers are then ready to be removed from the moulds. The casing with the moulds is removed from the oven and left to cool at room temperature for 2 mins, before disassembling. Once cooled, the moulds are gently pushed out of the casing. Using a scalpel, the PDMS layer is then scored at the edges to remove any excess material. To ease the removal of the PDMS layer off the moulds, the edges of the cured layer are gently squeezed a few times to enable detachment from moulds. The PDMS layer is then slowly removed to avoid tearing and carefully stored in a petri dish for plasma treatment.

### 3.5.7 Bonding of the VOC PDMS layers

To form the layers of the VOC platform, PDMS layers were treated using a handheld corona (BlackHole Labs, FRA). The plasma treatment was applied for approximately 2 mins across the surface of the layers that require bonding. Plasma treatment is a method used extensively in microfluidic fabrication. The treatment is mainly used to clean the substrate of contaminants and for bonding. By activating the surface of PDMS, the process alters the properties causing PDMS change from hydrophobic to hydrophilic state. This then allows the surface to bond with other treated surfaces.

PDMS is made from repeating units of  $(C_2H_6OSi)_n$ , but when treated this causes plasma to form free radicals which modifies the surface by removing the hydrocarbon groups and exposing silanol groups (-OH) at the surface of the PDMS. This results in strong covalent bonds (Si-O-Si) between PDMS and glass or PDMS to PDMS (Figure 3.6). This surface modification provides strong conformal bonds between surfaces that when oxidised, surfaces brought in to contact can cause irreversible bonding which occurs between the PDMS-PDMS layers (Tan *et al.*, 2010; Pasirayi *et al.*, 2012).

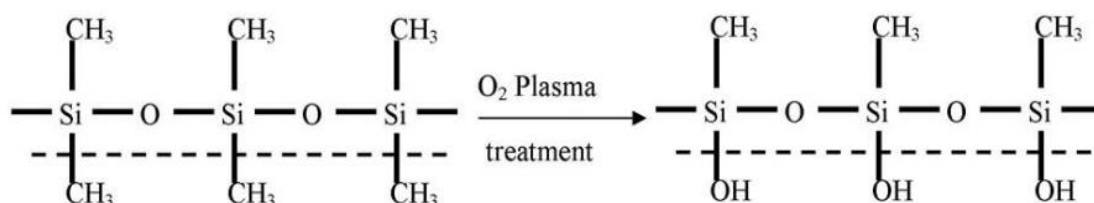


Figure 3.6 Surface modification of PDMS after oxygen plasma treatment (Pasirayi *et al.*, 2012).

As each layer of the VOC was treated, the individual PDMS layers were placed in descending order starting with the VOC base, central base, electrospun membrane, central top and finally the top layer to form the VOC platform, assembly of the VOC platform can be seen in Appendix A, 9.7.1. The final VOC platform was left in the oven over night at 45°C to ensure sufficient bonding between each layer before testing.

### 3.6 Design iterations and evaluation

Below discusses the design iteration and evaluation conducted on the VOC platform designs. Each design was tested, evaluated and re-designed to produce the final platform. A summary of the evaluation process can be seen in Table 3.2.

#### 3.6.1 Initial Design

The initial VOC model contained two microfluidic channels and alignment posts placed at the corners of the moulds to assist with assembling of the VOC layers (Figure 3.7). This design was carried out to evaluate, analyse, identify the challenges of the design and how a third layer could be introduced to the system i.e., the membrane which would be held in suspension between two fluidic channels to form the VOC model. From this, changes were made, further design iterations tested and analysed until the optimal design was achieved. Table 3.2 provides a summary of the different VOC designs outlining the design features, advantages, disadvantages and the benefits that were drawn and reflected on, to optimise and create the next model.

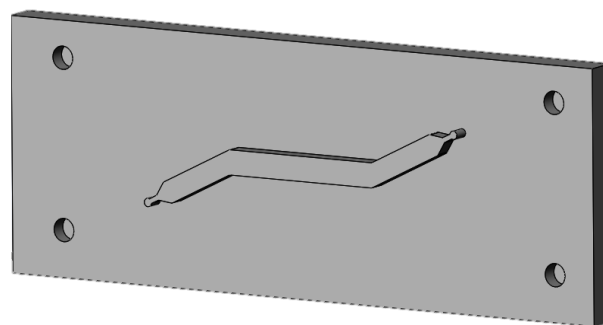
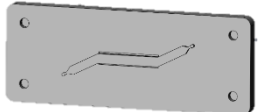
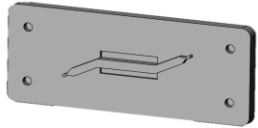
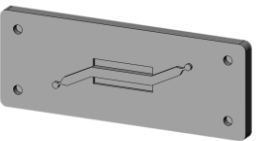
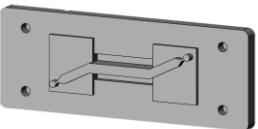
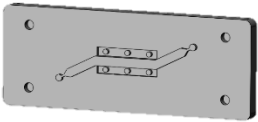


Figure 3.7 Initial concept of the VOC design mould with fluidic channel and alignment posts at the corners of the mould.



Table 3.2 Summary table of the VOC designs presenting the features, evaluation and benefits of each design.

Summary of VOC Designs				
Design No.	Design	Design Features	Evaluation	Benefits
2		<ul style="list-style-type: none"> <li>Membrane holders (0.5 x 19.50 mm) added on either side of the membrane to hold the membrane in suspension between the two fluidic channels to create the middle layer of the chip.</li> </ul>	<ul style="list-style-type: none"> <li>Size of holders were too small, causing the electrospun membrane to slide and not hold in place, resulting in sagging of the membrane and leakage of coloured solution into bottom channel.</li> </ul>	<ul style="list-style-type: none"> <li>Third layer is created.</li> <li>Membrane holders ideal feature to hold the membrane but need to increase the width to avoid sliding and leakage.</li> </ul>
3		<ul style="list-style-type: none"> <li>Membrane holders (1 x 19.50 mm) increase in width to provide support for the membrane held in position at the centre of the chip.</li> </ul>	<ul style="list-style-type: none"> <li>The increased width of the membrane holder held the membrane in place, but still experienced sagging and sliding of the membrane. In/outlets had a small orifice for tubing attachment which often led to blockage.</li> </ul>	<ul style="list-style-type: none"> <li>Increased width of the membrane holder improved the performance of the chip slightly, by holding the membrane in suspension.</li> </ul>
4		<ul style="list-style-type: none"> <li>Diameter for the in/outlet increased from <math>\varnothing 0.5</math> to <math>\varnothing 1.0</math> mm to improved attachment of tubing 0.5 mm OD X 1.00 mm ID (Atlec, UK ), for flow experiment.</li> </ul>	<ul style="list-style-type: none"> <li>Adding the tubing to the in/out lets of the mould, ensured tubing was attached to the PDMS layers, making it easier to run flow experiments.</li> </ul>	<ul style="list-style-type: none"> <li>Reduce blockage.</li> <li>Tubing attached to the mould to secure bonding of tubing to the in/outlets of the channels.</li> <li>Avoid leakage around the in/outlets</li> </ul>
5		<ul style="list-style-type: none"> <li>Layer added around the channels to seal the opposite channel during bonding, to prevent leakage into the opposite channel.</li> </ul>	<ul style="list-style-type: none"> <li>The extra layer increased the depth of the channels which was not necessary. The chip was set to have 1mm depth channels.</li> </ul>	<ul style="list-style-type: none"> <li>To ensure opposite channels were sealed.</li> <li>Reduce the sagging effect of the membrane exposing the channels</li> </ul>
6		<ul style="list-style-type: none"> <li>Posts added to the membrane holders to sandwich the membrane in position between the layers.</li> </ul>	<ul style="list-style-type: none"> <li>Due the small area on the membrane holders, the post accumulated space preventing the membrane from being held in place.</li> <li>Removing PDMS from small features proved tricky as PDMS would get stuck or tear, damaging the layers.</li> </ul>	<ul style="list-style-type: none"> <li>Design discarded but, inspired the creation of a gasket layer containing the membrane holders to support the membrane.</li> <li>Top and bottom layers would consist of the fluidic channels only, to simplify the design.</li> </ul>

### 3.6.2 Design 7 – The Final Model

To develop the final model, a performance evaluation of the previous designs was undertaken, taking into account the positives and negatives of each design using Table 3.2 as a reference. The novel design comprised of four moulds, that when combined would create the three layers of the VOC platform. The top and bottom moulds (Figure 3.8 A and B) contained the fluidic channels that would flow over and under the membrane based at the centre of the final chip. Expanding on the idea of design 5 (Table 3.2) two moulds were made to create the gasket layer (Figure 3.8 C and D). This layer was designed to support the membrane held in suspension at the centre of the chip between two fluidic channels. It also prevents sagging of the membrane and leakage into opposing channels. The idea was to sandwich the membrane as the middle layer of the VOC platform. The gasket layer not only seals the channels when layers are combined but, has been designed to cover the exposing areas of the channels at the meeting point of where the channels align with the membrane area at the centre of the chip. Moulds were all 3D printed in VeroWhite with an outer dimension of 30 x 80 mm to fit into the steel casing and with an inner dimension of 25 x 75 mm which resembles the same size of a glass slide. All four moulds included the alignments posts to aid with the assembling the layers of the VOC platform.

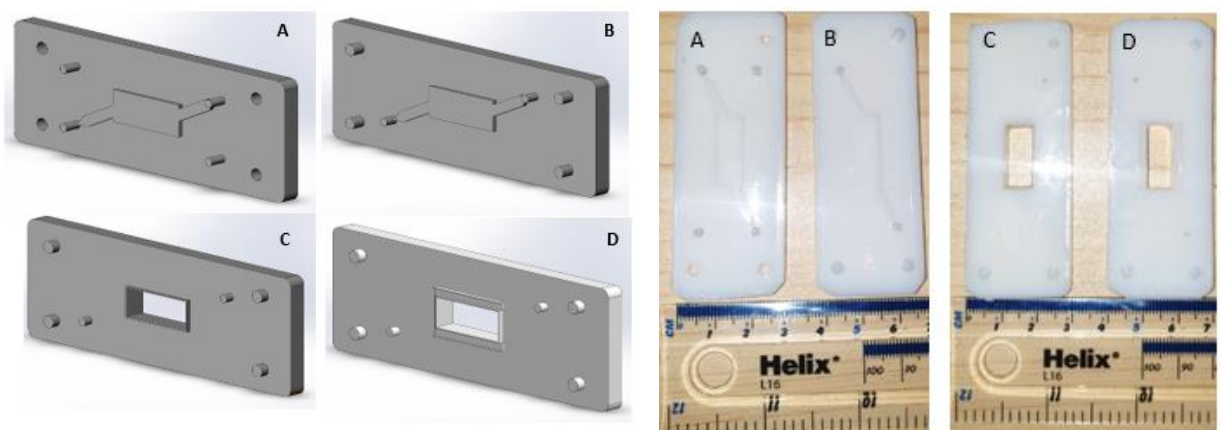


Figure 3.8 Presents the SolidWorks and 3D printed moulds for the VOC platform (A) Top VOC mould; (B) Base VOC mould; (C) Central top mould and (D) Central base mould.

### 3.7 Assembling of VOC platform

To create the final VOC platform, each layer is stacked on top of one another to create a complete model. In total, there are 5 individual layers of the platform that create the three main layers of the VOC as demonstrated in Figure 3.9. Top VOC layer (A) represents the first layer, central top layer (B), electrospun membrane (C) and central base layer (D) combined together form the middle layer and finally the base VOC layer (E) represents the final layer. Figure 3.10 illustrates the final assembly of the VOC layers to form the final model. The total thickness of the VOC platform is approximately 6mm.

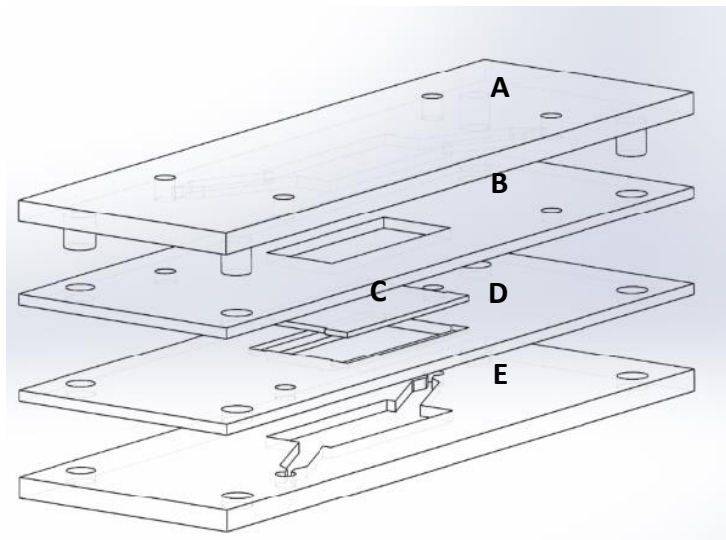


Figure 3.9 Final VOC platform in exploded view showing the separate layers in order (A) Top VOC layer; (B) Central top layer; (C) Electrospun membrane; (D) Central base layer and (E) Base VOC layer.

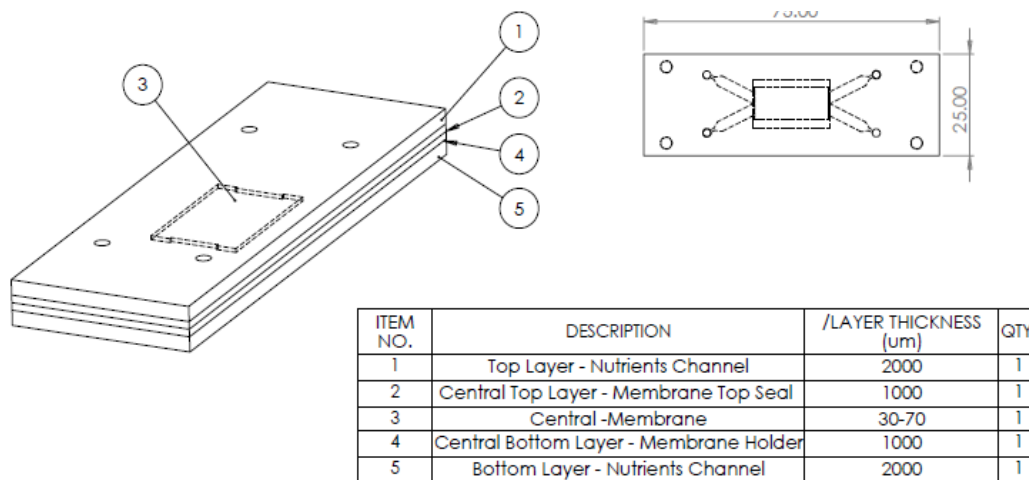


Figure 3.10 Final assembly of the VOC platform from a top view and isometric view with the membrane at the centre held in suspension between the channels.

### 3.7.1 Channel Dimension

The VOC platform prototype was designed to resemble the width and length of a microscopic glass slide 25x75 mm for easy handling of the platform. The channels dimensions have been designed with a width size of 2.75mm and height of 1mm (Appendix A, 9.1). Dimensions are large in scale when compared to the width and height of the channels for both the lung-on-chip and gut-on chip which have channels dimension of (400 $\mu$ m x 100 $\mu$ m). The VOC was designed to allometric scale with larger channels to provide sufficient nutrients to the membrane. The channels meet at the centre of the chip where the membrane is located (Appendix A, 9.1). A wider opening of the channels near the membrane will provide a dynamic flow of media to cells to mimic similar conditions that cells experience on a daily basis.

### 3.7.2 Top and Base VOC Moulds

Both the top and bottom VOC moulds have the same dimensions however, the top VOC mould contains extra in/out lets circled in red, Figure 3.11(A). The extra in/out-lets provides an access point for tubing to be inserted from the top layer. This allows the tubing to connect the top layer to the base layer to provide nutrient flow to the base nutrient channel. It is important that the layers are aligned properly for the tubing to reach the base channel.

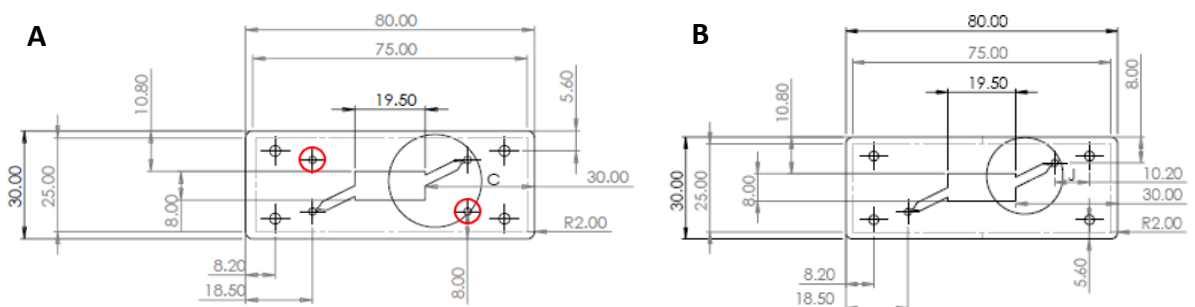


Figure 3.11 (A) Top VOC mould with extra in/outlet circled in red and (B) Base VOC mould with no extra in/outlets.

The membrane area 8 X 19.50mm seen in Figure 3.11 (A and B) was design in such a way to provide a larger surface area for 3D cell culture. Unlike other OOC model that mainly uses PDMS as the porous membrane, the VOC contains an electrospun membrane made from bio and synthetic polymers fabricated to support the growth of 3D vaginal tissue. However due to the thickness of the membrane with an average

depth of 0.2-0.7mm, being light in weight, it can be quite difficult to handle the sample manually. Therefore, a large membrane sample was required for easy assembly into the device as well as provide a large surface area for cell attachment.

### **3.7.3 Central top and base membrane layers**

To support the membrane in suspension the central top and base layers were designed as a gasket layer. The gasket layer also ensured the separation of the fluidic channels. As the nutrient channels cross over each in opposite directions, the central and base membrane layers provide sealing of the top and bottom fluidic channels when bonded to the middle layer of the platform. This also prevents leakage of nutrients into opposing channels. The central base layer contains membrane holders with a width and depth of 0.5mm on either side of the membrane area seen in Appendix A, 9.2.1 and 9.3.1. The electrospun membrane is placed between the central top and base and sealed by bonding, forming the middle layer of the VOC model.

### **3.8 Testing of VOC platform**

Initial testing of the VOC platform was conducted using blue and green colour dyes using the Fusion 200 two channel syringe pump (KR Analytical Ltd, UK). 5mL of dye was added to 15mL syringe (BD plastics, UK). Blunt 22G needles with an end of 0.5" were attached to the syringe via the Luer lock and silicone tubing 0.5 mm OD X 1.00 mm ID (Atlec, BEL). To connect the silicone tubing to the chip, 1cm of Polytetrafluoroethylene (PTFE) tubing, 1.58mm OD x 0.5mm ID (Sigma Aldrich, UK) was placed into the inlet and outlets of the chip. The syringe pump was set at a flow rate of 15  $\mu$ l/hr to produce a laminar flow that would mimic the dynamic flow cells and tissue would normally experience in the body. A steady flow rate was selected to prevent the chip from leaking, layers separating and cells from detaching from the surface of the membrane.

Figure 3.12 presents three individual VOC platforms and how the platform appears in three stages; (A) the VOC platform without the membrane, to visualise the channels positions on the chip; (B) the VOC platform with an electrospun membrane at the centre of the chip separating the top and bottom fluidic channels and (C) the outcome of the flow experiment conducted with both blue and green dyes passing through the channels. The membrane is held in suspension with no sagging or mixing of the fluidic

in opposing channels. However, leakage of the blue dye can be seen on the top layer, this may be due to partial bonding around the channels. The VOC is a working prototype at preliminary stages of testing which was tested by conducted wet experiments. Computational fluid dynamics (CFD) simulation but was not conducted on the prototype due to time constraints, but simulations would be beneficial for future experiments. With simulations, challenges can be predicted, designs optimised and reduce material waste and cost of manufacturing.

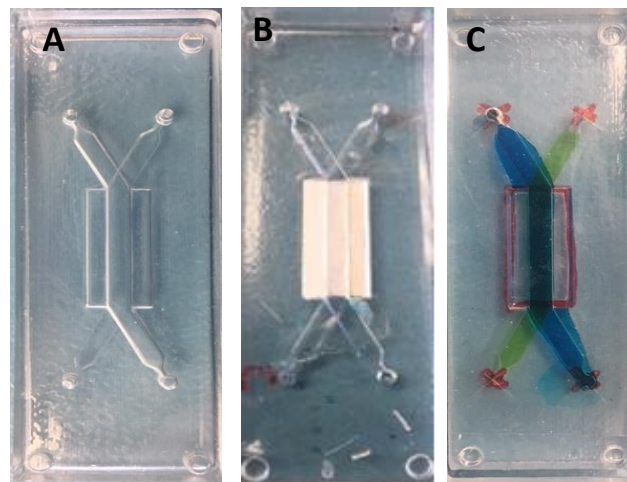


Figure 3.12 Three independent VOC chips (A) an empty VOC platform; (B) VOC platform with membrane between the two fluidic channels and (C) flow experiment conducted on VOC platform with colour dyes.

### 3.9 Summary

The main aim of the VOC platform design requirements was to contain a layer that would hold the membrane in suspension to support 3D cell culture. The VOC was designed to contain 3 main layers, two microfluidic channels and an electrospun membrane. The model also included alignment post to help with aligning of the layers. Alignment post features have never been used on an OOC device, but as the VOC contains multiple layers, it was essential to include these markers assist with alignment of the layers. The VOC design went through seven iterations (Table 3.2) to reach an optimised design for the final moulds that would be used to fabricate the VOC platform.

In Figure 3.9, layers of the VOC were shown in an exploded view to demonstrate the order of layer fabrication. The VOC, being at its preliminary stages of prototyping was

designed in the allometric scale i.e., microfluidic channel with a height of 1 mm and width of 2.75mm in comparison to the Lung-on-chip that has a channel size of 1mm in width and final chip size of 25 x 40 mm (Huh *et al.*, 2013). This was done to ensure nutrients were provided to the cells at the centre of the chip. The membrane area also contained a larger membrane sample of 8 mm x 19.50 mm ensure there was sufficient cell embodiment on the membrane as well as provide a large sample for further testing i.e., sample biopsies.

The channel height and membrane area of 1mm height was selected to provide enough space for 3D cell culture. The wider channels minimise the shear stress that cells may experience during the flow experiments. The role of the membrane holders which for the gasket layers was design to support the membrane in suspension between the fluidic channels but, also provided space between the channels to support 3D cell culture. As the membrane is porous, this would allow the cells to infiltrate the membrane by gaining support from the surrounding fibres and eventually forming vaginal tissues. With a larger surface area for cell adhesion, the VOC platform would provide larger samples to conduct statical data analysis.

The size of the VOC platform was designed to have a final dimension of 25 mm x 75 mm corresponding to the same size of a glass microscopic slide. This made it easier to manually handle the platform during experimentation. The platform underwent initial testing with colour dyes to observe the performance of the design, alignment and bonding of the layers. The next stages of testing would be to introduce the cells to the final VOC system to evaluate its performance, whether the VOC has the ability to mimic the function of to form 3D vaginal tissue. This test would then be carried out using the Elveflow system, a system designed to controlled flow and pressure within the VOC. Once established further, the system could then be challenged with bacterial strains to mimic the vaginal environment.

## Chapter 4 – Electrospun Membrane Fabrication and Evaluation

Electrospinning has been recognised as an effective technique to fabricate polymers into ultrafine fibrous mats. Due to their fibrous characteristics, they are commonly used as scaffolds to support various biomedical applications which include wound dressing, tissue engineering and drug delivery platforms (Z. M. Huang *et al.*, 2003). Electrospinning has been around since the 1930's and was mainly used in the textile industry to manufacture non-woven fibres. However, over the years the procedure had become increasingly popular especially in biomedical research, as polymer solutions and parameters were easily adjustable in developing scaffolds for tissue engineering applications (Kim *et al.*, 2009). The technique has the ability to produce electrospun mimic the structure of ultrathin fibres with a diameter than mimics the extra cellular matrix (ECM) (Kim *et al.*, 2009; Cipitria *et al.*, 2011). It also delivers a large surface area which, favours cell attachment and due to its porosity characteristics. This allows the scaffolds for the exchange of nutrients and waste material, ideal for drug loading applications (Cipitria *et al.*, 2011). Electrospun scaffolds can be fabricated using biopolymers which include gelatine (GE), collagen (COL), chitosan (CS) and synthetic polymers poly ( $\epsilon$ -caprolactone) (PCL), poly (lactic acid) (PLA) and polyurethane (PU).

Electrospun scaffolds can be fabricated using two methods, single and co-axial electrospinning which are described in the methods section 4.5 and 4.6. Kim *et al.*, 2009 stated that fabricating scaffolds using a single solution often produces higher fibre density which, leads to the growth of cells being restricted within the scaffold. Therefore, to overcome such drawbacks many researchers have explored the composite or blending of fibres to create scaffolds. This consisted of combining both bio and synthetic polymers. These scaffolds normally do not require a crosslinking agent to stabilise the fibres. This is due to their gel-solid like state transition during the hydration phase, unlike single or co-axial electrospinning. Single and co-axial spinning usually undergoes post treatment with a crosslinking agent like glutaraldehyde (GTA) or plasma treatment to stabilise the fibres (Cipitria *et al.*, 2011; Wang *et al.*, 2014). With the composite/ blended technique the synthetic polymer plays a vital role in supporting the



biopolymer as a nanofibrous backbone whilst the biopolymer acts as a promoter supporting the growth and adhesion of cells to the surface of the scaffolds (Kim *et al.*, 2009). For scaffolds, electrospinning is seen as the most favourable method in comparison to other methods like soft lithography, photolithography and bio-plotting which all can be costly and time consuming. Whereas electrospinning requires low-cost laboratory equipment, is versatile and multiple bio and synthetic polymers are readily available for use in research. Furthermore, electrospinning also provides the opportunity to control fibre diameter, alignment and reproducibility (Cipitria *et al.*, 2011).

In this chapter the development of nanofibrous membranes via electrospinning technique using biopolymers GE, COL and synthetic polymer PCL is presented. The membrane is part of the central layer of the VOC platform, designed to support the growth of vaginal tissue. GE, COL biopolymers and PCL a synthetic polymer were selected to fabricate the membranes due to their biodegradability, biocompatibility and mechanical properties. A combination of electrospinning methods was used to identify which method and type of membrane would be suitable for the VOC application.

#### **4.1 Requirement for a suitable membrane**

- Act as a scaffold to support the growth of vaginal tissue.
  - GE and COL biopolymers were selected for their biocompatibility and biodegradability properties to mimic the ECM to support 3D tissue growth.
  - PCL was chosen for its mechanical strength to support GE and COL fibres.
- To have a porous structure to control cell function and formation of new tissues.
  - The porosity of the membrane should facilitate cell seeding, infiltration and distribution of nutrients to the cells.
- A biocompatible surface suitable for cell adhesion, differentiation, and proliferation.

## **4.2 Biopolymers**

Biopolymers are natural polymers derived from cells of living organisms. They are mostly used in tissue engineering for the purpose of mimicking the ECM of tissue of interest. This is due to their biocompatibility, biodegradability, cell specific binding sites and fluid retention properties (Ramalingam *et al.*, 2019). However, biopolymers tend to have poor mechanical strength, degradability and usually requires crosslinking or combined with synthetic polymers to enhance their mechanical properties.

### **4.2.1 Gelatin**

Gelatin (GE) is a protein biopolymer which is derived from partial hydrolysis of collagen. Due to its good properties of being biocompatible, biodegradable, cell - specific binding sites, non-immunogenic and is commercially available at a low cost, makes this material favourable in the use of biomedical research (Zhang *et al.*, 2006; Daelemans *et al.*, 2018). However, gelatin being a polyelectrolyte, contains rigid chain conformations due a high number of hydrogen and ionising groups which makes it difficult to fabricate scaffolds via electrospinning (Nuge *et al.*, 2013). It is commonly combined with synthetic polymers to form fibrous scaffolds. Due to its solubility, scaffolds with gelatin often require crosslinking chemically or physically to ensure fibre stability.

### **4.2.2 Collagen**

Collagen (COL) is known to be the most abundant fibrous protein in the ECM for various connective tissue found in the body of animals and humans. It plays a major role in connective tissue that make up the skin, tendon, cartilage and bone. The main function of collagen in the body is to provide structure to the ECM, regulate cell function as well as strengthening of the bones. Collagen is generally weak in nature and has poor mechanical strength. Therefore, it is commonly crosslinked or blended with a synthetic polymer to enhance its mechanical properties without affecting the biological activity. Collagen has been widely utilised as a scaffold due to its benefits i.e., high surface to area volume ratio, cell adhesion, reasonable diameter and porosity for cell embedment and transportation of nutrients and provides mechanical cues to define cellular behaviour and formation of tissue (Law *et al.*, 2017a).

### **4.3 Synthetic polymer**

Synthetic polymers, derived from petroleum oil or man-made is commonly used for a variety of products ranging from medical devices to household items. They are often used in tissue engineering due to their beneficial attributes e.g., good mechanical properties, greater flexibility, highly durability and tensile strength. However, they can exhibit certain disadvantages for example being hydrophobic, lack cell-specific recognition sites and slow degradability, therefore requiring further characterisation to improve the surface properties for use in biomedical applications (Ramalingam *et al.*, 2019).

#### **4.2.3 Poly ( $\epsilon$ -caprolactone)**

Polycaprolactone (PCL) is a hydrophobic semi-crystalline polymer made from ring - opening polymerisation of epsilon-caprolactone which is commonly derived from carbon fossil (Nair *et al.*, 2017). PCL exhibits many benefits for example biodegradability, biocompatibility, easy to process and has desirable mechanical properties (Ramalingam *et al.*, 2019). Due to these properties, it is often used to make surgical implants, sutures, wound dressings and drug delivery application for tissue engineering. However, as PCL is hydrophobic it lack cell-specific recognition sites which affect cell affinity (Haslauer *et al.*, 2011; Daelemans *et al.*, 2018; Ramalingam *et al.*, 2019). PCL has a slow degradation rate of at least 3-4 years in water (Woodruff and Hutmacher, 2010)(Guarino *et al.*, 2017) however, it can be controlled by the use of enzymes and microorganisms (Nair *et al.*, 2017).

### **4.4 Materials and Methods**

Materials used to fabricate the electrospun membranes have been listed below, see section 4.4.1. The method used to fabricate the membranes was conducted by electrospinning. Each solution preparation and method has also been explained below, see section 4.5 - 4.6.1.

#### **4.4.1 Materials**

Polymers of gelatin Type A (gel strength 300) from porcine skin in powder form, Collagen Type 1 from rat tail in solution form, PCL ( $M_n$  80,000), solvents 2,2,2-

Trifluoroethanol (TFE) purity  $\geq 99.0\%$ , Glacial acetic acid (AA) purity  $\geq 99.0\%$ , Methanol purity  $\geq 99.8\%$ , Chloroform purity  $\geq 99.5\%$ , glutaraldehyde (GTA) grade I were all purchased from Sigma-Aldrich, UK. All chemicals were used as received. Teflon tubing with ID X1.00mm (Sigma-Aldrich, UK) and blunt needles 10G, 21G, 22G and 23G (RS, UK).

#### **4.5 Preparation of spinning solutions**

There are three ways of preparing electrospinning solutions depending on the method used. Single, composite and co-axial solutions for GE, COL and PCL which can be seen in section 4.5.1 - 4.5.3 for further details.

##### **4.5.1 Single solutions**

To make PCL 10% (w/v) solution, 1g of PCL pellets were dissolved at ratio 3:1 (chloroform: methanol). PCL was left to dissolve in 7.5 ml chloroform overnight on a magnetic stirrer at 300 rpm. Once dissolved, 2.5 ml of methanol was then added to the solution and left to mix for 1-2 hours until a honey like solution was produced (Spraybase, 2018).

##### **4.5.2 Composite solution**

Composite PCL (8% w/v)/GE (4% w/v) solution were made by dissolving 0.8g of PCL pellets and 0.4g of gelatin powder in TFE separately before combining together into one homogenous solution at 50:50 volume ratio and left to stir overnight on a magnetic plate at 300 rpm. Before using the composite solution, 100  $\mu$ l of acetic acid was added to the mixture and left to stir at 300 rpm for 1-2 hours to improve the miscibility of the solution before use. (Fu *et al.*, 2014 and Ramalingam *et al.*, 2019).

##### **4.5.3 Co-axial solution**

For the core-shell fibrous membranes, PCL/GE and PCL/COL solutions were made separately. For both membranes PCL (10% w/v) at (75:25) solution was made using the single solution method, see section 4.5.1 for the inner core of the fibres. GE (10% w/v.) and COL (4% w/v.) were both dissolved in TFE overnight at 300rpm. GE and COL were both used as the shell of the fibres respectively (Coimbra *et al.*, 2017 and Burugapalli *et al.*, 2018).

#### **4.2.4 Crosslinking**

Crosslinking is a chemical reaction that forms covalent bonds or short sequences of bonds that join two polymers together. Due to the nature of the biopolymers, gelatin and collagen are mechanically weak and soluble in water. Therefore, to improve their fibre stability and solubility in water PCL/GE and composite membranes were chemically cross-linked with GTA vapour (Burugapalli *et al.*, 2018). Samples were placed into a vacuum desiccator for 3 days with 10 ml of 25% aqueous GTA solution. Whereas PCL/COL samples were physically cross-linked under UV radiation for 30 mins before being used for further experimentation (Coimbra *et al.*, 2017).

#### **4.6 Electrospinning setup and single method**

The electrospinning setup, manufactured by AC solutions Ltd, UK seen in Figure 4.1 consists of a syringe pump Fusion 100 (KR Analytic, UK) placed in the horizontal position. The electrospun solution is placed into a 10mL syringe (BD, US), where a flow rate is applied and controlled by the syringe pump. The syringe is then attached to Teflon tubing with an internal diameter of 1.0 mm. Placed at the end of the tubing a long blunt needle also known as the spinneret, where the positive electrode is clamped to. Depending on the solution being spun, the distance between the needle and collective plate can be modified accordingly to produce nanofibers. The negative electrode is attached to a metal static plate covered in aluminium foil, non-shiny side up which makes it easier to remove as-spun fibre membranes for analysis and further experimentation. An adjustable high voltage supply (EL30R1.5, Glassman High Voltage Inc., UK) located at the top of the electrospinning unit is used to stimulate an electrical field required to establish the electrospinning process.

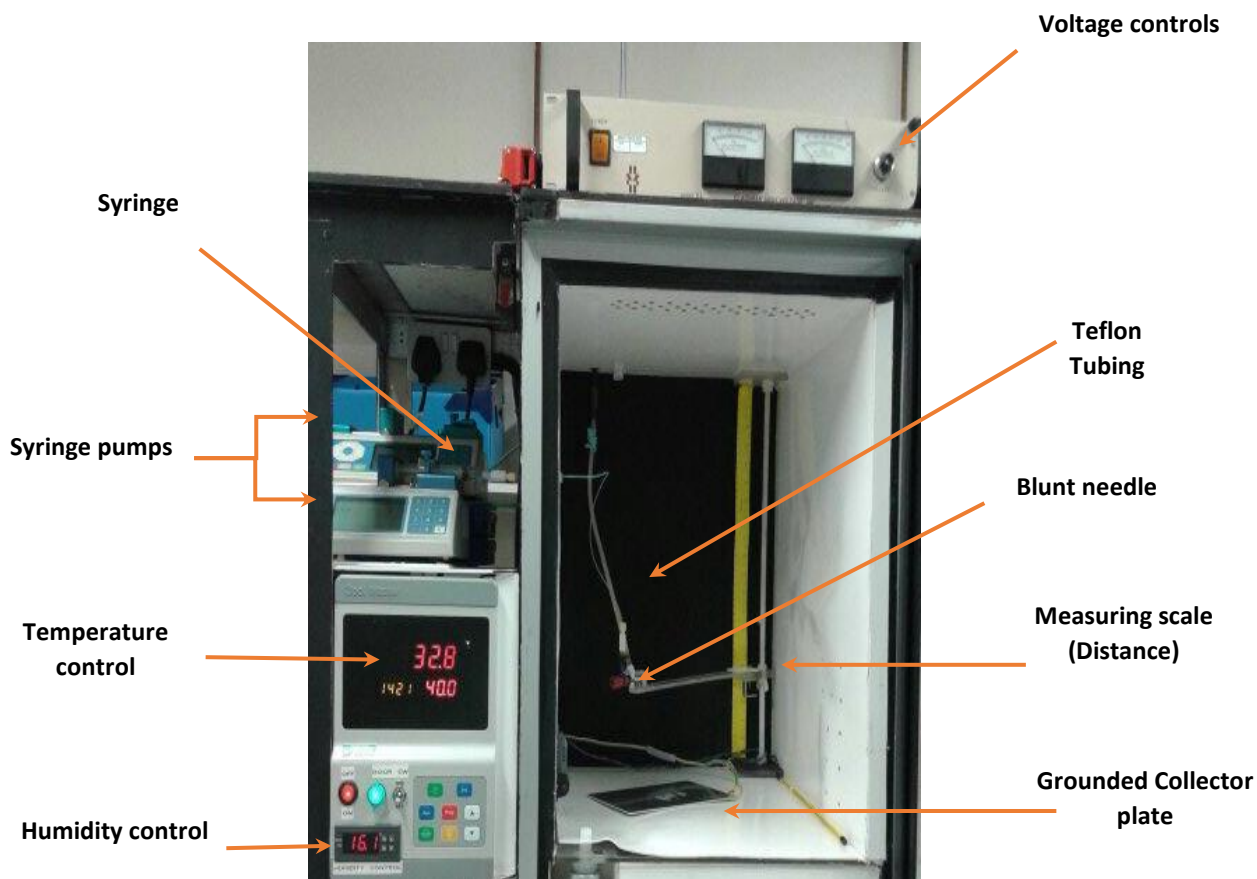


Figure 4.1 Electrospinning setup manufactured by AC solutions Ltd, UK.

The following solution parameters concentration, temperature, humidity, voltage, distance and flow rate were applied in reference to protocols for each sample and method which can be found in Table 4.1.

Table 4.1 Parameter settings used for electrospinning nanofiber membranes.

Electrospinning Parameters									
Method	Solution	Concentration	Solvent	Spinneret (G)	Height (cm)	Flow Rate (mL/hr)	Voltage (kV)	Temperature (C°)	Humidity (%)
Single	PCL	10% (w/v)	(75:25), Chloroform: Methanol	22	20	0.5	22.5	23-24	20-38
Single	PCL and GEL (Composite)	8%, 4% (w/v)	TFE	23	13-15	0.8 -1	17.5	24-25	55-65
Co-axial	PCL and GEL	10%, 10% (w/v)	TFE	21 (core) 10 (shell)	15	0.5, 0.8	12.5	23-24	40-50
Co-axial	PCL and COL	10%, 4% (w/v)	TFE		16-17	0.5, 0.3	17.5	23-24	23-24

#### 4.6.1 Co-axial spinning

The set up for co-axial spinning involves electrospinning two polymer solutions simultaneously to fabricate nanofibrous membranes. This is done by using a T-junction spinneret made with two blunt needles sharing an axis which, allows one solution to flow through the other creating the inner 'core' and outer 'shell' arrangement seen in

Figure 4.2 B. This method consists of two pumps placed at the horizontal position fusion 100 pumps (KR Analytic, UK), with two syringes connected to Teflon tubing. The samples were fed through at specific flow. Voltage and the height between the spinneret and collective plate were adjusted respectively to ensure stable fibre formation (Figure 4.2 A). Co-axial electrospinning parameters for both PCL/GEL (Coimbra *et al.*, 2017) and PCL/COL (Haslauer *et al.*, 2011) can be seen in Table 4.1. All experiments were carried out under ambient temperature and humidity. Membranes were left to crosslink and stored under sterilised conditions for a few days before being used for experiments.

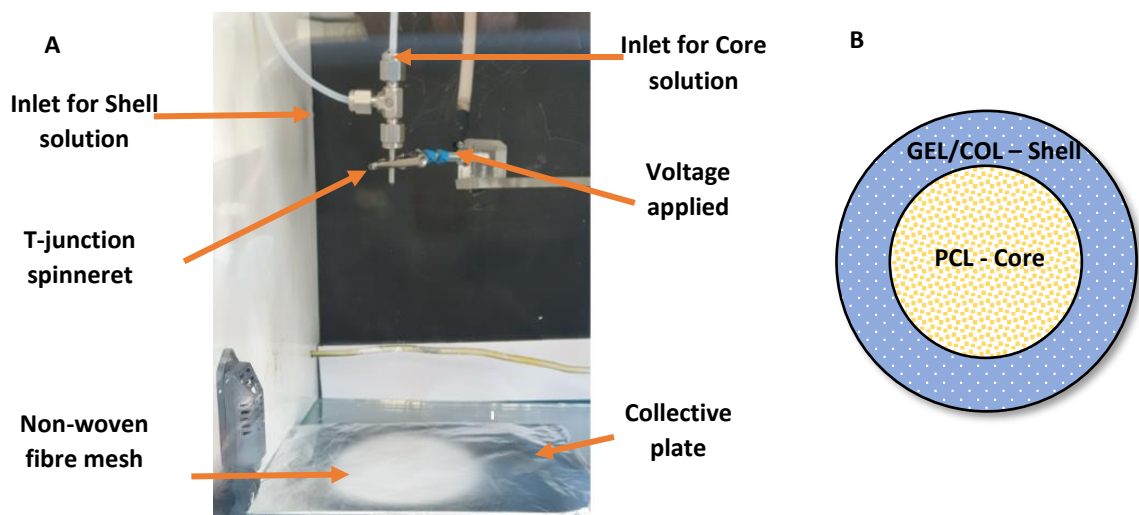


Figure 4.2 (A) Co-axial electrospinning set up; (B) Schematic of co-axial fibres with core (PCL) and shell (GEL or COL).

#### 4.6.2 Evaluation of Fibre Diameter and Morphology

Surface morphology and fibre diameter of the electrospun membranes were observed under scanning electron microscopy (SEM) (JEOL JCM-6000, Japan). Prior to SEM, small membrane samples were cut into 1 cm x 2 cm rectangles and placed onto stub holders with carbon tape to increase conductivity for coating. The samples were sputter coated in gold for 2 mins at 1.5 kV (OM-SC7640 Sputter Coater, UK) seen in Figure 4.3. SEM was then used to visualise the fibres of the membranes at an operating voltage of 15 kV.

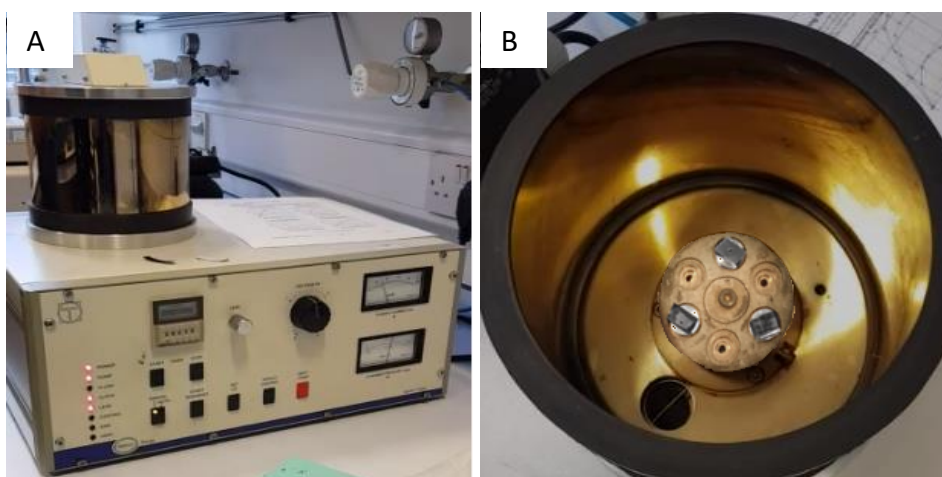


Figure 4.3 (A) Sputter coater device (OM-SC7640, UK); (B) 1 cm x 2 cm electrospun samples placed onto stub holders using carbon tape to sputter coat samples in gold for 2 mins.

#### 4.6.3 Fibre Diameter Measurement

SEM images were used to measure the fibre diameter of the membranes. Image J software (National Institute of Health, Bethesda, MD, USA) was used to calculate the average fibre diameter by randomly selecting and measuring at least 100 fibres per sample ( $n=3$ ) for each membrane ( $n=4$ ) to determine the average fibre diameter. SPSS Statistics (IBM software, USA) was used to analyse the data which were expressed as mean  $\pm$  standard deviation (SD).

#### 4.6.4 Contact angle measurements

Contact angle measurements were conducted on the electrospun membranes PCL, PCL/GEL, PCL/COL, and composite using the FTA32 a video-based goniometer (FLC, USA). The FTA32A and software, drop shape analysis was used to evaluate the wettability of each membrane. A syringe with a needle of 30G (ID 0.121 mm and OD 0.305 mm) was loaded with deionised water was manually moved to dispense a water droplet approximately 0.5 $\mu$ L on the membranes seen in Figure 4.4. The software captures the droplets shape automatically and calculates the angle between the slope of the droplet and the liquid-solid-vapor interface i.e., the surface of the membrane.



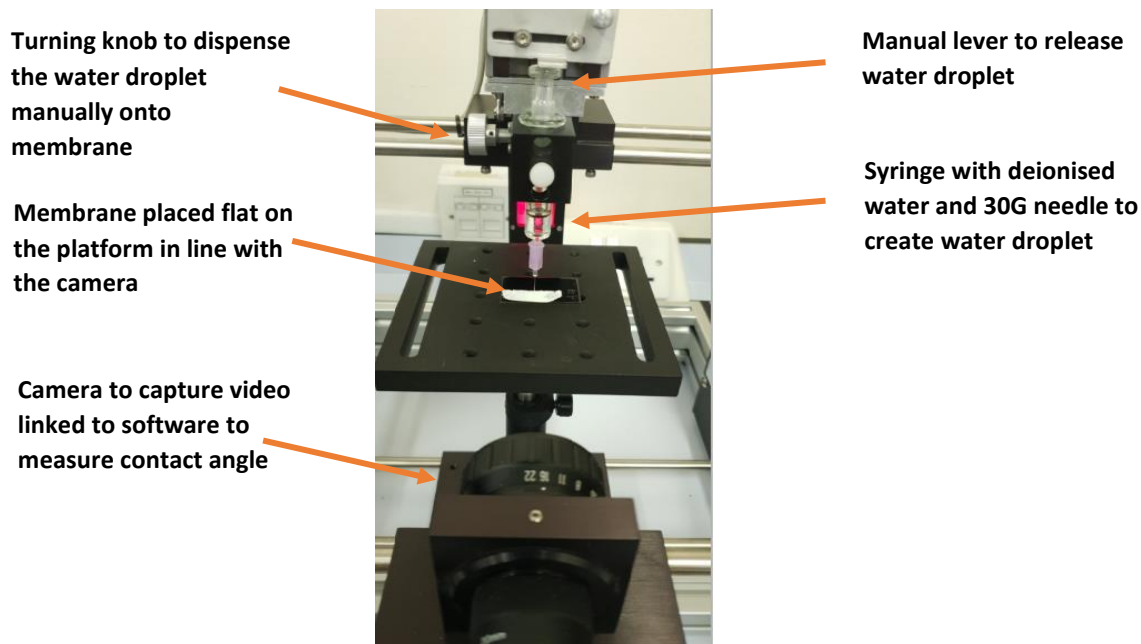


Figure 4.4 FTA 32A goniometer instrument use to measure contact angle of membranes (n=4)

#### 4.6.5 Uniaxial Tensile Measurements

Tensile strength measurements were conducted on the four (PCL, PCL/GEL, PCL/COL and composite) samples to determine the mechanical properties of each membrane. This test was performed using the Tensile Stress Testing Stage (TSTS350, Linkam Scientific Instruments, UK) equipped with a 20N load cell. Rectangular-shaped samples (3 cm x 1 cm) with an average thickness of 10-70  $\mu\text{m}$  were stretched in the y – axis at a constant crosshead speed of 250 $\mu\text{m}/\text{sec}$  (Figure 4.5). The samples were clamped and screwed down at the both ends to prevent samples from sliding during the testing (Ramalingam *et al.*, 2019).

LINK Control software was used to perform the mechanical tests. The thickness, length of sample, load cell and velocity parameters were entered into the software to run the experiments. Mechanical tests were conducted and repeated three times per sample in ambient conditions and ran until sample failure. Data sets from each membrane were combined and averaged to produce a stress-strain graph for analysis seen in Figure 4.7.

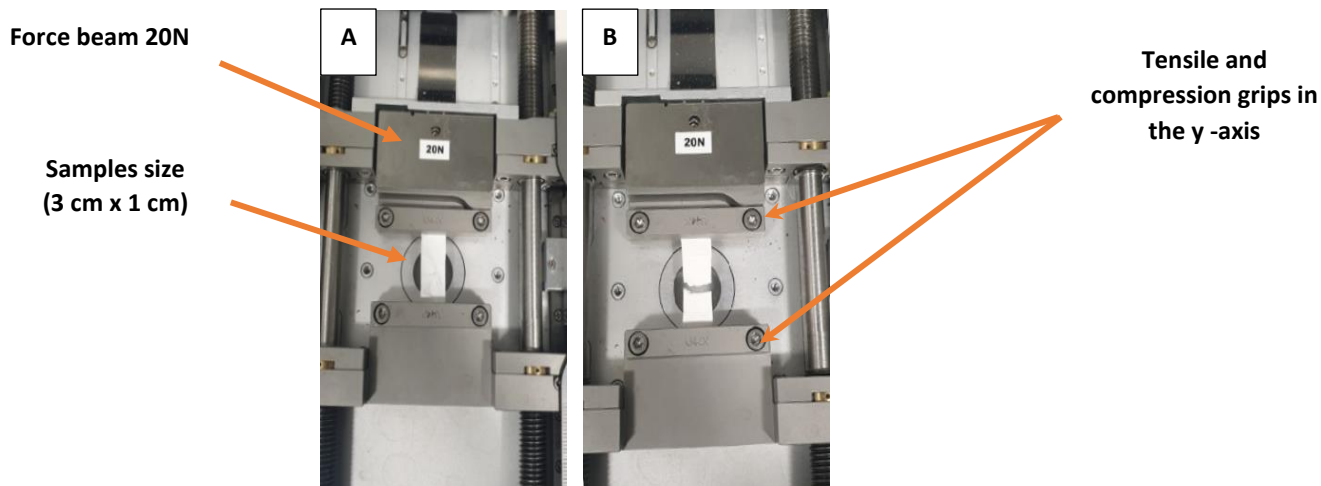


Figure 4.5 TSTS350, (Linkam Scientific Instruments, UK) measuring the tensile strength of an electrospun membrane under 20N load cell and pulled in the y-axis direction with a speed of 250 $\mu$ m/sec until sample failure. (A) sample at the stationary position; (B) Sample at failure.

## 4.7 Results

Below, presents the results of measurements and statistical analysis conducted on each membrane. These tests were done to evaluate performance of each membrane and to identify which sample would be suitable for the VOC platform.

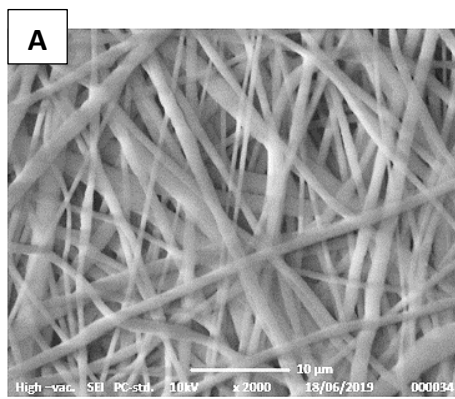
### 4.7.1 Morphology of Membranes

The following membranes PCL, PCL/GE, PLC/COL and composite were prepared using either the single, co-axial or composite methods as described above in section 4.5. SEM imaging was conducted on the membranes to observe the morphology of the fibres. Frequency percentage is usually measured as general practice to evaluate the average fibre diameter which was then analysed in SPSS (IBM Software, US). Figure 4.6 presents SEM images of each membrane with their corresponding fibre distributions. As seen in Figure 4.6 (A) PCL membrane, (C) PCL/GE membrane and (G) composite membrane the nanofibers appeared to be smooth, bead-free and uniformed, whereas in Figure 4.6 (E) PCL/COL membrane, displays smooth fibres but lacked uniformity.

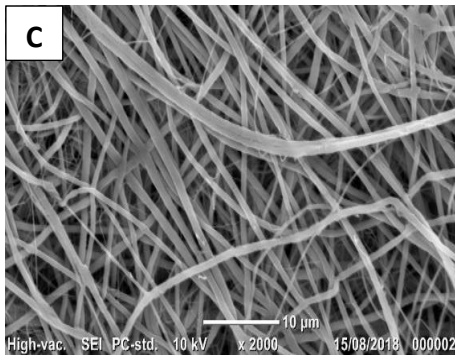
The membrane contained a mixture of large and small nanofibers that varied in diameter. In Figure 4.6 (B) PCL membrane had an average fibre diameter of 761.67  $\pm$ 237.296 nm, PCL/GEL membrane 575.65  $\pm$ 142.628 nm, PCL/COL membrane 540.55  $\pm$ 293.09 nm and Composite membrane 257.25  $\pm$ 72.919 nm. In comparison to PCL/GE and PCL/COL membrane, the composite membrane contained smaller nanofibers in

diameter due to the difference in concentrations used to make the composite solution. Composite membrane was made with a lower concentration of 8% PCL and 4% GEL which resulted in thinner fibres.

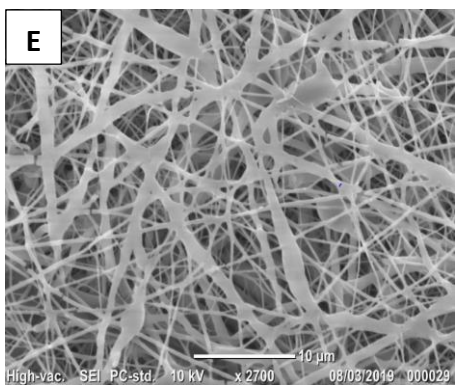
For tissues engineering it is desirable for electrospun membranes to have no beads with fibre diameters that closely resembles the ECM morphology to stimulate cellular growth. The membranes were fabricated to identify a suitable scaffold to support the growth of vaginal epithelial cells which are approximately 12-14 $\mu$ m in size. SEM was conducted on each membrane to examine the morphology of the fibres. A total of 300 fibre diameter measurements per membrane (n =4) were observed. Results indicated that all membranes exhibited thin, smooth and bead- free fibres, varied in size with a mean diameter between 260 nm - 765 nm, fibre diameter range that is suitable to support vaginal tissue.



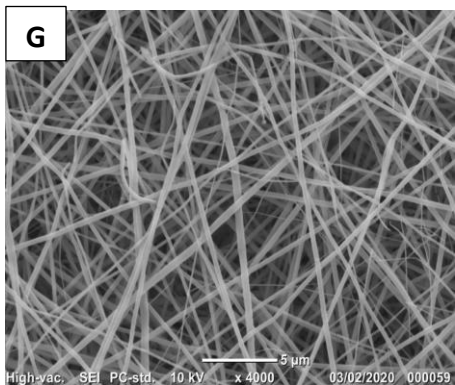
**PCL 10%(w/v)**



**PCL 10%(w/v)/GEL 10%(w/v)**



**PCL 10%(w/v)/COL 4%(w/v)**



**PCL 8%(w/v)/GEL 4%(w/v)**

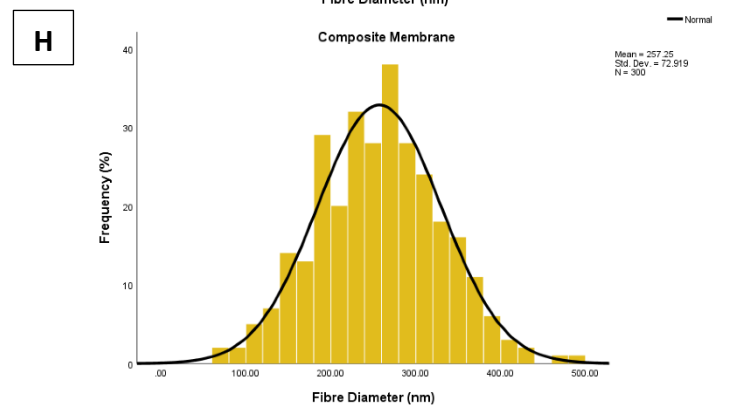
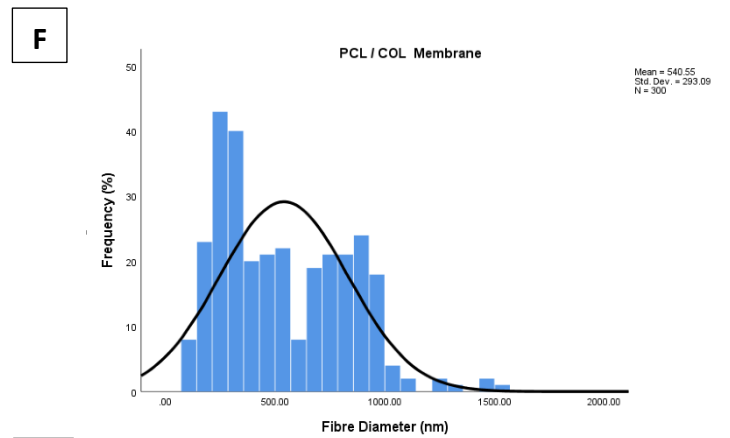
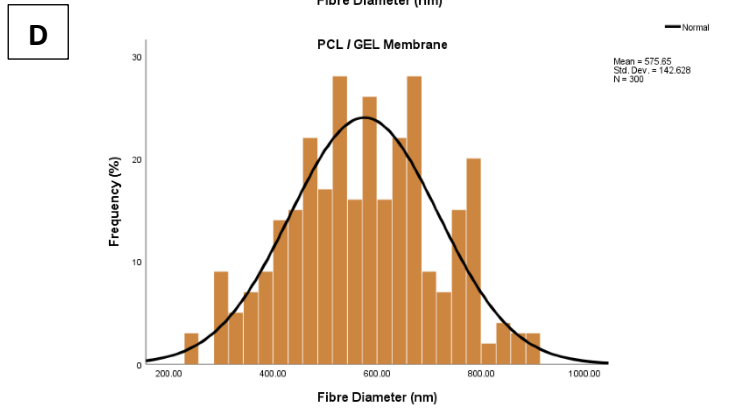
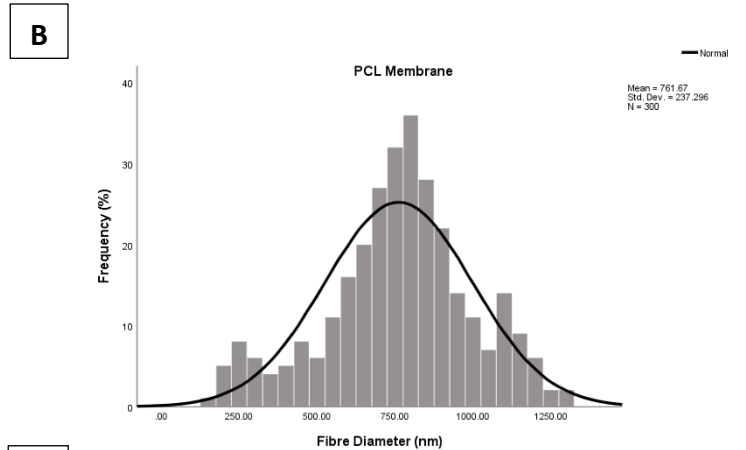


Figure 4.6. SEM of electrospun membranes (A) PCL membrane (2000x); (C) PCL/GE membrane (2000x); (E) PCL/COL membrane (2700x); (G) Composite membrane (4000x) with their respective fibre diameter distributions (B) PCL membrane; (D) PCL/GE membrane; (F) PCL/COL membrane and (H) Composite membrane.

#### 4.7.2 Stress-strain Curves

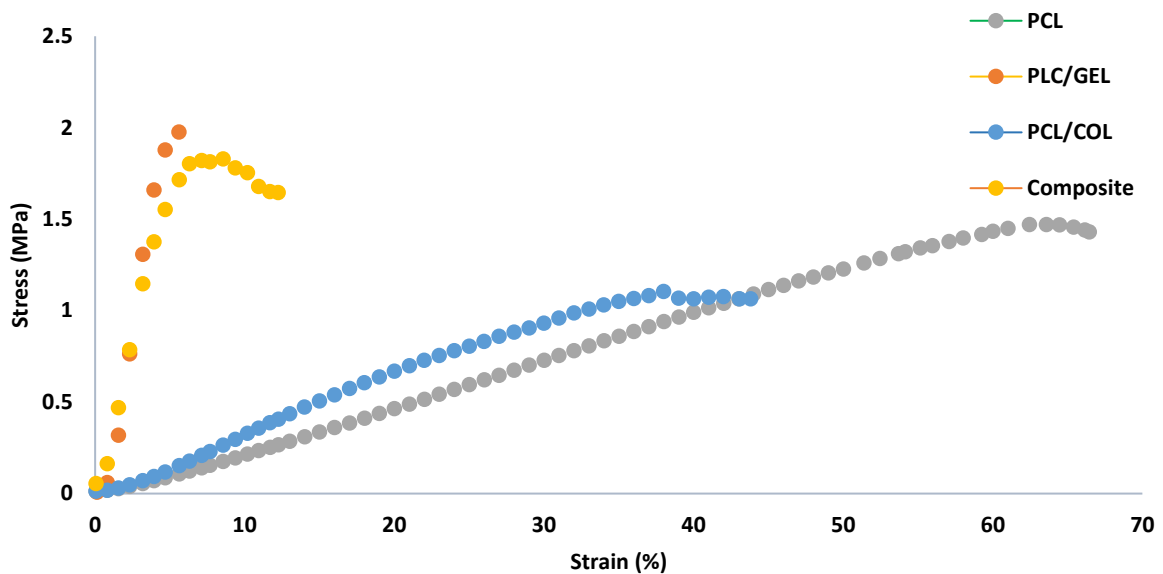


Figure 4.7. Stress -Strain curves on all electrospun membranes (n = 4)

The role of the fabricated membranes was to provide a scaffold that would mimic the ECM to support the growth of vaginal tissue at the centres of the VOC platform. However, it is important that the membranes also express similar properties to vaginal tissue. In order to understand the mechanical properties of the membranes, tensile strength measurements were conducted to evaluate the stress-strain behaviour in comparison to mechanical properties of vaginal tissue. The mechanical properties were compared to vaginal tissue from women with prolapse during prolapse repair surgery. Baah-Dwomoh *et al.*, 2016 indicated that strain at failure ranging from 19-41% and stress at failure ranging from 2.12-6.06 MPa for prolapsed tissue, whereas non-prolapsed tissue indicated strain at failure ranging from 20-46% and stress at failure ranging from 0.82-2.62 MPa.

Figure 4.7 expresses the stress-strain behaviour of the four membranes. The PCL membrane had a strain at failure of 65% and a stress at rupture of 1.4 MPa. The PCL/GE membrane had a strain at failure of 8% and a stress at rupture of 1.7 MPa. The PCL/COL membrane had a strain at failure of 43% and a stress at rupture of 1.2 MPa. The composite membrane had a strain at failure of 12% and a stress at rupture of 1.6 MPa. Figure 4.8 presents the PCL/GEL and composite membranes' stress-strain relationship more closely. The Young's modulus was also calculated and determined for the four membranes: (PCL) 25.8 kPa, (PCL/GE) 0.60 MPa, (PCL/COL) 35.5 kPa, and (composite) 0.42 MPa. Young's modulus measures the stiffness

of the material which, is defined by the relationship between stress and strain of a material. The results of the fabricated membranes indicated a variation in stiffness which expressed the composite membrane to show similarities of stress and strain values of non-prolapsed tissue, making it most suitable membranes for the VOC application. Due to the limitation of data available on the mechanical properties of healthy vaginal tissue the membranes were compared to tissue undergoing prolapsed repair surgery. For further statistical analysis, mechanical properties from at least 10 healthy vaginal epithelial tissue are required. The data could then be used to examine variance between healthy tissue and electrospun membranes, providing the target values as guidance to identify the mechanical properties required to fabricate a suitable membrane for the VOC platform.

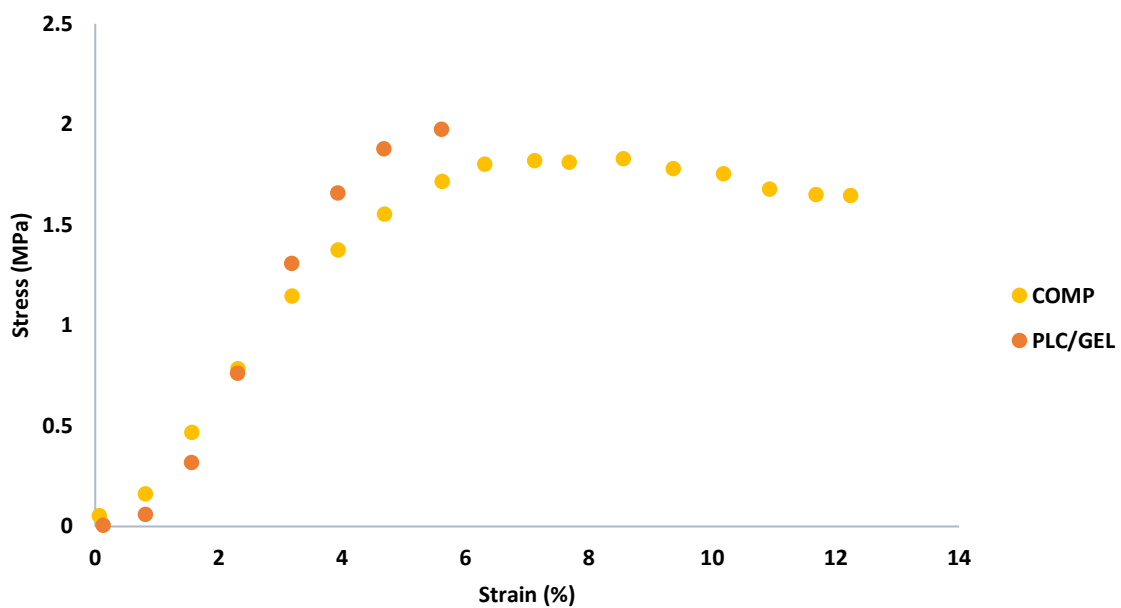


Figure 4.8 Stress -Strain curves of PCL/GE and Composite electrospun membranes (n=2).

### 4.7.3 Contact Angle

Contact angle (CA) measurements were conducted on all four membranes to identify the membranes wettability surface properties. CA measurement measures the angle between the solid surface and the water droplet dispensed onto the surface. The angle indicates whether the surface is hydrophobic or hydrophilic (Figure 4.9). The membranes have been experienced mechanical testing and fibre morphology observations to identify the best membrane for VOC platform. Therefore, it is essential that CA measurements is also considered has this parameter can have effect on cell attachment, migration and proliferation and the movement of the fluid flow in the channels of the VOC.

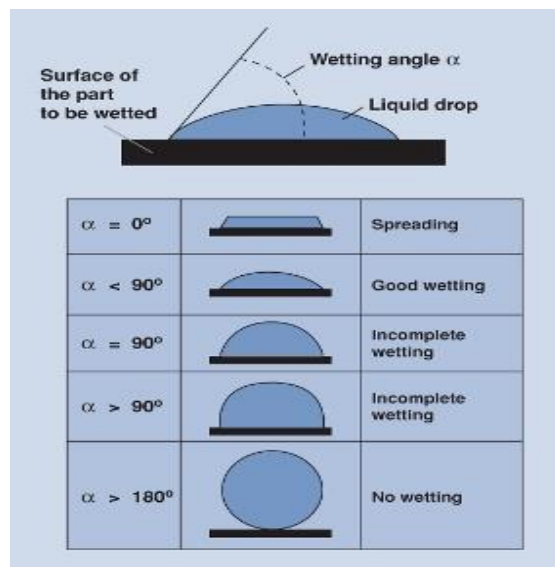


Figure 4.9 Contact angle measurement table presenting the angles for spreading to no wetting which informs whether a surface is hydrophobic or hydrophilic (Solving the Problems of Plastics Adhesion | Adhesion Bonding, 2012).

The results in Figure 4.10 demonstrates the contact angle for PCL, PLC/GEL, PLC/COL and composite electrospun membranes ( $n = 4$ ) at 0 seconds and 5 seconds which was repeated three times to refine the experiment observation for each membrane. From the results it was expected that PCL membrane would have a high CA as it is a polymer known to be hydrophobic gave a CA value of  $121.54^\circ$ . From 0 seconds to 5 seconds the angle did not change. In relation to the Figure 4.9 the angle is between  $90^\circ$ - $180^\circ$ , the water droplet indicated incomplete wetting the PCL surface. If PCL was selected as the membrane for VOC platform, the wettability properties must be altered to make the surface more hydrophilic for cell retention. To improve cell specific binding site, PCL can

be coated with collagen, fibrin or Arginyglycylaspartic acid (RGD) a peptide that can simulate cell adhesion to the ECM.

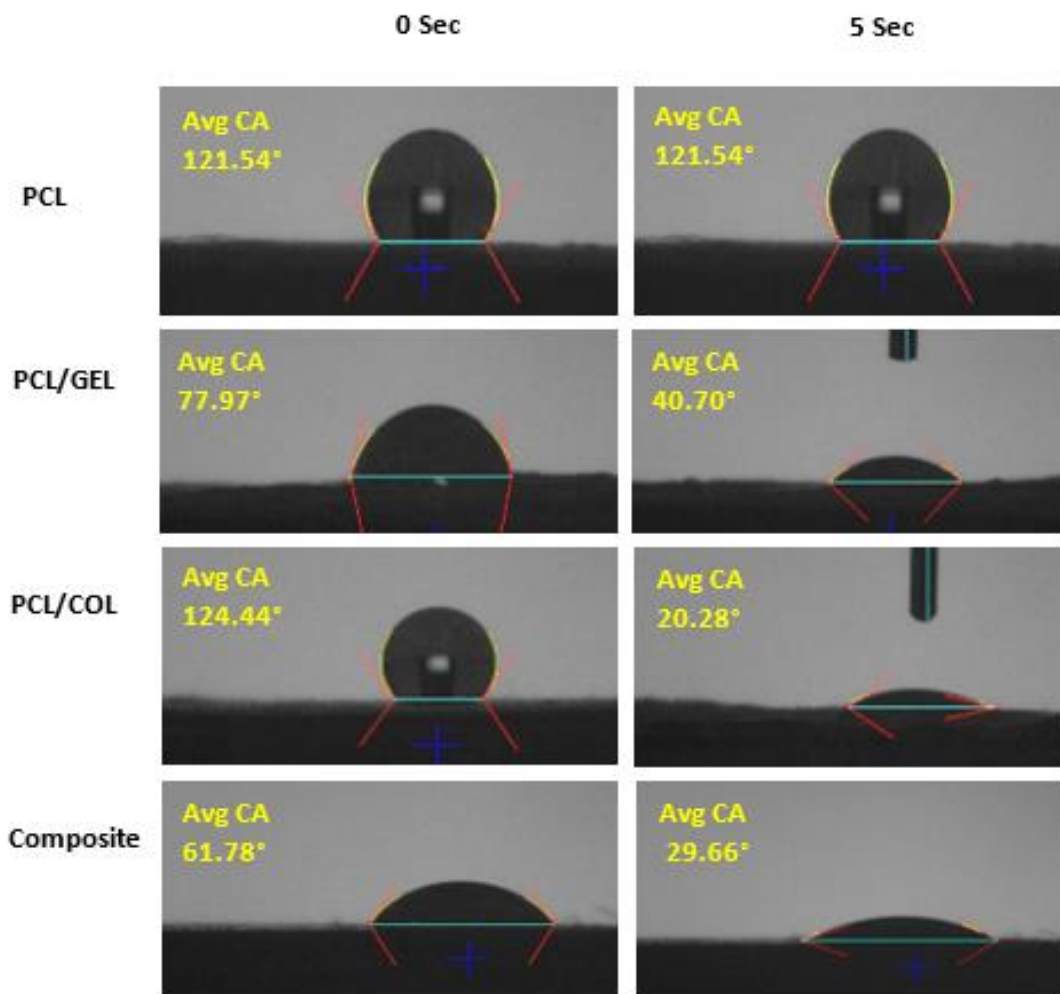


Figure 4.10 Water contact angle of PCL, PCL/GEL, PCL/COL and Composite membranes at 0 seconds and 5 seconds (n=4).

PCL/GE membrane had a CA of 77.97° at 0 seconds which decreased after 5 seconds to 40.70° indicating the surface had a good wettability angle from the beginning which gradually decreased over time. PCL/GEL membrane was electrospun via the co-axial method with the fibres in shell-core formation. Gelatin is known to be hydrophilic and is commonly used for biomedical applications like wound dressings and tissue engineering scaffolds. This is because of its good biocompatibility and cell adhesion properties. It was noted that the CA angle changed as the water wicked through the porous membrane. PCL/COL membrane had a CA of 124.44° at 0 seconds which at first exhibited an incomplete wetting angle but decreased to 20.2° after 5 seconds indicating the surface expressed good wettability. However, having a larger angle at the beginning



may cause issues during loading of sample to the surface of the membrane, which could lead to lack of cell adhesion. It would be ideal for the contact angle to be below  $90^\circ$  to improved cell adhesion and migration. The composite membrane expressed similar wettability properties to PLC/GE with a CA of  $61.78^\circ$  at 0 seconds which then decreased to  $29.66^\circ$  after 5 seconds, indicating the surface had a good wettability angle overall. Both the composite and PCL/GE membrane expressed good wettability, signifying they both could be ideal choice of membranes for culturing the vaginal cells.

#### **4.8 Electrostatics Forces**

Electrostatic force is a phenomenon where the properties of stationary or slow-moving electric charges are involved. This phenomenon arises from the forces that electric charges exert on each other and are described by Coulomb's law. The force can be attractive or repulsive and its strength can be easily higher than that of the van der Waals forces. The forces have been taken into consideration to understand the involvement electrostatic forces impact on cell adhesion which is curial for the VOC platform as the model contains an electrospun membrane to support the growth of vaginal tissue.

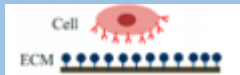
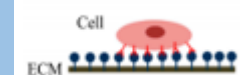
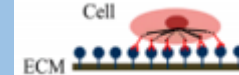



Van der Waals force is a term used to define the attraction of intermolecular forces between molecules. There are two types, London Dispersion Force and dipole-dipole forces. LDF is the weakest intermolecular force, it temporarily creates dipole forces when two adjacent atoms come into position. Whereas dipole-dipole force is similar to LDF but occurs in molecules that are permanently polar, meaning when polar molecular being positive attracts the negative pole of another molecular creating the dipole-dipole force.

Capillary force is the ability of a liquid that flows through narrow space without the need of external forces such gravity; this is due to two opposing forces; cohesion and adhesion. Cohesion is when there are attractive forces between similar molecular or atoms that can bond with neighbouring molecules. Whereas adhesion is the attractive force that happens between different molecules and atoms, for example molecule of cells adhering to the molecule of the polymers based in the electrospun membrane. Capillary force of a liquid is usually higher when adhesion force is greater than cohesion

force but when cohesion force is higher than adhesion force the capillary force is lower. Darcy law equation is considered for the VOC device, the law describes the flow of a fluid through a porous medium, the pressure in the y- direction is higher than that in the x-direction. The change in pressure is negative therefore the flow will be in the positive x-direction.

Cells are normally negative in charge, to ensure the cells adhere to the surface of a biopolymer/synthetic polymer the surface must be characterised. There are two ways to distinguish the surface charge of electrospun fibre mesh or other types of material being used as a scaffold 1) to measure the resistance across the membrane using the 2 / 4-point probe and by using the conductivity equation determine the resistance. 2) Working in reserve by using FTIR spectroscopy, an analytical technique used to identify organic, polymeric and inorganic material. The FTIR analysis uses infrared light to scan samples and determine the chemical properties. The chemical properties provide information of the chemical structure of the material for example the side chains which determines the surface charge of the material.

Table 4.2 Evaluation of passive In vitro cell adhesion intervention and stages (Khalili and Ahmad, 2015).

Cell Adhesion Phases	Phase I	Phase II	Phase III
Schematic diagram of cell adhesion			
Schematic diagram of the transformation of cell shape	 Initial attachment	 Flattening	 Fully spreading and structural organisation
Cell adhesion intervention	Electrostatic Interaction	Integrin Bonding	Focal Adhesion
Adhesion stages	Sedimentation	Cell attachment	Cell spreading and stable adhesion

In general, electrostatic interactions are repulsive because both cell and particle surfaces are negatively charged. In contrast, hydrophilic interactions and van der Waals forces tend to be attractive. Initial adhesion occurs when attractive forces overcome repulsive forces. Porous medium properties in conjunction with cell surface properties determine the relative importance of each of these interactions. Table 4.2 illustrates how the interaction of electrostatic and van der Waals forces governs reversible adhesion at various distances between the cell and particle surfaces. When a cell surface is in actual contact with, or very close to, a particle surface, the attractive forces are very strong, creating a primary minimum.

The forces governing the primary minimum are short-range forces which include hydrogen bonding and ion pair formation. As the two surfaces are separated slightly e.g., by several nanometres, repulsive forces grow quickly and prohibit adhesion. At slightly longer distances, another shallower minimum exists called the secondary minimum. It is the secondary minimum that is responsible for the initial reversible adhesion of microbes. The figures in Table 4.2 show the cell and particle surfaces are not in actual contact at the secondary minimum. As a result, cells can be removed from the surface easily, for example, by increasing the water flow velocity or by changing the chemistry of the porous medium solution, e.g., ionic strength.

#### **4.9 Summary**

This chapter introduced the electrospinning technique and how biopolymers GE and COL and synthetic polymer PCL were used to fabricate the membranes for the centre layer of the VOC model. Observation of fibre morphology and fibre diameter indicated all four membranes contained smooth, bead-free nanofibers suitable for the VOC application. Tensile strength measurements of the membranes compared to vaginal tissue of prolapsed women undergoing prolapse repair surgery indicated the composite membranes to be closely related to the mechanical properties of non-prolapsed vaginal tissue and ideal for the VOC platform. Finally, contact angle was conducted to examine the wettability properties of each membrane. Results suggested that PCL/GEL, PCL/COL and composite membranes were the suitable scaffolds due to their CA angles being below 90°, exhibiting good wettability, ideal for wicking cells across the membrane and

supporting the growth of vaginal tissue. From the experiments conducted on the membranes it is clear that the PCL/GE and composite membrane seem more favourable choice of membranes for the VOC platform. To classify the choice of membrane, the membranes must be subjected to further experimentation i.e., biocompatibility and viability tests see chapter 5.

## **Chapter 5 – Assessment of VOC membrane biocompatibility using VK2/E6E7 (vaginal epithelial cells)**

To accomplish the central layer of the VOC, membranes were created using the electrospinning techniques and underwent mechanical testing, contact angle and Image analysis to identify which membrane would be ideal for the use of supporting vaginal tissue growth. Four membranes were fabricated using biopolymers GE and COL and synthetic polymer PCL. These materials were chosen for their biodegradability and biocompatibility but to ensure these were suitable for the VOC platform, cell culture and cell viability experiments were conducted on the membranes. Immortal cell line VK2/E6E7 vaginal epithelial cells was kindly provided by from Dr Fichorova (Brigham & Women's Hospital, Department of Obstetrics and Gynaecology, Laboratory of Genital Tract Biology) and was used for the experiments conducted in this chapter. The cell line is also available from the ATCC website, categorised under ATCC CRL-2616.

### **5.1 Materials**

Materials used for all the cell culture procedures and cell viability tests and fluorescence imaging have been listed below in further detail.

#### **5.1.1 Cell line**

Vaginal epithelial cells VK2/E6E7 was originally derived from the vaginal mucosal tissue from a 32-year-old patient who had endometriosis in 1996. Tissue samples were collected during anterior-posterior vaginal repair surgery. The cell line was created in 1997 which contained normal vaginal epithelial cells, immortalized through infection of human papillomavirus (HPV) type 16 (Fichorova *et al.*, 1997).

#### **5.1.2 Growth Media for VK2/E6E7**

The following ingredients were required for the growth media of VK2/E6E7 cell line: Keratinocyte serum free medium (SFM) 1X, 500mL, which contains L- Glutamine and a phenol red indicator. Additional supplements, epidermal growth factor (EGF 0.5mL, final concentration 0.1ng/mL) and bovine pituitary extract (1 vial BPE 2.5mL, final

concentration 50µg/mL) were provided separately. Penicillin-streptomycin (P/S 100X, 5ml with a final concentration of 100 units/mL) all components were purchased from Gibco Thermo Fisher, UK. Calcium chloride (CaCl<sub>2</sub>) (22.05mg with a final concentration of 0.4mM) was purchased from Sigma Aldrich, UK.

To make the correct composition of growth media for VK2/E6E7 cells, the following ingredients presented in table 5.1 were added to the 500mL of SFM 1X.

Table 5.1. Ingredients for VK2/E6E7 Keratinocyte serum free medium.

Ingredients	Volume
EGF – 0.0324ng/ul	1.54mL
BPE – 25mg	2.5mL (1 Vial)
CaCl <sub>2</sub> , – 22.05mg with a final concentration of 0.4mM	500µl
Penicillin-Streptomycin (P/S) 100 units/mL	2mL*

\* 2mL of (P/S) was only used for the first time when culturing the cells for stock keeping. To maintain the cells media without P/S was used, this was done for the purpose of using the cells for experiments with bacterial.

Two vials of VK2/E6E7 cells with passage numbers P37 and P42 were provided by Dr Fichorova. P37 was stored immediately for future use due to the low passage number with respect to the passage numbers provided. Though both passage numbers were high, this was taken into consideration to monitor and evaluate the performance of the cells especially during experiments as cells with high passage numbers tend to experience changes in morphology, growth rates and protein expression.

After preparing the media, vial P42 was taken out of the dry ice and left to thaw at room temperature in preparation for cell culturing. To ensure cells were proliferating well, two types of media were created, one with P/S and one without. Cells were first grown with media containing P/S to achieve sterile and optimal growth to freeze cells for stock. P/S is commonly used in cell culture protocols to maintain sterilisation, inhibit bacteria growth and to prevent contamination. However, a vial of cells was taken and continuously grown in media without P/S to achieve cell culture. This was done to

ensure cells were able to grow without the need for antibiotics and to conduct experiments with bacterial species i.e., *Lactobacillus Crispatus*.

### **5.1.3 Growth Media for Resuspending**

Gibco DMEM/F12 (Dulbecco's Modified Eagle Medium/Nutrient Mixture F-12) – widely used basal medium used for growing many different mammalian cells. The medium was supplemented with 10% of Horse serum. Both were purchased from Gibco, Thermo Fisher, UK.

### **5.1.4 Trypsin – EDTA (0.05%), phenol red**

Gibco Trypsin-EDTA is a proteolytic enzyme mixture derived from porcine which is used to dissociate adherent cells from the surface of the flask they are cultured in. The trypsin breaks down the protein that allows cells to adhere to the surface. It is commonly used for cell dissociating and routine cell culture passaging.

## **5.2 Methodology**

The following methods presented below in section 5.2.1 -5.2.7.1 were carried out to conduct the cell culture, cell viability and fluorescent imaging experiments.

### **5.2.1 Thawing and culturing of VK2/E6E7 cells**

Cells are taken out of liquid nitrogen or dry ice and placed on ice. They are then transferred onto a water bath at 37°C until completely thawed (inverting occasionally). Once thawed, 1 ml of cell suspension was then transferred into a 15 ml centrifuge tube (Thermo fisher, UK). 9 mL of DMEM/F12 media supplemented with 5% Horse serum was added drop wise to the cell suspension. This step was done slowly to avoid media and cells mixing. A total of 10 ml cell suspension was then centrifuged for 5 mins at 1000 rpm to remove freezing media of which the cells were stored in, when in liquid nitrogen. The cell supernatant was then removed, leaving the pellet of cells, which is then carefully resuspended in 1 ml of pre-warmed (37°C) SFM media. 9 ml of fresh pre-warmed (37°C) SFM media was then added to a T75 flask (Thermo Fisher, UK) and to this, 1 ml of cell suspension was transferred. Cell culture procedures are always conducted under the laminar flow cabinet to prevent contamination. The flask is then

gently moved in a north to south, east to west movement for the cells to spread evenly across the flask. The cells are then checked under a light microscope to ensure they are in single cell suspension and not in clumps. The flask is sprayed with 70% ethanol and placed into the incubator at 37°C with 5% CO<sub>2</sub> for 48 hours for cells to start proliferating in optimal conditions.

### **5.2.2 Maintaining cells**

Media is changed every 2-3 days depending on the colour of the media. For T75 flask 10ml -15 ml of media can be fed to the cells; for T25 flask 5-7 ml of media. SFM is light pink in colour and as cells start to proliferate and absorb nutrients from the media a change in colour can be noticed. If media is left unchanged for longer than 3 days, the media will start to appear orange/yellow in colour, this is due to metabolites being released by the cells which causes the media to become more acidic, resulting in a lower pH. Therefore, cells must always be monitored and handled carefully to avoid contamination and human error.

### **5.2.3 Health of a cell line**

To maintain a healthy cell line, the growth of the cells is maintained by evaluating the standard growth curve. Growth curves are used to understand the growth characteristic patterns of cell lines. After seeding the cells, the cells enter the lag phase where cells grow slowly as they begin to adapt to their environment. This is then followed by an exponential growth called the log phase (Figure 5.1). During this phase, cells begin to consume all the nutrients in the growth media and expanded with no room left to develop further. It is at this stage the cells should then be sub-cultured or harvested to maintain optimal cell density for future experiments, where cells would stimulate and proliferate further. When cells have exceeded the capacity of its growth media, the cells then enter the stationary phase where proliferation is significantly reduced or terminates completely. Passaging at varying cell densities provides the opportunity to monitor cell behaviour and to achieve the optimal growth and yield appropriate for the cell line of interest. To ensure optimal growth, cells must be monitored. Changes in media (colour and pH), turbidity, contamination or environmental factors i.e., changes in temperature or gas can indicate the culture is unhealthy. This can be seen at



macroscopic level by eye, but further examination can then be performed using an inverted light microscope to check cell morphology and growth patterns. It is important to understand the cell line and maintain a cell culture protocol to make sure cells are grown at optima conditions (Straube and Müller, 2016).

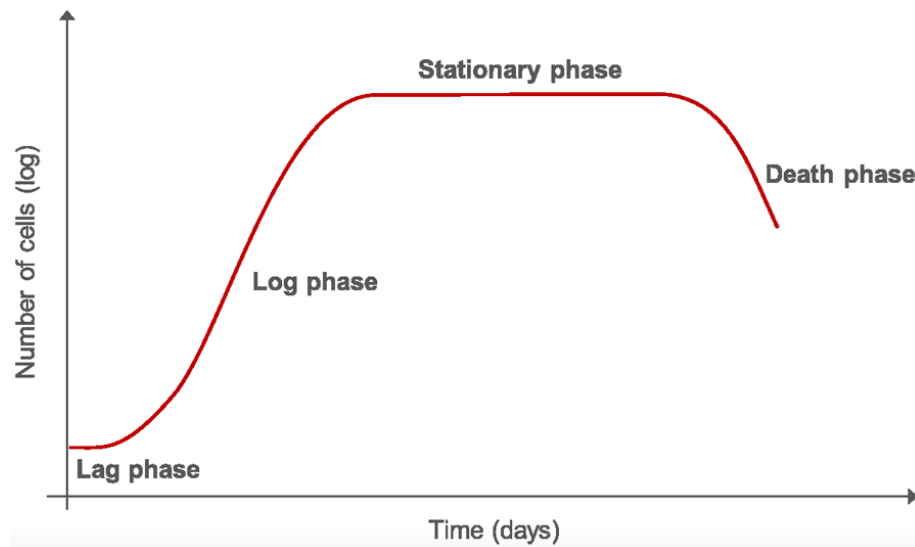


Figure 5.1 Growth curve presenting the four phases' cells go through during cell culture. Lag phase, cells grow slowly adapting to their environment. The log phase is where cells experience exponential growth by consuming the nutrients from the growth media. At the stationary phase cell growth begins to reduced significantly leading to the death phase where cells die, caused by lack of nutrients and inhabitable conditions (Straube and Müller, 2016).

#### 5.2.4 Subculture cells

It is important that cell lines are passaged and harvested before cells reach confluence, this is to ensure cells maintain their phenotype and culture quality. If cells are left to reach confluency, they take longer to recover. VK2/E6E7 cells were harvested at approximately 60% in confluence. If experiments required a large seeding density, cells are then sub-cultured into different dilution factors of 1:10 and 1:5. Experiments should be completed within 10 passages as cell lines will start to changes in morphology, growth rate, protein expression and response rate compared to lower passaged cells.

To subculture VK2/E6E7 cells, cells are observed under a light microscope to confirm cells had reached a confluence level of approximately 60%. Once confirmed, media was then removed from the flask and briefly rinsed with 5 mL of (pre-warmed at 37°C) Trypsin – EDTA (0.05%) for a T75 or 3 mL for a T25. The Trypsin – EDTA (0.05%) was

immediately removed and replaced with 5mL Trypsin – EDTA (0.05%) for a T75 or 2 mL for a T25. Flasks were then sprayed with 70% ethanol and placed into the incubator at 37°C for about 10 mins for cells to detach from the surface of the flasks. Detachment of cells were then checked under the light microscope.

To terminate the trypsinisation, 10 ml of neutralisation buffer (pre-warmed DMEM/F12 media with 5% horse serum) was added to the cells for a T75 or 5 ml for a T25. During this step, neutralisation buffer was pipetted up and down a few times to capture all cells on the surface on the flask. 13 ml of cell suspension from a T75 or 7ml from a T25 flask was then transferred into a 15 mL centrifuge tube and centrifuged for 5 mins at 1000 rpm. The cell supernatant was then removed, and the remaining pellet was resuspended with pre-warmed (37°C) SFM media depending on the dilution factor required. Cells are then distributed accordingly into flasks with fresh pre-warmed (37°C) SFM media. Cells are then checked again under the light microscope for single cell suspension before being placed into the incubator at 37°C with 5% CO<sub>2</sub>.

### **5.2.5 Cell counting**

Cell counting is important, to identify the cell density in a flask for either freezing cells or for experiments. Cell are counted and diluted, respectively. During the sub-culture process 1 ml of suspension is taken aside for counting. A plastic disposable haemocytometer was used for counting cells manually. Approximately 10-20 µl of cell suspension is pipetted onto two chambers that contain a grid of 10 large square that measures 1 x 1 mm, each square contained a smaller grid of squares 4x4 (16 cells). The haemocytometer is then placed onto a light microscope and cells are manually counted. All 10 squares were calculated for both chambers and averaged. Once the total number of cells have been calculated the cell concentration can then be determined by using the following equation (1). Usually a T75 flask with VK2/E6E7 cells has a total cell concentration of ~3million cells. For T25 has a total cell concentration of about 1.5-2 million cells.

Limited studies have worked with VK2 E6/E7 cell line but according to the following studies by Fichorova *et al.*, 1997; and Saha *et al.*, 2017 the cell line maintained a stable phenotype after passaging continuously for more than a year. Whereas, Radwan-

Pragłowska *et al.*, 2020 conducted their experiemnts with cells at passage 1 and 5. The cells took over a week to reach 60% in confluence but this may be due to the high passage number which influence the growth rate. A grow curve was not conducted but would have been helpful to evaluate the health of the cell line before experimenting. This would be beneficial for future work with the cell line.

$$(1) \text{ Total no. of cells/ml} \frac{\text{Total number of cells counted}}{\text{no. of 4x4 squares}} \times (\text{Dilution factor}) \\ \times 10000 \text{ cells/ml}$$

### 5.2.6 Cryopreservation of cells

To stock the cell line for future experiments cells were frozen at their earliest passage number in respect to the passage number provided. When cells have reached a confluence level of about 60-70% they are then ready to be frozen. First, freezing media is made using the following the procedure in table 5.2. The freezing media was made to a total volume of 20 ml.

Table 5.2. Components required freezing media

Components	Volume
70% DMEM	14ml
10% DMSO (Dimethyl sulfoxide)	2ml
20% serum (if using DMEM complete media it already contains 5% serum therefore only need 15% of serum)	3ml

DMSO is added to the media before adding the serum to the mixture. All components were thoroughly mixed well and stored at 4°C until further use. A Mr frosty container with isopropanol (IPA) was left to refrigerate at 4°C until use. Cells to be frozen go through the subculture process of being trypsinised, neutralised and centrifuged to obtain the pellet. Just before centrifuging an aliquot of cell suspension was used to calculate the cell concentration for each vial to contain 1 million cells.

Once centrifuged the supernatant is removed and an appropriate volume of freezing media is added to the pellet. Cells are gently resuspended with 1 ml of freezing media and transferred to the 1.2 ml cryovials (Alpha Laboratories, UK); special vials used for cryopreservation. The vials are then labelled with the cell line name, passage number

before trypsinisation, date and initials. The vials are then placed into the Mr frosty and refrigerated at - 80°C. This allows the vials to freeze at a rate of 1° C/min. The vials are left for overnight at - 80°C before being transferred to liquid nitrogen.

### 5.2.7 Observing cells

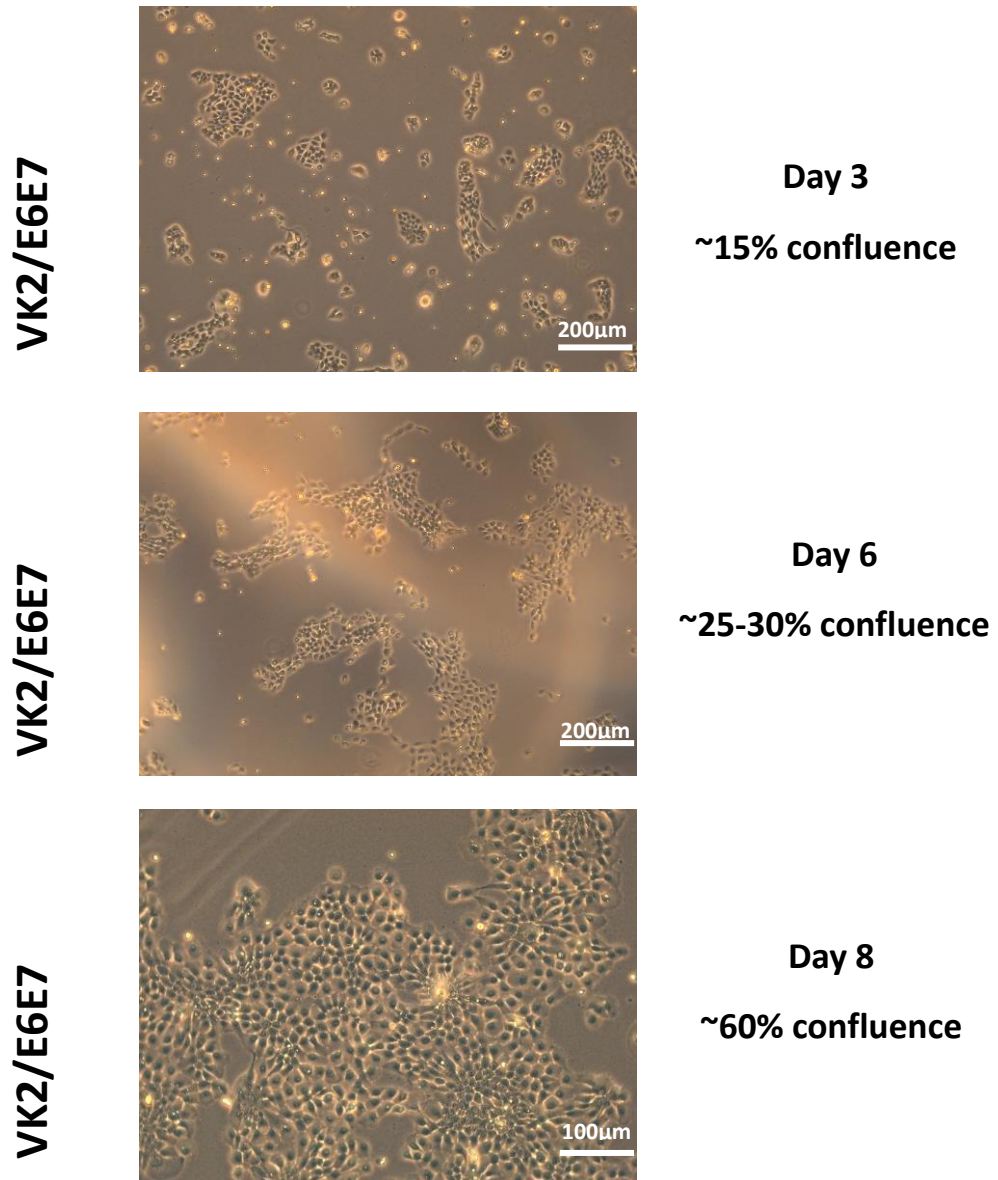


Figure 5.2 Cells observed on days 3,6 and 8 on the Lecia microscope x40 magnification.

Figure 5.2 presents the VK2/E6E7 cells progression of proliferating over 8 days. On day 3 cells were observed at approximately 15%, by day 8 it had reached about 60% in confluence. From examining the cells morphology under the light microscope, cells begin to form small colonies after 3 days in incubation and the proliferate into large clusters by day 8. During observation cells at the centre of the clusters would turn into

a start formation, die and shone brightly but was always surrounded by live cells. This can be seen in Figure 5.2 at day 8 which is particular behaviour of this cell line which has not been seen in other epithelial cell lines.

Cells were continuously observed and maintain carefully to avoid contamination resulting from human error or ambient environment. Culturing procedures were always conducted under the laminar flow cabinet. All equipment were sprayed with 70% ethanol before use to prevent contamination. When contamination occurred cell culture experiments were terminated. The incubator and flow cabinet used were deep cleaned with 1% of distal solution to clean infected areas and then sprayed with 70% ethanol. Cell culture was carefully planned to guarantee cells would be ready in time of experiments i.e., biocompatibility and cell viability tests using MTT assays on membranes, bacterial work, and fluorescent imaging on the electrospun membranes.

### **5.3 Cell viability test (MTT) – Electrospun membranes (24 well plate)**

The materials selected to make the electrospun membranes were specifically chosen due to their mechanical, biodegradable and biocompatible properties. As mentioned in chapter 4 both GE and COL, biopolymers will provide anchoring properties for cells adhesion to occur at the surface of the membranes. Synthetic polymer PCL was used to provide the mechanical strength to the nanofibers to support the growth of vaginal tissue. After successfully growing the vaginal cells in T75/T25 flasks the next step was to culture cells onto the electrospun membranes to test for biocompatibility. This was done to identify the potential scaffold that would be implemented in the VOC system.

MTT assay is a colourmetric assay that is used to measure the cell proliferation through cellular metabolic activity. A yellow dye, MTT 3-(4,5-dimethylthiazol-2-yl)-2,5-diphenyltetrazolium bromide (Tetrazole) was applied to the cells which passed into the mitochondria where it is reduced by mitochondria reductase enzyme into purple insoluble formazan crystals. These crystals can only be found in the mitochondria of living cells (Riss. T.L, et al 2004). It is a simple method that provides visual and quantitative results by measuring the optical density of living cells (Figure 5.3).



the membranes to prevent them from floating during the experiment. A 168 hrs, 72 hrs and 24 hrs were the set time points for data collection. Each column contained two membranes as replicates and two controls for that data point. VK2/E6E7 cells were first seeded on the first column of wells which represented 168hrs, the second column 72hrs, third column 24 hrs with the fourth column set as the control (well with cells only).



Figure 5.4 24 well plate with membranes held down in the well with nitrile O-rings to prevent samples from floating during experiments.

Cells were monitored and media was changed when necessary. The experiment lasted a week and on the final day of the experiment the MTT assay was performed. Cultured media was carefully removed from the well without disrupting the membrane and cells. Then to the well, 500  $\mu$ l of MMT solution (1/20 dilution added to DMEM media) was added to the membranes and left to incubate at 37°C for about an hour until crystals were formed. When crystal could be seen, the MTT solution was then removed from membranes and control samples. This was followed by a wash step of 500  $\mu$ l of HBSS (Hank's solution, Gibco Thermo Fisher, UK). Once all HBSS solution was removed from the wells 500  $\mu$ l of DMSO was added to the samples to dissolve the formazan crystals. The plates were then left on the shaker for 30mins and covered with aluminium foil due to DMSO being light sensitive. After shaking, the crystals dissolved producing a purple solution. The darker the solution to more viable cells is present in the sample. 20  $\mu$ l of each sample is then transferred into a 96 well plate, labelled and placed on a spectrophotometer to read the absorbance at 570 nm and 620 nm. Then optical density

data of the samples were collected and then compared to the controls to identify the biocompatibility of the membrane.

#### **5.4 Statistical Analysis**

The MTT experiments were repeated three times for each membrane. Each membrane had two replicate samples each ( $n = 4$ ). MTT assay was conducted three times at different data points, 24hrs, 72hrs and 168hrs to investigate significance of vial cells between the different time points on the different membranes. Experimental data was presented as  $\pm$  standard deviation (SD). ANOVA test was conducted to compare the difference between two groups in this case between the membranes for statistical comparison. The difference between the mean values of each group were evaluated by using a two-sample t-Test assuming equal variance in which p - value less than 0.05 was considered significant. The two-sample t-Test was conducted in Excel, where the data from each membrane for 24hrs, 72hrs, 168hrs and controls of each independent test were pooled together and normalised. The difference means from each membrane were compared with each other and against the control to identify which membrane was the most biocompatible in terms of cell viability.

#### **5.5 Results and discussion**

Results and discussion of the biocompatibility tests, fluorescence and SEM imaging performed on the electrospun membranes have been discussed below.

##### **5.5.1 MTT results conducted on Electrospun membranes**

The following results depicted in Figure 5.5 -5.7 represents the data obtained from the MTT assay experiments. The MTT assay was conducted to measure the number of viable cells that remained attached to the membranes after incubation period. This was then compared to the control. The experiment was carried out on following membranes PCL, PCL/GE, PCL/COL and composite to investigate the compatibility of membranes in order to identify a suitable membrane for the VOC system. The cells were incubated with the membranes for three time points: 24 hrs, 72hrs and 168hrs. These time points were selected to ensure cells would have enough time to adhere to the membrane and replicated for data collection. Controls were cultured on the 24 well plates at the same



time points but without a membrane to act as the standard reference. The data presented results from three independent experiments conducted on each membrane. A two-sample t-Test assuming equal variance in which,  $p$ -value  $< 0.05$  was considered significant.

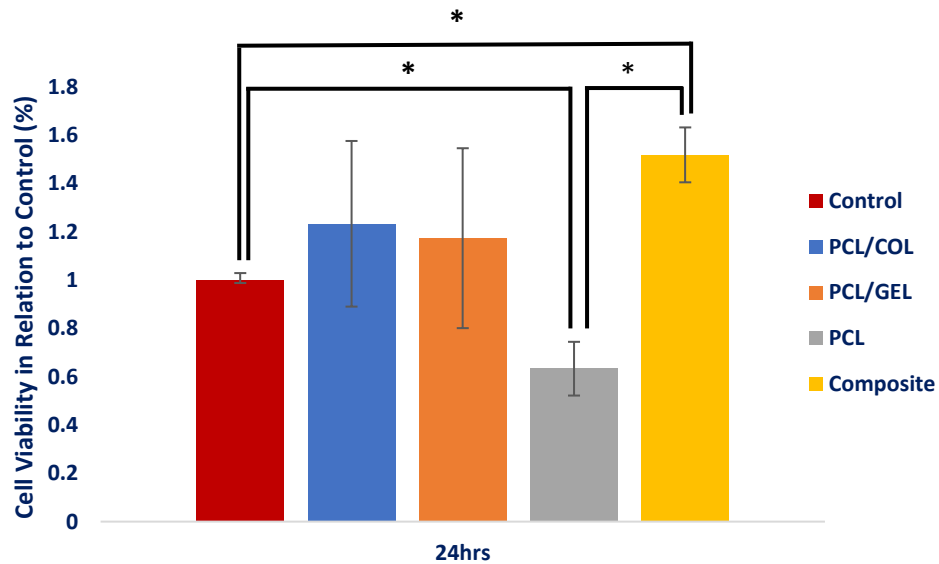


Figure 5.5. Represents all membranes cell viability in relation to the control ( $P < 0.05$ ) after 24hrs ( $n=4$ ).

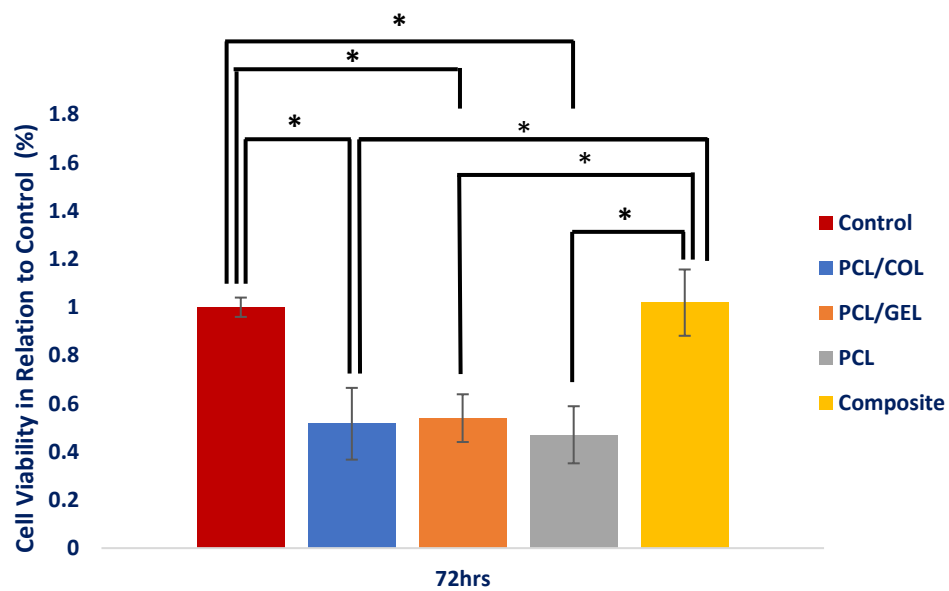


Figure 5.6. Represents all membranes cell viability in relation to the control ( $P < 0.05$ ) after 72hrs ( $n=4$ ).

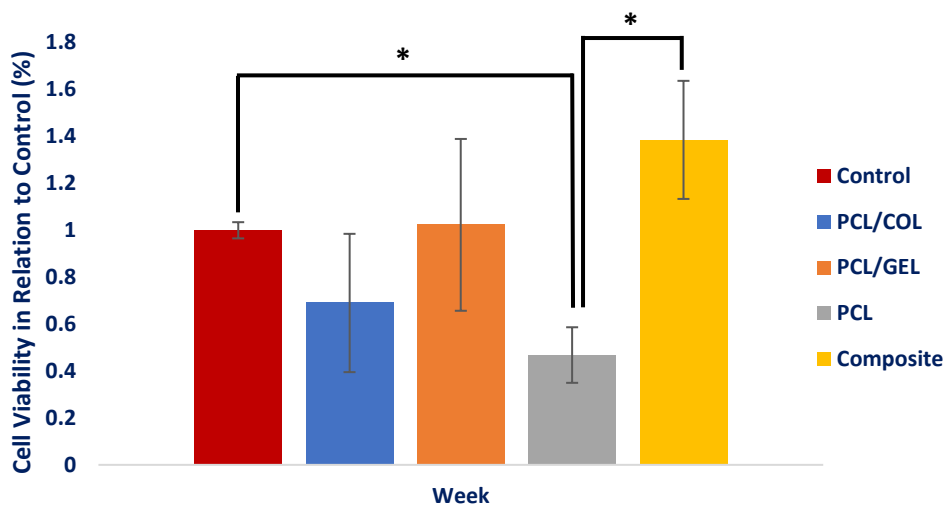


Figure 5.7. Represents all membranes cell viability in relation to the control ( $P < 0.05$ ) after 168 hrs ( $n=4$ )

The data presented in Figures 5.5, 5.6 and 5.7 indicated PCL/GEL, PCL/COL and composite membranes were biocompatible to support VK2/E6E7 cells. Each membrane expressed the expected growth pattern in relation to cell viability at different time points in relation to the control. After 24hr a significant difference can be seen between the membranes and control. This is due normal characteristic of cell growth after seeding cells enter the lag phase in which they begin to adapt to their environment before proliferating. A low seeding cell density of  $25 \times 10^3/\text{mL}$  was applied to each membrane but due to the low density may not have been a sufficient sample. Cells also were exposed to new material, the membrane which may needed longer for the cells to adapt and adhere to the surfaces of the membranes.

The VK2/E6E7 cells under normal cell culture procedure took roughly 48-72 hrs to express signs of proliferation, this may be due to the high passage cell sample which may have influenced the cell growth. At 72 hrs a decrease in cell number was observed. The cell viability compared to the controls showed that there were fewer cells at 72 hours in comparison to cells at 24 hours. This was observed in all the membranes, suggesting the cell required more time to proliferate, adhere and adapt to their surroundings or died due insufficient conditions. MTT assay only considers the mitochondria of living cells attached to the membrane and floating. The cell absorbance increased with subsequent time points as more cells attached to the membrane proliferated.

In Figure 5.5 -5.7 PCL membrane showed clear significance of viable cells with the control and between the composite membrane at 24 hrs, 72 hrs and 168 hrs. There was a minimal change in cell growth at these time points. This is due to PCL being a hydrophobic synthetic polymer. Though it is known for its good mechanical properties, it lacks cell recognition sites to exhibit cell adhesion. PCL expresses a contact angle of  $>90^\circ$  which represents incomplete wettability, cells applied to the scaffold floated on the surface of the membrane rather than wick through the nanofibers, inhibiting and reducing cell adhesion. PCL samples used in this experiment had a contact angle of  $121.54^\circ$  seen Figure 4.10 in chapter 4 was not treated to improve cell adhesion. To improve cell attachment to PCL membranes can be further functionalised by adding RDGs to enhance integrin bonding and focal adhesion (Bellis, 2011; Khalili and Ahmad, 2015). At 168 hrs, a decrease in proliferation can be seen for PCL membranes at 0.29-fold change indicating that PCL membrane alone is not suitable for the VOC platform without further treatment.

Both the co-axial scaffolds PCL/GE and PCL/COL seen in Figures 5.6 and 5.7 have shown an increase in cell number from 72 hrs to 168 hrs, indicating cell number increased on the PCL/GE membrane due to proliferation from 54% to 100% whereas, PCL/COL only had a minimal increase from 44% to 48% in relation to the control. Both the co-axial membranes contained biopolymers of GE and COL and it is expected that cell proliferation would be higher in both membranes as they have good fluid retention, porosity and cell specific binding sites (Ramalingam *et al.*, 2019). However, PCL/GE scaffold performed better in terms of cell absorbance than PCL/COL which indicates that PCL/COL membrane may not be a suitable membrane for maintaining cells longer than a month. This may be due to the fabrication process of the membrane and the diameter of the fibres. Though the membrane was crosslinked to stabilise the fibres of collagen, cross-linking treatment can reduce the antigenicity and immunogenicity (Chen *et al.*, 2019).

Both the co-axial membranes were cross linked with glutaraldehyde solution (GTA) to stabilise the fibres of gelatin and collagen as they exhibit poor mechanical strength and degradability (Ramalingam *et al.*, 2019). The co-axial method was used to fabricate both membranes with gelatin and collagen as the shell and PCL as the core. This technique allows the less spinnable polymers with low solubility and molecular weight;

gelatin and collagen to form fibres as the shell with the support of a spinnable polymer, PCL to provide the desirable mechanical properties at the core (Law *et al.*, 2017b). However, collagen structure is known to be unstable and may have denatured causing the number of cells to decrease and resulting in lack of proliferation on the membrane.

Composite membrane PCL/GE (50:50), a membrane fabricated by blending GE and PCL into one homogeneous solution and spun using the single method (Zhang *et al.*, 2005; Nuge *et al.*, 2013; Lim *et al.*, 2015; Ramalingam *et al.*, 2019). Within 24 hrs seen in Figure 5.5 a clear significance can be seen between the control and composite membrane. More viable cells were present on the composite membrane compared to the control indicating the cells to had adapted well to the composite membrane. At 72 hrs though a decrease in cell number was observed in all membranes in relation to the control, composite membrane remained significantly higher in cell viability at 100%. However, between 72 -1 68 hrs cell number accelerated, possibly due to the hydrophilic surface of the composite fibres enhancing fluid retention and increasing cell adhesion. As the composite membrane contains GE, cells specific binding sites could also be promoting cell adhesion properties and therefore increasing the cell absorbance. The process of cell adhesion is characterised by three stages. Phase 1 is the initial attachment which involve electrostatic interaction, creating specific integrin bonds between the cells and membranes.

During phase 2 cells begin to flatten and spread across the membrane decreasing in height and attaching to the membrane. At phase 3 cells are structurally organised and spread across the membrane this is known as focal adhesion (Khalili and Ahmad, 2015). In the study by (Lim *et al.*,2015) which examined *In vitro* biological evaluation of electrospun polycaprolactone/gelatine nanofibrous scaffold for tissue engineering the PCL/GE composite membrane expressed a higher cell count than the control suggesting it to be a suitable scaffold for tissue engineering as it combines the merits of natural and synthetic polymers making the membrane biocompatible, hydrophilic and with good mechanical properties (Fu *et al.*, 2014) to support the growth tissue. This was clearly shown in Figure 5.5-5.7 that compared to the other membranes, the composite membrane preformed the best in terms of the number of viable cells compared to the

control, informing that the composite membrane is the most fitted membrane to use for the VOC platform.

To conclude, four membranes tested for biocompatibility to grow the VK2/E6E7 cells, but PCL/GE, PCL/COL and composite (PCL/GE) membranes were identified as potential membranes suitable for the VOC model. Overall, PCL/GE and composite membrane produced higher cell viability than PCL/COL and PCL membranes and therefore considered as the suitable membranes for the VOC platform. As OOC models are trying to replace animal derived membranes, materials like PCL can be used. With further functionalisation by adding RGD's to the surface, peptide motifs would improve cell adhesion by attaching to the ECM, making this a potential membrane for not only for the VOC platform but for other OOC model too.

### **5.5.2 Cell morphology observations on membranes**

To observe cell attachment on the electrospun membranes cells were cultured for a week and prepared for fluorescent and SEM imaging separately. To prepare samples for fluorescent microscopy, the media was removed from the cell cultured membranes and washed in 1x PBS. This was then followed by a fixation process of 1:1 ratio of Acetone: Methanol and left to incubate for 20mins at -20°C. This step was done to ensure cells were fixed to the surface of the membrane for further analysis. After incubation, the samples were then washed again with 1xPBS for 5 mins, the membranes were then gently moved onto a microscopic glass slide. 3-4 drops of Vectashield mounting medium with DAPI (Abcam, US) was added directly on the samples. DAPI was used to stain the nucleus of cells on the membranes and covered with a glass coverslip to be observed under the fluorescent microscope (Leica DM1400, Germany).

### **5.5.3 Fluorescent staining o VK2/E6E7 cells on membranes**

Fluorescent staining with DAPI was performed on the PCL/GE, PCL/COL coaxial membranes and composite (PCL/GE) membrane to visualise the fixated cells attached to the nanofibers of the membranes. These three membranes were selected for further analyses as the MTT results identified these membranes as potential scaffolds for the VOC model. The samples were captured using the Leica DM1400 fluorescent microscope at magnification x10 Figure 5.8 shows the distribution of VK2/E6E7 vaginal

cells attached on the membranes (A) PCL/GE; (B) PCL/COL and (C) composite (PCL/GE). DAPI staining showed the fixated cells on the nanofibers and provided a visualisation of how well the membrane preformed after a week of experimenting with respect to cell adhesion, spread and proliferation.

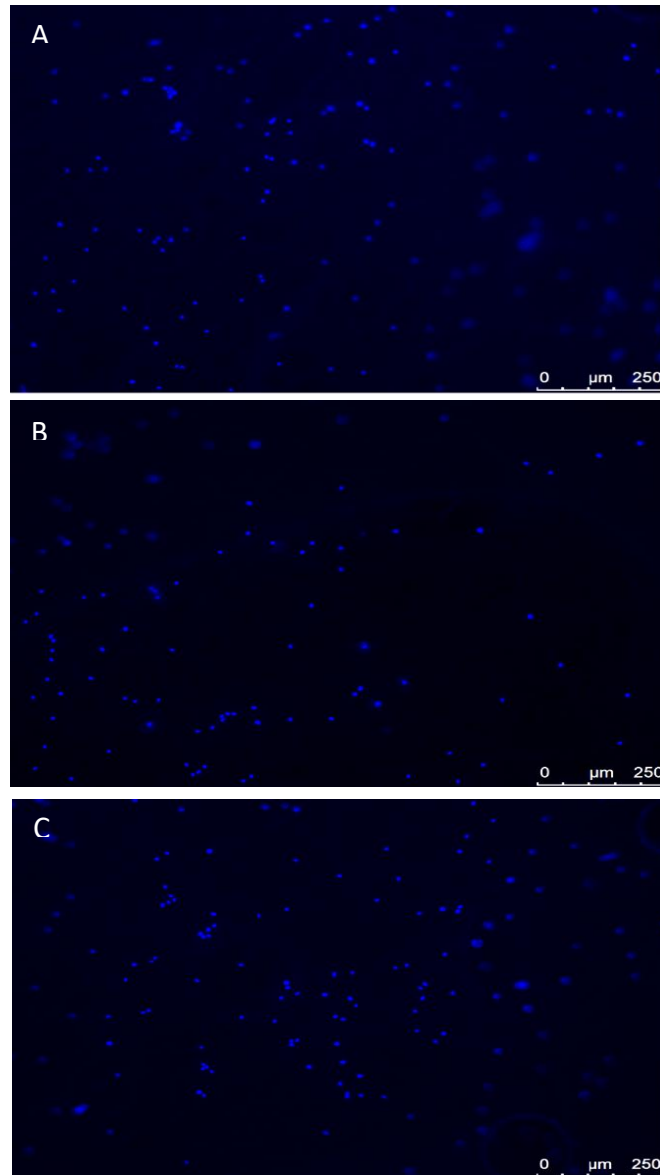


Figure 5.8 Fluorescent microscopy images of DAPI staining of VK2/E6E7 cells on (A) PCL/GE; (B) PCL/COL and (C) composite (PCL/GE) membrane at x10 magnification.

Cell density of  $25 \times 10^3$  were seeded onto the circular membranes with a diameter of 1.5cm. The electrospun membranes are made of multiple layers of randomised fibres spun on top of each other forming a 3D scaffold, due to this, cells can attach at different depths and therefore can be difficult to visualise as they may not appear in the same field of view. As the membranes are porous, this allows cells to migrate within in the membrane.

As experiments ran for a week it was expected that cells would proliferate and form colonies but under observation, cells remained single. This may be due to cells attaching at different location points on the membrane. It was noted that during conventional cell culture of VK2/E6E7 cells, it should normally take 3 days to proliferate into small colonies and only after a week would become confluent. Therefore, further experimentation is required to evaluate the growth of vaginal tissue over a longer duration to observe focal adhesion where cells have differentiated, migrated and proliferated forming tissue. For better cell observation, confocal microscopy to observe the membranes in 3D to examine if cells have infiltration within the membrane.

#### 5.5.4 SEM imaging of VK2/E6E7 cells on membranes

SEM was conducted to visualise cell attachment to the membrane fibres. To prepare the membranes for SEM, media was removed, and membranes were again washed with 1xPBS and underwent the same fixation process of 1:1 ratio of Acetone: Methanol and left to incubate for 20mins at  $-20^{\circ}\text{C}$ . Fixative solution was removed, and samples went through a series of washes again with 1xPBS followed by series of washes in 70% ethanol for 1 hour. The scaffolds were left to dry and were placed under UV to sterilise for 30mins. The membranes were sputter coated (OM-SC7640, UK) in gold for 2mins at 1.5 kV. Samples were then examined under the desktop SEM (JCM-6000, Japan) at an acceleration voltage of 10 kV.

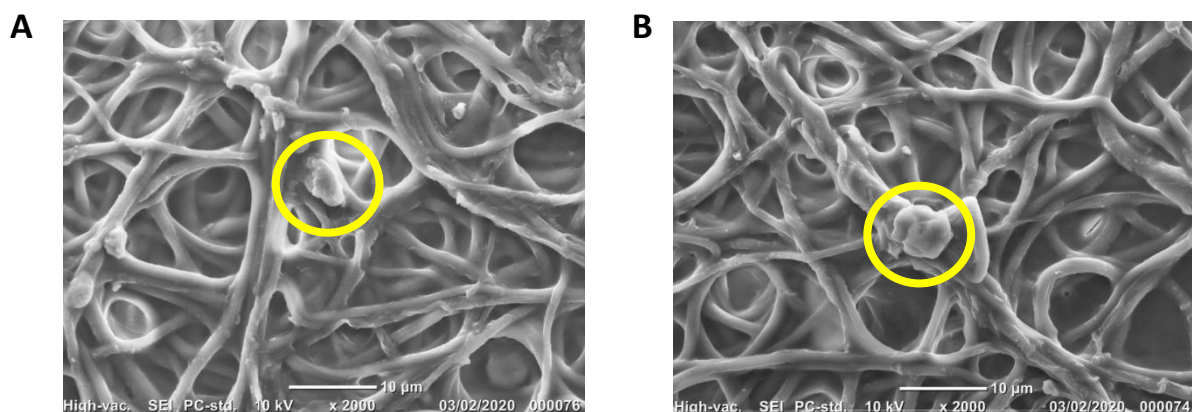


Figure 5.9 Scanning Electron Microscopy image of VK2/E6E7 cells on (A and B) PCL/GE coaxial membrane x2000 magnification.

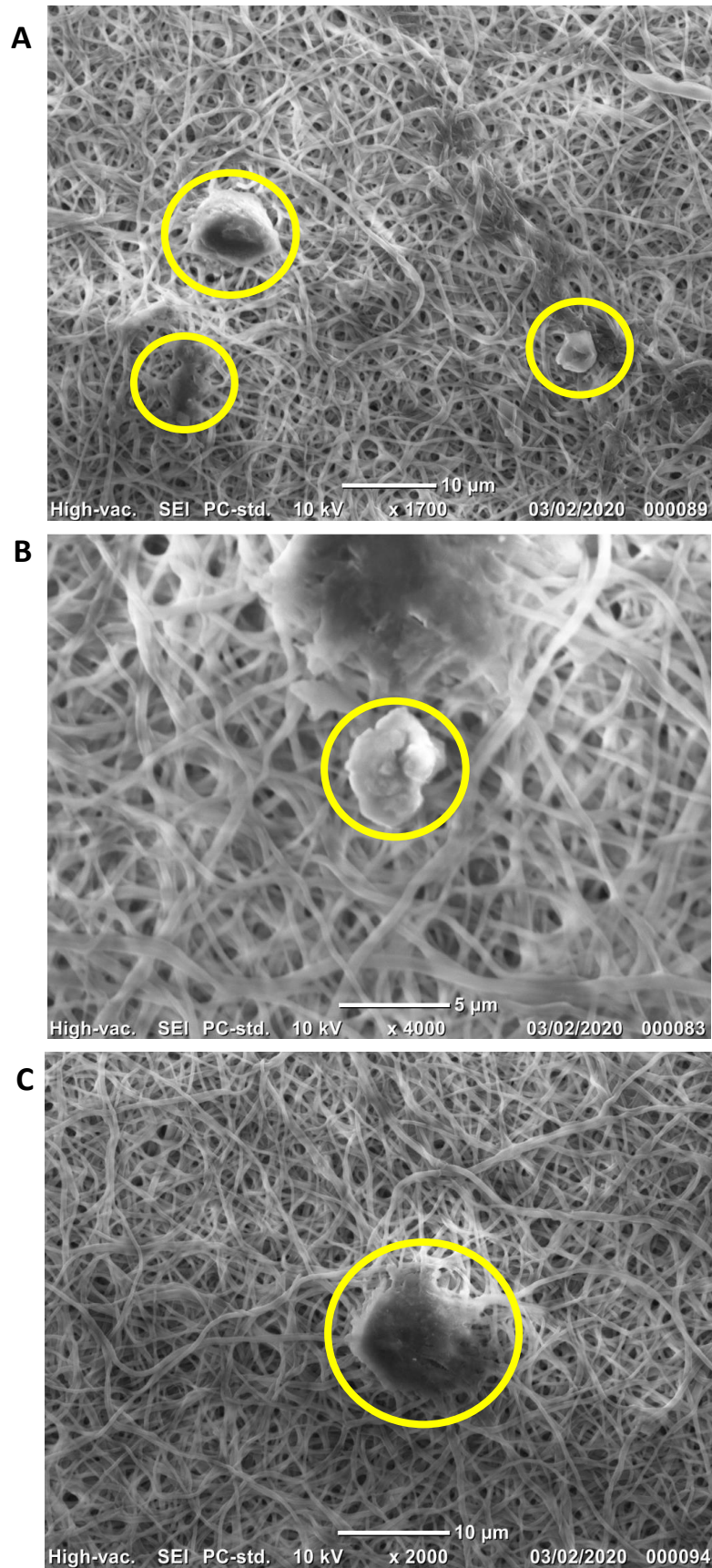


Figure 510 Scanning Electron Microscopy image of VK2/E6E7 cells on (A, B and C) PCL/COL coaxial membrane x2000 magnification.



Figures 5.9 and 5.10 presents the SEM images of the early development of VK2/E6E7 cells on both PCL/GE and PCL/COL membranes at a high magnification of x2000. Circled in yellow in Figure 5.9 is thought to be vaginal cells but looked more like debris on the surface of the membrane. PCL/GE samples were limited during this experiment resulting to unavailable data, for future analysis more samples should be prepared to avoid lack of data. As the fluorescent image in Figure 5.8 (A) showed many vaginal cells had adhered to the surface, it would be beneficial to repeat this experiment to capture cells on the membrane as evidence to prove that this membrane is biocompatible.

Figure 5.10 presents vaginal cells attached to the surface of the PCL/COL membrane, highlighted in yellow. As seen in Figure 10 (C) the cells have begun to attach to the fibres resulting in focal adhesion, spreading across the fibres. Further experimentation is required to understand the performance of cells and the membrane fibres for at least 2 weeks to a month. Figure 5.11 shows a potential 3D cell on the surface of the membrane. However, after analysing the image closely, it was suggested that it could be an artefact, as cells after a week should adhere to the surface of the membrane.

Unfortunately, composite membranes were unavailable for SEM analysis due to damaged samples. As cells were present on the membrane in Figure 5.8 (C), it would be beneficial to repeat SEM on this membrane to reflect the performance of cell attachment to confirm that composite membrane is suitable for the VOC platform.

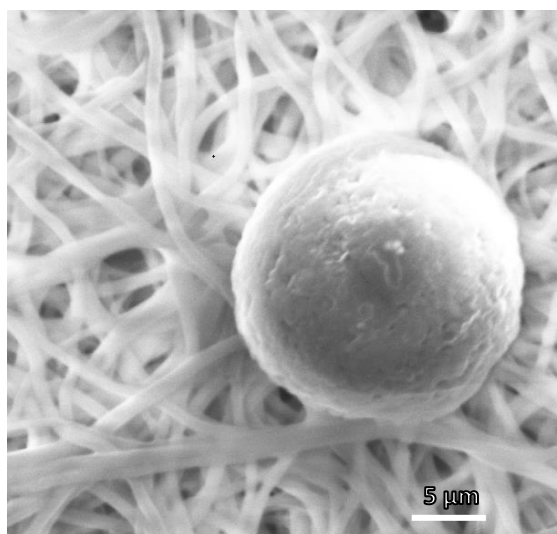


Figure 5.11 Scanning Electron Microscopy image of VK2/E6E7 cells on PCL/COL coaxial membrane x2000 magnification.

Fluorescent image of PCL/GE membrane seen in Figure 5.8 (A) showed several cells attached to the surface of the membrane, however under SEM this was a difficult to process to identify them due to cells location on the fibres. As the membranes are porous, cells migrate within the mesh. SEM was only able to capture the cells attached to the top surface of the membrane and not within. Both membranes respectively had smooth and bead free nanofibers.

## 5.6 Summary

Vaginal epithelium cells are approximately 12-14 $\mu$ m in diameter, therefore it is essential to find a suitable membrane that vaginal cells would require to form tissue at the centre of the VOC platform. SEM was conducted on the following members to examine the morphology of the fibre diameter of PCL/GE 575.65 $\pm$  142.628 nm, PCL/COL 540.55  $\pm$  293.09, composite (PLC/GE) 257.25 $\pm$  72.92 nm. With thin nanofibers closely distributed to each other on the membrane, this provided more connection points between the fibres increasing the mechanical strength to support cell culture (Ramalingam *et al.*, 2019). The fabricated scaffolds must be able to withstand the mechanical forces exerted by the cells, which results in actin-myosin binding to the cytoskeleton, influencing the cell shape and cellular functions that determine differentiation, proliferation and cell migration (Nuge *et al.*, 2013). In Figure 5.10, it is assumed that cells were attached to the fibres as they seem to merge into the fibres indicating possible passive cell attachment. Due to limited literature available on the morphology of 3D vaginal cells on electrospun membranes, cells observed in Figure 5.10 were compared to bone-marrow stromal cells grown on gelatin/PCL membranes reported by Zhang *et al.*, 2005 to obtain a reference of cell interaction to an electrospun membrane( Figure 5.12).

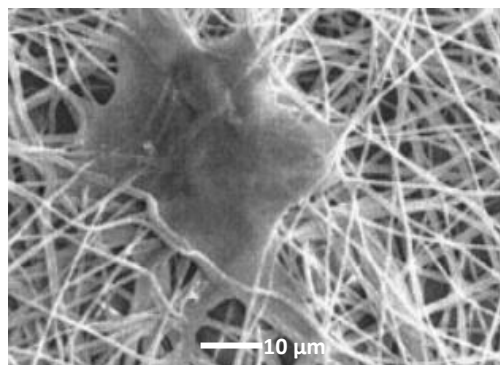


Figure 5.12 Interaction of bone-marrow stromal cells with gelatin/PCL composite fibrous scaffolds after 7 days of cell culture: cell interaction with scaffold, at 1000 x magnification (Zhang *et al.*, 2005)

To ensure the membranes selected for the VOC were capable of growing cells for longer than a week, further experiments must be conducted. As SEM images only provided a topological view of the cells attached to the fibres, Transmission electron microscopy (TEM) would be a suitable method to capture the internal structure of the membrane and how cells infiltrate the membrane.

## Chapter 6 – Discussion and VOC Platform Integration

The aim of this research was to develop a microfluidic device that could mimic the *in-vivo* vaginal tissue, within an *in-vitro* system to gain a better understanding of BV. This was done by conducting individual experiments in design and mould fabrication, scaffold fabrication and cell culture. In chapter 3, the VOC platform designs were constructed and evaluated through 7 iterations. Moulds were created using material jetting for rapid prototyping and to provide a smooth surface finish for the easy removal of PDMS layers. PDMS material was selected as the favourable material to fabricate the VOC layers due to its versatile properties i.e., flexibility, processibility, and transparency. Transparency of PDMS offered the ability to visually see what was happening within the chip during experimentation e.g., flow experiments and fluorescent microscopy without having to disrupt the layers of the chip.

As PDMS is permeable it allows for gas exchange to take place which is essential during cell culture. Though PDMS has its limitations especially being hydrophobic which results in non-specific absorption of protein at the surface, PDMS still remains the favourable material for fabricating OOC devices. This is due it being cost effective, easily utilised, processed and modified for wide applications especially in biomedical research (Gökaltun *et al.*, 2019).

From the designs conducted in chapter 3 the final designed contained alignment posts to help with assembling the layers of the VOC platform. The alignment posts were inspired by Lego microfluidics (Vittayarukskul and Lee, 2017). Using these posts positioned at the corners of the moulds, this allowed the designs of each VOC layers to link and align perfectly. The alignment is crucial when integrating the platform as many aspects are involved. Design 2 in chapter 3, Table 3.1 contained small membrane holders on either side of the membrane area but due to the small size was not able to hold the static membrane in place. During the flow experiments, flow that passed over the membrane caused the membrane to sag exposing the corresponding channels which resulted in cross flow. The design was then reevaluated a gasket layer was introduced in the final design to support the membrane suspension forming the central

layer of the VOC platform. The gasket layer is then positioned in line with the microfluidic channels that run above and below the membrane and sealing any exposed channels to prevent leakage.

In chapter 4 PCL, PCL/GE, PCL/COL and composite membranes were fabricated to find the suitable scaffold to support vaginal tissue for the VOC platform. SEM was conducted on the membranes to identify the fibre morphology. From the SEM results PCL membrane had an average fibre diameter of  $761.67 \pm 237.296$  nm, PCL/GEL membrane  $575.65 \pm 142.628$  nm, PCL/COL membrane  $540.55 \pm 293.09$  nm and Composite membrane  $257.25 \pm 72.919$  nm. PCL, PCL/GE and composite membrane presented uniformed, bead free fibres. However, PCL/COL, though presented bead-free and smooth fibres, did not exhibit uniformity and contained large pores seen in chapter 4 Figure 4.6.1 (E). It is difficult to successfully electrospin collagen as its structure is unstable causing it to denature therefore, collagen is usually spun with the combination of a synthetic polymers to enhance its mechanical properties and fibre stability (Zheng *et al.*, 2014).

The composite membrane produced ultrathin fibres compared to PCL, PCL/GE and PCL/COL. PCL 8% and GEL 4% were combined to make a homogenous solution thus creating non-beaded, continuous and thin fibre distribution with an average fibre size of  $250.34 \pm 79.257$ nm. This was in line with the literature, Ramalingam *et al.*, 2019 reported that composite membranes have an average fibres diameter of  $243 \pm 52$ nm. Whereas He *et al.* , 2014 reported composite membrane to have an average fibre size of  $386.9 \pm 102.5$  nm indicating that blended solutions produce ultrathin fibres in comparison to single or coaxal spinning. Composite membrane also expressed similar mechanical properties to non-prolapsed vaginal tissues (Baah-Dwomoh *et al.*, 2016) with a strain value of 12% and stress rupture at 1.6 MPa compared to PCL, PCL/GE and PCL/COL membrane (Figure 4.7). However, the blending of the PCL and gelatin did not enhance the strength of fibres but produced thin fibrous mesh. This is probably due to immiscibility and microphase separation which causes slippage of chains under loading caused by weak physical interactions amongst the chains in composite solutions (Zhang *et al.*, 2005).

Most OOC devices have used PDMS as the scaffold to support cell culture because of the many advantages the material provides i.e., biocompatible, flexible, transparent and permeable which are all ideal for cell culture. However, PDMS is hydrophobic and therefore is usually coated to modify the surface to hydrophilic. With this in mind, electrospinning technique was used to fabricate membranes as an alternative solution for the VOC device. Contact angle measurements were carried out on the membranes to evaluate their wettability properties for the purpose of sample loading during cell culture and flow experiments. PCL, known to be hydrophobic had a contact angle of  $121.54^\circ$  which expressed incomplete wettability. However, when PCL is combined with biopolymers GE and COL the contact angle is reduced resulting with a more hydrophilic surface. PCL/GE and PCL/COL as well as composite membranes presented contact angles of below  $<90^\circ$  indicating good wetting.

Furthermore, biocompatibility experiments were conducted to identify a suitable membrane for the VOC platform. MTT assay was performed to test for cell viability. After conducting a two-sample t-test with equal variance results indicated that there was a significant difference between the cell viability and the control at 95% confidence for the composite membrane with a *p-value*  $<0.05$ . After week in culture the composite membrane expressed 140% in cell viability compared to the control at 100% clearly emphasizing it to be the most suitable membrane of choice for the VOC platform.

However, in contrast the PCL membrane showed a significant difference in cell viability between the control and PCL membrane with a *p-value*  $< 0.05$ . After a week the cell viability on the PCL remained at 40% compared to PCL/GE at 100% and PCL/COL at 65% in relation to the control sample, signifying that PCL was not a suitable membrane for the VOC platform (Figure 5.7). PCL/GE and PCL/COL presented good cell viability but composite membrane remained to be the most appropriate membrane at 24 hrs, 72 hrs and 168 hrs. The two-sample t-test was also used to compare any differences between the membranes. It was noted that the composite membrane revealed a significant difference with PCL, PCL/GE, PCL/COL membrane during the 72 hrs (Figure 5.6). At 168 hrs, composite membrane proved to be the most suitable membrane with a cell viability of 140% compared to the control suggesting good viability in comparison to PCL/GE and PCL/COL seen in chapter 5 Figure 5.7.

MTT assay was done to confirm cell viability but to ensure cells had attached to the membrane fluorescent imaging. DAPI was used to stain the nucleus of the viable cells to visualise cell attachment. PCL/GE, PCL/COL and composite membranes were available for analysis. In chapter 5 Figure 5.8. demonstrated fluorescent microscopy images of DAPI staining on VK2/E6E7 cells attached to (A) PCL/GE, (B) PCL/COL and (C) composite (PCL/GE) membrane at x10 magnification. The images indicated cells had attached to the membranes but remained as single cells after a week in culture. As membranes are 3D scaffolds, cells attach to the fibres in different locations making it difficult to see whether cells have proliferated on the fibres or whether they have infiltrated the membrane. SEM analysis was also conducted to visualise the interaction of cells with the scaffold which can be seen in chapter 5 Figure 5.10. From observation it was noted that cells started to merge with the fibres. However, SEM is unable to capture cells embedded within the fibres. Therefore, it is recommended to conduct confocal microscopy to examine the migration and infiltration of cells within in the membrane.

Tensile strength measurements were conducted on the membrane which indicated similar stress and strain values in comparison to vaginal tissue from non-prolapsed women. Baah-Dwomoh et al 2016 reported that non-prolapsed tissue indicated a strain at failure ranging from 20-46% and stress at failure ranging from 0.82-2.62MPa. The composite membrane demonstrated similar properties with strain at failure 12 % and stress at rupture 1.6 MPa (Figure 4.8) suggesting that it would be a suitable membrane to support vaginal tissue. Whereas PCL membrane had a strain at failure 65% and stress at rupture 1.4 MPa, PCL/GE membrane strain at failure 8% and stress at rupture 1.7 MPa (Figure 4.7), PCL/COL membrane strain at failure 43% and stress at rupture 1.2 MPa and composite membrane strain at failure 12 % and stress at rupture 1.6 MPa (Figure 4.7). The young's modulus expressed the stiffness of each membrane evaluated PCL 25.8kPa, PCL/GE 0.60MPa, PCL/COL 35.5kPa and composite 0.42MPa. PCL/COL and PCL (Figure 4.7) expressed viscoelastic properties whereas PCL/GE and composite membrane demonstrated elastic properties with respect to vaginal tissue. It was indicated that vaginal tissue has an elastic modulus in the range of 2.5-9.5MPa but was

suggested by Baah-Dwomoh et al 2016 that vaginal tissue is nonlinear elastic and undergoes large deformations.

With design implementation and chip fabrication conducted in chapter 3, the final design for the VOC platform was selected. This was then followed by the fabrication of four electrospun membranes in Chapter 4. The membranes were designed to mimic the ECM to support vaginal tissue, once implemented into the VOC model. In chapter 5 biocompatibility experiments were conducted on the membranes to identify the most appropriate scaffold for the VOC platform. Each element of the VOC platform was carried out individually, the final step of this research was to combine all the individual components together to form a working VOC prototype.

## 6.1 VOC Integration

The initial flow experiment for the VOC platform was to provide nutrients to the epithelial cells grown at the centre of the chip. The VOC contains two microfluidic channels, top and bottom channel to provide nutrients to the vaginal epithelial. The platform is currently at this stage in testing. Once the working prototype has successfully formed vaginal epithelial tissue the platform will then introduce the second cell type, the endothelial cells to form the blood capillaries (Figure 6.1). As seen in Figure 6.1 the VOC platform has been designed with two microfluidic channels for the purpose of future experiments to combining two cell types.

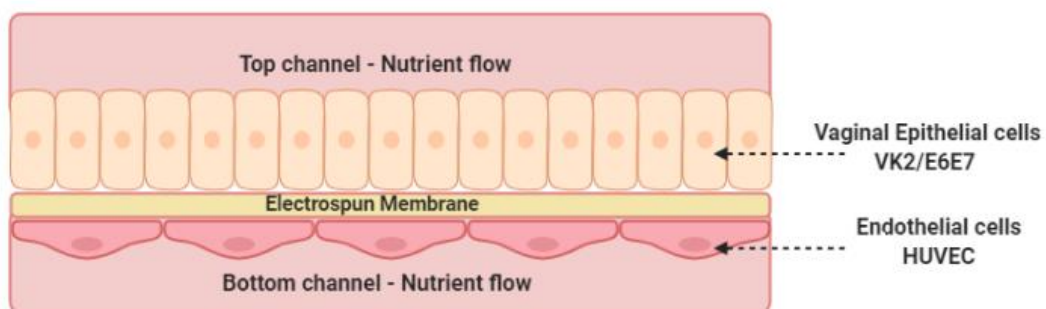


Figure 6.1 presents the potential layers of the VOC platform (created in BioRender.com)

The VOC platform contains a membrane that has been fabricated using bio and synthetic polymers via electrospinning to mimic the ECM for the prospects of 3D cell culture. VOC devices previously manufacture utilises PDMS as their porous membrane due to its advantageous properties of being flexible, semi permeable, transparent and



biocompatible, however it has its limitations. PDMS is known to absorb small hydrophobic molecules which can compromise measuring drug efficacy and toxicity (Huh *et al.*, 2013). Therefore, the electrospun membrane is used as the scaffold for the VOC platform to support the growth of vaginal tissue. The membrane is made with biodegradable material that has biocompatible and mechanical properties to aid the formation of 3D cells. Biodegradable material was chosen for the VOC platform as cells would eventually release chemical cues which would slowly degrade the nanofibers of the membrane leaving only vaginal tissue at the centre of the VOC platform. The platform has the potential to be used as a research tool to understand conditions like BV and other pathogens that affect the vaginal ecosystem. The VOC can be used by researchers and clinicians to develop improved treatment and eventually personalised medicine.

Another method was also investigated as an alternative approach to fabricating the VOC platform. 3D printing is an alternative method to creating a rapid prototype, Figure 6.2 (A) presents the first 3D printed VOC model in VeroClear (Stratasys, US). The layers of the chip were printed on the Objet30 Pro (Stratasys, US). The final design from chapter 3 Figure 3.9. Includes the alignment posts that aid to connect each layer into one device. However, with 3D printed layers treatment is required to bond layers, preventing the chip from leaking. Unlike the PDMS VOC models, tubing must be connected to the chip using Luer locks to run flow experiments. This method has the potential for manufacturing multiple chips rapidly for larger experiments, but materials can be costly, and printing can be time consuming.



Figure 6.2(A) 3D printed VOC platform in VeroClear; (B) Design concept for TPU VOC platform.

Seen in Figure 6.2 (B) another design was implemented for 3D printing layers of the VOC platform using TPU. The design was based around the Lego concept, but the layers were confined into a single unit containing the top and bottom channel layers as an enclosure. This idea was to create a chip containing a completely sealed chip with interlocking layers. With the interlocking feature the design potentially replace the need for bonding treatment and can prevent leakage. TPU is a thermoplastic polymer that is high in durability and flexibility and has similar characteristics to rubber, commonly used to for fabricating wires, breathable films and textile coatings. With great versatility, it provides another alternative approach to fabricating OOC device. However, TPU is opaque making it difficult to visualise cells for microscopy image analyses and difficult to bond to surfaces but, has the potential to replace PDMS as the main material used for fabricating OOC devices.

## Chapter 7 – Conclusion

The aim of this research was to create a 3D microfluidic device that would have the ability to mimic *in-vivo* vaginal tissue, within an *in-vitro* system. The VOC platform was based on the OOC concept, a novel approach combining biology and engineering to mimic the biochemical, mechanical and physical aspects of vaginal tissue. To create this microfluidic device a combination of techniques was used to construct the individual components of the chip. The process was split into three different areas, design and chip manufacturing, membrane fabrication and cell culture.

In chapter 3 design and fabrication, an engineering design process was conducted to identify the optimal design. The seventh design containing alignment posts and a gasket later was fabricated using soft lithography method. The layers of the VOC were manufacture using PDMS, a flexible transparent elastomer ideal for rapid prototype. The alignment posts were a vital addition to the design to improve alignment of the three main layers that make up the VOC platform. Initial flow testing was conducted on the VOC prototype using a syringe pump, which presented preliminary results on the performance of the VOC design. However, further testing is required to fully evaluate the VOC platform as a whole unit including the electrospun membrane and cells to obtain a fully developed model.

One of the objectives mentioned in chapter 1.2 was to create a biocompatible membrane. In chapter 4, membranes were fabricated using the electrospinning technique. This method was chosen as an alternative method to PDMS to create a biodegradable and biocompatible membrane that would mimic the ECM to support vaginal epithelial cells at the centre of the VOC platform. Biopolymers GE and COL were both selected due to their biodegradability, biocompatibility and fluid retention properties but lack mechanical strength. To improve their mechanical strength synthetic polymer PCL was used in combination with the biopolymers to fabricate membranes via co-axial and composite electrospinning. Membranes PCL/GE, PCL/COL and composite provided good mechanical strength and biocompatibility characteristics to support the growth of vaginal tissue. Fibre diameter measurements, mechanical testing and contact angle were conducted on all four membranes to help identified the

appropriate membrane for the VOC platform. To conclude PCL/GE and composite membranes indicated the most suitable for the platform.

In Chapter 5 the membranes were analysed for their biocompatibility with vaginal cell line VK2/E6E7. Cell viability tests were conducted on the membranes and concluded that the composite membrane was the most suitable membrane for the VOC platform. This was highlighted in the statistical analysis conducted on the membranes. The composite membrane had a significant difference in relation to the control but also with the other membranes. More cells were viable on the composite membrane than on the PCL/GE and PCL/COL membrane. From the statistical analysis it was concluded that PCL membrane would not be suitable for the VOC platform and would require further treatment to enhance the surface properties to become more biocompatible. Fluorescent imaging conducted on the PCL/GE, PCL/COL and composite membranes demonstrated cells were adherent to the surface of the membrane and distributed evenly across the membrane. SEM done on the PCL/GE and PCL/COL membrane showed the cells merging with the fibres indicating integrin bonding, cell attached after a week in culture. To conclude PCL/GE, PCL/COL and composite membrane expressed biocompatibility but overall, the composite membrane is the most fitting membrane for the VOC platform.

The final step in this research project was to amalgamate each component of the VOC system into one integrated platform and to validate the platform by conducting fluidic experiments. However, due to the unforeseen circumstances of the pandemic the final flow experiments were not achieved. Therefore, to conclude further experimentation is required to validate the performance of the VOC platform before challenging the system with bacterial strains to investigate what causes BV.

## **7.1 Contribution to knowledge**

The research conducted in this thesis has contributed knowledge to the following areas: -

- **OOO Design**

The VOC has been designed to contain 3 layers with the central layer acting as a gasket to hold the membrane in suspension. The gasket layer has also been designed to cover

exposing channels to prevent leakage. Unlike other OOC devices that require additional casing to hold the chip together, the VOC platform design includes additional feature i.e., alignment posts based at the corners of the chip for easy assembling similar to Lego. This provides a plug and connect system which helps with alignment of the layers and supports the membrane.

- **New membrane on which vaginal cells have been successfully seeded**

Vaginal cells have only been grown using conventional 2D methods and 3D models including the RWV but an electrospun membrane has been developed using a mixture of bio and synthetic polymers to support the growth of vaginal epithelial cells.

- **VOC platform an alternative solution to replacing animal testing**

A novel approach to understanding BV, the VOC platform is a working prototype in its initial stages of development designed to mimic the function of the human vagina, physiology and model its natural microbiome environment. The VOC is a realistic platform designed to examine the interaction between vaginal epithelial cells, bacterial strains and pathogens that affect the vaginal environment. Development of new drugs and treatment for BV can be directly tested on this platform and has the potential to cater for personalised medicine.

## Chapter 8 – Future Work

The VOC platform has the potential to replace animal testing and provide a model researchers and clinicians could use to understand BV. However, the platform requires further validation as an integrated system therefore the following suggestions have been recommended as future work: -

- **Flow experiments with the Elveflow system to test the integrated platform and its performance.**

To test the VOC platform as a fully integrated system using the ELVEFLOW microfluidic flow controller and sensor to control cell culture experiment on the VOC platform for at least a week to validate the platform performance.

### 8.1 Set up of ELVEFLOW Experiment

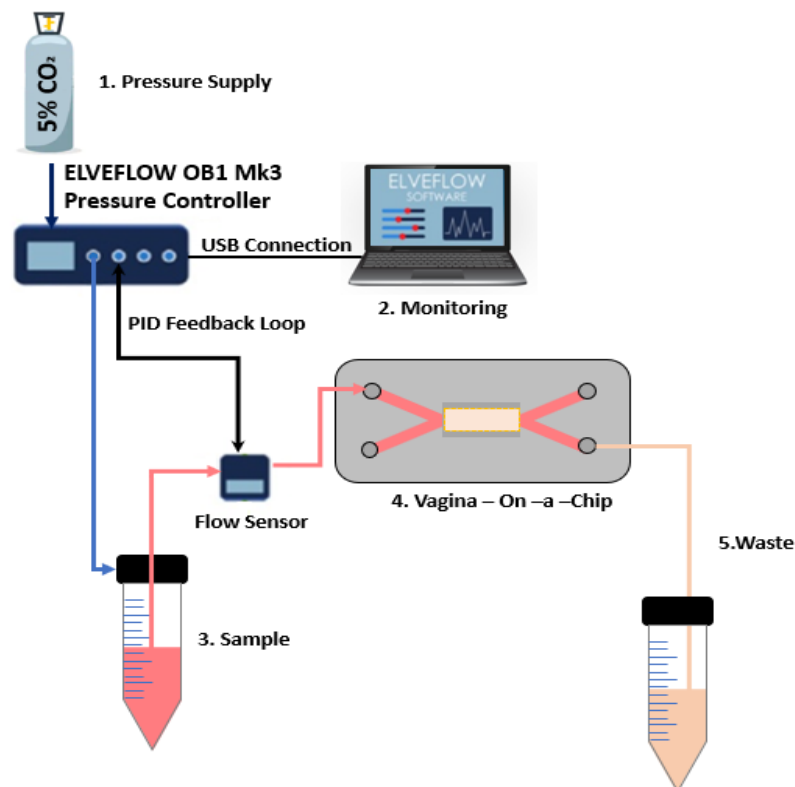


Figure 8.1 Integrated VOC platform under flow experiment through with the Elveflow system.

To conduct the experiment, the VOC platform would be prepared in advance, sterilised under UV for 20mins before the experiment and stored ready for use. The VOC must be contaminated free during the experiments. To run the experiment a flask of vaginal cells must be grown separately prior to the set up in order seed the VOC with single cell

suspension of approximately 25,000 cells/ml. This step is done under the flow cabinet before attaching to the flow system. The cells should then be carefully passed through the inlet till the membrane and channels are completely full of media and cells suspension. The VOC platform should then be left for 24 hours in the incubator at 37°C with 5% CO<sub>2</sub>. This is so the cells can attach to the surface of the membrane. The composite membrane is used at the centre of the chip to support the growth of vaginal epithelial cells.

After 24 hours incubation period, media is slowly pumped out and replaced with fresh media. The VOC is then connected to the Elveflow OB1 Mk3 pressure controlling system seen in Figure 8.1. The inlet of the chip is connected to a reservoir with KSF media to provide nutrients to the vaginal cells growing at the centre of the chip. Between the reservoir and the chip, a flow sensor is located which is set as a PID feedback loop in order to monitor the flow rate and pressure exerted by the OB1 Mk3 system. The outlet of the chip is connected to a 50 ml centrifuge tube to collect waste. To initiate the flow, the OB1 Mk3 pressure controlling system is supplied with 5% CO<sub>2</sub>. The pressure limits are set to a minimum and maximum of 80 mbar, with a pressure set to 15 mbar to run the experiment. During the experiment, the flow sensor monitors the flow rate during the experiment.

Once the VOC platform is connected to the system and media is flowing through the channels, the chip is then placed into the incubator at 37°C with 5% CO<sub>2</sub> to conduct the cell culture experiment. The OB1 Mk3 pressure controller has the ability to conduct multiple chips in one set up, ideal for larger data collection and analysis. As the membrane is opaque once the tissue has formed on the membrane it can then be used for further biological and fluorescent imaging analysis. With the Elveflow set up the VOC platform can be evaluated by observing the design performance by checking for leakage or blockage during the experiments, whether the layers have completely bonded and can be easily separated without interfering with the membrane.

- **Successfully try to grow 3D vaginal tissue on the VOC platform.**

To ensure the membrane can support the growth of 3D vaginal tissue, the VOC platform can be used to run 2 weeks to a month-long experiment to examine the membranes and their ability to form 3D cells. SEM and TEM can then be conducted to study the morphology of the vaginal tissue from the VOC platform.

- **To check infiltration by conducting confocal microscopy image analysis.**

To examine cells migration within the fibers of the membrane, confocal imaging would be beneficial. Fiber diameter of the membrane can affect the migration of cells, therefore confocal imaging would provide an insight to whether the appropriate membrane has been selected for the VOC platform.

- **Seed bacterial strains to the top layer of the VOC to establish the vaginal microbiome environment.**

Once the VOC platform has formed vaginal tissues, *Lactobacillus* spp. can then be introduced to the system to mimic the microbiome of the vagina. The model can then be used to investigate the interaction between vaginal epithelial cells and bacterial strains like BV and other pathogen. This can then be monitored over a period of time to investigate whether *GV* biofilm emerges. To test the formation of the biofilm, pH bacterial proliferation and viability assay will be conducted. To verify bacterial adhesion to the epithelial cells TEM will be performed on dissected cross section of the VOC tissue.

- **To measure porosity and degradation tests on membranes.**

To measure porosity of the membranes to ensure the appropriate membrane is used for the VOC platform. Degradation tests must also be considered to evaluate how long it would take the membrane to degrade. Over time as the cells grow and attached the membrane the material should degrade leaving behind 3D vaginal tissue. To test degradation rate, membrane samples will be exposed in media and monitored over a time frame. At each data point SEM images of the samples will be taken to capture the degradation of the membrane. Membranes will also be exposed to media with bacteria, monitored and compared to membranes only with media to examine if there is any significant difference in degradation rate with the addition of bacteria.



## References

- Aleshkin, V. A., Voropaeva, E. A. and Shenderov, B. A. (2006) 'Vaginal microbiota in healthy women and patients with bacterial vaginosis and nonspecific vaginitis', *Microbial Ecology in Health and Disease*. Taylor & Francis, 18(2), pp. 71–74. doi: 10.1080/17482960600891473.
- Aroutcheva, A. *et al.* (2001) 'Defense factors of vaginal lactobacilli', *American Journal of Obstetrics and Gynecology*. Am J Obstet Gynecol, 185(2), pp. 375–379. doi: 10.1067/mob.2001.115867.
- Ashammakhi, N. *et al.* (2012) 'Nanofiber-based scaffolds for tissue engineering', *European Journal of Plastic Surgery*, 35(2), pp. 135–149. doi: 10.1007/s00238-008-0217-3.
- Baah-Dwomoh, A. *et al.* (2016) 'Mechanical Properties of Female Reproductive Organs and Supporting Connective Tissues: A Review of the Current State of Knowledge', *Applied Mechanics Reviews*, 68(6), pp. 1–12. doi: 10.1115/1.4034442.
- Bein, A. *et al.* (2018) 'Microfluidic Organ-on-a-Chip Models of Human Intestine', *CMGH*. Elsevier Inc, pp. 659–668. doi: 10.1016/j.jcmgh.2017.12.010.
- Bellis, S. L. (2011) 'Advantages of RGD peptides for directing cell association with biomaterials', *Biomaterials*. Elsevier Ltd, 32(18), pp. 4205–4210. doi: 10.1016/j.biomaterials.2011.02.029.
- Bitew, A. *et al.* (2017) 'Prevalence of bacterial vaginosis and associated risk factors among women complaining of genital tract infection', *International Journal of Microbiology*, 2017. doi: 10.1155/2017/4919404.
- Boskey, E. R. *et al.* (2001) 'Origins of vaginal acidity: High D/L lactate ratio is consistent with bacteria being the primary source', *Human Reproduction*. Oxford University Press, 16(9), pp. 1809–1813. doi: 10.1093/humrep/16.9.1809.
- Boskey, E. R. (2005) 'Alternative therapies for bacterial vaginosis: A literature review and acceptability survey', *Alternative Therapies in Health and Medicine*, 11(5), pp. 38–43.
- Boskey ER, Telsch KM, Whaley KJ, Moench TR, C. R. (1999) *Acid production by vaginal flora in vitro is consistent with the rate and extent of vaginal acidification.*, *Infect Immun* 67. Available at: [https://www.researchgate.net/publication/12803174\\_Boskey\\_ER\\_Telsch\\_KM\\_Whaley\\_KJ\\_Moench\\_TR\\_Cone\\_RA\\_Acid\\_production\\_by\\_vaginal\\_flora\\_in\\_vitro\\_is\\_consistent\\_with\\_the\\_rate\\_and\\_extent\\_of\\_vaginal\\_acidification\\_Infect\\_Immun\\_67\\_5170-5175](https://www.researchgate.net/publication/12803174_Boskey_ER_Telsch_KM_Whaley_KJ_Moench_TR_Cone_RA_Acid_production_by_vaginal_flora_in_vitro_is_consistent_with_the_rate_and_extent_of_vaginal_acidification_Infect_Immun_67_5170-5175) (Accessed: 13 September 2020).

- Bournias Varotsis, A. (2019) 'Introduction to Material Jetting 3D Printing', *3DHubs*. Available at: <https://www.3dhubs.com/knowledge-base/introduction-material-jetting-3d-printing/#what> (Accessed: 2 October 2020).
- Bradshaw, C. S. and Brotman, R. M. (2015a) 'Making inroads into improving treatment of bacterial vaginosis - striving for long-term cure.', *BMC infectious diseases*. *BMC Infectious Diseases*, 15(1), p. 292. doi: 10.1186/s12879-015-1027-4.
- Bradshaw, C. S. and Brotman, R. M. (2015b) 'Making inroads into improving treatment of bacterial vaginosis – striving for long-term cure'. doi: 10.1186/s12879-015-1027-4.
- Bradshaw, C. S. and Sobel, J. D. (2016) 'Current Treatment of Bacterial Vaginosis- Limitations and Need for Innovation', *Journal of Infectious Diseases*, 214(Suppl 1), pp. S14–S20. doi: 10.1093/infdis/jiw159.
- Branavan, M. *et al.* (2016) 'Modular development of a prototype point of care molecular diagnostic platform for sexually transmitted infections', *Medical Engineering and Physics*, 38(8). doi: 10.1016/j.medengphy.2016.04.022.
- Brusie, C. (2019) *What Happens to Your Vagina After Pregnancy and Birth?* Available at: <https://www.verywellfamily.com/what-happens-to-your-vagina-after-pregnancy-4156275> (Accessed: 20 September 2020).
- Burton, J. P., Cadieux, P. A. and Reid, G. (2003) 'Improved understanding of the bacterial vaginal microbiota of women before and after probiotic instillation', *Applied and Environmental Microbiology*. *Appl Environ Microbiol*, 69(1), pp. 97–101. doi: 10.1128/AEM.69.1.97-101.2003.
- Burton, J. P. and Reid, G. (2002) 'Evaluation of the bacterial vaginal flora of 20 postmenopausal women by direct (Nugent score) and molecular (polymerase chain reaction and denaturing gradient gel electrophoresis) techniques', *Journal of Infectious Diseases*. *J Infect Dis*, 186(12), pp. 1770–1780. doi: 10.1086/345761.
- Burugapalli, K. *et al.* (2018) 'Biomimetic electrospun coatings increase the in vivo sensitivity of implantable glucose biosensors', *Journal of Biomedical Materials Research - Part A*, 106(4), pp. 1072–1081. doi: 10.1002/jbm.a.36308.
- Charati, S. G. and Stern, S. A. (1998) 'Diffusion of Gases in Silicone Polymers : Molecular Dynamics Simulations', 9297(98), pp. 5529–5535.
- Chen, D. *et al.* (2019) '<p>Electrospun polycaprolactone/collagen nanofibers cross-linked with 1-ethyl-3-(3-dimethylaminopropyl) carbodiimide/<em>N-</em>hydroxysuccinimide and genipin facilitate endothelial cell regeneration and may be a promising candidate for vascular scaffolds</p>', *International Journal of Nanomedicine*. Dove Press, 14, pp. 2127–2144. doi: 10.2147/IJN.S192699.
- Choktaweasap, N. *et al.* (2007) 'Electrospun gelatin fibers: Effect of solvent system on

morphology and fiber diameters', *Polymer Journal*. Nature Publishing Group, 39(6), pp. 622–631. doi: 10.1295/polymj.PJ2006190.

Cipitria, A. *et al.* (2011) 'Design, fabrication and characterization of PCL electrospun scaffolds - A review', *Journal of Materials Chemistry*, 21(26), pp. 9419–9453. doi: 10.1039/c0jm04502k.

Coimbra, P. *et al.* (2017) 'Coaxial electrospun PCL/Gelatin-MA fibers as scaffolds for vascular tissue engineering', *Colloids and Surfaces B: Biointerfaces*. Elsevier B.V., 159, pp. 7–15. doi: 10.1016/j.colsurfb.2017.07.065.

Daelemans, L. *et al.* (2018) 'Nanostructured hydrogels by blend electrospinning of polycaprolactone/gelatin nanofibers', *Nanomaterials*, 8(7), pp. 1–12. doi: 10.3390/nano8070551.

Devillard, E. *et al.* (2004) 'Novel insight into the vaginal microflora in postmenopausal women under hormone replacement therapy as analyzed by PCR-denaturing gradient gel electrophoresis', *European Journal of Obstetrics and Gynecology and Reproductive Biology*, 117(1), pp. 76–81. doi: 10.1016/j.ejogrb.2004.02.001.

Donia, M. S. *et al.* (2014) 'A systematic analysis of biosynthetic gene clusters in the human microbiome reveals a common family of antibiotics.', *Cell*, 158(6), pp. 1402–1414. doi: 10.1016/j.cell.2014.08.032.

Easmon, C. S., Hay, P. E. and Ison, C. A. (1992) 'Bacterial vaginosis: a diagnostic approach', *Genitourinary medicine*, 68(2), pp. 134–138.

England, N. (2018a) *Bartholin's cyst*. Available at: <https://www.nhs.uk/conditions/bartholins-cyst/> (Accessed: 20 September 2020).

England, N. (2018b) *Is my vagina normal? - NHS*. Available at: <https://www.nhs.uk/live-well/sexual-health/vagina-shapes-and-sizes/> (Accessed: 20 September 2020).

Fasnacht, A. (2017) *SLA vs. PolyJet: What You Need to Know | CADimensions*. Available at: <https://www.cadimensions.com/blog/sla-vs-polyjet-need-know/> (Accessed: 1 October 2020).

Fertala, A., Han, W. B. and Ko, F. K. (2001) 'Mapping critical sites in collagen II for rational design of gene-engineered proteins for cell-supporting materials', *Journal of Biomedical Materials Research*. J Biomed Mater Res, 57(1), pp. 48–58. doi: 10.1002/1097-4636(200110)57:1<48::AID-JBM1140>3.0.CO;2-S.

Fethers, K. A. *et al.* (2008) 'Sexual risk factors and bacterial vaginosis: A systematic review and meta-analysis', *Clinical Infectious Diseases*. Clin Infect Dis, pp. 1426–1435. doi: 10.1086/592974.

Fichorova, R. N. *et al.* (2011) 'Novel vaginal microflora colonization model providing new

insight into microbicide mechanism of action', *mBio*, 2(6), pp. 1–10. doi: 10.1128/mBio.00168-11.

Fichorova, R. N. and Anderson, D. J. (1999) 'Differential expression of immunobiological mediators by immortalized human cervical and vaginal epithelial cells', *Biology of Reproduction*. *Biol Reprod*, 60(2), pp. 508–514. doi: 10.1095/biolreprod60.2.508.

Fichorova, R. N., Rheinwald, J. G. and Anderson, D. J. (1997) 'Generation of papillomavirus-immortalized cell lines from normal human ectocervical, endocervical, and vaginal epithelium that maintain expression of tissue-specific differentiation proteins', *Biology of Reproduction*, 57(4), pp. 847–855. doi: 10.1095/biolreprod57.4.847.

Forsum, U. *et al.* (2005) 'Bacterial vaginosis - A microbiological and immunological enigma', *Apmis*, 113(2), pp. 81–90. doi: 10.1111/j.1600-0463.2005.apm1130201.x.

Fu, W. *et al.* (2014) 'Electrospun gelatin / PCL and collagen / PLCL scaffolds for vascular tissue engineering', pp. 2335–2344.

Fujisawa, T. *et al.* (1992) 'Taxonomic study of the *Lactobacillus acidophilus* group, with recognition of *Lactobacillus gallinarum* sp. nov. and *Lactobacillus johnsonii* sp. nov. and synonymy of *Lactobacillus acidophilus* group A3 (Johnson *et al.* 1980) with the type strain of *Lactobacillus amylovorus* (Nakamura 1981)', *International Journal of Systematic Bacteriology*. *Int J Syst Bacteriol*, 42(3), pp. 487–491. doi: 10.1099/00207713-42-3-487.

Garg, K. and Bowlin, G. L. (2011) 'Electrospinning jets and nanofibrous structures', *Biomicrofluidics*. American Institute of Physics Inc., 5(1). doi: 10.1063/1.3567097.

Gilbert, N. M., Lewis, W. G. and Lewis, A. L. (2013) 'Clinical Features of Bacterial Vaginosis in a Murine Model of Vaginal Infection with *Gardnerella vaginalis*', *PLoS ONE*, 8(3). doi: 10.1371/journal.pone.0059539.

Gillet, E. *et al.* (2011) 'Bacterial vaginosis is associated with uterine cervical human papillomavirus infection: A meta-analysis', *BMC Infectious Diseases*, 11. doi: 10.1186/1471-2334-11-10.

Ginkel, P. D. *et al.* (1993) 'Vaginal Flora in Postmenopausal Women: The Effect of Estrogen Replacement', *Infectious Diseases in Obstetrics and Gynecology*. *Infect Dis Obstet Gynecol*, 1(2), pp. 94–97. doi: 10.1155/S1064744993000225.

Gökaltun, A. *et al.* (2019) 'Simple Surface Modification of Poly(dimethylsiloxane) via Surface Segregating Smart Polymers for Biomicrofluidics', *Scientific Reports*. Springer US, 9(1), pp. 1–14. doi: 10.1038/s41598-019-43625-5.

Gold, J. M. and Shrimanker, I. (2019) *Physiology, Vaginal*, *StatPearls*. StatPearls Publishing. Available at: <http://www.ncbi.nlm.nih.gov/pubmed/31424731> (Accessed:

20 September 2020).

Guarino, V. *et al.* (2017) 'Polycaprolactone: Synthesis, Properties, and Applications', in *Encyclopedia of Polymer Science and Technology*. Hoboken, NJ, USA: John Wiley & Sons, Inc., pp. 1–36. doi: 10.1002/0471440264.pst658.

Haslauer, C. M. *et al.* (2011) 'Collagen-PCL sheath-core bicomponent electrospun scaffolds increase osteogenic differentiation and calcium accretion of human adipose-derived stem cells', *Journal of Biomaterials Science, Polymer Edition*, 22(13), pp. 1695–1712. doi: 10.1163/092050610X521595.

Haubert, K., Drier, T. and Beebe, D. (2006) 'PDMS bonding by means of a portable, low-cost corona system', *Lab on a Chip*. Royal Society of Chemistry, 6(12), pp. 1548–1549. doi: 10.1039/b610567j.

Herbst-Kralovetz, M. M. *et al.* (2008) 'Quantification and comparison of toll-like receptor expression and responsiveness in primary and immortalized human female lower genital tract epithelia', *American Journal of Reproductive Immunology*. Wiley-Blackwell, 59(3), pp. 212–224. doi: 10.1111/j.1600-0897.2007.00566.x.

Herbst-Kralovetz, M. M. *et al.* (2016) 'New Systems for Studying Intercellular Interactions in Bacterial Vaginosis', *Journal of Infectious Diseases*. Oxford University Press, 214(Suppl 1), pp. S6–S13. doi: 10.1093/infdis/jiw130.

Hjelm, B. E. *et al.* (2010) 'Development and Characterization of a Three-Dimensional Organotypic Human Vaginal Epithelial Cell Model', *Biology of Reproduction*, 82(3), pp. 617–627. doi: 10.1095/biolreprod.109.080408.

Hoffmann, J. N. *et al.* (2014) 'Prevalence of Bacterial Vaginosis and Candida among Postmenopausal Women in the United States', *Journals of Gerontology, Series B: Psychological Sciences and Social Sciences*, 69(8), pp. 205–214. doi: 10.1093/geronb/gbu105.

Horuz, T. İ. and Bülent Belibağlı, K. (2017) 'Production of electrospun gelatin nanofibers: An optimization study by using Taguchi's methodology', *Materials Research Express*. Institute of Physics Publishing, 4(1), p. 015023. doi: 10.1088/2053-1591/aa57ea.

Huang, H., Song, L. and Zhao, W. (2014) 'Effects of probiotics for the treatment of bacterial vaginosis in adult women: A meta-analysis of randomized clinical trials', *Archives of Gynecology and Obstetrics*. Springer Verlag, 289(6), pp. 1225–1234. doi: 10.1007/s00404-013-3117-0.

Huang, Z.-M. *et al.* (2003) 'A review on polymer nanofibers by electrospinning and their applications in nanocomposites'. doi: 10.1016/S0266-3538(03)00178-7.

Huang, Z. M. *et al.* (2003) 'A review on polymer nanofibers by electrospinning and their applications in nanocomposites', *Composites Science and Technology*, 63(15), pp. 2223–

2253. doi: 10.1016/S0266-3538(03)00178-7.

Huang, Z. M. *et al.* (2004) 'Electrospinning and mechanical characterization of gelatin nanofibers', *Polymer*. Elsevier BV, 45(15), pp. 5361–5368. doi: 10.1016/j.polymer.2004.04.005.

Huh, D. *et al.* (2010) 'Reconstituting organ-level lung functions on a chip.', *Science (New York, N.Y.)*. American Association for the Advancement of Science, 328(5986), pp. 1662–8. doi: 10.1126/science.1188302.

Huh, D. *et al.* (2013a) 'Microfabrication of human organs-on-chips', *Nature Protocols*. Nature Publishing Group, 8(11), pp. 2135–2157. doi: 10.1038/nprot.2013.137.

Huh, D. *et al.* (2013b) 'Microfabrication of human organs-on-chips', *Nature Protocols*, 8(11), pp. 2135–2157. doi: 10.1038/nprot.2013.137.

Huh, D. *et al.* (2013c) 'Microfabrication of human organs-on-chips', *Nature Protocols*, 8(11), pp. 2135–2157. doi: 10.1038/nprot.2013.137.

Ingber, D. (2017) *Human Organs-on-Chips*. Available at: <https://wyss.harvard.edu/technology/human-organs-on-chips/> (Accessed: 17 September 2020).

J. Gordon Betts, Kelly A. Young, James A. Wise, Eddie Johnson, Brandon Poe, Dean H. Kruse, Oksana Korol, Jody E. Johnson, Mark Womble, P. D. and OpenStax, P. (2013) *Anatomy and Physiology of the Female Reproductive System*. OpenStax.

J.Paavone (1983) *Physiology and ecology of the vagina*, *Scand J Infect Dis Suppl*. Available at: <https://pubmed.ncbi.nlm.nih.gov/6582587/> (Accessed: 20 September 2020).

Jin, H. J. *et al.* (2002) 'Electrospinning Bombyx mori silk with poly(ethylene oxide)', *Biomacromolecules*. American Chemical Society , 3(6), pp. 1233–1239. doi: 10.1021/bm025581u.

Johnson, A. P. *et al.* (1984) 'A study of the susceptibility of three species of primate to vaginal colonization with Gardnerella vaginalis', *British Journal of Experimental Pathology*. Wiley-Blackwell, 65(3), pp. 389–396. Available at: </pmc/articles/PMC2040981/?report=abstract> (Accessed: 29 September 2020).

Johnson, J. L. *et al.* (1980) *Taxonomy of the Lacto bacillus acidophilus Group*, *INTERNATIONAL JOURNAL OF SYSTEMATIC BACTERIOLOGY*.

Johnson, T. C. (2020) *Mycoplasma Genitalium STD: Symptoms, Treatment, and Prevention*. Available at: <https://www.webmd.com/sexual-conditions/mycoplasma-genitalium#1> (Accessed: 29 September 2020).

Kapałczyńska, M. *et al.* (2018) '2D and 3D cell cultures – a comparison of different types

of cancer cell cultures', *Archives of Medical Science*. Termedia Publishing House Ltd., 14(4), pp. 910–919. doi: 10.5114/aoms.2016.63743.

Khalili, A. A. and Ahmad, M. R. (2015) 'A Review of Cell Adhesion Studies for Biomedical and Biological Applications', pp. 18149–18184. doi: 10.3390/ijms160818149.

Khil, M. S. *et al.* (2003) 'Electrospun Nanofibrous Polyurethane Membrane as Wound Dressing', *Journal of Biomedical Materials Research - Part B Applied Biomaterials*. John Wiley and Sons Inc., 67(2), pp. 675–679. doi: 10.1002/jbm.b.10058.

Khoruzhenko, A. I. (2011) '2D- and 3D-cell culture', *Biopolymers and Cell*, 27(1), pp. 17–24. doi: 10.7124/bc.00007D.

Kim, S. E. *et al.* (2009) 'Electrospun gelatin/polyurethane blended nanofibers for wound healing', *Biomedical Materials*, 4(4). doi: 10.1088/1748-6041/4/4/044106.

Kuramoto, H., Tamura, S. and Notake, Y. (1972) 'Establishment of a cell line of human endometrial adenocarcinoma in vitro', *American Journal of Obstetrics and Gynecology*. Am J Obstet Gynecol, 114(8), pp. 1012–1019. doi: 10.1016/0002-9378(72)90861-7.

Laniewski, P. *et al.* (2017) 'Human three-dimensional endometrial epithelial cell model to study host interactions with vaginal bacteria and *Neisseria gonorrhoeae*', *Infection and Immunity*. American Society for Microbiology, 85(3). doi: 10.1128/IAI.01049-16.

Lauer, E., Helming, C. and Kandler, O. (1980) 'Heterogeneity of the Species *Lactobacillus acidophilus* (Moro) Hansen and Moquot as Revealed by Biochemical Characteristics and DNA-DNA hybridisation', *Zentralblatt für Bakteriologie: I. Abt. Originale C: Allgemeine, angewandte und ökologische Mikrobiologie*. Elsevier BV, 1(2), pp. 150–168. doi: 10.1016/s0172-5564(80)80037-6.

Laurencin, C. T. *et al.* (1999) 'Tissue engineering: Orthopedic applications', *Annual Review of Biomedical Engineering*. Annual Reviews Inc., 1(1), pp. 19–46. doi: 10.1146/annurev.bioeng.1.1.19.

Law, J. X. *et al.* (2017a) 'Electrospun Collagen Nanofibers and Their Applications in Skin Tissue Engineering', *Tissue Engineering and Regenerative Medicine*. Korean Tissue Engineering and Regenerative Medicine Society, pp. 699–718. doi: 10.1007/s13770-017-0075-9.

Law, J. X. *et al.* (2017b) 'Electrospun Collagen Nanofibers and Their Applications in Skin Tissue Engineering', *Tissue Engineering and Regenerative Medicine*. Korean Tissue Engineering and Regenerative Medicine Society, 14(6), pp. 699–718. doi: 10.1007/s13770-017-0075-9.

Leclerc, E., Sakai, Y. and Fujii, T. (2003) 'Cell Culture in 3-Dimensional Microfluidic Structure of PDMS', 1, pp. 109–114.

Li, Z. and Wang, C. (2013) 'Effects of Working Parameters on Electrospinning', in, pp. 15–28. doi: 10.1007/978-3-642-36427-3\_2.

Lim, M. M., Sun, T. and Sultana, N. (2015) 'In vitro biological evaluation of electrospun polycaprolactone/gelatine nanofibrous scaffold for tissue engineering', *Journal of Nanomaterials*, 2015. doi: 10.1155/2015/303426.

Marois, Y. and Be, M. C. (2001) 'Studies of Primary Reference Materials Low-Density Polyethylene and Polydimethylsiloxane : A Review', pp. 467–477.

Martin, D. H. and Marrazzo, J. M. (2016) 'The Vaginal Microbiome: Current Understanding and Future Directions', *Journal of Infectious Diseases*, 214(Suppl 1), pp. S36–S41. doi: 10.1093/infdis/jiw184.

*Microfluidics Background* (no date). Available at: <http://bme240.eng.uci.edu/students/06s/bmosadeg/microback.htm> (Accessed: 2 October 2020).

Min, B. M. *et al.* (2004) 'Electrospinning of silk fibroin nanofibers and its effect on the adhesion and spreading of normal human keratinocytes and fibroblasts in vitro', *Biomaterials*. Elsevier BV, 25(7–8), pp. 1289–1297. doi: 10.1016/j.biomaterials.2003.08.045.

Nair, N. R. *et al.* (2017) *Current Developments in Biotechnology and Bioengineering / ScienceDirect*. Edited by C. R. S. Ashok Pandey, Sangeeta Negi. Elsevier. doi: <https://doi.org/10.1016/B978-0-444-63662-1.00032-4>.

Ness, R. B. *et al.* (2002) 'Douching in relation to bacterial vaginosis, lactobacilli, and facultative bacteria in the vagina', *Obstetrics and Gynecology*. *Obstet Gynecol*, 100(4), pp. 765–772. doi: 10.1016/S0029-7844(02)02184-1.

NIH (2017) *Modeling the Female Reproductive Tract in 3-D: The Birth of EVATAR™ / National Center for Advancing Translational Sciences*. Available at: <https://ncats.nih.gov/pubs/features/evatar> (Accessed: 21 September 2020).

Noguchi K, Tsukumi K, U. T. (2003) 'Qualitative and quantitative differences in normal vaginal flora of conventionally reared mice, rats, hamsters, rabbits, and dogs - PubMed', *Comp Med.*, 53(4), pp. 404–12. Available at: <https://pubmed.ncbi.nlm.nih.gov/14524417/> (Accessed: 30 September 2020).

Nuge, T. *et al.* (2013) 'Electrospun gelatin composite nanofibres: A review on structural and mechanical characterizations', *Regenerative Research*, 2(2), pp. 39–42. Available at: [http://www.regres.tesma.org.my/pdf/RR-271113-009 R1 \(7\) final.pdf](http://www.regres.tesma.org.my/pdf/RR-271113-009 R1 (7) final.pdf).

Nye, M. B. *et al.* (2020) 'Prevalence of Mycoplasma genitalium infection in women with bacterial vaginosis', *BMC Women's Health*. *BMC Women's Health*, 20(1), pp. 1–5. doi: 10.1186/s12905-020-00926-6.



Pasirayi, G. *et al.* (2012) 'Microfluidic Bioreactors for Cell Culturing: A Review', *Micro and Nanosystemse*. Bentham Science Publishers Ltd., 3(2), pp. 137–160. doi: 10.2174/1876402911103020137.

Patterson, J. L. *et al.* (2007) 'Effect of biofilm phenotype on resistance of *Gardnerella vaginalis* to hydrogen peroxide and lactic acid', *American Journal of Obstetrics and Gynecology*. Mosby Inc., 197(2), pp. 170.e1-170.e7. doi: 10.1016/j.ajog.2007.02.027.

Patton, D. L. *et al.* (1996) 'The vaginal microflora of pig-tailed macaques and the effects of chlorhexidine and benzalkonium on this ecosystem', *Sexually Transmitted Diseases*. Lippincott Williams and Wilkins, 23(6), pp. 489–493. doi: 10.1097/00007435-199611000-00009.

Pleil, M. (2009) *Photolithography Overview for MEMS*. Available at: [www.scme-nm.org](http://www.scme-nm.org) (Accessed: 1 October 2020).

Poonia, B. *et al.* (2006) 'Cyclic changes in the vaginal epithelium of normal rhesus macaques', *Journal of Endocrinology*, 190, pp. 829–835. doi: 10.1677/joe.1.06873.

Pot, B. *et al.* (1993) 'Identification and classification of *Lactobacillus acidophilus*, *L. gasseri* and *L. johnsonii* strains by SDS-PAGE and rRNA-targeted oligonucleotide probe hybridization', *Journal of General Microbiology*. J Gen Microbiol, 139(3), pp. 513–517. doi: 10.1099/00221287-139-3-513.

*Professional 3D printing made accessible | Ultimaker* (2011). Available at: <https://ultimaker.com/> (Accessed: 1 October 2020).

*Promising Future of Human Organ Microchips* (2017). Available at: <https://wittysparks.com/human-organ-on-a-chip-technology/> (Accessed: 17 September 2020).

Qin, D., Xia, Y. and Whitesides, G. M. (2010) 'Soft lithography for micro- and nanoscale patterning', *Nature Protocols*. Nature Publishing Group, 5(3), pp. 491–502. doi: 10.1038/nprot.2009.234.

Quayle, A. J. (2002) 'The innate and early immune response to pathogen challenge in the female genital tract and the pivotal role of epithelial cells', in *Journal of Reproductive Immunology*. J Reprod Immunol, pp. 61–79. doi: 10.1016/S0165-0378(02)00019-0.

Radtke, A. L. and Herbst-Kralovetz, M. M. (2012) 'Culturing and applications of rotating wall vessel bioreactor derived 3D epithelial cell models', *Journal of Visualized Experiments*. Journal of Visualized Experiments, (62). doi: 10.3791/3868.

Radwan-Pragłowska, J. *et al.* (2020) 'The potential of novel chitosan-based scaffolds in pelvic organ prolapse (POP) treatment through tissue engineering', *Molecules*, 25(18). doi: 10.3390/molecules25184280.

- Ramalingam, R. *et al.* (2019) 'Poly- $\epsilon$ -caprolactone/gelatin hybrid electrospun composite nanofibrous mats containing ultrasound assisted herbal extract: Antimicrobial and cell proliferation study', *Nanomaterials*, 9(3). doi: 10.3390/nano9030462.
- Reneker, D. H. *et al.* (2000) 'Bending instability of electrically charged liquid jets of polymer solutions in electrospinning', *Journal of Applied Physics*. American Institute of Physics Inc., 87(9 I), pp. 4531–4547. doi: 10.1063/1.373532.
- Rosa R. Yu, Andrew T. Cheng, Laurel A. Lagenaur, Wenjun Huang, D. E. W. *et al.* (2009) *A Chinese rhesus macaque (Macaca mulatta) model for vaginal Lactobacillus colonization and live microbicide development*, *J Med Primatol*.
- Saha, D. *et al.* (2017) 'Expression of hemoglobin- $\alpha$  and  $\beta$  subunits in human vaginal epithelial cells and their functional significance', *PLoS ONE*. Public Library of Science, 12(2). doi: 10.1371/JOURNAL.PONE.0171084.
- Senok, A. C. *et al.* (2009) 'Probiotics for the treatment of bacterial vaginosis', *Cochrane Database of Systematic Reviews*. John Wiley and Sons Ltd. doi: 10.1002/14651858.CD006289.pub2.
- Sha, B. E. *et al.* (2005) 'Utility of amsel criteria, nugent score, and quantitative PCR for Gardnerella vaginalis, Mycoplasma hominis, and Lactobacillus spp. for diagnosis of bacterial vaginosis in human immunodeficiency virus-infected women', *Journal of Clinical Microbiology*. American Society for Microbiology (ASM), 43(9), pp. 4607–4612. doi: 10.1128/JCM.43.9.4607-4612.2005.
- Siddique, S. A. (2003) 'Vaginal Anatomy and Physiology', in *Journal of Pelvic Medicine and Surgery*, pp. 263–272. doi: 10.1097/01.spv.0000094481.95144.3d.
- Solving the Problems of Plastics Adhesion | Adhesion Bonding* (2012). Available at: <http://www.adhesionbonding.com/2012/05/03/solving-the-problems-of-plastics-adhesion/> (Accessed: 8 October 2020).
- Spraybase (2018) *Application notes for Electrospinning PCL Electrospinning Polycaprolactone (PCL) onto a flat plate collector*.
- Straube, T. and Müller, C. (2016) 'How to do a Proper Cell Culture Quick Check'.
- Sugiritama, W. (2009) *histologic structure of female genital system*. Available at: <https://www.slideshare.net/sugiritama/histologic-structure-of-female-genital-system-1630453> (Accessed: 20 September 2020).
- Sun, H. *et al.* (2020) 'Combining additive manufacturing with microfluidics: an emerging method for developing novel organs-on-chips', *Current Opinion in Chemical Engineering*. Elsevier Ltd, 28, pp. 1–9. doi: 10.1016/j.coche.2019.10.006.
- Tan, S. H. *et al.* (2010) 'Oxygen plasma treatment for reducing hydrophobicity of a

sealed polydimethylsiloxane microchannel'. doi: 10.1063/1.3466882.

Taylor, T. (2020) *Vagina - Anatomy Pictures and Information*. Available at: [https://www.innerbody.com/image\\_repfov/repo12-new.html](https://www.innerbody.com/image_repfov/repo12-new.html) (Accessed: 20 September 2020).

Teo, W. (2015) *Handbook Electrospinning parameters and fiber control*. Available at: <http://electrospintech.com/hb-espInParameter.html> (Accessed: 12 October 2020).

Thulkar, J., Kriplani, A. and Agarwal, N. (2010) 'Probiotic and metronidazole treatment for recurrent bacterial vaginosis', *International Journal of Gynecology and Obstetrics*. John Wiley and Sons Ltd, 108(3), pp. 251–252. doi: 10.1016/j.ijgo.2009.09.029.

Todar, K. (2008) *The Normal Bacterial Flora of Humans*. Available at: [http://textbookofbacteriology.net/normalflora\\_1.html](http://textbookofbacteriology.net/normalflora_1.html) (Accessed: 12 September 2021).

Truter, I. (2013) 'Bacterial vaginosis: Literature review of treatment options with specific emphasis on non-antibiotic treatment', *African Journal of Pharmacy and Pharmacology*, 7(48), pp. 3060–3067. doi: 10.5897/ajppx2013.0001.

Turovskiy, Sutyak Noll, and C. (2012) 'THE ETIOLOGY OF BACTERIAL VAGINOSIS', *Microbiol*, 110(5), pp. 1105–1128. doi: 10.1038/jid.2014.371.

Ustyugov, A. A. *et al.* (2018) 'Development of 3D Cell Culture on Ultra-High Molecular Weight Polyethylene (UHMWPE) as the Basis of Cellular Matrix', *Biomedical Chemistry: Research and Methods*. Institute of Biochemistry, 1(3), p. e00048. doi: 10.18097/bmcrm00048.

Vanechoutte, M. (2017) 'The human vaginal microbial community', *Research in Microbiology*. Elsevier Masson SAS, 168(9–10), pp. 811–825. doi: 10.1016/j.resmic.2017.08.001.

Varotsis, A. B. (2020a) *Introduction to FDM 3D printing | 3D Hubs*. Available at: <https://www.3dhubs.com/knowledge-base/introduction-fdm-3d-printing/#what> (Accessed: 2 October 2020).

Varotsis, A. B. (2020b) *Introduction to SLA 3D printing | 3D Hubs*. Available at: <https://www.3dhubs.com/knowledge-base/introduction-sla-3d-printing/#what> (Accessed: 1 October 2020).

Verma, A. *et al.* (2013) 'Fabrication of 3D charged particle trap using through-silicon vias etched by deep reactive ion etching', *Journal of Vacuum Science & Technology B, Nanotechnology and Microelectronics: Materials, Processing, Measurement, and Phenomena*. American Vacuum Society, 31(3), p. 032001. doi: 10.1116/1.4799662.

Verowhite - Sculpteo (no date). Available at:

<https://www.sculpteo.com/en/materials/polyjet-resin-material/verowhite-polyjet-resin-material/> (Accessed: 31 August 2020).

Verreck, G. *et al.* (2003) 'Incorporation of drugs in an amorphous state into electrospun nanofibers composed of a water-insoluble, nonbiodegradable polymer', *Journal of Controlled Release*. *J Control Release*, 92(3), pp. 349–360. doi: 10.1016/S0168-3659(03)00342-0.

Vittayarukskul, K. and Lee, A. P. (2017) 'A truly Lego®-like modular microfluidics platform', *Journal of Micromechanics and Microengineering*. IOP Publishing, 27(3), p. aa53ed. doi: 10.1088/1361-6439/aa53ed.

Wang, N. *et al.* (2014) 'Electrospun polyurethane-core and gelatin-shell coaxial fibre coatings for miniature implantable biosensors', *Biofabrication*, 6(1). doi: 10.1088/1758-5082/6/1/015002.

Wang, Z., He, Y. and Zheng, Y. (2019) 'Probiotics for the treatment of bacterial vaginosis: A meta-analysis', *International Journal of Environmental Research and Public Health*. MDPI AG. doi: 10.3390/ijerph16203859.

Ward, A. (2015) *Presenting the Form 1+ SLA 3D Printer*. Available at: <https://www.rs-online.com/designspark/presenting-the-form-1-sla-3d-printer> (Accessed: 1 October 2020).

Watson, S. (2019) *Vaginal pH Balance: Normal Levels, Correcting Unbalanced pH & More*. Available at: [https://www.healthline.com/health/womens-health/vaginal-ph-balance#\\_noHeaderPrefixedContent](https://www.healthline.com/health/womens-health/vaginal-ph-balance#_noHeaderPrefixedContent) (Accessed: 12 September 2021).

van de Wijgert, J. H. H. M. *et al.* (2020) 'Intermittent Lactobacilli-containing Vaginal Probiotic or Metronidazole Use to Prevent Bacterial Vaginosis Recurrence: A Pilot Study Incorporating Microscopy and Sequencing', *Scientific Reports*. Nature Research, 10(1), pp. 1–15. doi: 10.1038/s41598-020-60671-6.

Woodruff, M. A. and Hutmacher, D. W. (2010) 'The return of a forgotten polymer - Polycaprolactone in the 21st century', *Progress in Polymer Science (Oxford)*. Elsevier Ltd, pp. 1217–1256. doi: 10.1016/j.progpolymsci.2010.04.002.

Woodruff, T. K. (2013a) *Evatar: The Mother of MicroHumans | Woodruff Lab*. Available at: <https://www.woodrufflab.org/Evatar> MPS (Accessed: 14 October 2020).

Woodruff, T. K. (2013b) *Ex Vivo Female Reproductive Tract Integration in a 3D Microphysiologic System (active) | Woodruff Lab*. Available at: <https://www.woodrufflab.org/FemKUBE> (Accessed: 14 October 2020).

Wu, Q. *et al.* (2020) 'Organ-on-a-chip: Recent breakthroughs and future prospects', *BioMedical Engineering Online*. BioMed Central, 19(1), pp. 1–19. doi: 10.1186/s12938-020-0752-0.

- Xiao, S. *et al.* (2017) 'A microfluidic culture model of the human reproductive tract and 28-day menstrual cycle', *Nature Communications*. Nature Publishing Group, 8, pp. 1–13. doi: 10.1038/ncomms14584.
- Yang, Q., Lian, Q. and Xu, F. (2017) 'Perspective : Fabrication of integrated organ-on-a-chip via bioprinting', 031301, pp. 1–5. doi: 10.1063/1.4982945.
- Yi, H. G., Lee, H. and Cho, D. W. (2017) '3D printing of organs-on-chips', *Bioengineering*. MDPI AG. doi: 10.3390/bioengineering4010010.
- Zhang, Y. *et al.* (2005) 'Electrospinning of gelatin fibers and gelatin/PCL composite fibrous scaffolds', *Journal of Biomedical Materials Research - Part B Applied Biomaterials*. doi: 10.1002/jbm.b.30128.
- Zhang, Y. Z. *et al.* (2006) 'Crosslinking of the electrospun gelatin nanofibers', *Polymer*, 47(8), pp. 2911–2917. doi: 10.1016/j.polymer.2006.02.046.
- Zheng, W. *et al.* (2014) 'Functionalization of PCL fibrous membrane with RGD peptide by a naturally occurring condensation reaction', *Chinese Science Bulletin*. Science in China Press, 59(22), pp. 2776–2784. doi: 10.1007/s11434-014-0336-0.
- Zhou, X. *et al.* (2004) 'Characterization of vaginal microbial communities in adult healthy women using cultivation-independent methods', *Microbiology*. Society for General Microbiology, 150(8), pp. 2565–2573. doi: 10.1099/mic.0.26905-0.
- Zong, X. *et al.* (2003) 'Control of structure, morphology and property in electrospun poly(glycolide-co-lactide) non-woven membranes via post-draw treatments', *Polymer*. Elsevier BV, 44(17), pp. 4959–4967. doi: 10.1016/S0032-3861(03)00464-6.
- Aleshkin, V. A., Voropaeva, E. A. and Shenderov, B. A. (2006) 'Vaginal microbiota in healthy women and patients with bacterial vaginosis and nonspecific vaginitis', *Microbial Ecology in Health and Disease*. Taylor & Francis, 18(2), pp. 71–74. doi: 10.1080/17482960600891473.
- Aroutcheva, A. *et al.* (2001) 'Defense factors of vaginal lactobacilli', *American Journal of Obstetrics and Gynecology*. Am J Obstet Gynecol, 185(2), pp. 375–379. doi: 10.1067/mob.2001.115867.
- Ashammakhi, N. *et al.* (2012) 'Nanofiber-based scaffolds for tissue engineering', *European Journal of Plastic Surgery*, 35(2), pp. 135–149. doi: 10.1007/s00238-008-0217-3.
- Baah-Dwomoh, A. *et al.* (2016) 'Mechanical Properties of Female Reproductive Organs and Supporting Connective Tissues: A Review of the Current State of Knowledge', *Applied Mechanics Reviews*, 68(6), pp. 1–12. doi: 10.1115/1.4034442.
- Bein, A. *et al.* (2018) 'Microfluidic Organ-on-a-Chip Models of Human Intestine', *CMGH*.

Elsevier Inc, pp. 659–668. doi: 10.1016/j.jcmgh.2017.12.010.

Bellis, S. L. (2011) 'Advantages of RGD peptides for directing cell association with biomaterials', *Biomaterials*. Elsevier Ltd, 32(18), pp. 4205–4210. doi: 10.1016/j.biomaterials.2011.02.029.

Bitew, A. *et al.* (2017) 'Prevalence of bacterial vaginosis and associated risk factors among women complaining of genital tract infection', *International Journal of Microbiology*, 2017. doi: 10.1155/2017/4919404.

Boskey, E. R. *et al.* (2001) 'Origins of vaginal acidity: High D/L lactate ratio is consistent with bacteria being the primary source', *Human Reproduction*. Oxford University Press, 16(9), pp. 1809–1813. doi: 10.1093/humrep/16.9.1809.

Boskey, E. R. (2005) 'Alternative therapies for bacterial vaginosis: A literature review and acceptability survey', *Alternative Therapies in Health and Medicine*, 11(5), pp. 38–43.

Boskey ER, Telsch KM, Whaley KJ, Moench TR, C. R. (1999) *Acid production by vaginal flora in vitro is consistent with the rate and extent of vaginal acidification.*, *Infect Immun* 67. Available at: [https://www.researchgate.net/publication/12803174\\_Boskey\\_ER\\_Telsch\\_KM\\_Whaley\\_KJ\\_Moench\\_TR\\_Cone\\_RA\\_Acid\\_production\\_by\\_vaginal\\_flora\\_in\\_vitro\\_is\\_consistent\\_with\\_the\\_rate\\_and\\_extent\\_of\\_vaginal\\_acidification\\_Infect\\_Immun\\_67\\_5170-5175](https://www.researchgate.net/publication/12803174_Boskey_ER_Telsch_KM_Whaley_KJ_Moench_TR_Cone_RA_Acid_production_by_vaginal_flora_in_vitro_is_consistent_with_the_rate_and_extent_of_vaginal_acidification_Infect_Immun_67_5170-5175) (Accessed: 13 September 2020).

Bournias Varotsis, A. (2019) 'Introduction to Material Jetting 3D Printing', *3DHubs*. Available at: <https://www.3dhubs.com/knowledge-base/introduction-material-jetting-3d-printing/#what> (Accessed: 2 October 2020).

Bradshaw, C. S. and Brotman, R. M. (2015a) 'Making inroads into improving treatment of bacterial vaginosis - striving for long-term cure.', *BMC infectious diseases*. BMC Infectious Diseases, 15(1), p. 292. doi: 10.1186/s12879-015-1027-4.

Bradshaw, C. S. and Brotman, R. M. (2015b) 'Making inroads into improving treatment of bacterial vaginosis – striving for long-term cure'. doi: 10.1186/s12879-015-1027-4.

Bradshaw, C. S. and Sobel, J. D. (2016) 'Current Treatment of Bacterial Vaginosis- Limitations and Need for Innovation', *Journal of Infectious Diseases*, 214(Suppl 1), pp. S14–S20. doi: 10.1093/infdis/jiw159.

Branavan, M. *et al.* (2016) 'Modular development of a prototype point of care molecular diagnostic platform for sexually transmitted infections', *Medical Engineering and Physics*, 38(8). doi: 10.1016/j.medengphy.2016.04.022.

Brusie, C. (2019) *What Happens to Your Vagina After Pregnancy and Birth?* Available at: <https://www.verywellfamily.com/what-happens-to-your-vagina-after-pregnancy->

4156275 (Accessed: 20 September 2020).

Burton, J. P., Cadieux, P. A. and Reid, G. (2003) 'Improved understanding of the bacterial vaginal microbiota of women before and after probiotic instillation', *Applied and Environmental Microbiology*. Appl Environ Microbiol, 69(1), pp. 97–101. doi: 10.1128/AEM.69.1.97-101.2003.

Burton, J. P. and Reid, G. (2002) 'Evaluation of the bacterial vaginal flora of 20 postmenopausal women by direct (Nugent score) and molecular (polymerase chain reaction and denaturing gradient gel electrophoresis) techniques', *Journal of Infectious Diseases*. J Infect Dis, 186(12), pp. 1770–1780. doi: 10.1086/345761.

Burugapalli, K. *et al.* (2018) 'Biomimetic electrospun coatings increase the in vivo sensitivity of implantable glucose biosensors', *Journal of Biomedical Materials Research - Part A*, 106(4), pp. 1072–1081. doi: 10.1002/jbm.a.36308.

Charati, S. G. and Stern, S. A. (1998) 'Diffusion of Gases in Silicone Polymers : Molecular Dynamics Simulations', 9297(98), pp. 5529–5535.

Chen, D. *et al.* (2019) 'Electrospun polycaprolactone/collagen nanofibers cross-linked with 1-ethyl-3-(3-dimethylaminopropyl) carbodiimide/N-hydroxysuccinimide and genipin facilitate endothelial cell regeneration and may be a promising candidate for vascular scaffolds', *International Journal of Nanomedicine*. Dove Press, 14, pp. 2127–2144. doi: 10.2147/IJN.S192699.

Choktaweasap, N. *et al.* (2007) 'Electrospun gelatin fibers: Effect of solvent system on morphology and fiber diameters', *Polymer Journal*. Nature Publishing Group, 39(6), pp. 622–631. doi: 10.1295/polymj.PJ2006190.

Cipitria, A. *et al.* (2011) 'Design, fabrication and characterization of PCL electrospun scaffolds - A review', *Journal of Materials Chemistry*, 21(26), pp. 9419–9453. doi: 10.1039/c0jm04502k.

Coimbra, P. *et al.* (2017) 'Coaxial electrospun PCL/Gelatin-MA fibers as scaffolds for vascular tissue engineering', *Colloids and Surfaces B: Biointerfaces*. Elsevier B.V., 159, pp. 7–15. doi: 10.1016/j.colsurfb.2017.07.065.

Daelemans, L. *et al.* (2018) 'Nanostructured hydrogels by blend electrospinning of polycaprolactone/gelatin nanofibers', *Nanomaterials*, 8(7), pp. 1–12. doi: 10.3390/nano8070551.

Devillard, E. *et al.* (2004) 'Novel insight into the vaginal microflora in postmenopausal women under hormone replacement therapy as analyzed by PCR-denaturing gradient gel electrophoresis', *European Journal of Obstetrics and Gynecology and Reproductive Biology*, 117(1), pp. 76–81. doi: 10.1016/j.ejogrb.2004.02.001.

Donia, M. S. *et al.* (2014) 'A systematic analysis of biosynthetic gene clusters in the

human microbiome reveals a common family of antibiotics.', *Cell*. Cell, 158(6), pp. 1402–1414. doi: 10.1016/j.cell.2014.08.032.

Easmon, C. S., Hay, P. E. and Ison, C. A. (1992) 'Bacterial vaginosis: a diagnostic approach', *Genitourinary medicine*, 68(2), pp. 134–138.

England, N. (2018a) *Bartholin's cyst*. Available at: <https://www.nhs.uk/conditions/bartholins-cyst/> (Accessed: 20 September 2020).

England, N. (2018b) *Is my vagina normal? - NHS*. Available at: <https://www.nhs.uk/live-well/sexual-health/vagina-shapes-and-sizes/> (Accessed: 20 September 2020).

Fasnacht, A. (2017) *SLA vs. PolyJet: What You Need to Know | CADimensions*. Available at: <https://www.cadimensions.com/blog/sla-vs-polyjet-need-know/> (Accessed: 1 October 2020).

Fertala, A., Han, W. B. and Ko, F. K. (2001) 'Mapping critical sites in collagen II for rational design of gene-engineered proteins for cell-supporting materials', *Journal of Biomedical Materials Research*. J Biomed Mater Res, 57(1), pp. 48–58. doi: 10.1002/1097-4636(200110)57:1<48::AID-JBM1140>3.0.CO;2-S.

Fethers, K. A. *et al.* (2008) 'Sexual risk factors and bacterial vaginosis: A systematic review and meta-analysis', *Clinical Infectious Diseases*. Clin Infect Dis, pp. 1426–1435. doi: 10.1086/592974.

Fichorova, R. N. *et al.* (2011) 'Novel vaginal microflora colonization model providing new insight into microbicide mechanism of action', *mBio*, 2(6), pp. 1–10. doi: 10.1128/mBio.00168-11.

Fichorova, R. N. and Anderson, D. J. (1999) 'Differential expression of immunobiological mediators by immortalized human cervical and vaginal epithelial cells', *Biology of Reproduction*. Biol Reprod, 60(2), pp. 508–514. doi: 10.1095/biolreprod60.2.508.

Fichorova, R. N., Rheinwald, J. G. and Anderson, D. J. (1997) 'Generation of papillomavirus-immortalized cell lines from normal human ectocervical, endocervical, and vaginal epithelium that maintain expression of tissue-specific differentiation proteins', *Biology of Reproduction*, 57(4), pp. 847–855. doi: 10.1095/biolreprod57.4.847.

Forsum, U. *et al.* (2005) 'Bacterial vaginosis - A microbiological and immunological enigma', *Apmis*, 113(2), pp. 81–90. doi: 10.1111/j.1600-0463.2005.apm1130201.x.

Fu, W. *et al.* (2014) 'Electrospun gelatin / PCL and collagen / PLCL scaffolds for vascular tissue engineering', pp. 2335–2344.

Fujisawa, T. *et al.* (1992) 'Taxonomic study of the *Lactobacillus acidophilus* group, with recognition of *Lactobacillus gallinarum* sp. nov. and *Lactobacillus johnsonii* sp. nov. and



synonymy of *Lactobacillus acidophilus* group A3 (Johnson et al. 1980) with the type strain of *Lactobacillus amylovorus* (Nakamura 1981)', *International Journal of Systematic Bacteriology*. *Int J Syst Bacteriol*, 42(3), pp. 487–491. doi: 10.1099/00207713-42-3-487.

Garg, K. and Bowlin, G. L. (2011) 'Electrospinning jets and nanofibrous structures', *Biomicrofluidics*. American Institute of Physics Inc., 5(1). doi: 10.1063/1.3567097.

Gilbert, N. M., Lewis, W. G. and Lewis, A. L. (2013) 'Clinical Features of Bacterial Vaginosis in a Murine Model of Vaginal Infection with *Gardnerella vaginalis*', *PLoS ONE*, 8(3). doi: 10.1371/journal.pone.0059539.

Gillet, E. *et al.* (2011) 'Bacterial vaginosis is associated with uterine cervical human papillomavirus infection: A meta-analysis', *BMC Infectious Diseases*, 11. doi: 10.1186/1471-2334-11-10.

Ginkel, P. D. *et al.* (1993) 'Vaginal Flora in Postmenopausal Women: The Effect of Estrogen Replacement', *Infectious Diseases in Obstetrics and Gynecology*. *Infect Dis Obstet Gynecol*, 1(2), pp. 94–97. doi: 10.1155/S1064744993000225.

Gökaltun, A. *et al.* (2019) 'Simple Surface Modification of Poly(dimethylsiloxane) via Surface Segregating Smart Polymers for Biomicrofluidics', *Scientific Reports*. Springer US, 9(1), pp. 1–14. doi: 10.1038/s41598-019-43625-5.

Gold, J. M. and Shrimanker, I. (2019) *Physiology, Vaginal, StatPearls*. StatPearls Publishing. Available at: <http://www.ncbi.nlm.nih.gov/pubmed/31424731> (Accessed: 20 September 2020).

Guarino, V. *et al.* (2017) 'Polycaprolactone: Synthesis, Properties, and Applications', in *Encyclopedia of Polymer Science and Technology*. Hoboken, NJ, USA: John Wiley & Sons, Inc., pp. 1–36. doi: 10.1002/0471440264.pst658.

Haslauer, C. M. *et al.* (2011) 'Collagen-PCL sheath-core bicomponent electrospun scaffolds increase osteogenic differentiation and calcium accretion of human adipose-derived stem cells', *Journal of Biomaterials Science, Polymer Edition*, 22(13), pp. 1695–1712. doi: 10.1163/092050610X521595.

Haubert, K., Drier, T. and Beebe, D. (2006) 'PDMS bonding by means of a portable, low-cost corona system', *Lab on a Chip*. Royal Society of Chemistry, 6(12), pp. 1548–1549. doi: 10.1039/b610567j.

Herbst-Kralovetz, M. M. *et al.* (2008) 'Quantification and comparison of toll-like receptor expression and responsiveness in primary and immortalized human female lower genital tract epithelia', *American Journal of Reproductive Immunology*. Wiley-Blackwell, 59(3), pp. 212–224. doi: 10.1111/j.1600-0897.2007.00566.x.

Herbst-Kralovetz, M. M. *et al.* (2016) 'New Systems for Studying Intercellular

Interactions in Bacterial Vaginosis', *Journal of Infectious Diseases*. Oxford University Press, 214(Suppl 1), pp. S6–S13. doi: 10.1093/infdis/jiw130.

Hjelm, B. E. *et al.* (2010) 'Development and Characterization of a Three-Dimensional Organotypic Human Vaginal Epithelial Cell Model1', *Biology of Reproduction*, 82(3), pp. 617–627. doi: 10.1095/biolreprod.109.080408.

Hoffmann, J. N. *et al.* (2014) 'Prevalence of Bacterial Vaginosis and Candida among Postmenopausal Women in the United States', *Journals of Gerontology, Series B: Psychological Sciences and Social Sciences*, 69(8), pp. 205–214. doi: 10.1093/geronb/gbu105.

Horuz, T. İ. and Bülent Belibağlı, K. (2017) 'Production of electrospun gelatin nanofibers: An optimization study by using Taguchi's methodology', *Materials Research Express*. Institute of Physics Publishing, 4(1), p. 015023. doi: 10.1088/2053-1591/aa57ea.

Huang, H., Song, L. and Zhao, W. (2014) 'Effects of probiotics for the treatment of bacterial vaginosis in adult women: A meta-analysis of randomized clinical trials', *Archives of Gynecology and Obstetrics*. Springer Verlag, 289(6), pp. 1225–1234. doi: 10.1007/s00404-013-3117-0.

Huang, Z.-M. *et al.* (2003) 'A review on polymer nanofibers by electrospinning and their applications in nanocomposites'. doi: 10.1016/S0266-3538(03)00178-7.

Huang, Z. M. *et al.* (2003) 'A review on polymer nanofibers by electrospinning and their applications in nanocomposites', *Composites Science and Technology*, 63(15), pp. 2223–2253. doi: 10.1016/S0266-3538(03)00178-7.

Huang, Z. M. *et al.* (2004) 'Electrospinning and mechanical characterization of gelatin nanofibers', *Polymer*. Elsevier BV, 45(15), pp. 5361–5368. doi: 10.1016/j.polymer.2004.04.005.

Huh, D. *et al.* (2010) 'Reconstituting organ-level lung functions on a chip.', *Science (New York, N.Y.)*. American Association for the Advancement of Science, 328(5986), pp. 1662–8. doi: 10.1126/science.1188302.

Huh, D. *et al.* (2013a) 'Microfabrication of human organs-on-chips', *Nature Protocols*. Nature Publishing Group, 8(11), pp. 2135–2157. doi: 10.1038/nprot.2013.137.

Huh, D. *et al.* (2013b) 'Microfabrication of human organs-on-chips', *Nature Protocols*, 8(11), pp. 2135–2157. doi: 10.1038/nprot.2013.137.

Huh, D. *et al.* (2013c) 'Microfabrication of human organs-on-chips', *Nature Protocols*, 8(11), pp. 2135–2157. doi: 10.1038/nprot.2013.137.

Ingber, D. (2017) *Human Organs-on-Chips*. Available at: <https://wyss.harvard.edu/technology/human-organs-on-chips/> (Accessed: 17

September 2020).

J. Gordon Betts, Kelly A. Young, James A. Wise, Eddie Johnson, Brandon Poe, Dean H. Kruse, Oksana Korol, Jody E. Johnson, Mark Womble, P. D. and OpenStax, P. (2013) *Anatomy and Physiology of the Female Reproductive System*. OpenStax.

J.Paavone (1983) *Physiology and ecology of the vagina*, *Scand J Infect Dis Suppl*. Available at: <https://pubmed.ncbi.nlm.nih.gov/6582587/> (Accessed: 20 September 2020).

Jin, H. J. *et al.* (2002) 'Electrospinning Bombyx mori silk with poly(ethylene oxide)', *Biomacromolecules*. American Chemical Society , 3(6), pp. 1233–1239. doi: 10.1021/bm025581u.

Johnson, A. P. *et al.* (1984) 'A study of the susceptibility of three species of primate to vaginal colonization with Gardnerella vaginalis', *British Journal of Experimental Pathology*. Wiley-Blackwell, 65(3), pp. 389–396. Available at: </pmc/articles/PMC2040981/?report=abstract> (Accessed: 29 September 2020).

Johnson, J. L. *et al.* (1980) *Taxonomy of the Lacto bacillus acidophilus Group*, *INTERNATIONAL JOURNAL OF SYSTEMATIC BACTERIOLOGY*.

Johnson, T. C. (2020) *Mycoplasma Genitalium STD: Symptoms, Treatment, and Prevention*. Available at: <https://www.webmd.com/sexual-conditions/mycoplasma-genitalium#1> (Accessed: 29 September 2020).

Kapałczyńska, M. *et al.* (2018) '2D and 3D cell cultures – a comparison of different types of cancer cell cultures', *Archives of Medical Science*. Termedia Publishing House Ltd., 14(4), pp. 910–919. doi: 10.5114/aoms.2016.63743.

Khalili, A. A. and Ahmad, M. R. (2015) 'A Review of Cell Adhesion Studies for Biomedical and Biological Applications', pp. 18149–18184. doi: 10.3390/ijms160818149.

Khil, M. S. *et al.* (2003) 'Electrospun Nanofibrous Polyurethane Membrane as Wound Dressing', *Journal of Biomedical Materials Research - Part B Applied Biomaterials*. John Wiley and Sons Inc., 67(2), pp. 675–679. doi: 10.1002/jbm.b.10058.

Khoruzhenko, A. I. (2011) '2D- and 3D-cell culture', *Biopolymers and Cell*, 27(1), pp. 17–24. doi: 10.7124/bc.00007D.

Kim, S. E. *et al.* (2009) 'Electrospun gelatin/polyurethane blended nanofibers for wound healing', *Biomedical Materials*, 4(4). doi: 10.1088/1748-6041/4/4/044106.

Kuramoto, H., Tamura, S. and Notake, Y. (1972) 'Establishment of a cell line of human endometrial adenocarcinoma in vitro', *American Journal of Obstetrics and Gynecology*. Am J Obstet Gynecol, 114(8), pp. 1012–1019. doi: 10.1016/0002-9378(72)90861-7.

Laniewski, P. *et al.* (2017) 'Human three-dimensional endometrial epithelial cell model

to study host interactions with vaginal bacteria and *Neisseria gonorrhoeae*', *Infection and Immunity*. American Society for Microbiology, 85(3). doi: 10.1128/IAI.01049-16.

Lauer, E., Helming, C. and Kandler, O. (1980) 'Heterogeneity of the Species *Lactobacillus acidophilus* (Moro) Hansen and Moquot as Revealed by Biochemical Characteristics and DNA-DNA hybridisation', *Zentralblatt für Bakteriologie: I. Abt. Originale C: Allgemeine, angewandte und ökologische Mikrobiologie*. Elsevier BV, 1(2), pp. 150–168. doi: 10.1016/s0172-5564(80)80037-6.

Laurencin, C. T. *et al.* (1999) 'Tissue engineering: Orthopedic applications', *Annual Review of Biomedical Engineering*. Annual Reviews Inc., 1(1), pp. 19–46. doi: 10.1146/annurev.bioeng.1.1.19.

Law, J. X. *et al.* (2017a) 'Electrospun Collagen Nanofibers and Their Applications in Skin Tissue Engineering', *Tissue Engineering and Regenerative Medicine*. Korean Tissue Engineering and Regenerative Medicine Society, pp. 699–718. doi: 10.1007/s13770-017-0075-9.

Law, J. X. *et al.* (2017b) 'Electrospun Collagen Nanofibers and Their Applications in Skin Tissue Engineering', *Tissue Engineering and Regenerative Medicine*. Korean Tissue Engineering and Regenerative Medicine Society, 14(6), pp. 699–718. doi: 10.1007/s13770-017-0075-9.

Leclerc, E., Sakai, Y. and Fujii, T. (2003) 'Cell Culture in 3-Dimensional Microfluidic Structure of PDMS', 1, pp. 109–114.

Li, Z. and Wang, C. (2013) 'Effects of Working Parameters on Electrospinning', in, pp. 15–28. doi: 10.1007/978-3-642-36427-3\_2.

Lim, M. M., Sun, T. and Sultana, N. (2015) 'In vitro biological evaluation of electrospun polycaprolactone/gelatine nanofibrous scaffold for tissue engineering', *Journal of Nanomaterials*, 2015. doi: 10.1155/2015/303426.

Marois, Y. and Be, M. C. (2001) 'Studies of Primary Reference Materials Low-Density Polyethylene and Polydimethylsiloxane : A Review', pp. 467–477.

Martin, D. H. and Marrazzo, J. M. (2016) 'The Vaginal Microbiome: Current Understanding and Future Directions', *Journal of Infectious Diseases*, 214(Suppl 1), pp. S36–S41. doi: 10.1093/infdis/jiw184.

*Microfluidics Background* (no date). Available at: <http://bme240.eng.uci.edu/students/06s/bmosadeg/microback.htm> (Accessed: 2 October 2020).

Min, B. M. *et al.* (2004) 'Electrospinning of silk fibroin nanofibers and its effect on the adhesion and spreading of normal human keratinocytes and fibroblasts in vitro', *Biomaterials*. Elsevier BV, 25(7–8), pp. 1289–1297. doi:

10.1016/j.biomaterials.2003.08.045.

Nair, N. R. *et al.* (2017) *Current Developments in Biotechnology and Bioengineering / ScienceDirect*. Edited by C. R. S. Ashok Pandey, Sangeeta Negi. Elsevier. doi: <https://doi.org/10.1016/B978-0-444-63662-1.00032-4>.

Ness, R. B. *et al.* (2002) 'Douching in relation to bacterial vaginosis, lactobacilli, and facultative bacteria in the vagina', *Obstetrics and Gynecology*. *Obstet Gynecol*, 100(4), pp. 765–772. doi: 10.1016/S0029-7844(02)02184-1.

NIH (2017) *Modeling the Female Reproductive Tract in 3-D: The Birth of EVATAR™ / National Center for Advancing Translational Sciences*. Available at: <https://ncats.nih.gov/pubs/features/evatar> (Accessed: 21 September 2020).

Noguchi K, Tsukumi K, U. T. (2003) 'Qualitative and quantitative differences in normal vaginal flora of conventionally reared mice, rats, hamsters, rabbits, and dogs - PubMed', *Comp Med.*, 53(4), pp. 404–12. Available at: <https://pubmed.ncbi.nlm.nih.gov/14524417/> (Accessed: 30 September 2020).

Nuge, T. *et al.* (2013) 'Electrospun gelatin composite nanofibres: A review on structural and mechanical characterizations', *Regenerative Research*, 2(2), pp. 39–42. Available at: [http://www.regres.tesma.org.my/pdf/RR-271113-009 R1 \(7\) final.pdf](http://www.regres.tesma.org.my/pdf/RR-271113-009 R1 (7) final.pdf).

Nye, M. B. *et al.* (2020) 'Prevalence of Mycoplasma genitalium infection in women with bacterial vaginosis', *BMC Women's Health*. *BMC Women's Health*, 20(1), pp. 1–5. doi: 10.1186/s12905-020-00926-6.

Pasirayi, G. *et al.* (2012) 'Microfluidic Bioreactors for Cell Culturing: A Review', *Micro and Nanosystemse*. Bentham Science Publishers Ltd., 3(2), pp. 137–160. doi: 10.2174/1876402911103020137.

Patterson, J. L. *et al.* (2007) 'Effect of biofilm phenotype on resistance of Gardnerella vaginalis to hydrogen peroxide and lactic acid', *American Journal of Obstetrics and Gynecology*. Mosby Inc., 197(2), pp. 170.e1-170.e7. doi: 10.1016/j.ajog.2007.02.027.

Patton, D. L. *et al.* (1996) 'The vaginal microflora of pig-tailed macaques and the effects of chlorhexidine and benzalkonium on this ecosystem', *Sexually Transmitted Diseases*. Lippincott Williams and Wilkins, 23(6), pp. 489–493. doi: 10.1097/00007435-199611000-00009.

Pleil, M. (2009) *Photolithography Overview for MEMS*. Available at: [www.scme-nm.org](http://www.scme-nm.org) (Accessed: 1 October 2020).

Poonia, B. *et al.* (2006) 'Cyclic changes in the vaginal epithelium of normal rhesus macaques', *Journal of Endocrinology*, 190, pp. 829–835. doi: 10.1677/joe.1.06873.

Pot, B. *et al.* (1993) 'Identification and classification of Lactobacillus acidophilus, L.

gasseri and L. johnsonii strains by SDS-PAGE and rRNA-targeted oligonucleotide probe hybridization', *Journal of General Microbiology*. J Gen Microbiol, 139(3), pp. 513–517. doi: 10.1099/00221287-139-3-513.

*Professional 3D printing made accessible | Ultimaker* (2011). Available at: <https://ultimaker.com/> (Accessed: 1 October 2020).

*Promising Future of Human Organ Microchips* (2017). Available at: <https://wittysparks.com/human-organ-on-a-chip-technology/> (Accessed: 17 September 2020).

Qin, D., Xia, Y. and Whitesides, G. M. (2010) 'Soft lithography for micro- and nanoscale patterning', *Nature Protocols*. Nature Publishing Group, 5(3), pp. 491–502. doi: 10.1038/nprot.2009.234.

Quayle, A. J. (2002) 'The innate and early immune response to pathogen challenge in the female genital tract and the pivotal role of epithelial cells', in *Journal of Reproductive Immunology*. J Reprod Immunol, pp. 61–79. doi: 10.1016/S0165-0378(02)00019-0.

Radtke, A. L. and Herbst-Kralovetz, M. M. (2012) 'Culturing and applications of rotating wall vessel bioreactor derived 3D epithelial cell models', *Journal of Visualized Experiments*. Journal of Visualized Experiments, (62). doi: 10.3791/3868.

Radwan-Pragłowska, J. *et al.* (2020) 'The potential of novel chitosan-based scaffolds in pelvic organ prolapse (POP) treatment through tissue engineering', *Molecules*, 25(18). doi: 10.3390/molecules25184280.

Ramalingam, R. *et al.* (2019) 'Poly- $\epsilon$ -caprolactone/gelatin hybrid electrospun composite nanofibrous mats containing ultrasound assisted herbal extract: Antimicrobial and cell proliferation study', *Nanomaterials*, 9(3). doi: 10.3390/nano9030462.

Reneker, D. H. *et al.* (2000) 'Bending instability of electrically charged liquid jets of polymer solutions in electrospinning', *Journal of Applied Physics*. American Institute of Physics Inc., 87(9 I), pp. 4531–4547. doi: 10.1063/1.373532.

Rosa R. Yu, Andrew T. Cheng, Laurel A. Lagenaur, Wenjun Huang, D. E. W. *et al.* (2009) *A Chinese rhesus macaque (Macaca mulatta) model for vaginal Lactobacillus colonization and live microbicide development*, *J Med Primatol*.

Saha, D. *et al.* (2017) 'Expression of hemoglobin- $\alpha$  and  $\beta$  subunits in human vaginal epithelial cells and their functional significance', *PLoS ONE*. Public Library of Science, 12(2). doi: 10.1371/JOURNAL.PONE.0171084.

Senok, A. C. *et al.* (2009) 'Probiotics for the treatment of bacterial vaginosis', *Cochrane Database of Systematic Reviews*. John Wiley and Sons Ltd. doi: 10.1002/14651858.CD006289.pub2.

- Sha, B. E. *et al.* (2005) 'Utility of amsel criteria, nugent score, and quantitative PCR for Gardnerella vaginalis, Mycoplasma hominis, and Lactobacillus spp. for diagnosis of bacterial vaginosis in human immunodeficiency virus-infected women', *Journal of Clinical Microbiology*. American Society for Microbiology (ASM), 43(9), pp. 4607–4612. doi: 10.1128/JCM.43.9.4607-4612.2005.
- Siddique, S. A. (2003) 'Vaginal Anatomy and Physiology', in *Journal of Pelvic Medicine and Surgery*, pp. 263–272. doi: 10.1097/01.spv.0000094481.95144.3d.
- Solving the Problems of Plastics Adhesion | Adhesion Bonding* (2012). Available at: <http://www.adhesionbonding.com/2012/05/03/solving-the-problems-of-plastics-adhesion/> (Accessed: 8 October 2020).
- Spraybase (2018) *Application notes for Electrospinning PCL Electrospinning Polycaprolactone (PCL) onto a flat plate collector*.
- Straube, T. and Müller, C. (2016) 'How to do a Proper Cell Culture Quick Check'.
- Sugiritama, W. (2009) *histologic structure of female genital system*. Available at: <https://www.slideshare.net/sugiritama/histologic-structure-of-female-genital-system-1630453> (Accessed: 20 September 2020).
- Sun, H. *et al.* (2020) 'Combining additive manufacturing with microfluidics: an emerging method for developing novel organs-on-chips', *Current Opinion in Chemical Engineering*. Elsevier Ltd, 28, pp. 1–9. doi: 10.1016/j.coche.2019.10.006.
- Tan, S. H. *et al.* (2010) 'Oxygen plasma treatment for reducing hydrophobicity of a sealed polydimethylsiloxane microchannel'. doi: 10.1063/1.3466882.
- Taylor, T. (2020) *Vagina - Anatomy Pictures and Information*. Available at: [https://www.innerbody.com/image\\_repfov/repo12-new.html](https://www.innerbody.com/image_repfov/repo12-new.html) (Accessed: 20 September 2020).
- Teo, W. (2015) *Handbook Electrospinning parameters and fiber control*. Available at: <http://electrospintech.com/hb-espInParameter.html> (Accessed: 12 October 2020).
- Thulkar, J., Kriplani, A. and Agarwal, N. (2010) 'Probiotic and metronidazole treatment for recurrent bacterial vaginosis', *International Journal of Gynecology and Obstetrics*. John Wiley and Sons Ltd, 108(3), pp. 251–252. doi: 10.1016/j.ijgo.2009.09.029.
- Todar, K. (2008) *The Normal Bacterial Flora of Humans*. Available at: [http://textbookofbacteriology.net/normalflora\\_1.html](http://textbookofbacteriology.net/normalflora_1.html) (Accessed: 12 September 2021).
- Truter, I. (2013) 'Bacterial vaginosis: Literature review of treatment options with specific emphasis on non-antibiotic treatment', *African Journal of Pharmacy and Pharmacology*, 7(48), pp. 3060–3067. doi: 10.5897/ajppx2013.0001.

Turovskiy, Sutyak Noll, and C. (2012) 'THE ETIOLOGY OF BACTERIAL VAGINOSIS', *Microbiol*, 110(5), pp. 1105–1128. doi: 10.1038/jid.2014.371.

Ustyugov, A. A. *et al.* (2018) 'Development of 3D Cell Culture on Ultra-High Molecular Weight Polyethylene (UHMWPE) as the Basis of Cellular Matrix', *Biomedical Chemistry: Research and Methods*. Institute of Biochemistry, 1(3), p. e00048. doi: 10.18097/bmcrm00048.

Vanechoutte, M. (2017) 'The human vaginal microbial community', *Research in Microbiology*. Elsevier Masson SAS, 168(9–10), pp. 811–825. doi: 10.1016/j.resmic.2017.08.001.

Varotsis, A. B. (2020a) *Introduction to FDM 3D printing | 3D Hubs*. Available at: <https://www.3dhubs.com/knowledge-base/introduction-fdm-3d-printing/#what> (Accessed: 2 October 2020).

Varotsis, A. B. (2020b) *Introduction to SLA 3D printing | 3D Hubs*. Available at: <https://www.3dhubs.com/knowledge-base/introduction-sla-3d-printing/#what> (Accessed: 1 October 2020).

Verma, A. *et al.* (2013) 'Fabrication of 3D charged particle trap using through-silicon vias etched by deep reactive ion etching', *Journal of Vacuum Science & Technology B, Nanotechnology and Microelectronics: Materials, Processing, Measurement, and Phenomena*. American Vacuum Society, 31(3), p. 032001. doi: 10.1116/1.4799662.

Verowhite - Sculpteo (no date). Available at: <https://www.sculpteo.com/en/materials/polyjet-resin-material/verowhite-polyjet-resin-material/> (Accessed: 31 August 2020).

Verreck, G. *et al.* (2003) 'Incorporation of drugs in an amorphous state into electrospun nanofibers composed of a water-insoluble, nonbiodegradable polymer', *Journal of Controlled Release*. J Control Release, 92(3), pp. 349–360. doi: 10.1016/S0168-3659(03)00342-0.

Vittayarukkul, K. and Lee, A. P. (2017) 'A truly Lego®-like modular microfluidics platform', *Journal of Micromechanics and Microengineering*. IOP Publishing, 27(3), p. aa53ed. doi: 10.1088/1361-6439/aa53ed.

Wang, N. *et al.* (2014) 'Electrospun polyurethane-core and gelatin-shell coaxial fibre coatings for miniature implantable biosensors', *Biofabrication*, 6(1). doi: 10.1088/1758-5082/6/1/015002.

Wang, Z., He, Y. and Zheng, Y. (2019) 'Probiotics for the treatment of bacterial vaginosis: A meta-analysis', *International Journal of Environmental Research and Public Health*. MDPI AG. doi: 10.3390/ijerph16203859.

Ward, A. (2015) *Presenting the Form 1+ SLA 3D Printer*. Available at: <https://www.rs->



online.com/designspark/presenting-the-form-1-sla-3d-printer (Accessed: 1 October 2020).

Watson, S. (2019) *Vaginal pH Balance: Normal Levels, Correcting Unbalanced pH & More*. Available at: [https://www.healthline.com/health/womens-health/vaginal-ph-balance#\\_noHeaderPrefixedContent](https://www.healthline.com/health/womens-health/vaginal-ph-balance#_noHeaderPrefixedContent) (Accessed: 12 September 2021).

van de Wijgert, J. H. H. M. *et al.* (2020) 'Intermittent Lactobacilli-containing Vaginal Probiotic or Metronidazole Use to Prevent Bacterial Vaginosis Recurrence: A Pilot Study Incorporating Microscopy and Sequencing', *Scientific Reports*. Nature Research, 10(1), pp. 1–15. doi: 10.1038/s41598-020-60671-6.

Woodruff, M. A. and Hutmacher, D. W. (2010) 'The return of a forgotten polymer - Polycaprolactone in the 21st century', *Progress in Polymer Science (Oxford)*. Elsevier Ltd, pp. 1217–1256. doi: 10.1016/j.progpolymsci.2010.04.002.

Woodruff, T. K. (2013a) *Evatar: The Mother of MicroHumans | Woodruff Lab*. Available at: <https://www.woodrufflab.org/Evatar> MPS (Accessed: 14 October 2020).

Woodruff, T. K. (2013b) *Ex Vivo Female Reproductive Tract Integration in a 3D Microphysiologic System (active) | Woodruff Lab*. Available at: <https://www.woodrufflab.org/FemKUBE> (Accessed: 14 October 2020).

Wu, Q. *et al.* (2020) 'Organ-on-a-chip: Recent breakthroughs and future prospects', *BioMedical Engineering Online*. BioMed Central, 19(1), pp. 1–19. doi: 10.1186/s12938-020-0752-0.

Xiao, S. *et al.* (2017) 'A microfluidic culture model of the human reproductive tract and 28-day menstrual cycle', *Nature Communications*. Nature Publishing Group, 8, pp. 1–13. doi: 10.1038/ncomms14584.

Yang, Q., Lian, Q. and Xu, F. (2017) 'Perspective : Fabrication of integrated organ-on-a-chip via bioprinting', 031301, pp. 1–5. doi: 10.1063/1.4982945.

Yi, H. G., Lee, H. and Cho, D. W. (2017) '3D printing of organs-on-chips', *Bioengineering*. MDPI AG. doi: 10.3390/bioengineering4010010.

Zhang, Y. *et al.* (2005) 'Electrospinning of gelatin fibers and gelatin/PCL composite fibrous scaffolds', *Journal of Biomedical Materials Research - Part B Applied Biomaterials*. doi: 10.1002/jbm.b.30128.

Zhang, Y. Z. *et al.* (2006) 'Crosslinking of the electrospun gelatin nanofibers', *Polymer*, 47(8), pp. 2911–2917. doi: 10.1016/j.polymer.2006.02.046.

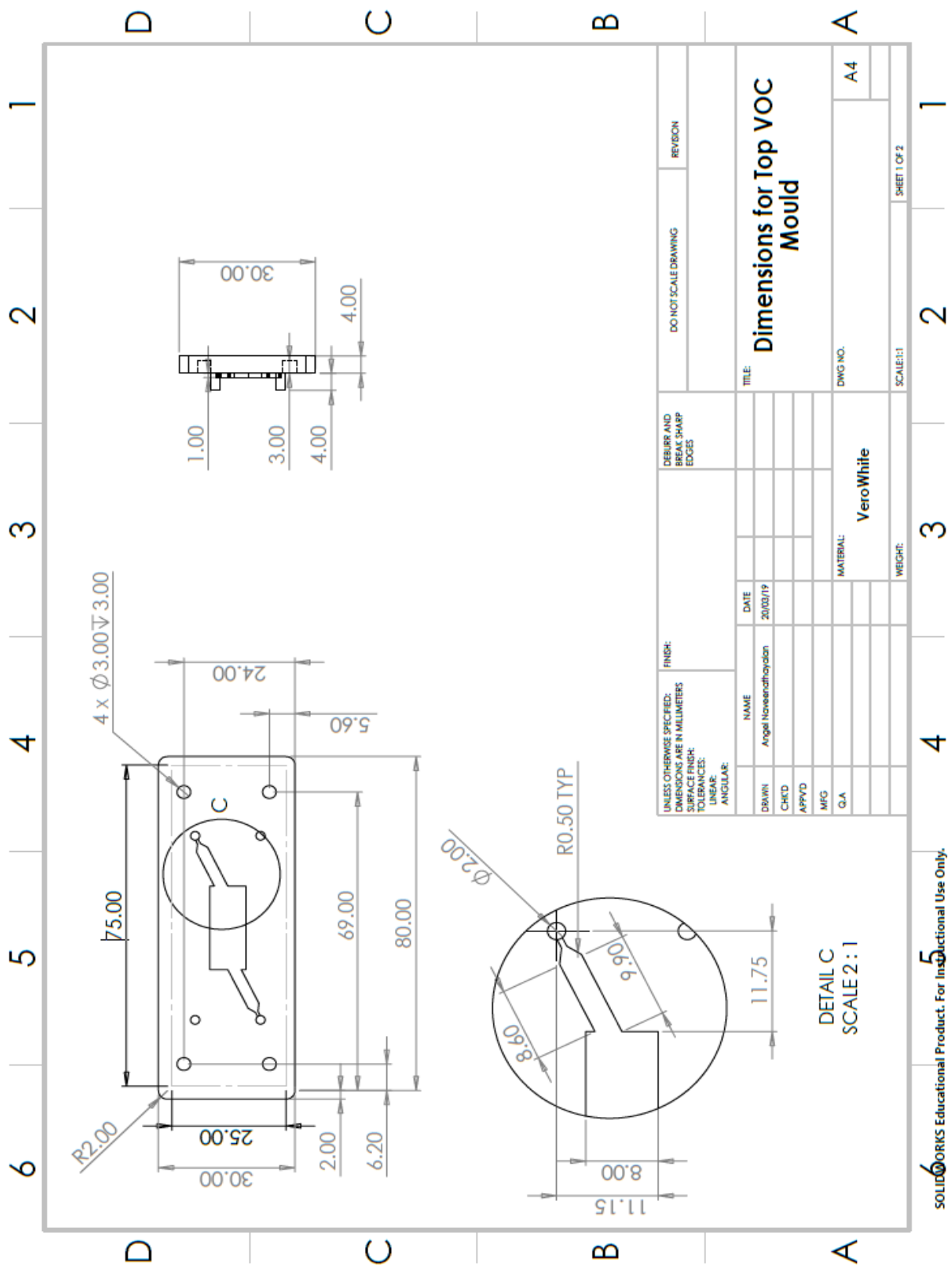
Zheng, W. *et al.* (2014) 'Functionalization of PCL fibrous membrane with RGD peptide by a naturally occurring condensation reaction', *Chinese Science Bulletin*. Science in China Press, 59(22), pp. 2776–2784. doi: 10.1007/s11434-014-0336-0.

Zhou, X. *et al.* (2004) 'Characterization of vaginal microbial communities in adult healthy women using cultivation-independent methods', *Microbiology*. Society for General Microbiology, 150(8), pp. 2565–2573. doi: 10.1099/mic.0.26905-0.

Zong, X. *et al.* (2003) 'Control of structure, morphology and property in electrospun poly(glycolide-co-lactide) non-woven membranes via post-draw treatments', *Polymer*. Elsevier BV, 44(17), pp. 4959–4967. doi: 10.1016/S0032-3861(03)00464-6.

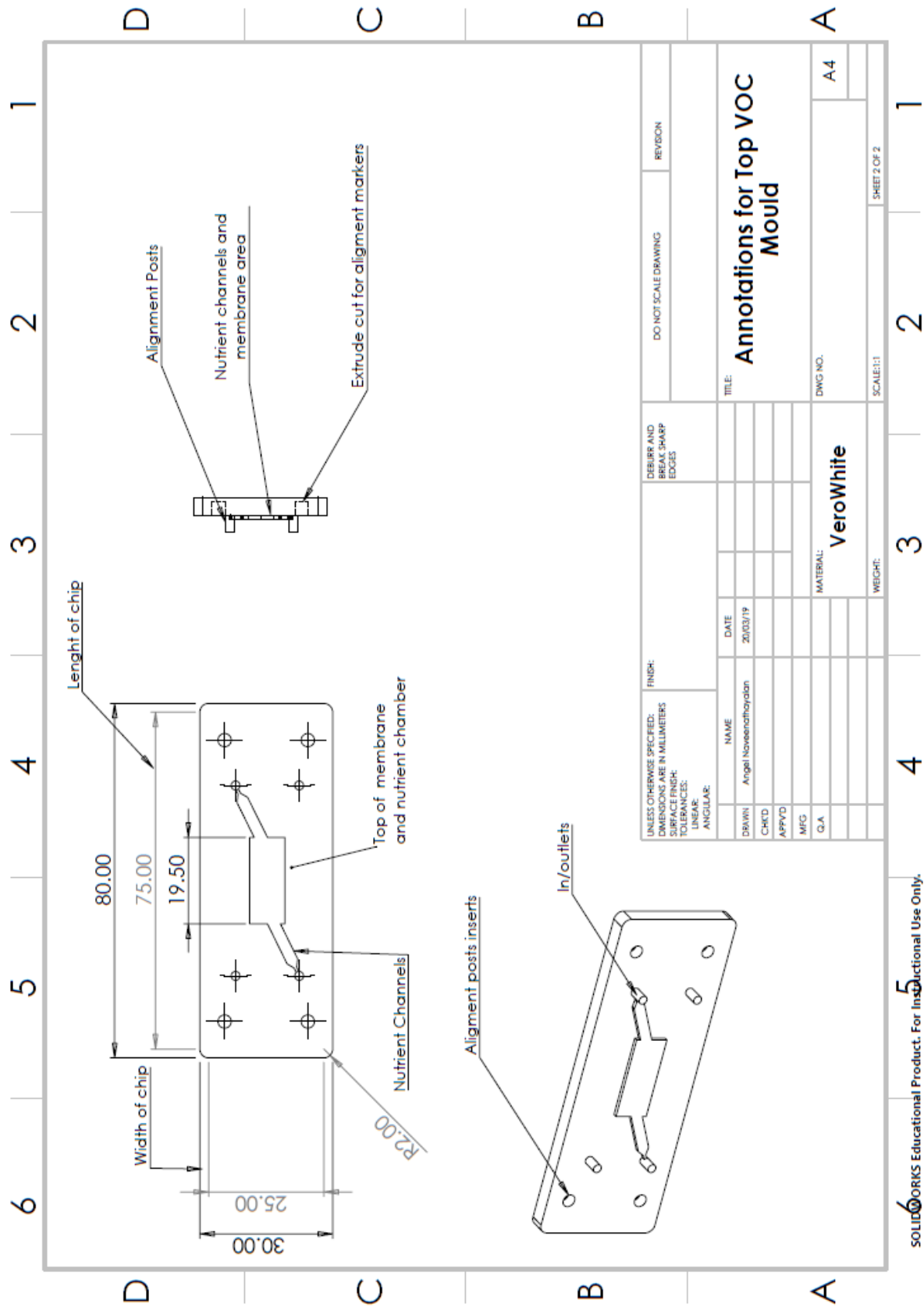
# Appendix A

## 9.1 Top VOC Mould Dimensions



SOLIDWORKS Educational Product. For Instructional Use Only.

### 9.1.1 Top VOC Mould Annotations

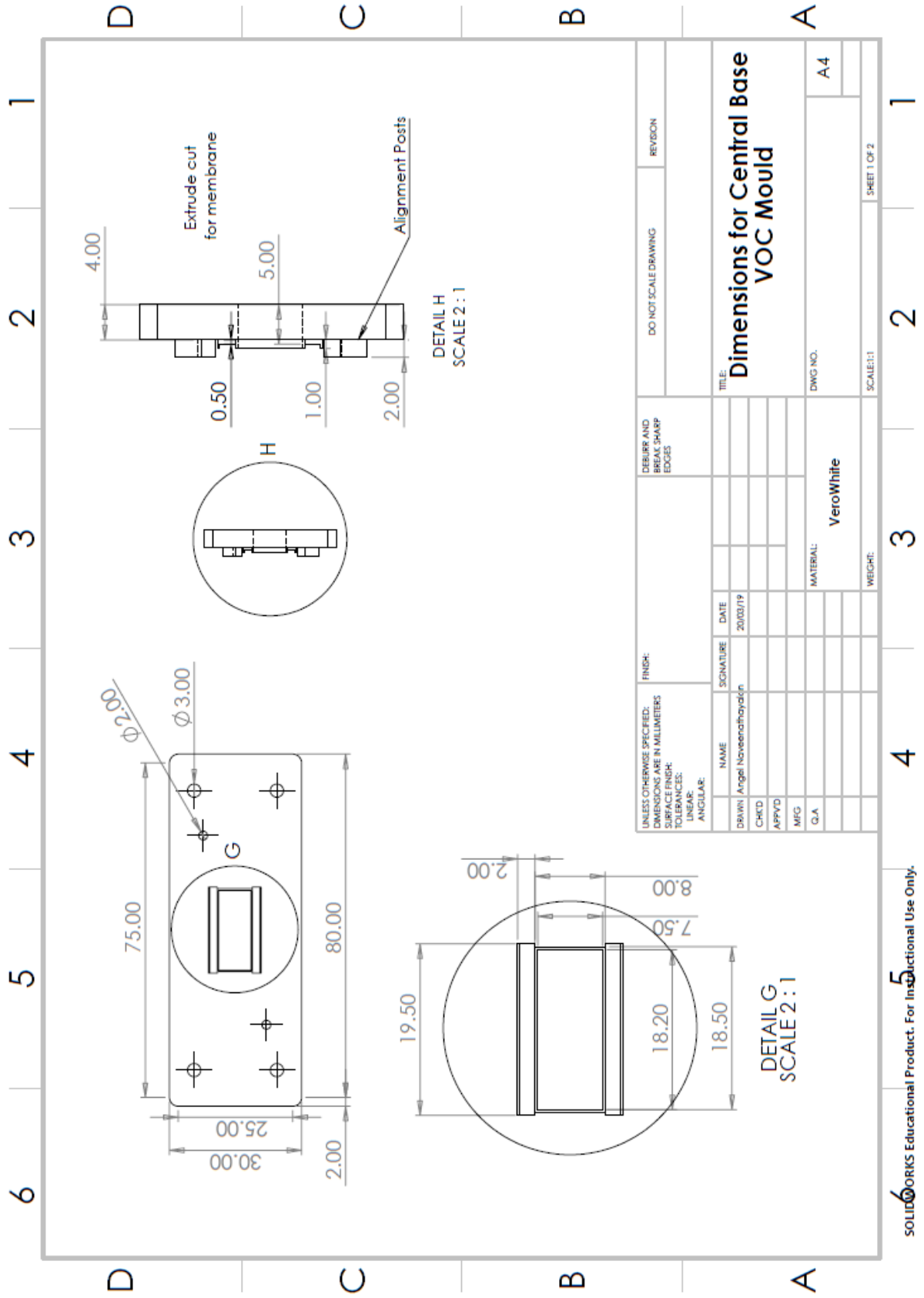


UNLESS OTHERWISE SPECIFIED: DIMENSIONS ARE IN MILLIMETERS		FINISH:		DEBUR AND BREAK SHARP EDGES		DO NOT SCALE DRAWING		REVISION	
SURFACE FINISH:		NAME		DATE		TITLE: <b>Annotations for Top VOC Mould</b>			
TOLERANCES:		DRAWN/ Angel Naveenathayalan		20/03/19		DWG NO. A4			
LINEAR:		CHKD				MATERIAL: <b>VeroWhite</b>			
ANGULAR:		APPROV				SCALE: 1:1			
		MFG				WEIGHT:			
		Q.A.				SHEET 2 OF 2			

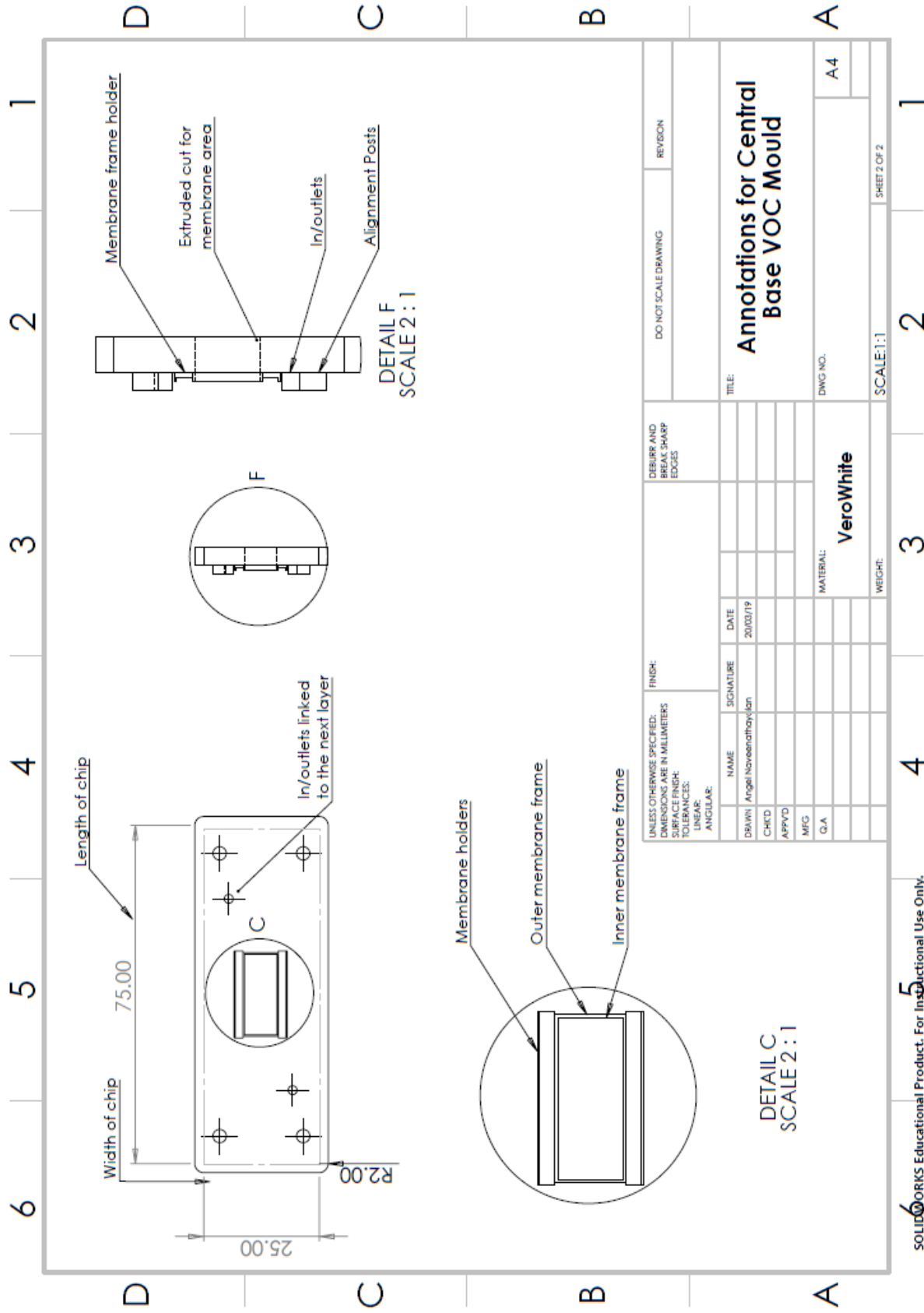




9.3 Central Base VOC Mould Dimensions



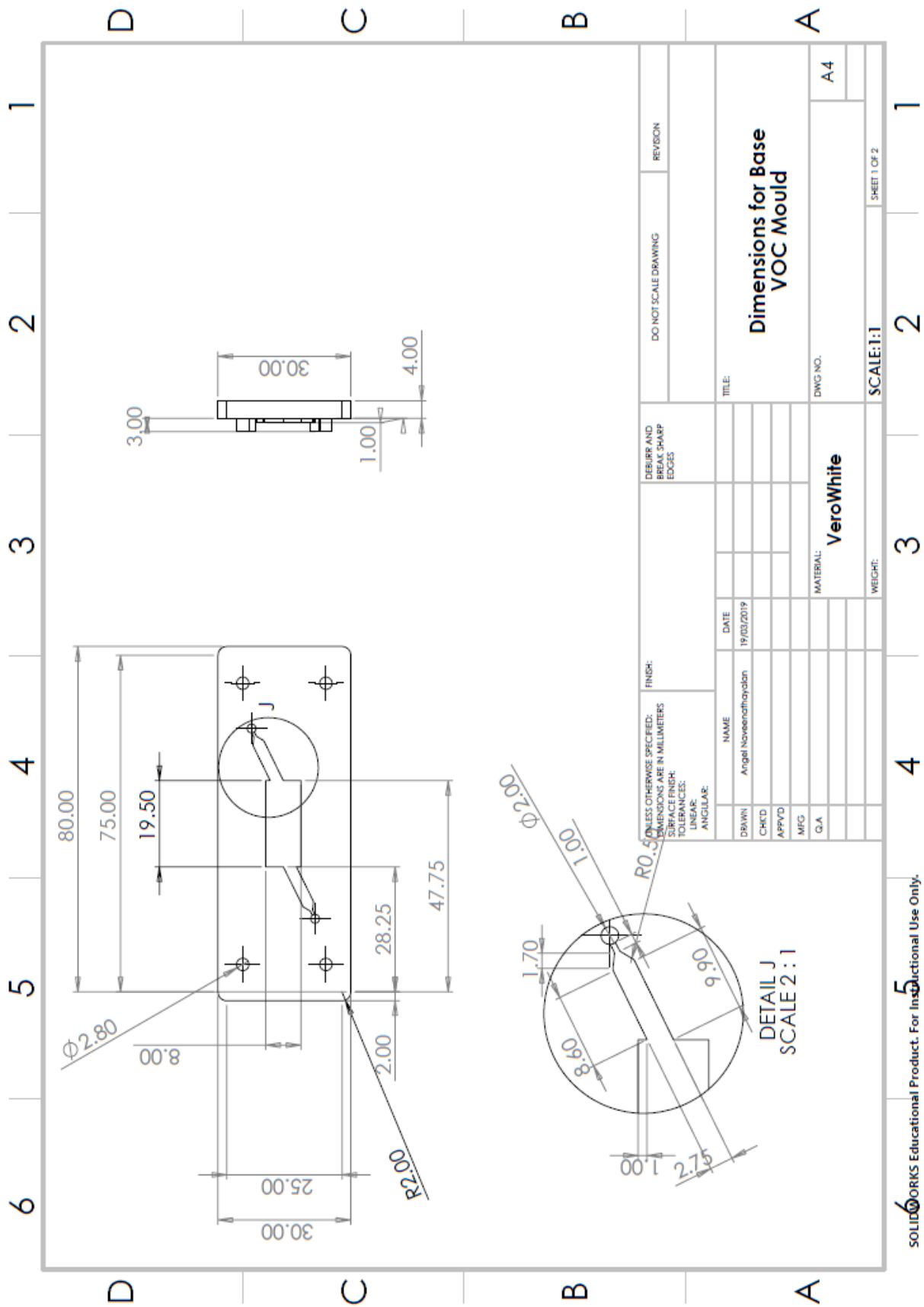
### 9.3.1 Central Base VOC Mould Annotations



SOLIDWORKS Educational Product. For Instructional Use Only.

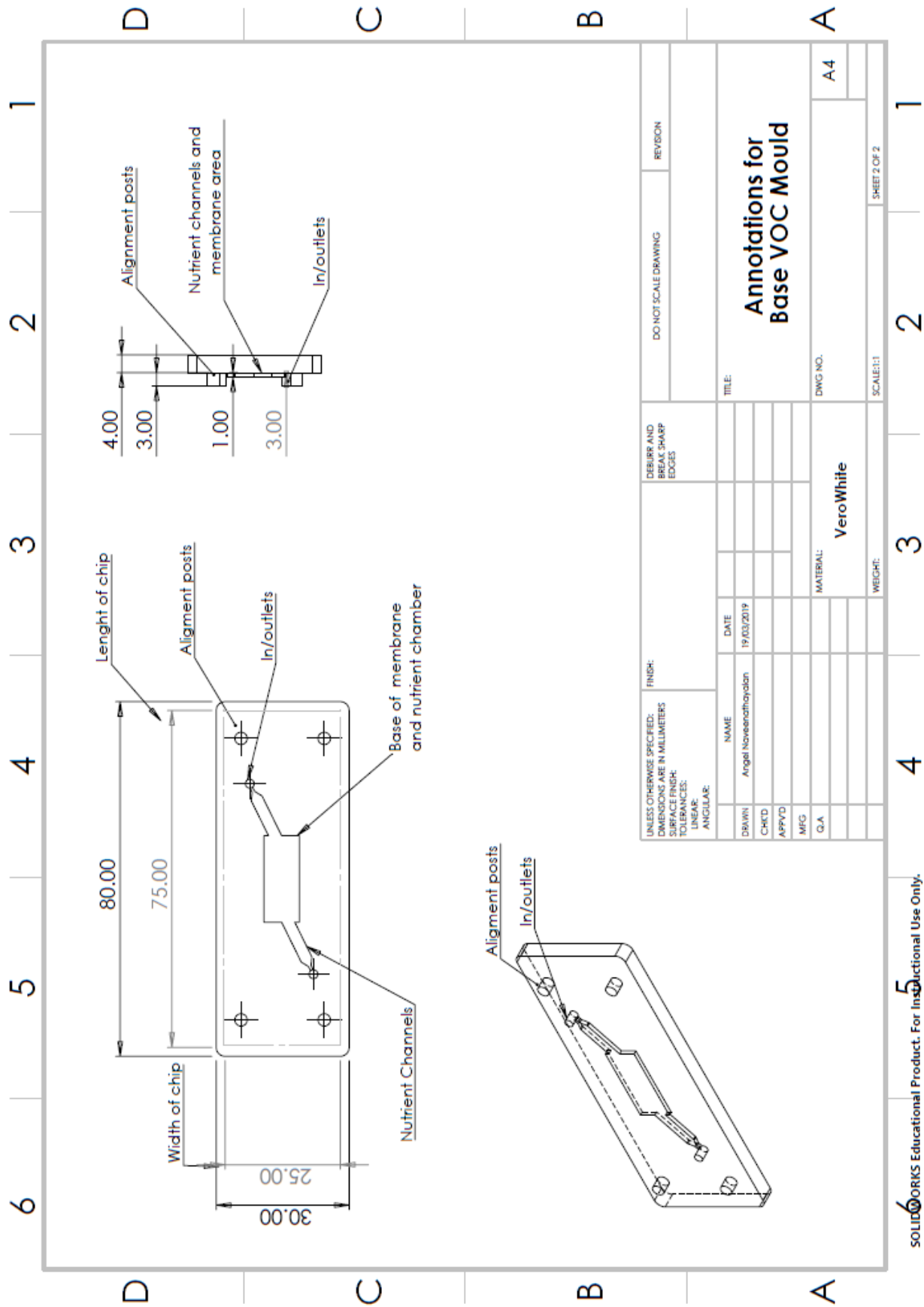


### 9.4 Base VOC Mould Dimensions



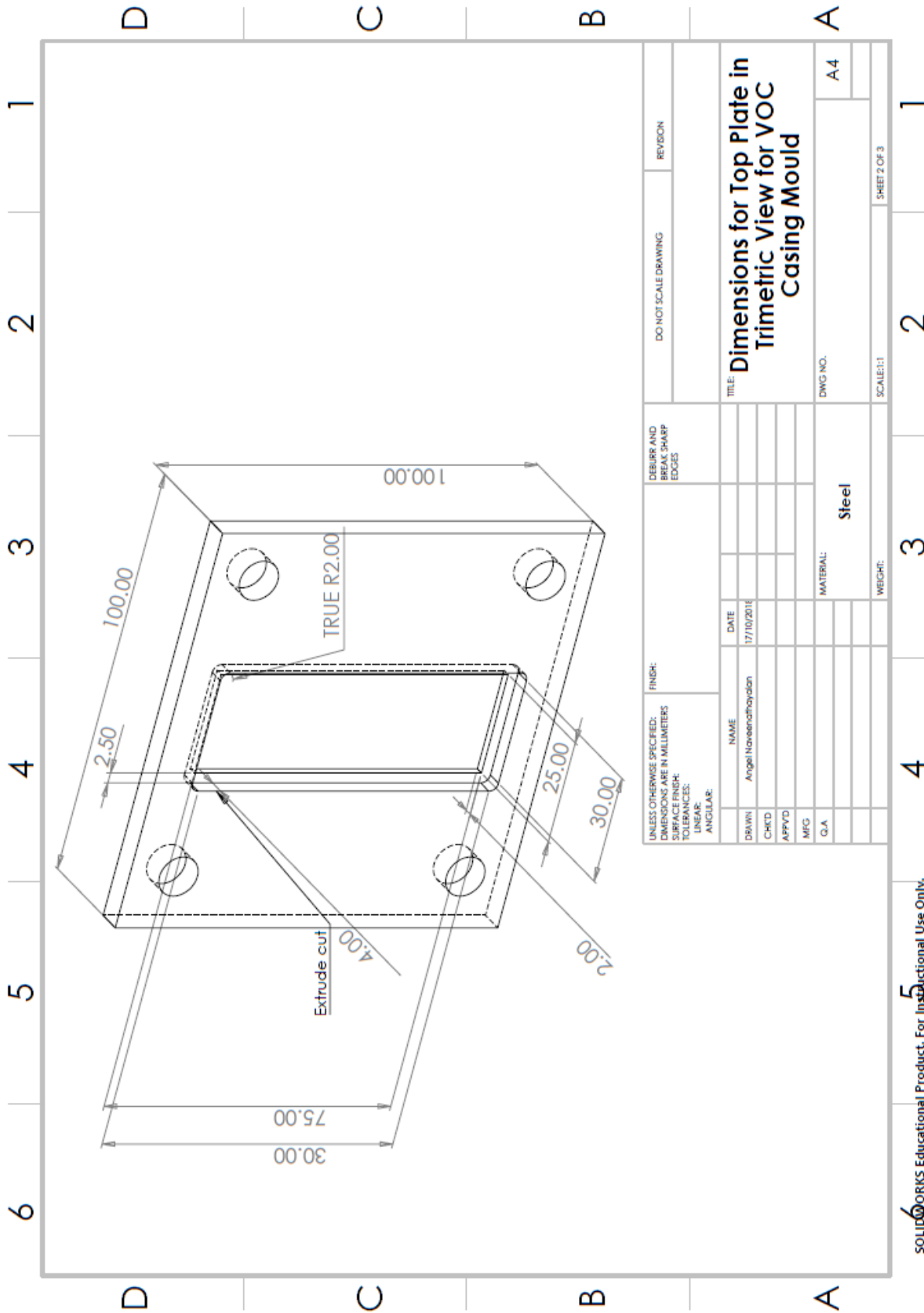
SOLIDWORKS Educational Product. For Instructional Use Only.

### 9.4.1 Base VOC Mould Annotations

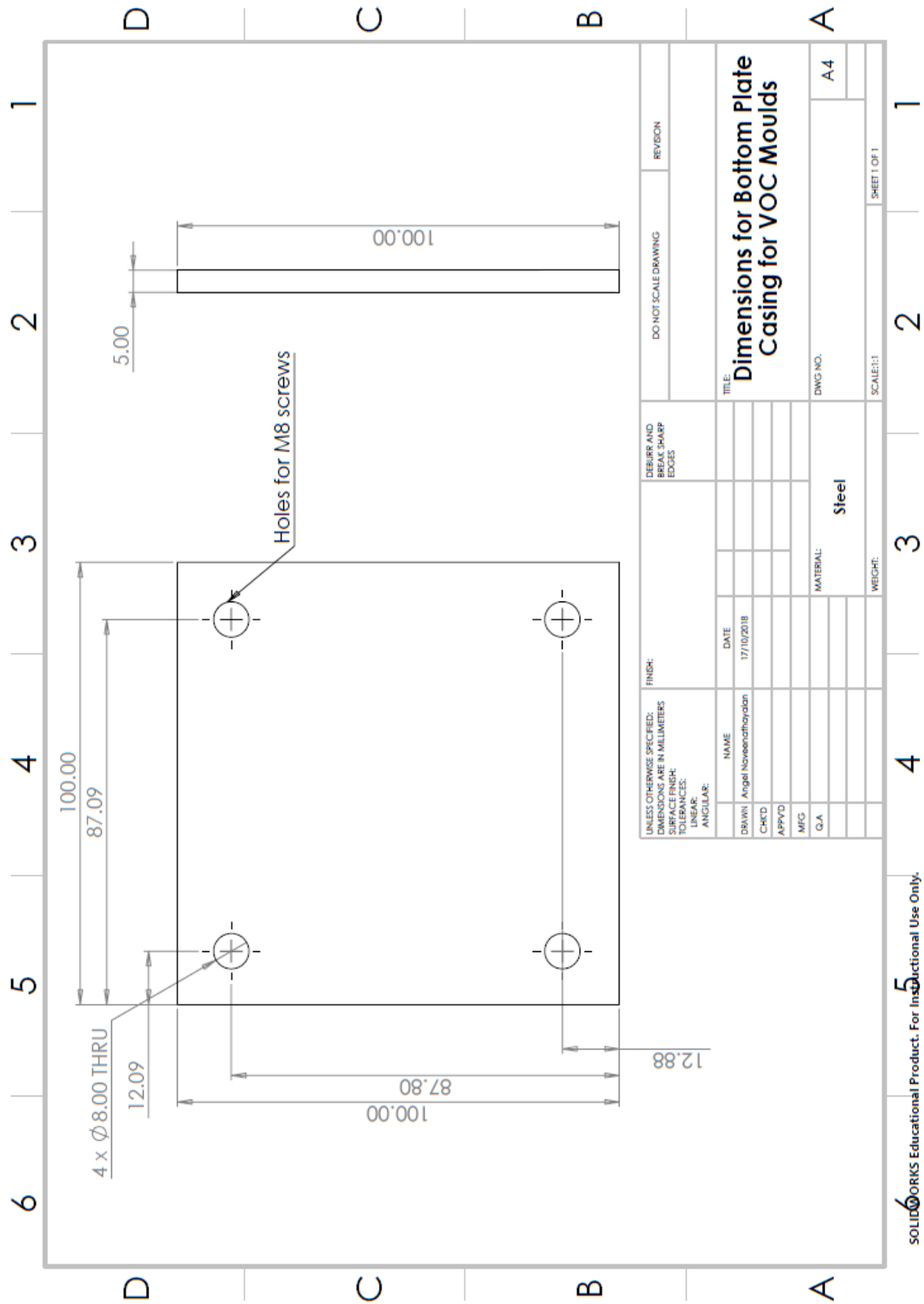




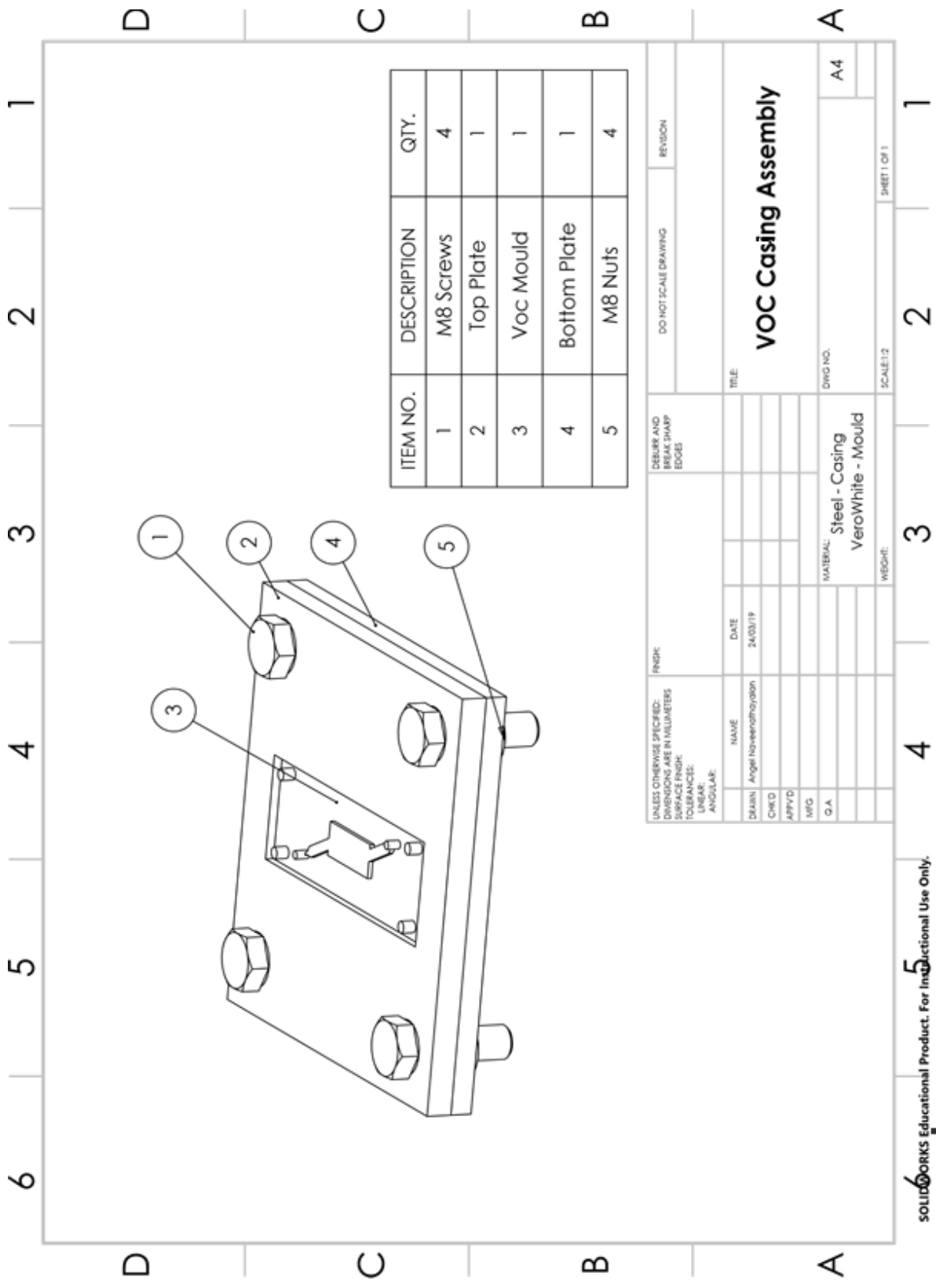
### 9.5.1 Top Plate Casing for VOC Mould Trimetric View



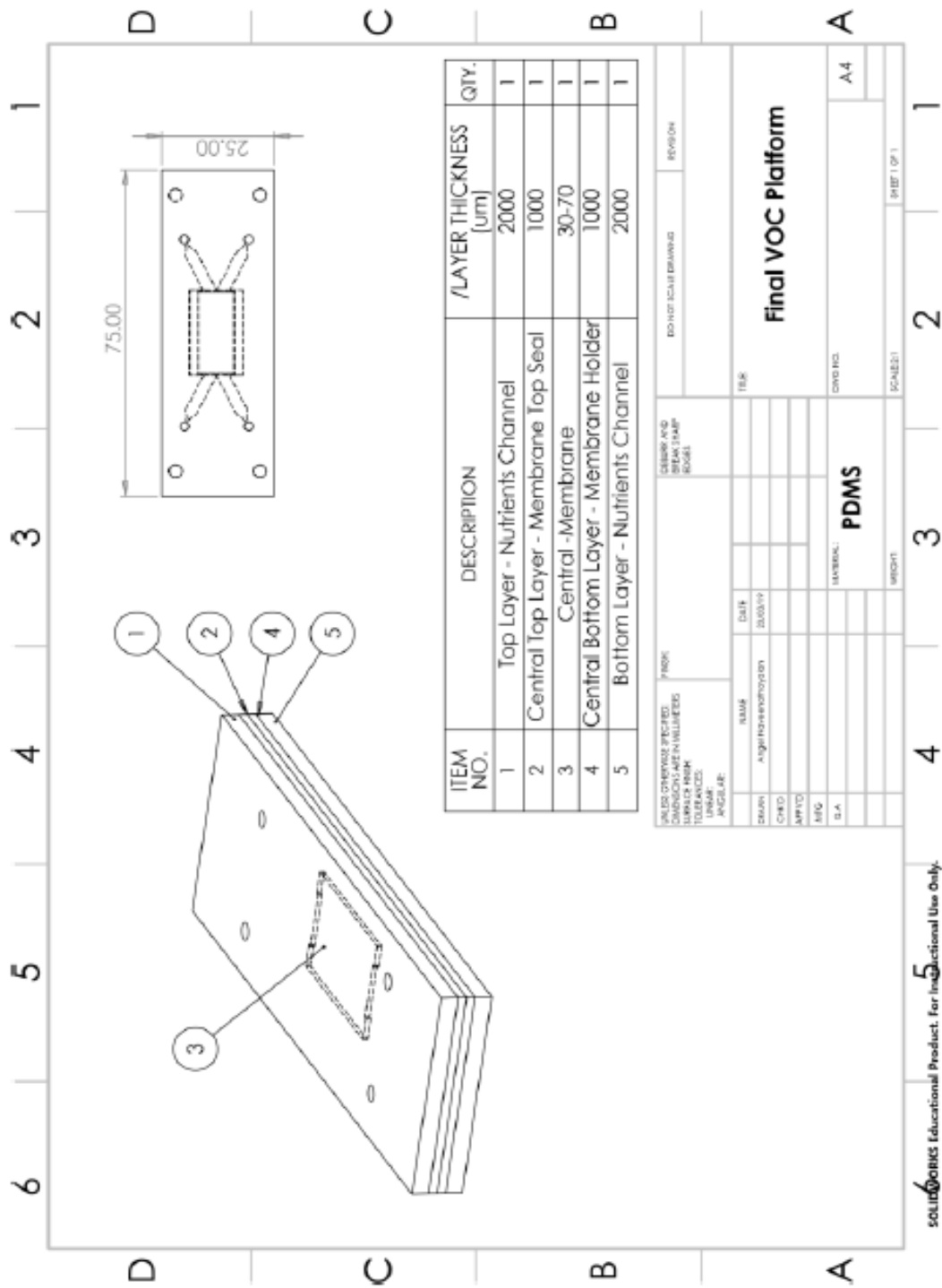
### 9.6 Bottom Plate Casing for VOC Mould Dimensions



### 9.7 VOC Mould in Casing Assembly



### 9.7.1 Assembly of the VOC Platform



SOLIDWORKS Educational Product. For Instructional Use Only.